MEASUREMENT AND ANALYSIS OF AMBIENT ATMOSPHERIC PARTICULATE MATTER IN URBAN AND REMOTE ENVIRONMENTS

A Dissertation
Presented to
The Academic Faculty

By

Gayle S.W. Hagler

In Partial Fulfillment
of the Requirements for the Degree
Doctor of Philosophy in the
School of Civil and Environmental Engineering

Georgia Institute of Technology

August 2007

MEASUREMENT AND ANALYSIS OF AMBIENT ATMOSPHERIC PARTICULATE MATTER IN URBAN AND REMOTE ENVIRONMENTS

Approved by:

Dr. Michael H. Bergin, Advisor
School of Civil and Environmental Engineering and
School of Earth and Atmospheric Sciences
Georgia Institute of Technology

Dr. James A. Mulholland
School of Civil and Environmental Engineering
Georgia Institute of Technology

Dr. Armistead G. Russell
School of Civil and Environmental Engineering
Georgia Institute of Technology

Dr. James J. Schauer
Department of Civil and Environmental Engineering
University of Wisconsin-Madison

Dr. Rodney J. Weber
School of Earth and Atmospheric Sciences
Georgia Institute of Technology

Date approved:
May 2, 2007

This thesis is dedicated to Ty,
who climbed this mountain with me.

ACKNOWLEDGEMENTS

There are quite a few people I wish mention for their tremendous support in my research and in my personal growth throughout graduate school.

I would like to thank my thesis committee, including my advisor, Mike Bergin, and committee members Ted Russell, Rodney Weber, Jim Mulholland, and Jamie Schauer. As a student in their classes, an author on collaborative papers, and a co-investigator on research problems, these five faculty members have been a catalyst in my development as a student and researcher. In particular, I would like to thank Mike for his endless patience, unconditional support, and commitment to excellent research. I would not have made it to this point without such an amazing advisor. In addition, I cannot thank enough the staff, faculty, and fellow students in the Environmental Engineering Department and School of Civil and Environmental Engineering. They have all made my graduate school experience rewarding from start to finish.

In my research studies in China, I am deeply thankful for positive collaboration with Lynn Salmon of Caltech, Mei Zheng and Bill Chameides at Georgia Tech, the scientists of the Hong Kong, Guangzhou, and Zhongshan Environmental Protection Departments, Christine Loh and Kylie Uebergang of Civic Exchange, Jianzhen Yu, Eric Wan, and all my friends at HKUST, Tao Wang at Hong Kong PolyU, C.S. Kiang, Xiaoyan Tang, Yuanghang Zhang, Zeng Limin, and Yang Qiang of Beijing University, and Sjaak Slanina of the Energy Institute of the Netherlands. In addition, I am thankful for the

access to meteorological data provided by the HKEPD, the Chinese Meteorological Association, and the Center for Coastal and Atmospheric Research at HKUST.

Moving to the Greenland Ice Sheet and the Colorado Rockies, I greatly appreciate the support of our co-investigators, including Erika von Schneidemesser and Martin Shafer at the University of Wisconsin-Madison, and Jack Dibb, Casey Anderson, and Rob Griffin at the University of New Hampshire. In addition, I am thankful for the research support provided by staff of the University of Colorado Mountain Research Station, Veco Polar Resources, New York Air National Guard 109th Airlift Wing, ETH Zürich, and members of the Russell lab (Sangil Lee, Hyeonkook Kim, Evan Cobb) and Weber lab (Chris Hennigan, Amy Sullivan, Rick Peltier, Arsineh Hecobian).

For my personal financial support, I am very grateful for graduate fellowships provided by Georgia Tech, the National Science Foundation, the American Association of University Women, and P.E.O. International.

Finally, there are never enough words to express how thankful I am for the endless support of my family. My parents and sisters would have formed an official uniformed cheerleading squad if I had let them. My husband's family, the Hagler and Livesay clan, have adopted me as one of their own and have been a constant source of support throughout graduate school. Finally, I am so grateful for my husband, Ty. Whether in the lab with me late at night helping process snow samples or sending me off to study while he moved us into a new apartment, Ty has been a saint.

TABLE OF CONTENTS

ACKNOWLEDGEMENTS iv

LIST OF TABLES ix

LIST OF FIGURES x

NOMENCLATURE xvii

SUMMARY xix

INTRODUCTION 1

PART 1: FINE PARTICULATE MATTER IN URBAN CHINA 6

CHAPTER 2: INTRODUCTION 7
2.1 Foreword 7
2.2 Human Health and Economic Impact of Particulate Matter in China 7
2.3 Particulate Matter in the Pearl River Delta Region of China 12
2.4 Research Objectives 15

CHAPTER 3: METHODS 16
3.1 Field Sampling 16
3.2 Chemical Analyses 20

CHAPTER 4: RESULTS AND DISCUSSION 22
4.1 Concentrations of Major Fine Particulate Species 22
4.2 Enrichment Factors and Concentrations of Fine Particulate Elements 24
4.3 Meteorology Case Studies 30
4.3.1 Southerly Flow 35
4.3.2 Northerly Flow 39
4.3.3 Mixed Flow 42
4.4 Correlative Analysis 45
4.5 Factor Analysis 53

CHAPTER 5: CONCLUSIONS AND RECOMMENDATIONS 55
5.1 Conclusions 55
5.2 Policy Implications 58
5.3 Recommendations for Further Research 60

PART 2: PARTICULATE MATTER ON THE GREENLAND ICE SHEET 64

CHAPTER 6: INTRODUCTION 65
6.1 Foreword 65
6.2 Background on the Greenland Ice Sheet 65
6.2.1 Climate Change and Ice Loss 66
6.2.2 Archival of Atmospheric History 67
6.2.3 Modern Origin of Pollutants Reaching the Greenland Ice Sheet 69
6.3 Carbonaceous Particulate Matter and the Greenland Ice Sheet 70
6.3.1 Atmospheric Carbonaceous Particulate Matter 70
6.3.2 Archival and Post-Depositional Processing in Snow 71
6.4 Research Objectives 75

CHAPTER 7: METHODS 77
7.1 Field Sites and Sampling Overview 77
7.1.1 Summit, Greenland 77
7.1.2. Niwot Ridge, Colorado 80
7.2 Field Sampling and Instrumentation 82
7.2.1 Surface Snow Sampling 82
7.2.2 Snow Pit Sampling 83
7.2.3 Atmospheric Sampling 84
7.3 Laboratory Analyses 88
7.3.1 Snow Samples 88
7.3.2 Integrated Filter Samples 91

CHAPTER 8: RESULTS AND DISCUSSION 92
8.1 Foreword 92
8.2 Organic Carbon Record in Snow on the Greenland Ice Sheet 92
8.2.1 Concentrations and Dating of Snow Pit Samples 92
8.2.2 Comparison With Past Measurements 94
8.2.3 Trends Observed in Snow Pit Carbonaceous Species 96
8.3 Time Series of Organic and Elemental Carbon on the Greenland Ice Sheet 99
8.3.1 Atmospheric Concentrations and Transport 99
8.3.2 Surface Snow Concentrations 106
8.3.3 Comparison of Air and Snow 112
8.4 Investigation of Camp Contamination at Summit, Greenland 115
8.4.1 Camp Emissions and Atmospheric Samples 115
8.4.2 Impact of Camp Emissions on Snow Concentrations 119
8.5 Related Measurements at Niwot Ridge, Colorado 122
8.5.1 Atmospheric Concentrations 122
8.5.2 Snow Concentrations 126

CHAPTER 9: CONCLUSIONS AND RECOMMENDATIONS 130
9.1 Conclusions 130
9.2 Recommendations for Further Research 135

APPENDIX A: CHINA – FIELD DOCUMENTATION 138

APPENDIX B: CHINA – ADDITIONAL DATA AND ANALYSES 154

APPENDIX C: GREENLAND ICE SHEET AND NIWOT RIDGE – FIELD SAMPLING PREPARATION AND CALCULATIONS 204

APPENDIX D: GREENLAND ICE SHEET – ADDITIONAL DATA 224

REFERENCES 244

VITA 259

LIST OF TABLES

Table 1. Sampling sites in the Pearl River Delta Region of China 17

Table 2. Concentrations of major fine particulate species 24

Table 3. Elemental Composition of $PM_{2.5}$ ($\mu g\ m^{-3}$) 29

Table 4. Sampling days categorized into Southerly, Northerly, or Mixed Flow 31

Table 5. Average concentrations of measured species during Southerly Flow, Northerly Flow, and Mixed Flow 33

Table 6. Least-squares fit of developed sites in Hong Kong versus rural Tap Mun 49

Table 7. Principle Components Analysis of measurements made at sites in Hong Kong (Tap Mun, Tung Chung, Central/Western), and Shenzhen 54

Table 8. Description of field sampling at Summit, Greenland 80

Table 9. Description of field sampling at Niwot Ridge, Colorado 81

Table 10. Comparison of surface snow with buried summer snow layers 98

Table 11. Concentrations of atmospheric species at Summit, Greenland during Summer 2006 99

Table 12. Concentrations of snow-phase species at Summit, Greenland during Summer 2006 108

Table 13. 1-meter snow pit locations near Summit, Greenland 119

LIST OF FIGURES

Figure 1. China's energy consumption from 1978 to 1999 8

Figure 2. A view of Shenzhen, China, located in the Pearl River Delta Region, in September 2002 12

Figure 3. Map of southeastern China, with the Pearl River Delta Region of China (PRD) highlighted 13

Figure 4. Location of monitoring sites used in the PRD study 16

Figure 5. Schematic of $PM_{2.5}$ samplers used in the PRD study 18

Figure 6. Intercomparison of overall $PM_{2.5}$ concentration and speciation of major particulate components 19

Figure 7. Four-month average enrichment factors of elements at seven sites in the Pearl River Delta Region of China 26

Figure 8. Four-month average seawater enrichment factors of elements at seven sites in the Pearl River Delta Region of China 26

Figure 9. Measurements of wind speed, wind direction and precipitation at the Shenzhen meteorology site for selected days categorized as Northerly Flow, Southerly Flow, and Mixed Flow 32

Figure 10. Normalized concentrations and standard error of species measured at seven sites in the Pearl River Delta, categorized by wind pattern 34

Figure 11a. Sulfur measured at the Hong Kong background site, Tap Mun, compared with the more developed sites in Hong Kong, Central/Western and Tung Chung 46

Figure 11b. Potassium measured at the Hong Kong background site, Tap Mun, compared with the more developed sites in Hong Kong, Central/Western and Tung Chung 46

Figure 11c. Sodium measured at rural Tap Mun, compared with Central/Western and Tung Chung. 47

Figure 11d. Nickel measured at rural Tap Mun, compared with Central/Western and Tung Chung. 47

Figure 12. Pearson correlation coefficient calculated between pairings of Hong Kong sites Tap Mun, Tung Chung, and Central/Western 48

Figure 13a. Pearson correlation coefficient calculated between pairings of Hong Kong sites Tap Mun, Tung Chung, and Central/Western with Shenzhen, located immediately north of the Hong Kong Special Administrative Region 51

Figure 13b. Pearson correlation coefficient calculated between pairings of Hong Kong sites Tap Mun, Tung Chung, and Central/Western with Zhongshan, located west of the Hong Kong Special Administrative Region 51

Figure 13c. Pearson correlation coefficient calculated between pairings of Hong Kong sites Tap Mun, Tung Chung, and Central/Western with Guangzhou, located northwest of the Hong Kong Special Administrative Region 52

Figure 14. Location of Summit, Greenland (source: zero.eng.ucmerced.edu) 77

Figure 15. A view of Summit, Greenland taken from the Swiss Tower, located in the clean air sector 78

Figure 16. Spatial layout of Summit Camp 79

Figure 17. Location of Niwot Ridge, Colorado field campaign ("Soddie Site") 81

Figure 18. Sampling a 1-meter snow pit located 20 km south of Summit, Greenland in 2006 84

Figure 19. Instrumentation used during the Niwot Ridge, Colorado field campaign 85

Figure 20. 3-meter snow pit profiles of elemental carbon, water-insoluble organic carbon, water-soluble organic carbon, deuterium ratio, calcium ion, potassium ion, and sulfate ion 93

Figure 21. A time series of particulate measurements in the atmosphere of Summit, Greenland during Summer 2006 100

Figure 22. Mean clustered 10-day back trajectories for 28 May - 19 July 2006 101

Figure 23. Relationship between atmospheric elemental carbon and organic carbon 104

Figure 24. Relationship between atmospheric elemental carbon and the absorption coefficient 105

Figure 25. 10-day back-trajectories and pressure altitude (hPa) during the high particulate matter concentrations observed on 13-14 June 2006 106

Figure 26. A time series of snow-phase water-soluble organic carbon, water-insoluble organic carbon, and elemental carbon. Observations of snow and fog are indicated. 108

Figure 27. 24-hour change in surface snow WSOC compared with 24-hour change in surface-snow WIOC 112

Figure 28. Comparison of atmospheric $PM_{0.1\text{-}1.0}$ concentrations versus surface snow WSOC 114

Figure 29. Comparison of carbon balance in air samples and surface snow 114

Figure 30. Wind patterns observed during 26 May 2006 – 18 July 2006. 116

Figure 31. Sector control power on/off and the unfiltered measurement of the absorption coefficient 117

Figure 32. Wind direction and speed during 2003-2005 at Summit, Greenland 118

Figure 33. Comparison of average snow pit concentrations in 1-meter snow pits located near and far from Summit Camp 121

Figure 34. A time series of atmospheric particulate matter species at Niwot Ridge, Colorado, including carbonaceous particulate matter, $PM_{0.1\text{-}1.0}$, number concentration, particulate absorption coefficient, particulate scattering coefficient, and single-scattering albedo 124

Figure 35. Relationship between ambient particulate absorption and scattering at Niwot Ridge, Colorado 125

Figure 36. Water-soluble organic carbon measured at 5 cm increments in a 1-meter snow pit at Niwot Ridge, Colorado 126

Figure 37. Water-soluble organic carbon in surface snow measured hourly starting at 10:00 am at Niwot Ridge, Colorado 127

Figure 38. Relationship between the fraction of WSOC that is hydrophilic and total WSOC 129

Figure B.1 Hourly wind vectors and 24-hour rainfall at six meteorological sites in the Pearl River Delta on 10/1/2002-10/2/2002 155

Figure B.2 Hourly wind vectors and 24-hour rainfall at six meteorological sites in the Pearl River Delta on 10/7/2002-10/8/2002 156

Figure B.3 Hourly wind vectors and 24-hour rainfall at six meteorological sites in the Pearl River Delta on 10/13/2002-10/14/2002 157

Figure B.4 Hourly wind vectors and 24-hour rainfall at six meteorological sites in the Pearl River Delta on 10/19/2002-10/20/2002 158

Figure B.5 Hourly wind vectors and 24-hour rainfall at six meteorological sites in the Pearl River Delta on 10/25/2002-10/26/2002 159

Figure B.6 Hourly wind vectors and 24-hour rainfall at six meteorological sites in the Pearl River Delta on 11/30/2002-12/1/2002 160

Figure B.7 Hourly wind vectors and 24-hour rainfall at six meteorological sites in the Pearl River Delta on 12/6/2002-12/7/2002 161

Figure B.8 Hourly wind vectors and 24-hour rainfall at six meteorological sites in the Pearl River Delta on 12/12/2002-12/13/2002 162

Figure B.9 Hourly wind vectors and 24-hour rainfall at six meteorological sites in the Pearl River Delta on 12/18/2002-12/19/2002 163

Figure B.10 Hourly wind vectors and 24-hour rainfall at six meteorological sites in the Pearl River Delta on 12/24/2002-12/25/2002 164

Figure B.11 Hourly wind vectors and 24-hour rainfall at six meteorological sites in the Pearl River Delta on 2/28/2003-3/1/2003 165

Figure B.12 Hourly wind vectors and 24-hour rainfall at six meteorological sites in the Pearl River Delta on 3/6/2003-3/7/2003 166

Figure B.13 Hourly wind vectors and 24-hour rainfall at six meteorological sites in the Pearl River Delta on 3/12/2003-3/13/2003 167

Figure B.14 Hourly wind vectors and 24-hour rainfall at six meteorological sites in the Pearl River Delta on 3/18/2003-3/19/2003 168

Figure B.15 Hourly wind vectors and 24-hour rainfall at six meteorological sites in the Pearl River Delta on 3/24/2003-3/25/2003 169

Figure B.16 Hourly wind vectors and 24-hour rainfall at six meteorological sites in the Pearl River Delta on 6/4/2003-6/5/2003 170

Figure B.17 Hourly wind vectors and 24-hour rainfall at six meteorological sites in the Pearl River Delta on 6/10/2003-6/11/2003 171

Figure B.18 Hourly wind vectors and 24-hour rainfall at six meteorological sites in the Pearl River Delta on 6/16/2003-6/17/2003 172

Figure B.19 Hourly wind vectors and 24-hour rainfall at six meteorological sites in the Pearl River Delta on 6/22/2003-6/23/2003 173

Figure B.20 Hourly wind vectors and 24-hour rainfall at six meteorological sites in the Pearl River Delta on 6/28/2003-6/29/2003 174

Figure B.21 24 hour back-trajectory of air parcels reaching sites Tap Mun and Conghua on 0000 local time, October 20th, 2002 175

Figure B.22 24 hour back-trajectory of air parcels reaching sites Tap Mun and Conghua on 0000 local time, June 5th, 2003 175

Figure B.23 24 hour back-trajectory of air parcels reaching sites Tap Mun and Conghua on 0000 local time, June 23rd, 2003 176

Figure B.24 24 hour back-trajectory of air parcels reaching sites Tap Mun and Conghua on 0000 local time, June 29th, 2003 176

Figure C.1 Comparison of carbon mass in ultraclean water in Kaptclean^{TM} bottles, before and after cleaning. 206

Figure C.2. Calculated inorganic carbon in water given P_{CO2} of $10^{-3.5}$ atm 208

Figure C.3 OC and IC concentrations in aged ultrapure water during acidification tests 209

Figure C.4 OC/TC fraction during acidification tests 209

Figure C.5 Tests for background addition by phosphoric acid 210

Figure C.6 Layered versus single punches measured on the Sunset Carbon Analyzer 212

Figure C.7 Absorption coefficient (Mm^{-1}) measured at Summit Camp 215

Figure C.8 Wind direction during the July 2005 field campaign 215

Figure C.9 Wind speeds measured during the July 2005 field campaign 216

Figure D.1 Calculated 10-day isobaric trajectories arriving at Summit, Greenland on 28-31 May 2006 225

Figure D.2 Calculated 10-day isobaric trajectories arriving at Summit, Greenland on 1-4 June 2006 226

Figure D.3 Calculated 10-day isobaric trajectories arriving at Summit, Greenland on 5-8 June 2006 227

Figure D.4 Calculated 10-day isobaric trajectories arriving at Summit, Greenland on 9-12 June 2006 228

Figure D.5 Calculated 10-day isobaric trajectories arriving at Summit, Greenland on 13-16 June 2006 229

Figure D.6 Calculated 10-day isobaric trajectories arriving at Summit, Greenland on 17-20 June 2006 230

Figure D.7 Calculated 10-day isobaric trajectories arriving at Summit, Greenland on 21-24 June 2006 231

Figure D.8 Calculated 10-day isobaric trajectories arriving at Summit, Greenland on 25-28 June 2006 232

Figure D.9 Calculated 10-day isobaric trajectories arriving at Summit, Greenland on 29 June - 2 July 2006 233

Figure D.10 Calculated 10-day isobaric trajectories arriving at Summit, Greenland on 3-6 July 2006 234

Figure D.11 Calculated 10-day isobaric trajectories arriving at Summit, Greenland on 7-10 July 2006 235

Figure D.12 Calculated 10-day isobaric trajectories arriving at Summit, Greenland on 11-14 July 2006 236

Figure D.13 Calculated 10-day isobaric trajectories arriving at Summit, Greenland on 15-18 July 2006 237

Figure D.14 Calculated 10-day isobaric trajectories arriving at Summit, Greenland on 19 July 2006 238

Figure D.15 Profiles of ions measured in a 3-meter snow pit at Summit, Greenland 239

Figure D.16 1-meter profile of elemental carbon (EC) at Summit, Greenland and up to 20 km North or South of Summit, Summer 2006 240

Figure D.17 1-meter profile of water-insoluble organic carbon (OC) at Summit, Greenland and up to 20 km North or South of Summit, Summer 2006 240

Figure D.18 3-meter snow pit carbonaceous species and oxygen-isotope ratio, Greenland Ice Sheet, July 2005 241

Figure D.19 3-meter snow pit ions and comparison of GT/UNH sampling with samples from a parallel 2-meter snow pit taken by the Laboratoire de Glaciologie et Géophysique de l'Environnement (LGGE), Greenland Ice Sheet, July 2005 242

Figure D.20 Water-insoluble organic carbon measured in the surface snow during the July 2005 field campaign in Summit, Greenland. 243

Figure D.21 Elemental carbon measured in the surface snow during the July 2005 field campaign in Summit, Greenland. 243

NOMENCLATURE

Al: Aluminum
AOD: aerosol optical depth
As: Arsenic
BC: Black carbon
Br: Bromide
Ca: Calcium
CH: Conghua
Cl: Chloride
Co: Cobalt
CO: Carbon monoxide
Cr: Chromium
CW: Central/Western
Cu: Copper
CV: Coefficient of variation
δ^2H or δD: Deuterium ratio
D_{50}: Particle diameter cut-point with 50% penetration
D_p: Particle diameter
E_{ap}: Mass absorption cross-section
EC: Elemental carbon
EF: Crustal enrichment factor
Fe: Iron
GD: Guangdong Province
GZ: Guangzhou
HK: Hong Kong Special Administrative Zone
HYSPLIT: Hybrid Single-Particle Lagrangian Integrated Trajectory
I or I_o: Light transmittance
K: Potassium
lpm: liters per minute
Mn: Manganese
Na: Sodium
NH_4^+: Ammonium
Ni: Nickel
NO_3^-: Nitrate
NO_x: Nitrogen dioxide (NO_2) plus nitrogen oxide (NO)
OC: Organic carbon
OM: Organic mass
PAHs: Polycyclic aromatic hydrocarbons
Pb: Lead
PCA: Principle Components Analysis
PMF: Positive Matrix Factorization
$PM_{0.1\text{-}1.0}$: Particulate matter with a diameter between 0.1 and 1.0 μm
$PM_{2.5}$: Particulate matter with a diameter of 2.5 μm or less
PM_{10}: Particulate matter with a diameter of 10 μm or less

PRD: Pearl River Delta
PSAP: Particle Soot Absorption Photometer
Rb: Rubidium
RSP: Respirable suspended particulate matter (synonymous with PM_{10})
σ_{ap}: Particulate absorption coefficient
σ_{ext}: Particulate extinction coefficient
σ_{sp}: Particulate scattering coefficient
SEF: Seawater enrichment factor
S: Sulfur
Se: Selenium
Si: Silica
SO_4^{2-}: Sulfate
Sn: Tin
Sr: Strontium
SZ: Shenzhen
TC: Tung Chung
Tl: Thallium
TM: Tap Mun
TSP: Total suspended particulate matter
V: Vanadium
ω: Particulate single-scattering albedo
WSOC: Water-soluble organic carbon
WIOC: Water-insoluble organic carbon
WTP: willingness-to-pay
XRF: X-Ray Fluorescence
ybp: years before present
Zn: Zinc
ZS: Zhongshan

SUMMARY

Atmospheric particulate matter pollution is a challenging environmental concern in both urban and remote locations worldwide. It is intrinsically difficult to control, given numerous anthropogenic and biogenic sources (e.g. fossil fuel combustion, biomass burning, dust, and seaspray) and undergoing atmospheric transport up to thousands of kilometers after production. In urban regions, $PM_{2.5}$ (particles with diameters under 2.5 μm) is of special concern for its ability to penetrate the human lung system and threaten cardiopulmonary health. A second major impact area is climate, with particulate matter altering Earth's radiative balance through scattering and absorbing solar radiation, modifying cloud properties, and reducing surface reflectivity after deposition in snow-covered regions. While atmospheric particulate matter is well-understood in many developed regions of the world, in developing nations and in remote areas it is relatively unexplored. This thesis characterizes atmospheric particulate matter in regions that represent the extreme ends of the spectrum in terms of air pollution – the rapidly-industrializing and heavily populated Pearl River Delta Region of China, the remote and pristine Greenland ice Sheet, and a remote area in the Colorado Rocky Mountains.

In China, fine particles were studied through a year-long field campaign at seven sites surrounding the Pearl River Delta. Fine particulate matter was analyzed for composition, regional variation, and transport. Average fine particulate matter (20 total samples) at the seven locations ranged from 29 μg m^{-3} at an undeveloped island in Hong Kong to 71 μg m^{-3} in urban Guangzhou. Main constituents of $PM_{2.5}$ were organic compounds (24–35% by mass) and sulfate (21–32%). Overall, the analyses presented in this thesis suggest that

regional air quality can be greatly improved by reducing emissions within the Pearl River Delta, with long-distance transport only appearing to significantly impact regional sulfate concentrations. The Guangzhou vicinity, located north of Hong Kong, was found to have a substantial impact on regional $PM_{2.5}$ concentrations, with levels observed to increase by 18-34 $\mu g\ m^{-3}$ at sites immediately downwind of Guangzhou. Local anthropogenic sources appear to be important as well, such as the site-to-site variability in species linked with vehicular traffic (EC) and fuel oil combustion (Ni, V).

On the Greenland Ice Sheet and in the Colorado Rocky Mountains, the carbonaceous fraction (organic and elemental carbon) of particulate matter was studied in the atmosphere and snow pack. Analyses include quantifying particulate chemical and optical properties, assessing atmospheric transport, and evaluating post-depositional processing of carbonaceous species in snow. In the atmosphere above the Greenland Ice Sheet, elemental carbon and the particulate absorption coefficient were detectable and highly correlated throughout the summer of 2006, illustrating the ever-present input of combustion emissions to the atmosphere above the Greenland Ice Sheet. Atmospheric organic carbon was found to be much more water-soluble (81% on average) than at less-remote locations in the Northern Hemisphere, which may be due to either the oxidation of primary organic carbon during transport and/or gas-to-particle formation of secondary organic carbon. In addition, measurement of snow-phase organic and elemental carbon determined that the organic fraction undergoes significant post-depositional degradation, likely due to photochemical processes. Thus, it appears that we must progress with caution towards using organic compounds as tracers in ice core research.

INTRODUCTION

Airborne liquid and solid particles, termed "aerosols" or "particulate matter", are ubiquitous in the lower atmosphere. Associated with urban haze, elevated levels of particulate matter in industrialized regions are a consequence of an increase in combustion of biomass and fossil fuels (e.g. coal, diesel, and gasoline). By-products of in-complete combustion include primary particulate species as well as particle precursors, gas-phase compounds that may eventually condense onto particle surfaces. In addition to particulate matter produced by human activity, natural sources such as wind-blown dust, spontaneous forest fires, and sea spray also contribute to atmospheric concentrations. While many atmospheric contaminants (e.g. ozone, carbon monoxide) consist of only one chemical compound, particulate matter incorporates a wide variety of constituents, including metals, ions, and carbonaceous species.

For populations living in developed regions with high particulate matter concentrations, fine particles (particles with a diameter less than 2.5 μm) are a public health concern, contributing to a higher rate of cardiopulmonary morbidity and mortality (Dockery, et al., 1993; Englert, 2004; Pope III, et al., 2002; Schwartz, et al., 1996). A second major concern is the ability of airborne particles to impact climate through absorption or scattering of solar radiation (Charlson, et al., 1992; Haywood and Shine, 1995; Schwartz, 1996), alteration of cloud properties (Boucher and Lohmann, 1995; Charlson et al., 1992; Haywood and Boucher, 2000; Jones, et al., 1994), and decreasing surface albedo after deposition to snow and ice (Hansen and Nazarenko, 2004; Jacobson, 2004; Roberts and

Jones, 2004). With an atmospheric residence time ranging from days to weeks, particulate matter is not only a local concern but a global one, the generation of pollutants in one region impacting the air quality of another. The combination of spatially varying sources, meteorology, and atmospheric chemistry poses special challenges on our ability to understand and control particulate matter pollution.

In some regions of the world, namely the developed nations, local and regional atmospheric particulate matter is monitored, regulated, and researched with state-of-the-art modeling and measurement techniques. In the United States, for example, fine particulate emissions inventories are in existence, routine government-led ambient monitoring is in place, and thus research is focused mainly on understanding the more elusive details of aerosol science. However, in a number of areas in the world, such as developing nations or remote locations, particulate matter characteristics are poorly known and basic field measurements can provide highly valuable information. This thesis work concerns atmospheric particulate matter at two locations that have not been previously well-studied and are of special interest to the scientific community – the Pearl River Delta Region of China and the Greenland Ice Sheet. An additional location, the Niwot Ridge section of the Colorado Rocky Mountains, was studied as a comparison to the Greenland Ice Sheet.

China has captured global attention for its astonishing rate of industrialization over the past ~30 years. The Pearl River Delta Region, containing the well-known cities of Guangzhou and Hong Kong, is a populous (~46 million citizens) southern section of

China that has been called “the fastest-growing part of the fastest-growing province in the fastest-growing large economy in the world” (Enright and Scott, 2002). Along with blazingly-fast economic growth (16.9 % per year from 1980 to 2000), however, came a palpable degradation in regional air quality. The increase in particulate matter pollution in the Pearl River Delta threatens the health of local citizens and positions the region as an important global source of primary and secondary particulate species. To better understand particulate matter pollution in the Pearl River Delta, a year-long air monitoring campaign took place at seven sites throughout the Pearl River Delta. The results from this study are provided and discussed in the first half of this thesis, including fine particulate composition, estimated source types, and an assessment of local versus regional influence on air quality.

In contrast to rapidly developing China, the Greenland Ice Sheet has virtually no particulate matter emissions and instead is a recipient of pollution transported long distances in the atmosphere. The ice cap’s 3000-meter depth (at its highest elevation) contains a record of the past chemical composition of the atmosphere as well as the climate of the Earth. In terms of this frozen record of history, the carbonaceous fraction (organic and elemental carbon) of particulate matter may potentially serve as historical markers of combustion emissions (biomass burning and fossil fuel combustion) in ice cores. However, currently little is known regarding the ambient levels and deposition of carbonaceous particulate matter to the Greenland Ice Sheet, as well as the chemical stability of carbonaceous species after deposition to the ice cap. In addition, particulate elemental carbon is also of interest as a warming influence in the local atmosphere and

for potentially impacting the reflectivity of the ice sheet. In order to understand the nature of carbonaceous particulate matter in the air and snow on the Greenland Ice Sheet, two summer series of field measurements were conducted at Summit, Greenland, the highest point of the ice cap. Additionally, closely-related measurements were conducted at a remote site in the Colorado Rocky Mountains and are discussed in comparison to the Greenland Ice Sheet.

Structure and Scope of This Work

This thesis covers field measurement and analysis of atmospheric particulate matter in urban and remote environments, characterizing physical and chemical properties of particulate matter and transport in the atmosphere. As described below, this document is split into two parts, with the first part of the thesis describing a large-scale air monitoring study in China and the second half of the thesis focused on particulate matter in the air and snow on the Greenland Ice Sheet.

Part I and **Appendices A-B** cover field measurements and ensuing analysis of fine particulate matter ($PM_{2.5}$) measured in urban China. **Chapter 2**, **"Introduction"**, provides a thorough literature review of air pollution associated with China's rapid development and the limited previous information on particulate matter pollution in the Pearl River Delta Region of China. **Chapter 3, "Methodology"**, covers the year-long set of field measurements that took place and describes the laboratory techniques employed to speciate $PM_{2.5}$. **Chapter 4, "Results and Discussion"**, discusses $PM_{2.5}$ composition and assesses the local vs. regional nature of particulate matter pollution in the Pearl River

Delta Region. **Chapter 5, "Conclusions and Recommendations",** discusses the major findings of the field study and suggests areas of future work.

Part II and **Appendices C-D** discuss measurements of carbonaceous particulate matter at the highest point of the Greenland Ice Sheet (Summit, Greenland) and supporting field work performed at the remote and high-elevation Niwot Ridge, Colorado. **Chapter 6, "Introduction",** provides an in-depth coverage of the properties of the Greenland Ice Sheet, present-day impacts of carbonaceous particulate matter on the ice cap, and issues surrounding the potentially useful ice core record of particulate matter concentrations. **Chapter 7, "Methodology",** describes the field measurements and laboratory analyses performed during two summertime field campaigns to Summit, Greenland and a wintertime field campaign in Niwot Ridge, Colorado. **Chapter 8, "Results",** discusses the concentrations and transport of atmospheric carbonaceous species on the Greenland Ice Sheet and studies the fate of carbonaceous species after deposition to the snow pack. Additionally, supporting measurements of carbonaceous particulate matter in the air and snow at Niwot Ridge, Colorado are discussed. **Chapter 9, "Conclusions and Recommendations",** covers the major discoveries from the field studies and provides ideas for future research.

PART 1: FINE PARTICULATE MATTER IN URBAN CHINA

CHAPTER 2: INTRODUCTION

2.1 Foreword

Part I of this thesis focuses on regional fine particulate matter measurements in the Pearl River Delta region of China and includes an extended version of the following publications:

(1) Hagler, G.S.W., Bergin, M.H., Salmon, L.G., Yu, J.Z., Wan, E.C.H., Zheng, M., Zeng, L.M., Kiang, C.S., Zhang, Y.H., Lau, A.K.H., and Schauer, J.J., 2006. Source areas and chemical composition of fine particulate matter in the Pearl River Delta region of China. *Atmospheric Environment*, 40(20): 3802-3815.

(2) Hagler, G.S.W., Bergin, M.H., Salmon, L.G., Yu, J.Z., Wan, E.C.H., Zheng, M., Zeng, L.M., Kiang, C.S., Zhang, Y.H., and Schauer, J.J., 2007. Local and regional anthropogenic influence on $PM_{2.5}$ elements in Hong Kong, *Atmospheric Environment*, doi:10.1016/j.atmosenv.2007.03.012

2.2 Human Health and Economic Impact of Particulate Matter in China

China's economic development since the end of Mao Zedong's reign has been awe-inducing, with its GDP quadrupling from 1978 to 2000. This rampant growth in economic performance supported significant quality of life improvements for China's 1.3 billion citizens, such as the average life expectancy increasing from 64 to over 70 in a matter of decades (Qian, 2003). However, an unfortunate marker of the nation's economic growth has been a surge in air pollutant emissions from increased coal burning, vehicular traffic, land disturbance, and combustion of biomass. Shown in Figure 1, it can

be seen how China's need for energy more than doubled from 1978 to 1999, with coal as the main fuel type consumed (National Bureau of Statistics, 2000).

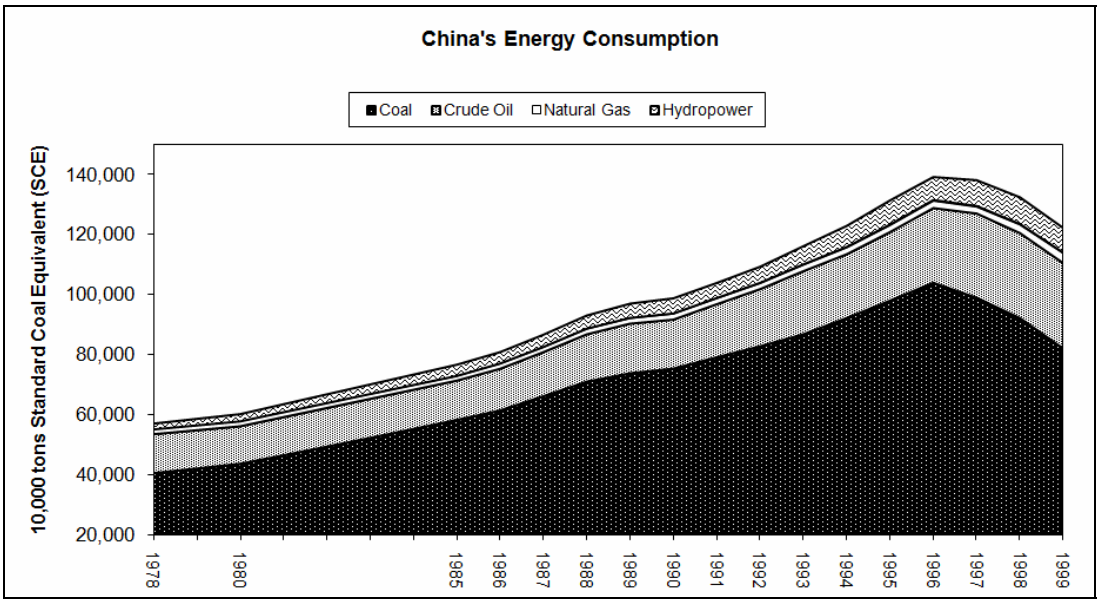

Figure 1. China's energy consumption from 1978 to 1999, with labeled years marking the data points. Data source: China's National Bureau of Statistics, 2000.

Even given the enormous increase in fuel use accounted for by the Chinese government and displayed in Figure 1, a recent study comparing energy statistics with satellite-derived column-NO_x asserted that recently (1996-2002) published coal combustion values may be underestimating the actual fuel consumption (Akimoto et al., 2006). Thus, it can be concluded that the data in recent years shown in Figure 1 may be assumed to be a lower estimate of fuel consumption. China's increased combustion of fossil fuels, without question, has been substantial over the past few decades.

As emitting sources grew in magnitude throughout China, emissions of primary and secondary particulate species have similarly increased. Sulfur dioxide, a precursor of

particulate sulfate and mainly produced by coal combustion, experienced a nation-wide increase from 23.0 Tg in 1990 to 25.2 Tg in 1995, with best-case scenario emissions projected to rise to 30.6 Tg by 2020. Lacking any improvement in emission controls, SO_2 may more than double 1995 levels to 60.7 Tg in 2020 (Streets and Waldhoff, 2000). China has also been reported to be a major global source of particulate organic carbon and black carbon, with emissions estimated at 4.1 Tg and 1.5 Tg, respectively (Cao et al., 2006). Comparing with global emissions estimates in 1984 and assuming the same levels roughly hold for 2000, China would constitute a quarter of global black carbon emissions (Cooke et al., 1999). Not only do China's emissions have potential health and economic impacts on Chinese citizens, they also position China as a significant global source of particulate matter.

Given the rapid degradation in air quality that has accompanied China's growth, much attention has been focused on understanding and quantifying the resulting impacts on Chinese citizens. Several studies in the city of Hong Kong, part of our project focus area, found significant linkages between PM_{10} levels and increased respiratory and cardiac hospital admissions (Wong et al., 2002), as well as significant associations between PM_{10} and respiratory mortality (Wong et al., 2001; Wong et al., 2002). An extensive review of epidemiological studies in China determined that per 1 $\mu g\ m^{-3}$ increase in PM_{10} are an associated 0.03% increase in all-cause mortality and 0.04% increase in cardiovascular deaths (Aunan and Pan, 2004). Also, they report 0.31% and 0.44% increase per PM_{10} $\mu g\ m^{-3}$ in chronic respiratory symptoms and diseases for adults and children, respectively.

The resulting economic impact of particulate pollution has been evaluated in several case studies. In Shanghai, economic loss due to health impacts of PM_{10} was estimated at 1.03% of the city's GDP (Kan and Chen, 2004). In Zaozhuang, a growing Chinese city of 3.5 million and an area of coal mining, regional health costs due to particulate matter (PM_{10} or $PM_{2.5}$) were estimated at up to 10% of the city's GDP (Wang and Mauzerall, 2006). One recent study combined the limited measurements of particulate matter in different areas of China (mainly measured as total suspended particulates (TSP)) to estimate a national economic cost due to particulate pollution. Using a general equilibrium approach, evaluating as a function of both labor loss and changes in consumption patterns (i.e. increased medical expenditures), air pollution was estimated to cause an economic burden of 0.38% of China's GDP. Evaluating the cost using a human capital approach, meaning studying economic cost as the loss of a person's wages due to work days missed from illness or premature death, the economic burden was higher at 1.26% of China's GDP (Wan et al., 2005). This study implies that the individual economic loss of Chinese citizens due to air pollution is greater than the negative impact to China's economic engine. However, despite the apparent greater economic loss felt by the Chinese population, an interesting recent study on willingness-to-pay (WTP) for air quality improvements found a complex response by Chinese citizens. Focused on citizens in Chongqing, a highly industrialized city of 15 million and one of the most polluted in China, the study found that while the overall WTP value ($34,458 per saved statistical life) fit the expected range relative to comparable studies in developed regions, their income elasticity response was quite different. A measure of increased WTP as a function of increased income, the high income elasticity (1.42) found in Chongqing

implies that Chinese citizens may currently consider clean air to be a luxury item reserved for those with greater wealth (Wang and Mullahy, 2006).

On top of the public health and associated economic cost from high levels of particulate matter, several studies in China have observed additional impacts of particulate levels on visibility and agriculture. In the Pearl River Delta region located in southern China, several studies found significant visibility impacts due to particulate pollution in Hong Kong (Lee and Sequeira, 2002; Man and Shih, 2001), with one study commenting on a measured visibility of only 200 m in the neighboring city of Guangzhou during a recent pollution episode (Wu et al., 2005). As shown in Figure 2, the poor visibility and aesthetic impact can be substantial during major episodes. As China sets the stage as the host of major world events, particularly the summer 2008 Olympics, they should expect to face major challenges in providing clean air for their visitors (Streets et al., 2007).

Related to the loss of visibility are the potential negative impacts on agriculture due to deposition of air pollutants to crop soil and a reduction in photosynthetically active radiation (PAR) reaching crops. In the Pearl River Delta Region, one study measured the high deposited levels of chromium (Cr), copper (Cu), lead (Pb), and zinc (Zn) (Wong et al., 2003) and another found agricultural soils in the Pearl River Delta to be enriched with Cu and Pb. The isotopic signature of Pb in the crop soils pointed to industrial and vehicular sources (Wong et al., 2002). Another interesting study assessed the Nanjing, China agricultural area and determined that regional haze may cause substantial decrease (~5-30%) in direct solar radiation reaching crops (Chameides et al., 1999). It is clear that

there are numerous human health and economic costs linked to the atmospheric emissions created by China's burgeoning industry.

Figure 2 A view of Shenzhen, China, located in the Pearl River Delta Region, in September 2002. The top image was taken during a regional haze episode, while the bottom picture is a few days later after rainfall.

2.3 Particulate Matter in the Pearl River Delta Region of China

The Pearl River Delta Region (PRD) of China, including the major cities of Hong Kong (population of 6.8 million), Guangzhou (7.5 million) and Shenzhen (1.8 million), is an area of particular interest for its incredible industrial growth, even relative to the rest of quickly-growing China. Home to a population of 46 million, the PRD encompasses the floodplains region of the Pearl River (Zhujiang) in the southern province of Guangdong as well as the southward mountainous New Territories and island regions of Hong Kong. The physical location of the PRD is shown in Figure 3. With Hong Kong established as a service sector (Cullinane and Cullinane, 2003) and Guangdong province focused on manufacturing and energy production (Warren-Rhodes and Koenig, 2001), the

intertwined economies have proven to be mutually beneficial to all members of the delta, where the regional GDP grew at a rate of ~17% per year from 1980 to 2000 (Cullinane and Cullinane, 2003). Such phenomenal growth, however, has also yielded high concentrations of fine particulate matter ($PM_{2.5}$) in many areas of the PRD, an issue of major concern to local governments and citizens.

Figure 3 Map of southeastern China, with the Pearl River Delta Region of China (PRD) highlighted. Source: www.hktrader.net

Recent measurements of fine particulate matter in Hong Kong and neighboring Guangdong (Cao et al., 2003; Cao et al., 2004; Cohen et al., 2004; Louie et al., 2005; Pathak et al., 2003; Qian et al., 2001; Wei et al., 1999) have confirmed the existence of unhealthy concentrations well-exceeding the current World Health Organization Air Quality Guidelines (AQG) of 10 μg m^{-3} (annual average) and 25 μg m^{-3} (24 hour average) (World Health Organization, 2006). A recent field campaign conducted by Cao et al. (2003, 2004) sampled for $PM_{2.5}$ and carbonaceous species (EC and OC) during the winter and summer of 2002 in four cities of the PRD, finding highest $PM_{2.5}$

concentrations in Guangzhou (106 μg m^{-3}), followed by Shenzhen (61 μg m^{-3}), Zhuhai (59 μg m^{-3}), and Hong Kong (55 μg m^{-3}).

Improving particulate matter pollution in the quickly developing Pearl River Delta is a challenging task, complicated by a mountainous island landscape that can impede pollutant dispersal (Liu et al., 2001) and numerous anthropogenic sources in the densely populated and industrialized region. In order to effectively manage regional air quality, it is essential to know the degree to which pollution is generated locally versus transported in from outside of the region. Previous studies, limited to measurement in the Hong Kong area, provided fine particulate source information through analysis of chemical composition and in combining chemical speciation with local meteorology. Two different studies found spatial differences in organic and elemental carbon levels among different sites in Hong Kong, pointing to the importance of local sources (Ho et al., 2002; Louie et al., 2005). Another field study at site located southwest of Hong Kong Island compared particulate concentrations during wind flow from the ocean versus from inland, and estimated the Pearl River Delta as a whole to contribute a major portion (48-57%) of particulate mass (Cheung et al., 2005). Finally, one study measured $PM_{2.5}$ at three sites in Hong Kong and, using back-trajectory modeling, estimated that long-range transport increased concentrations of particulate sulfate and ammonium by 49-383% and 33-302% (Pathak et al., 2003). These previous studies have shown that a combination of local and regional sources influence air quality in Hong Kong, although it is unclear from the results to what degree pollution is created locally, advected in from other nearby areas in the Pearl River Delta, or from an even further origin.

2.4 Research Objectives

In order to guide regional air quality management, an in-depth study linking regional $PM_{2.5}$ chemical characteristics with influencing factors (sources, source locations, and meteorology) is needed. This thesis presents an overview of a large-scale monitoring study that took place over the time span of October 2002 to June 2003, with simultaneous measurements of $PM_{2.5}$ mass and chemical composition at seven sites in the PRD. The major objectives of this study include the following:

1. Determine $PM_{2.5}$ levels and concentrations throughout the Pearl River Delta, including background and urban locations.
2. Study the impact of meteorology on pollutant patterns throughout the area.
3. Characterize the importance of local versus regional sources on air quality in the Pearl River Delta.
4. Assess the types of sources impacting local air quality.

CHAPTER 3: METHODS

3.1 Field Sampling

Characterization of fine particulate matter in the Pearl River Delta Region of China was performed via field measurements at seven locations throughout Hong Kong Special Administrative Region and Guangdong province. The sites were selected to be representative of the air shed, including sites monitoring regional background air, urban sources, and locations in close proximity to urban areas. In addition to the seven selected monitoring locations for fine particulate matter, local meteorological data was provided at six locations in Hong Kong and Guangdong. Figure 4 shows the locations of the seven monitoring and six meteorological sites. Coordinates and descriptions of the $PM_{2.5}$ monitoring sites are given in Table 1.

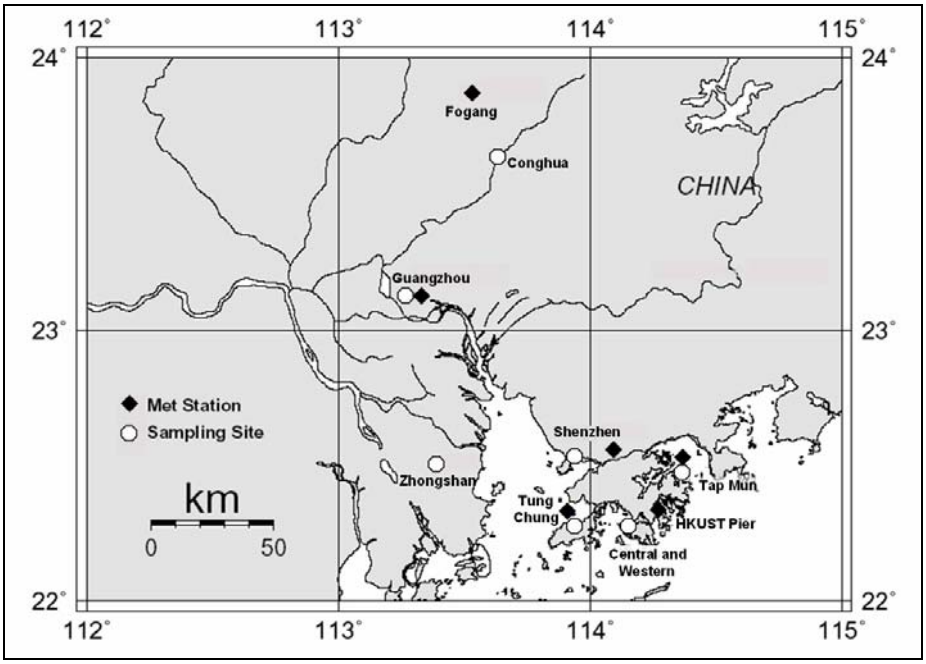

Figure 4. Location of monitoring sites in the PRD study

Table 1. Sampling sites in the Pearl River Delta Region of China

Site	Site Code	Location	Coordinates	Site description
Tap Mun	TM	Hong Kong	Lat: N 22 28.277 Lon: E 114 21.642	Background
Tung Chung	TC	Hong Kong	Lat: N 22 17.324 Lon: E 113 56.620	Downwind of urban source
Central and Western	CW	Hong Kong	Lat: N 22 17.122 Lon: E 114 08.713	Urban source
Shenzhen	SZ	Guangdong	Lat: N 22 32.183 Lon: E 113 56.340	Urban source
Zhongshan	ZS	Guangdong	Lat: N 22 30.660 Lon: E 113 24.429	Downwind of urban source
Guangzhou	GZ	Guangdong	Lat: N 23 07.969 Lon: E 113 15.585	Urban source
Conghua	CH	Guangdong	Lat: N 23 38.530 Lon: E 113 38.345	Background

At the $PM_{2.5}$ monitoring sites, 24-hour filter collections were performed every 6^{th} day in the months October 2002, December 2002, March 2003, and June 2003, yielding a total of 20 sampling days at each monitoring site. The sampling sites of Tap Mun (TM), Tung Chung (TC), Central and Western (CW), Guangzhou (GZ), and Shenzhen (SZ) used ThermoAnderson RAAS $PM_{2.5}$ chemical speciation samplers, while Conghua (CH) and Zhongshan (ZS) used California Institute of Technology Gray Box samplers that served as the original prototype design for the RAAS $PM_{2.5}$ instrument. A schematic of the sampler set-up is shown in Figure 5. Both samplers use cyclone separators to remove particles of diameter greater than 2.5 μm (John and Reischl, 1980), with particles collected downstream on filters in four channels (two 47 mm quartz fiber filters, two 47 mm Teflon filters). Each sampler had two flow lines of 24 L min^{-1}, which included a $PM_{2.5}$ cyclone followed by a manifold splitting each flow line into a quartz filter channel

(16.7 L min^{-1} for RAAS $PM_{2.5}$, 14.0 L min^{-1} for Caltech Gray Box) and a Teflon filter channel (7.3 L min^{-1} for RAAS $PM_{2.5}$, 10.0 L min^{-1} for Caltech Gray Box). Flow rates were controlled by critical orifices located upstream of a vacuum pump and were measured periodically with a calibrated dry gas meter (NIST Traceable-ID #C-0701). Intercomparison sampling performed between co-located Gray Box and ThermoAndersen RAAS samplers demonstrated measurements of $PM_{2.5}$ mass concentration to be within 5% of a reference ThermoAndersen RAAS sampler and thus suitable for joint use in the PRD field measurement campaign. This intercomparison is shown in Figure 6.

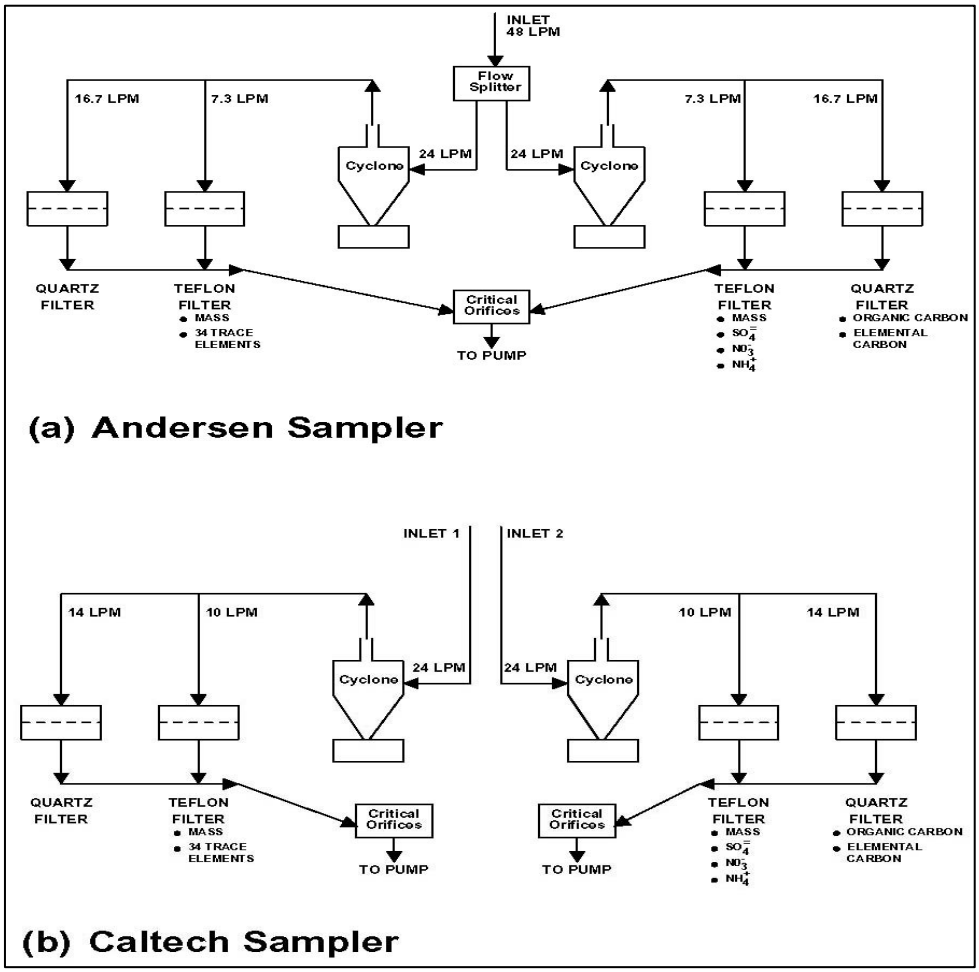

Figure 5. Schematic of $PM_{2.5}$ samplers used in the Pearl River Delta study.

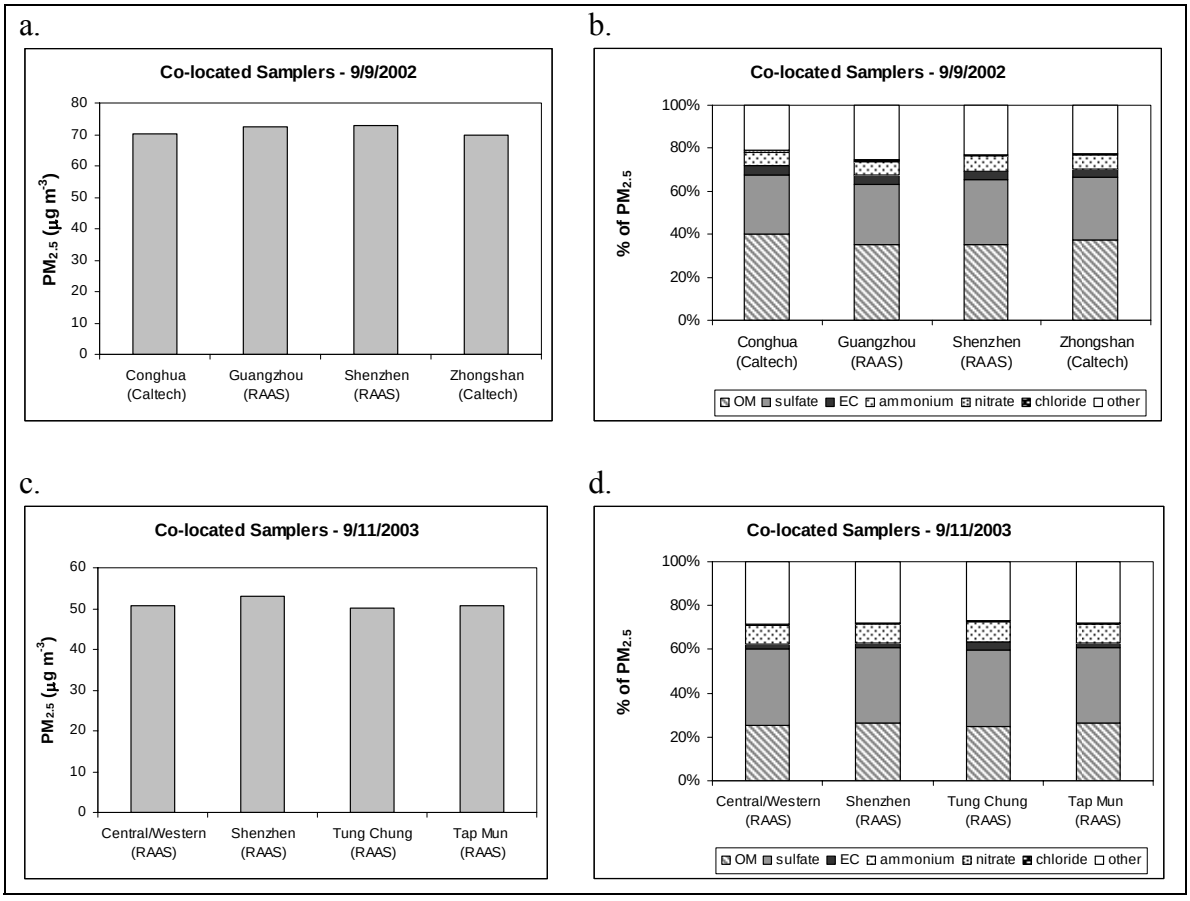

Figure 6. Intercomparison of overall $PM_{2.5}$ concentration (a, c) and speciation of major particulate components (b, d).

Operators at each of the seven sampling sites were carefully trained in filter handling and storage. A copy of the operations manual for the field sampling is included in Appendix A, in English and Chinese. After each sampling period, filter samples were sealed in Petri dishes and stored under freezing temperatures to minimize the loss of volatile species. Samples were later transported in ice-packed coolers to their eventual destinations in Hong Kong and California for mass measurement and chemical analyses. To track any contamination due to handling, four field blanks (one per sampling month) were taken at each site. The blank filters were stored and transported alongside the 24-

hour samples. To ensure the uniformity of sampler operation and filter handling, a field audit took place during October 2002, with audit team members including Peter Louie of the Hong Kong Environmental Protection Department, Sjaak Slanina of the Energy Research Foundation of the Netherlands, Zhang Yuanghang and Zeng Limin from Beijing University, and Gayle Hagler (author) from Georgia Institute of Technology. A sample of the audit checkpoints is provided in Appendix A.

3.2 Chemical Analyses

After sample collection, the Teflon filters were analyzed for $PM_{2.5}$ mass concentration, major ions (sulfate, nitrate, chloride, ammonium), and trace elements. Analysis of the quartz fiber filters included organic carbon (OC), elemental carbon (EC), and speciation of organics. $PM_{2.5}$ mass measurements were conducted via a microbalance (Mettler Instruments) following the guidelines laid out in the EPA Quality Assurance Document 2.12 (EPA, 1998), with repeat measurements performed on all samples to ensure accurate results. Concentrations of sulfate, nitrate, and chloride were determined using ion chromatography, comparing sampled concentrations with laboratory standards prepared from ACS grade analytical reagents. For the measurement of ammonium, indophenol colorimetric analysis was performed using a rapid flow analyzer (RFA-300 TM, Alpkem Corp.) (Bolleter et al., 1961). Specific elements were detected using X-ray fluorescence analysis (XRF), including sulfur (S), potassium (K), silica (Si), zinc (Zn), iron (Fe), sodium (Na), calcium (Ca), lead (Pb), aluminum (Al), manganese (Mn), copper (Cu), vanadium (V), arsenic (As), tin (Sn), bromide (Br), rubidium (Rb), nickel (Ni), selenium (Se), thallium (Tl), chromium (Cr), cobalt (Co), and strontium (Sr) (Watson et al., 1996).

Quartz fiber filters were measured for EC and OC using a carbon analyzer (Sunset Laboratory) following the NIOSH protocol of thermal evolution and combustion (Birch and Cary, 1996). A conversion factor of 1.4 is applied to the measured organic carbon values to estimate overall organic mass (OM). While the OM to OC ratio is not necessarily a constant value in ambient particulate matter, the value of 1.4 has been suggested as an appropriate adjustment factor to reconcile OC values to the original mass of organic compounds (Russell, 2003).

CHAPTER 4: RESULTS AND DISCUSSION

4.1 Concentrations of Major Fine Particulate Species

The average $PM_{2.5}$ concentration throughout the collection period (5 24-hour samples taken in October 2002, December 2002, March 2003, and June 2003) ranged from 37 μg m^{-3} at rural Conghua to 71 μg m^{-3} at urban Guangzhou for the sites in Guangdong province, with a lower range of 29 μg m^{-3} at rural Tap Mun to 34 μg m^{-3} at urban Central/Western in the Hong Kong region. Averages of chemical composition, presented in Table 2, show that fine particulate mass within the Pearl River Delta is dominated by organic compounds (24-35%) and sulfate (21-32%). Other important measured constituents include crustal material (7-13%), ammonium (6-8%), elemental carbon (3-8%), and nitrate (1-6%).

Particulate organic mass (OM), formed by both direct emissions and through gas-to-particle conversion, ranged annually from 6.9 to 9.3 μg m^{-3} at sites in Hong Kong, and from 12.7 to 24.6 μg m^{-3} in Guangdong. As shown in Table 2, annual mean elemental carbon (EC) concentrations were low at background sites Conghua (1.4 μg m^{-3}) and Tap Mun (0.8 μg m^{-3}), compared with a range of 1.9-4.4 μg m^{-3} for the five sites in more developed locations. Annual average OM/EC ratios had maximum values at background sites Conghua (9.0) and Tap Mun (8.4), with lower values of 4.0-5.9 for the remaining areas of the region. Previous studies have also measured the carbonaceous component of $PM_{2.5}$ in Hong Kong and Guangdong, although different OC and EC detection methods

were used and thus the data cannot be directly compared. Measurements in Hong Kong by Louie et al. (2005) throughout both Hong Kong and Guangdong by Cao et al. (2003, 2004) utilized thermal evolution analysis based on laser reflectance (IMPROVE) with a different temperature program than the laser transmittance method (NIOSH) that is used in this study. Chow et al. (2001) verified experimentally that the two methods have similar results for total carbon but variability exists in the division of carbon between EC and OC. Ho et al. (2003) measured EC and OC in Hong Kong using thermal manganese dioxide oxidation (TMO method), which has been found to closely compare to results from the IMPROVE protocol (Fung et al., 2002).

Average particulate sulfate concentrations, generated primarily through the oxidation of emitted gaseous SO_2, had lower values and a smaller range in Hong Kong (9.0-9.3 μg m^{-3}) compared with that in Guangdong (10.0-14.7 μg m^{-3}). The close range in measured sulfate at sites representing both urban and background locations in Hong Kong supports the notion that sulfate has regional and perhaps longer range sources. Our measurements at sites in Hong Kong are similar to those by Louie et al.(2005), who measured average $PM_{2.5}$ sulfate concentrations at three locations in Hong Kong in the range of 8.7-9.4 μg m^{-3} during 2000-2001. In comparing sulfate and ammonium ion concentrations, it is observed that the four-month average ammonium/sulfate molar charge ratio ranges from 0.60-0.85 among the seven sites in the Pearl River Delta. This indicates that the aerosol phase is acidic, with ammonium principally associated with sulfate. A recent emissions inventory by Streets et al. (2003) found agricultural activities to be the main source of

ammonia in China, which is the likely explanation for the higher levels of ammonium at the sites in Guangdong compared with Hong Kong.

Table 2. Concentrations of major fine particulate species

		Mean Concentration ($\mu g/m^3$)[a]																	
Site[b]	N	$PM_{2.5}$		OM[c]		EC		Nitrate		Sulfate		Ammonium		Crustal[d]		Trace[e]		Other	
TM	20	28.7	(13.8)	6.9	(3.9)	0.8	(0.5)	0.5	(0.3)	9.2	(4.7)	2.3	(1.2)	2.3	(1.7)	0.9	(0.4)	5.9	(4.5)
TC	20	32.5	(14.8)	8.8	(4.7)	2.0	(1.0)	0.8	(0.8)	9.0	(5.1)	2.5	(1.3)	2.2	(1.6)	1.0	(0.4)	6.1	(5.1)
CW	20	34.3	(14.1)	9.3	(4.3)	1.9	(1.0)	1.0	(0.7)	9.3	(4.5)	2.5	(1.2)	2.4	(1.6)	1.0	(0.3)	7.0	(4.5)
SZ	21	47.1	(21.3)	15.6	(7.9)	3.9	(2.3)	2.3	(1.8)	10.0	(5.3)	3.2	(1.6)	4.1	(2.3)	1.6	(0.9)	6.6	(5.1)
ZS	19	46.5	(23.0)	14.7	(9.1)	2.5	(1.2)	1.8	(1.8)	11.9	(5.7)	3.3	(1.6)	4.5	(3.5)	1.4	(0.9)	6.4	(6.1)
GZ	20	70.6	(30.2)	24.6	(11.6)	4.4	(1.8)	4.0	(3.7)	14.7	(6.1)	4.5	(2.2)	6.6	(3.1)	2.5	(1.3)	9.3	(7.1)
CH	19	36.8	(18.5)	12.7	(6.3)	1.4	(0.5)	0.3	(0.2)	10.4	(5.4)	2.4	(1.2)	4.6	(2.3)	1.4	(0.5)	3.7	(3.6)

[a] Values in parentheses represent standard deviation
[b] Site labels are as follows: Tap Mun (TM), Tung Chung (TC), Central/Western (CW), Shenzhen (SZ), Zhongshan (ZS), Guangzhou (GZ), and Conghua (CH)
[c] OM (organic mass) is calculated by multiplying the measured organic carbon by 1.4
[d] Crustal is the sum of the common oxides of Si, Al, Fe, Ti, Mn, Ca, and K, and uses a factor of 1.17 to include carbonate and the water of hydration.
[e] Trace species include elements determined from XRF analysis not included in "crustal", converted to their oxide forms where appropriate.

4.2 Enrichment Factors and Concentrations of Fine Particulate Elements

With the main aim of this analysis to determine sources and locations of sources affecting $PM_{2.5}$ in Hong Kong, crustal (EF) and seawater (SEF) enrichment factors provide the ability to determine which elements may be mainly of crustal or oceanic origin. EFs and SEFs were calculated relative to the average elemental composition of Earth's crust and ocean water (Weast, 1987). The crustal enrichment is calculated as follows: $EF = (X_i/Al)_{sample}/ (X_i/Al)_{crust}$, where X_i is a given element concentration and aluminum (Al) is assumed to be entirely from Earth's crust. Similarly, SEF is calculated as: $SEF = (X_i/Na)_{sample}/ (X_i/Na)_{ocean}$, where sodium (Na) is likewise assumed to solely originate from seaspray. Given that the Pearl River Delta is located near the ocean and has no local volcanic activity, elements highly enriched relative to both crustal and oceanic

sources are most likely generated by anthropogenic activity. However, it is also possible that human activity in land development may contribute to elements of apparent crustal origin (low EF). Shown in Figure 7, low enrichment factors (EF < 5.0) are found for Si, Ca, Sr, and Fe indicating that fine particulate levels of these species are most likely dominated by crustal material. In contrast, all other species are seen to be impacted by non-crustal sources, with very high enrichment (EF > 1000) observed for elements Zn, Tl, Br, Sn, As, S, Pb, and Se. In addition to the general grouping of elements by enrichment factor, the relative range of enrichment factors among the monitoring sites gives clues to the possible presence of sources. Among the highly enriched species, Cr, Ni, and As are seen to have high outliers occur at certain monitoring sites. Chromium and Ni both have significantly high enrichment factors at Zhongshan, with Shenzhen also highly enriched in Ni. Guangzhou stands out for highest enrichment in many species, with a particularly high As-enrichment in comparison with other sites in the area.

The influence of the surrounding ocean was similarly estimated by comparing the ratio of measured elements to measured Na with their associated seawater ratio. As displayed in Figure 8, the only species with a low seawater enrichment factor (SEF) at all sites is Cl (four-month average SEF = 0.1-0.9), with below-unity values expected as a chloride depletion reaction with nitrate is known to occur (Ho et al., 2003; Lee et al., 1999), the loss mechanism also making it difficult to determine from only its enrichment level whether the species is solely originated from the ocean. It is also of note that bromide is seen to have low enrichment at sites in Hong Kong (SEF = 1.6-2.6), though higher enrichment is observed at sites in Guangdong (SEF = 5.4-14.7), indicating a combination

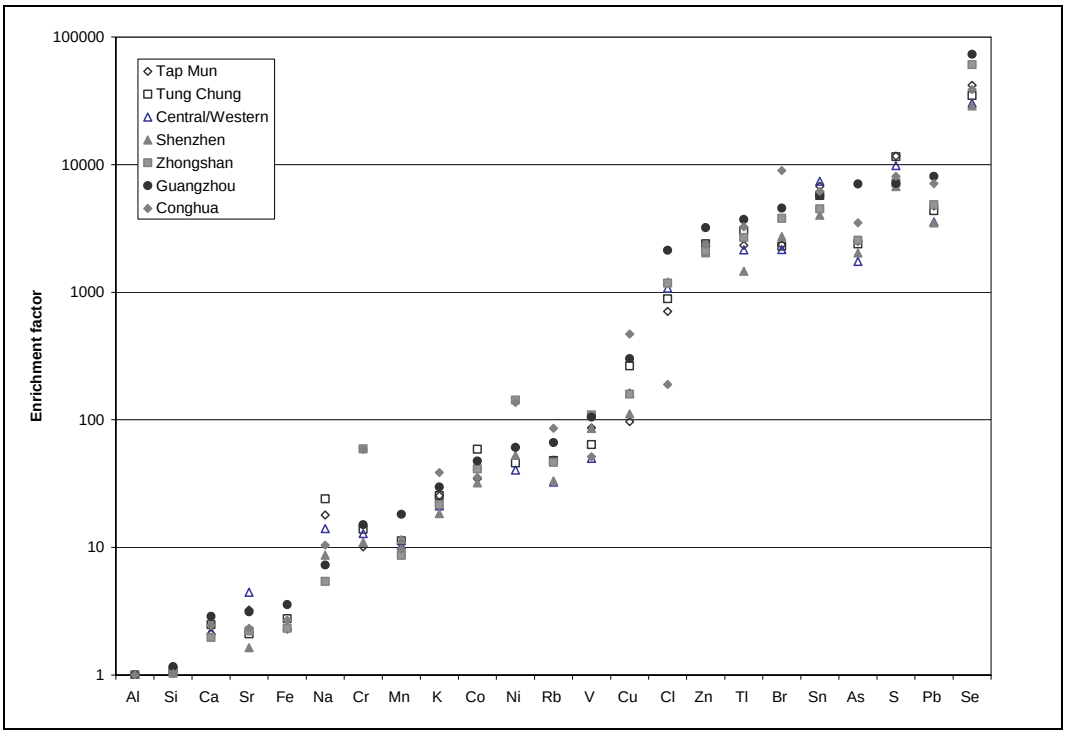

Figure 7. Four-month average crustal enrichment factors of elements at seven sites in the Pearl River Delta Region of China.

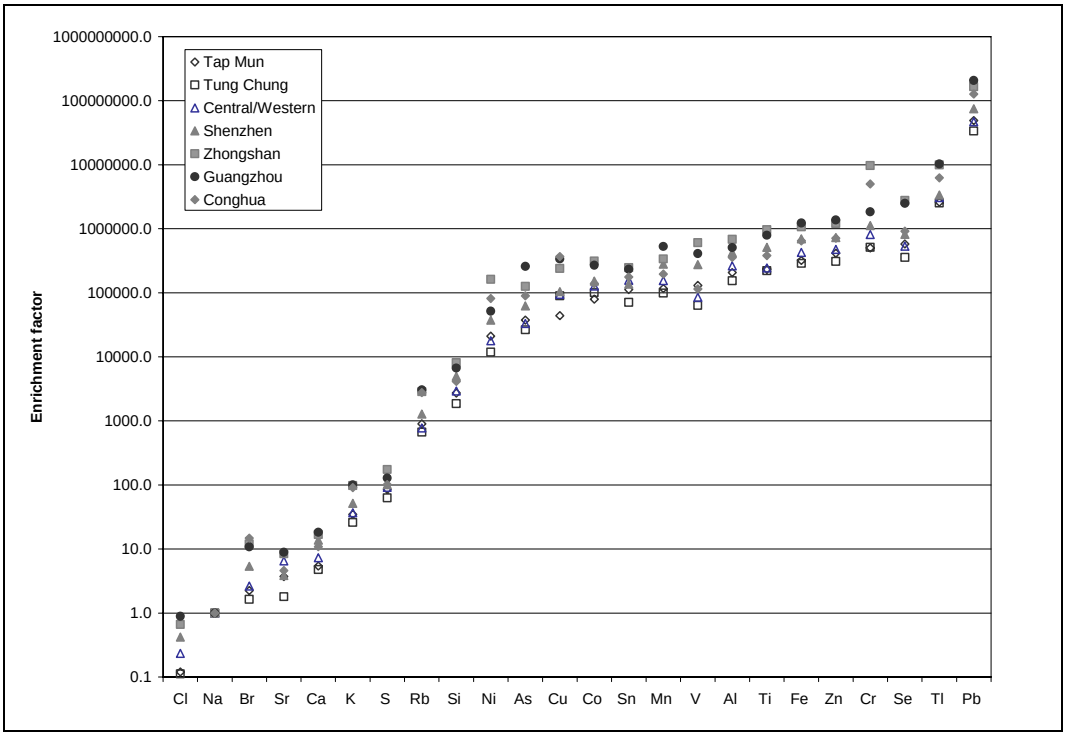

Figure 8. Four-month average seawater enrichment factors of elements at seven sites in the Pearl River Delta Region of China.

of oceanic and anthropogenic sources of bromide in the region. It is interesting that the Guangdong rural site, Conghua, has significantly higher bromide enrichment than elsewhere in the region. Potassium (K) and sulfur (S) are two species that are often used to indicate biomass burning and coal combustion, respectively, though they may each also have an oceanic component (Watson et al., 2001). In the Pearl River Delta, the high SEF values of K (26-100) and S (63-174) demonstrate that the ocean plays a minor role in the measured particulate levels of these species.

While the enrichment coefficient may indicate natural (oceanic and crustal sources) versus anthropogenic sources, a spatial difference in concentrations of certain species can point to potential locations of sources. The average element concentrations over the entire measurement period (October 2002, December 2002, March 2003, and June 2003) are summarized in Table 3. With the exception of three elements (As, Co, and Sr), average element concentrations at the remote site Tap Mun are seen to well-exceed their associated analytical uncertainty (raw data provided in Appendix B). Given the higher uncertainty for As, Co, and Sr, the results presented for these two species should be considered tentative. The average levels recorded in this study are similar to values measured by past researchers at comparable sites (urban and rural) within Hong Kong (Cohen et al., 2004; Ho et al., 2003; Louie et al., 2005) and in the city of Guangzhou (Wei et al., 1999). It is immediately striking to note that, with the exception of sodium, each measured element is highest at a Guangdong site and most frequently at urban Guangzhou. In fact, Guangzhou stands out as a significant industrial source area with average levels more than 30% higher than any other site for highly enriched (EF > 1000)

Zn, Tl, As, Pb, and Se. It is also interesting to note that species exhibiting crustal characteristics (EF < 5) are also seen to have significantly higher levels in Guangdong province compared with Hong Kong, indicating that human activity in Guangdong province may be increasing crustal material concentrations in the Pearl River Delta.

Among the Hong Kong sites, a difference in concentration between remote Tap Mun and more developed Central/Western and Tung Chung may point to the influence of local human activity on Hong Kong's air quality. For the majority of the species, the three sites are observed to be within close range of one another. However, a difference in concentration exceeding 50% is observed among the three sites for eight species (EC, Cl, V, Cr, Co, Cu, Sr, and Sn), pointing to local emissions. Vehicular emissions may be linked to a local spatial difference in EC (diesel exhaust) and Cu (brake wear) (Lough et al., 2005). A second possible source of Cu in the Hong Kong area is local printed circuit board manufacturing (Qin et al., 1997), although this source may have since re-located to other areas in the Pearl River Delta. While spatial variability in Hong Kong is commonly seen with elevated concentrations in urban areas, it is of note that both Ni and V are, on average, at increased levels (32% and 43% higher, respectively) at the remote Tap Mun island compared with the more developed sites in Hong Kong. The presence of V and Ni in the Hong Kong area has been previously related to fuel oil combustion (Lee et al., 1999) and thus the concentrations observed at Tap Mun may be linked to local shipping activity.

Table 3. Elemental Composition of $PM_{2.5}$ ($\mu g\ m^{-3}$)

	Tap Mun			Tung Chung			Central/Western			Shenzhen			Zhongshan			Guangzhou			Conghua		
Species	**N**	**Avg**	**CV[a]**	**N**	**Avg**	**CV**	**N**	**Avg**	**CV**	**N**	**Avg**	**CV**	**N**	**Avg**	**CV**	**N**	**Avg**	**CV**	**N**	**Avg**	**CV**
S	20	3.2E+00	0.55	20	3.1E+00	0.60	20	3.2E+00	0.51	21	3.5E+00	0.52	19	4.3E+00	0.47	20	4.9E+00	0.42	19	3.9E+00	0.50
K	20	5.7E-01	0.75	20	5.6E-01	0.73	20	5.6E-01	0.75	21	8.6E-01	0.63	19	1.0E+00	0.98	20	1.7E+00	0.53	19	1.5E+00	0.55
Na	17	4.5E-01	0.71	15	5.9E-01	0.54	19	4.2E-01	0.49	20	5.5E-01	0.89	17	2.9E-01	0.51	20	4.3E-01	0.67	17	4.5E-01	0.63
Si	20	3.5E-01	0.81	20	3.1E-01	0.79	20	3.5E-01	0.75	21	6.1E-01	0.57	19	6.8E-01	0.72	20	8.8E-01	0.48	19	5.3E-01	0.56
Zn	20	1.8E-01	0.81	20	1.7E-01	0.83	20	1.9E-01	0.64	21	3.1E-01	0.66	19	3.3E-01	0.84	20	6.1E-01	0.53	19	3.1E-01	0.68
Fe	20	1.4E-01	0.75	20	1.6E-01	0.68	20	1.7E-01	0.59	21	2.9E-01	0.48	19	3.0E-01	0.65	20	5.3E-01	0.75	19	2.8E-01	0.60
Cl	20	9.3E-02	0.84	20	1.1E-01	0.77	20	1.2E-01	0.67	21	2.3E-01	0.74	19	1.9E-01	0.94	20	3.2E-01	0.51	19	1.9E-01	0.54
Ca	20	8.9E-02	0.73	20	8.7E-02	0.88	20	1.1E-01	0.74	21	1.7E-01	0.61	19	1.9E-01	0.71	20	2.3E-01	0.63	19	1.5E-01	0.58
Al	19	6.3E-02	0.77	20	5.7E-02	0.82	19	5.6E-02	0.71	21	1.0E-01	0.77	19	1.4E-01	0.87	20	2.7E-01	0.43	19	1.6E-01	0.60
Pb	17	1.5E-02	1.08	16	1.2E-02	0.62	17	1.9E-02	0.59	19	1.6E-02	0.63	16	2.0E-02	0.58	19	3.0E-02	0.61	19	2.3E-02	0.82
Sn	20	1.1E-02	0.86	20	7.2E-03	0.81	20	6.8E-03	1.20	21	2.1E-02	0.67	19	3.4E-02	0.63	20	3.6E-02	0.66	19	9.8E-03	1.12
V	14	1.0E-02	0.98	13	1.2E-02	0.74	11	9.8E-03	0.78	19	2.3E-02	0.62	16	2.7E-02	0.82	19	3.2E-02	0.60	17	1.6E-02	1.11
Mn	20	1.0E-02	0.69	20	1.1E-02	0.65	20	1.2E-02	0.56	21	2.5E-02	0.51	19	1.9E-02	0.64	20	4.4E-02	1.15	19	1.7E-02	0.68
Br	20	6.3E-03	0.73	20	6.0E-03	0.61	20	6.8E-03	0.64	21	1.8E-02	1.02	19	2.2E-02	0.89	20	2.8E-02	0.97	18	4.3E-02	1.36
Cu	19	5.7E-03	0.71	20	1.5E-02	0.30	20	1.1E-02	0.49	21	1.4E-02	0.62	19	2.0E-02	0.74	20	4.3E-02	0.55	19	4.9E-02	1.06
Ni	20	4.9E-03	0.59	20	3.6E-03	0.77	20	3.8E-03	0.61	21	8.2E-03	0.55	19	2.4E-02	0.98	20	1.2E-02	0.63	19	2.0E-02	0.48
As	17	4.8E-03	0.66	17	4.5E-03	0.71	17	4.0E-03	0.82	19	8.7E-03	0.67	18	1.0E-02	0.80	20	3.4E-02	0.43	19	1.2E-02	0.75
Rb	19	4.7E-03	0.74	18	4.5E-03	0.71	20	3.7E-03	0.79	21	6.9E-03	0.73	19	9.5E-03	1.10	20	1.6E-02	0.58	19	1.4E-02	0.60
Se	18	2.2E-03	0.60	19	1.8E-03	0.71	20	1.9E-03	0.69	20	3.3E-03	0.67	18	6.9E-03	0.84	20	1.1E-02	0.92	19	3.6E-03	0.60
Sr	14	1.3E-03	0.58	16	8.2E-04	0.75	16	2.1E-03	1.43	20	1.2E-03	0.67	18	1.9E-03	0.70	16	3.1E-03	0.53	18	1.6E-03	0.93
Tl	18	1.1E-03	1.05	17	1.4E-03	0.47	15	1.2E-03	0.80	16	1.6E-03	0.81	18	2.8E-03	0.83	19	4.6E-03	0.48	18	2.8E-03	0.71
Cr	16	1.1E-03	0.62	14	1.4E-03	0.50	16	1.6E-03	0.63	19	2.6E-03	0.89	19	1.3E-02	1.43	18	3.9E-03	0.63	19	1.2E-02	0.61
Co	20	9.3E-04	0.53	20	1.5E-03	0.61	20	1.4E-03	0.56	20	1.9E-03	0.77	19	2.3E-03	0.75	20	3.1E-03	0.71	19	1.7E-03	0.70

[a]Coefficient of variation

4.3 Meteorology Case Studies

In order to provide insight into source area locations as well as meteorological influences (i.e. wind speed and precipitation) on fine particulate concentrations, daily surface wind patterns are compared with concentrations of fine particulate species at the seven sites in the Pearl River Delta. In the four months of sampling, three unique meteorological cases were identified which can be summarized as follows: (1) "Southerly Flow" characterized by low to moderate winds from the South; (2) "Northerly Flow" having moderate to strong winds from the North, and (3) "Mixed Flow" associated with weak winds (wind speed < 3 m/s) shifting in direction throughout the day. Table 4 lists the 13 sampling days (of 20 total) categorized into each meteorological case, with the remaining 7 days excluded for not clearly fitting into one of the three identified categories or for inconsistency in wind measurements among monitoring sites. Measured hourly wind speed, wind direction, and daily precipitation for each categorized day are shown in Figure 9. Though some variability exists among the meteorology sites, the presented measurements at the Shenzhen meteorology station (Lat: 22.5500, Long: 114.1000) represent general observed trends in wind and precipitation at the five other meteorological sites shown in Figure 4. The full set of observed hourly wind speed, wind direction, and daily precipitation for all sampling days and at all meteorological stations is available in Appendix B. It should be noted that surface wind measurements do not necessarily represent large-scale flow patterns, as local topography can affect surface measurements. However, the selected meteorological sites in the Pearl River Delta are strategically placed to represent regional rather than local winds.

Table 4. Sampling days categorized into Southerly, Northerly, or Mixed Flow

Meteorological Cases		
Southerly Flow	***Northerly Flow***	***Mixed Flow***
2002.10.20	2002.10.08	2002.10.14
2003.06.05	2002.12.13	2002.12.19
2003.06.23	2002.12.25	2003.03.13
2003.06.29	2003.03.07	2003.03.25
		2003.06.17

To relate upwind source regions with downwind concentrations of fine particulate matter, specific species linked with sources are examined for each meteorological category, including sulfate (coal combustion), organic compounds (combustion of fossil fuels, biomass burning, industrial sources, local cooking), elemental carbon (poor coal combustion, fuel oil combustion, combustion of diesel gasoline), potassium (biomass burning), and lead (combustion of leaded gasoline, industrial sources). In order to compare the grouped series of days, each daily measured species is normalized by the concentration of the identical species on the same day at the Guangzhou site and then the relative concentrations of the grouped days are averaged. Guangzhou was selected as a reference site because it is centrally located, has the highest average fine particulate matter concentration among the seven monitoring sites, and is hypothesized to be a major source area contributing to downwind concentrations. The normalization lessens any bias due to precipitation events and seasonally-changing source strengths, such as the variability of biomass burning events throughout the year. Assuming that source locations are remaining constant, the normalization allows a clear view into impacts of wind patterns on relative concentrations among the seven sites.

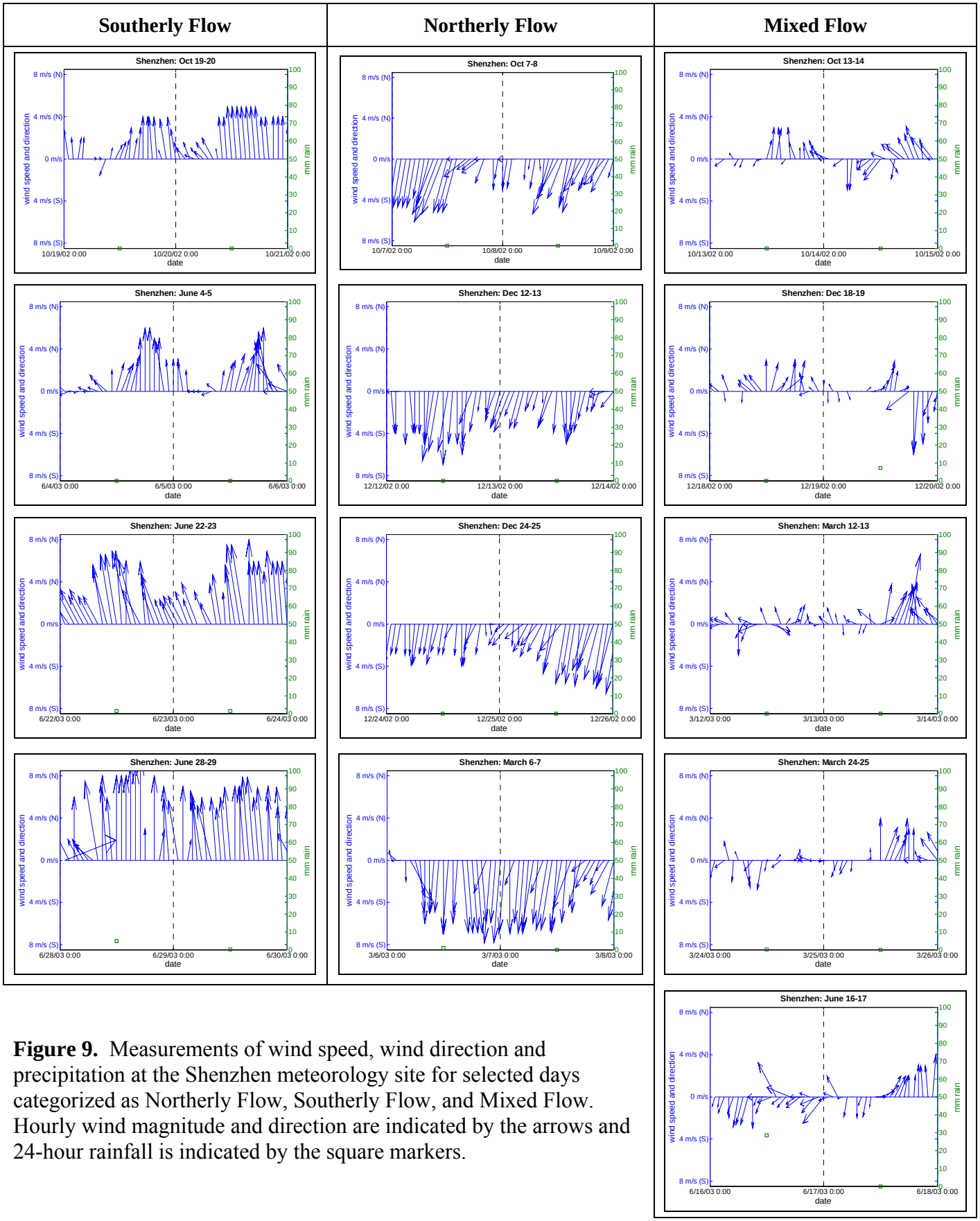

Figure 9. Measurements of wind speed, wind direction and precipitation at the Shenzhen meteorology site for selected days categorized as Northerly Flow, Southerly Flow, and Mixed Flow. Hourly wind magnitude and direction are indicated by the arrows and 24-hour rainfall is indicated by the square markers.

Shown in Figure 10, the average relative concentration and standard error of the selected species at each site are categorized into Southerly Flow, Northerly Flow, and Mixed Flow. Also, non-normalized average concentrations for each meteorological case are shown in Table 5, though it should be noted that looking at a single site's change between meteorological cases may be biased by an uneven distribution of precipitation events within each category.

Table 5. Average concentrations of measured species during Southerly Flow, Northerly Flow, and Mixed Flow

		Average Concentration in mg m^{-3}					
	Site	$PM_{2.5}$	Sulfate	OM	EC	Potassium	Lead
Southerly Flow	Tap Mun	18.0	6.0	3.3	0.30	0.194	0.013
	Tung Chung	22.1	6.8	3.4	0.65	0.235	0.016
	Central/Western	21.9	6.8	3.8	0.78	0.232	0.015
	Shenzhen	25.4	6.6	5.8	1.51	0.321	0.018
	Zhongshan	21.7	7.1	4.4	1.29	0.249	0.018
	Guangzhou	47.0	11.4	14.7	3.15	0.937	0.228
	Conghua	39.9	12.4	13.0	1.44	1.617	0.119
Northerly Flow	Tap Mun	32.8	9.2	10.0	1.29	1.025	0.099
	Tung Chung	39.5	9.2	13.5	2.72	1.102	0.117
	Central/Western	36.4	8.5	12.3	2.29	0.963	0.089
	Shenzhen	52.4	10.2	19.4	4.00	1.337	0.164
	Zhongshan	60.6	13.3	23.8	3.33	2.443	0.308
	Guangzhou	44.2	9.9	16.4	3.89	1.250	0.163
	Conghua	26.5	7.8	9.3	1.03	0.848	0.101
Mixed Flow	Tap Mun	38.9	12.3	8.5	0.94	0.592	0.071
	Tung Chung	38.5	11.6	10.3	2.11	0.529	0.051
	Central/Western	43.4	12.0	11.1	1.93	0.537	0.061
	Shenzhen	53.2	10.9	16.7	4.13	0.747	0.083
	Zhongshan	62.1	15.7	19.7	3.18	0.966	0.132
	Guangzhou	107.1	21.4	35.7	5.89	2.763	0.392
	Conghua	46.3	11.8	16.5	1.59	1.979	0.257

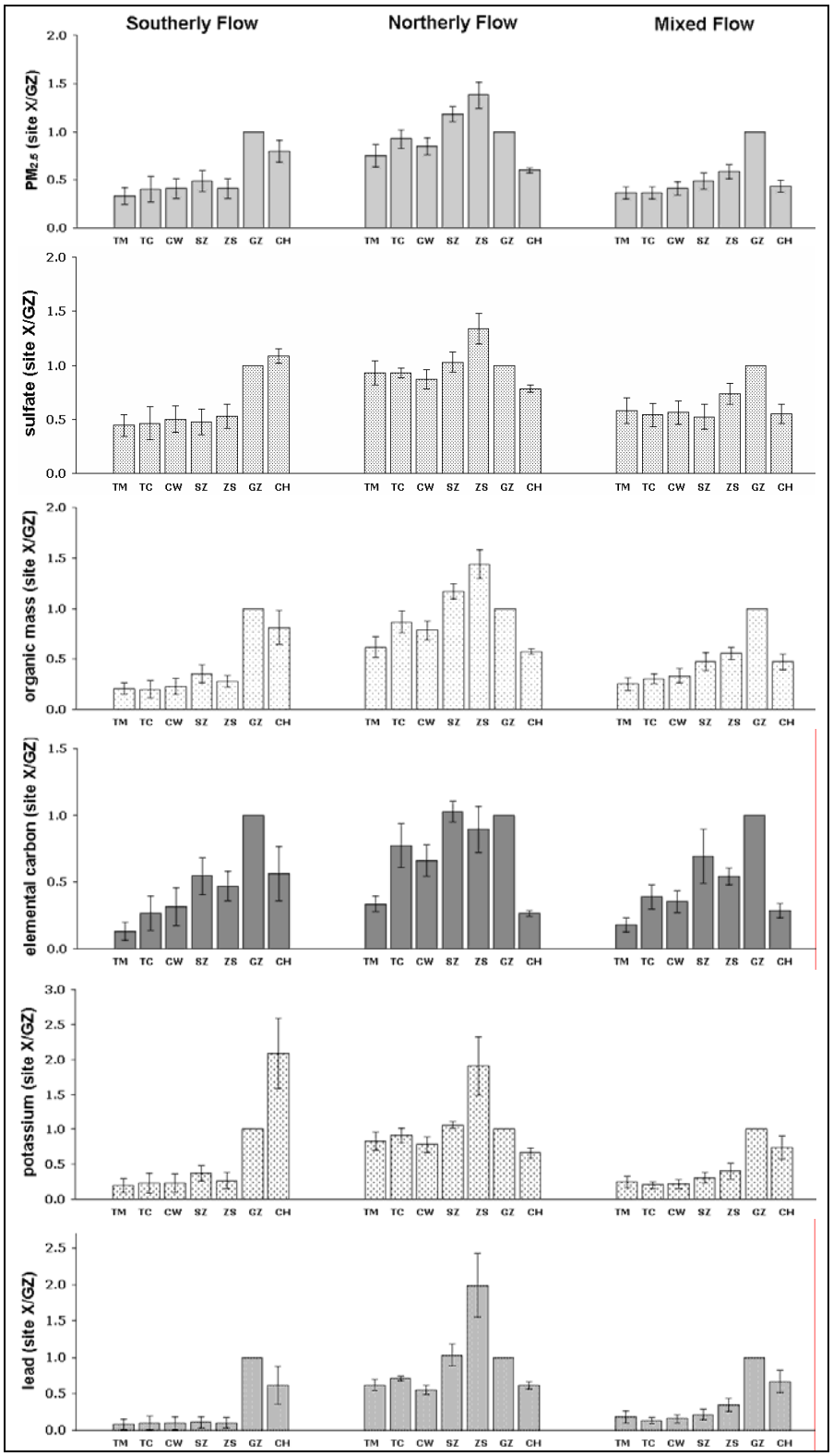

Figure 10. Normalized concentrations and standard error of species measured at seven sites in the Pearl River Delta, categorized by wind pattern. Site labels are as follows: Tap Mun (TM), Tung Chung (TC), Central/Western (CW), Shenzhen (SZ), Zhongshan (ZS). Guangzhou (GZ), and Conghua (CH).

4.3.1 Southerly Flow

Relative concentrations of $PM_{2.5}$ and specific chemical species for southerly flow conditions can be seen in the leftmost column of graphs in Figure 10. Average values for each of the flow conditions are given in Table 5. During days with southerly winds transporting air masses northward from the ocean, a large difference is seen between $PM_{2.5}$ average concentrations at the southernmost five sites (Tap Mun, Tung Chung, and Central/Western in Hong Kong; Shenzhen and Zhongshan in Guangdong) and the northern two (Guangzhou and Conghua in Guangdong). As shown in Table 5, mean values from the southern five sites range from 18-25 $\mu g\ m^{-3}$, as compared to 47 $\mu g\ m^{-3}$ measured at the more northerly urban Guangzhou site. The mean $PM_{2.5}$ concentration at the northern background site in Conghua is 40 $\mu g\ m^{-3}$, nearly twice as high as the sites south of Guangzhou. It is apparent that a source area must be located near Guangzhou to cause the observed accumulation of fine particulate mass over a relatively short distance. Comparing rural Conghua located north of Guangzhou with the Zhongshan site placed south of Guangzhou, an 18 $\mu g\ m^{-3}$ increase representing a near doubling of downwind $PM_{2.5}$ is observed and can be attributed to sources located in the region between the two sites, including the city of Guangzhou. In addition to the contribution to downwind $PM_{2.5}$ by the Guangzhou area, it should be noted that the levels at the upwind background site of Tap Mun (18 $\mu g\ m^{-3}$) indicate significant region-wide background $PM_{2.5}$. To investigate further the origin of the particulate matter, 24 hour back-trajectory modeling was performed on the four days of southerly flow, using the Hybrid Single-Particle Lagrangian Integrated Trajectory (HYSPLIT) model (Draxler and Rolph, 2003) with NCEP/GDAS FNL reanalysis meteorological data. Figures of these model runs are

displayed in Appendix B. Modeled trajectories were calculated for the two background sites, Tap Mun and Conghua, at elevations of 100, 500, and 1500 m. Although the rugged terrain of the region imparts uncertainty to meteorological modeling, the HYSPLIT model did confirm that the four southerly flow days had air parcels transported inland from the ocean area to the South. This implies that southerly flow fine particulate levels at rural Tap Mun may be due to long-range transport. Local shipping emissions may also affect overall levels at Tap Mun, but the relative influence of this source requires further investigation.

Sulfate is a dominant component of fine particulate matter in the PRD, on average contributing 21-32% of overall mass, as shown in Table 2. The relative concentrations of sulfate during southerly wind are highest at the Guangdong background site at Conghua (1.09), shown in Figure 10. As with overall $PM_{2.5}$, relative values of sulfate at the southern five sites are about half that measured in Conghua and are within a close range of one another (0.44-0.53), with absolute concentrations of 6.0-7.1 $\mu g\ m^{-3}$. It is apparent that a source of sulfate lies in the Guangzhou vicinity, leading to a doubling of concentrations from sites south of Guangzhou to northernmost Conghua. However, though levels of sulfate at the southern sites are far less than northern areas, the sulfate concentrations at the southernmost five sites are still substantial. With sulfate levels at remote Tap Mun similar to that at urban Shenzhen, it is expected that sulfate has regional background levels during southerly flow that results in approximately half of the Pearl River Delta's sulfate mass. This background sulfate may be due to long-distance transport from outside of the Pearl River Delta region.

Both primary and secondary in origin, relative concentrations of organic compounds at Conghua are more than double values measured at the southern five sites during southerly wind patterns, as shown in Figure 10. The change between the southern five sites and Guangzhou is even more extreme, with a near tripling of relative concentrations. Comparing the Southerly Flow distributions of OM and sulfate, a higher range of OM concentrations is observed among the southernmost five sites (3.3–5.8 $\mu g\ m^{-3}$), with mean normalized concentrations also showing a wider range (0.20-0.35). Some localized influence on OM is thus predicted in the Hong Kong vicinity, with a tripling of OM concentrations in Guangzhou attributed to both transport of precursors from the South and locally emitted organic species in the Guangzhou area. The relatively high OM concentrations observed in Guangzhou are perhaps not surprising given the size of the city and intense traffic congestion.

Elemental carbon during Southerly Flow has a unique pattern compared with $PM_{2.5}$, sulfate, and OM. Among the southern five sites, background Tap Mun has a low relative concentration of 0.13 while more developed sites at Shenzhen and Zhongshan are nearly three-fold higher with relative concentrations of 0.55 and 0.47, respectively. With normalized concentrations at the Hong Kong sites of Tung Chung and Central/Western more than doubling background Tap Mun and even higher increases at urban sites within Guangdong, local sources appear to strongly affect EC levels throughout the delta. Though EC concentrations seem to be mainly dominated by local sources, some impact of transport is apparent with high relative levels observed at Conghua (0.56), located downwind of Guangzhou. As with OM, the relatively high EC concentration in urban

Guangzhou strongly suggests the importance of local sources on particulate matter concentrations.

As shown in Figure 10, the Southerly Flow case for potassium shows extraordinarily high relative concentrations at rural site Conghua, more than doubling urban Guangzhou and higher than sites south of Guangzhou by a factor of five. A tracer for biomass burning, the significant increases moving northward throughout the delta lead to the conclusion that biomass burning sources are distributed within the northern section of the monitoring area, near Guangzhou and north of the city toward Conghua. Comparatively low measured potassium at sites south of Guangzhou points to a lack of biomass burning in close proximity to Hong Kong and southern Guangdong.

Of all observed species, lead appears to be the most heavily dominated by sources in Guangdong, with homogeneously low relative concentrations south of Guangzhou (ranging from .09-.11) and levels at Guangzhou and Conghua higher by more than six-fold. Shown in Figure 10, the sudden jump in lead levels moving from sites Zhongshan and Shenzhen to nearby Guangzhou indicates a localized source area of lead within the vicinity of Guangzhou and perhaps north of the city. Assuming no local production of lead near Conghua, the high lead concentrations at Conghua appear to be caused by transport from upwind Guangzhou.

4.3.2 Northerly Flow

As seen in Figure 10, Northerly Flow relative levels of $PM_{2.5}$ at sites south of Guangzhou more than double that observed during Southerly Flow, while normalized concentration at northernmost Conghua decreases by 0.2. A spatial gradient is seen among sites downwind of Guangzhou, with highest relative concentrations at Zhongshan (1.4) and Shenzhen (1.2) and lower levels in the Hong Kong area (0.75-0.93). Comparing upwind Conghua and downwind Zhongshan, an increase of 34 $\mu g\ m^{-3}$ can be linked to the Guangzhou region located in-between the two sites. With an attenuation of impact related to distance from Guangzhou, the increase in concentration at the background site of Tap Mun relative to Conghua is 6.3 $\mu g\ m^{-3}$. Overall, the doubling increase in relative concentrations at the three sites in Hong Kong as compared to Southerly Flow conditions points to the significant impact of the Guangzhou area on levels of fine particulate matter in Hong Kong. In addition to increases observed downwind of Guangzhou, Northerly Flow $PM_{2.5}$ measured upwind at rural Conghua is significantly high (~27 $\mu g\ m^{-3}$), indicating a regional background concentration that may be due to long-range transport from northern areas.

Similar to the reversal observed in $PM_{2.5}$ concentrations when comparing cases of Northerly Flow and Southerly Flow, particulate sulfate levels likewise increase at sites downwind of Guangzhou and decrease at Conghua, located upwind of Guangzhou. As observed in Figure 10, Zhongshan receives the heaviest dose of sulfate, with concentrations relative to Guangzhou at 1.34 compared with 0.53 under Southerly Flow. Conghua now has lowest relative concentrations in the region (0.78) compared with

ranking highest when downwind of Guangzhou. Assuming negligible local impact on particulate sulfate concentrations at Conghua, its Northerly Flow average sulfate concentration of 7.8 μg m^{-3} indicates significant background particulate sulfate advected into the Pearl River Delta that constitutes over half of the 13.3 μg m^{-3} of sulfate measured at Zhongshan. Examining Table 5, it is interesting to note that the average difference between the maximum at Conghua and upwind Zhongshan under Southerly flow is 5.3 μg m^{-3}, while the Northerly Flow difference between the same two sites is 5.5 μg m^{-3}. Thus, the direct contribution of the Guangzhou vicinity to particulate sulfate can be roughly estimated at 5-6 μg m^{-3}.

Having a nearly identical distribution as the Northerly Flow case of $PM_{2.5}$, OM concentrations appear to be influenced by a source area near Guangzhou. Impact based on proximity to Guangzhou is again observed, with Zhongshan and Shenzhen having much higher average OM levels relative to that seen during Southerly Flow and lesser increases in OM concentrations at sites in Hong Kong. Though OM concentrations appear to have a regional increase at sites in Hong Kong, a localized influence is still evident with normalized OM levels observed at rural Tap Mun ~20% lower than nearby Tung Chung and Central/Western, as shown in Figure 10. With expected biomass burning sources near Conghua, as indicated by high potassium levels during Southerly Flow, OM concentrations at Conghua may be likewise influenced by nearby sources and thus not indicative of regional background levels. Even with the possible presence of OM sources near Conghua, the impact of transported organic particulate species from Guangzhou is significant. Absolute OM concentrations displayed in Table 5 show a

Northerly Flow difference between downwind Zhongshan and upwind Conghua of 14.5 $\mu g\ m^{-3}$ and an 8.5 $\mu g\ m^{-3}$ increase from Zhongshan to Conghua during Southerly Flow.

With much lower relative concentrations at background sites (Tap Mun, Conghua) compared with urban areas (Shenzhen, Guangzhou), the distribution of EC during Northerly Flow appears to be dominated by local sources. However, it should be pointed out that some degree of transport is seen in concentrations at the background sites. Comparing the case of northerly winds to that of southerly winds, relative EC concentrations at Tap Mun increase by 0.21 during flow from the North, while normalized levels at Conghua decrease by 0.30, as shown in Figure 10. Despite the observed transport of EC, local influence appears to remain significant at the three sites in Hong Kong, with much higher EC concentrations at Central/Western and Tung Chung (2.3 and 2.7 $\mu g\ m^{-3}$, respectively) as compared with background Tap Mun (1.3 $\mu g\ m^{-3}$).

While normalized potassium at Conghua is seen to double levels at Guangzhou during Southerly Flow, as shown in Figure 10, Conghua ranks lowest among all sites during wind from the North, indicating significant biomass burning occurring south of Conghua. The reversal of flow causes highest relative levels at Zhongshan (1.9) with lessening impact moving southward to the sites in Hong Kong (.78-.91). Though Conghua has the lowest potassium concentration during the case of Northerly Flow, the level is still relatively high (0.85 $\mu g\ m^{-3}$) and indicates a background contribution that constitutes more than a third of the peak level observed at Zhongshan. The background potassium during Northerly Flow may be caused by biomass burning located near Conghua or due to transport from north of the Pearl River Delta region.

Normalized particulate lead concentrations are observed to dramatically increase at sites south of Guangzhou when comparing the case of Northerly Flow to Southerly Flow, with a maximum 20-fold increase observed at Zhongshan and a minimum 5-fold increase observed at Central/Western. With relative concentrations spiking at Zhongshan (2.0), attenuation is again seen moving southward to Shenzhen (1.0) and the sites in Hong Kong (0.56-0.71). While absolute lead concentrations, shown in Table 5, are observed to increase from 0.01 to 0.10 μg m^{-3} at the background site of Tap Mun, comparing cases of flow from the North and South, only a slight decrease of 0.02 μg m^{-3} in concentration is seen at Conghua. It is expected that particulate lead is regionally advected into the Pearl River Delta during flow from the North, maintaining high concentrations of lead at Conghua. However, local sources of lead at the background site in Guangdong cannot be ruled out. Even given a rise in background levels of lead during Northerly Flow, a tripling in absolute lead concentrations from Conghua to Zhongshan indicates lead emissions local to Guangzhou.

4.3.3 Mixed Flow

Even though larger rainfall was observed during days within the Mixed Flow category in comparison with Northerly and Southerly Flow, the stagnant conditions result in extremely high $PM_{2.5}$ concentrations at Guangzhou, with levels more than 60 μg m^{-3} higher than that observed for the other two flow categories, as presented in Table 5. In comparison to the dramatic change observed in Guangzhou, a more muted increase is seen at the remainder of sites in the delta, resulting in relative fine particulate levels at Guangzhou more than 40% higher than any other sampling site. This observed maximum at Guangzhou is similarly observed for all presented species (sulfate, OM, EC, potassium,

and lead). With limited transport of fine particulate concentrations, it is observed that sources within the vicinity of Guangzhou heavily impact local pollution during Mixed Flow. Throughout the delta, stagnant winds result in an accumulation of fine particulate matter from both local and regional sources, leading to higher $PM_{2.5}$ concentrations at both background sites at Conghua (46 $\mu g\ m^{-3}$) and Tap Mun (39 $\mu g\ m^{-3}$) than observed during Southerly or Northerly Flow. The relatively low wind speeds likely favor more local influences at the sampling stations.

Compared with all other examined species, the Mixed Flow distribution of normalized sulfate concentrations indicates the most significant degree of regional impact, with high relative concentrations (0.53-0.74) observed at the six sites surrounding Guangzhou. In contrast, the same six sites have lower relative levels of $PM_{2.5}$ (0.36-0.58) as shown in Figure 10. Though sulfate sources appear to have a regional influence on concentrations in the Pearl River Delta, sources in the vicinity of Guangzhou city cause sulfate concentrations at Guangzhou to measure more than 25% higher than any other site in the region.

With a nearly identical distribution as relative concentrations of $PM_{2.5}$, normalized OM has a maximum at Guangzhou during stagnant conditions, significantly higher than the remainder of sites (ranging from 0.25 to 0.55). In comparison to the distribution of sulfate among the seven monitoring sites during Mixed Flow, OM levels appear to have a more localized impact. Major sources of OM are expected to be located near Guangzhou, causing a doubling of average OM concentrations at Guangzhou in comparison with Southerly and Northerly Flow, despite higher precipitation during Mixed Flow days.

Although a doubling in absolute OM is observed at Guangzhou, comparing Mixed Flow to Northerly Flow, a 10-20% decrease is observed at the southernmost five sites, indicating an isolation of high OM levels to Guangzhou.

As observed during Northerly and Southerly Flow, a localized influence on EC is again apparent during Mixed Flow, with relative concentrations at the urban areas of Guangzhou and Shenzhen (0.69) much higher than background levels at Conghua (0.29) and Tap Mun (0.18). Localized sources are also apparent within the Hong Kong region, with normalized EC at Central/Western and Tung Chung more than doubling that measured at background Tap Mun.

The distribution of potassium concentrations during Mixed Flow supports a source area located near Guangzhou and Conghua. Ranked highest in the region during stagnant conditions, levels of potassium at Guangzhou (2.8 $\mu g\ m^{-3}$) are more than double concentrations measured during both Southerly and Northerly Flow, in spite of higher rainfall during Mixed Flow days. Though potassium levels increase at Conghua by 130%, comparing the case of Mixed Flow to Northerly Flow, a decrease of 40-60% is measured among the five sites south of Guangzhou. The stagnant winds appear to isolate high concentrations of potassium to the northern Pearl River Delta region and indicate a source area affecting concentrations at both Guangzhou and Conghua.

With a nearly identical distribution as particulate potassium, levels of lead during Mixed Flow similarly appear to be dominated by sources in the northern Pearl River Delta and have little transport to sites south of Guangzhou. Compared with Northerly Flow, the

southernmost five sites have a 30-60% reduction in absolute levels of lead while Guangzhou and Conghua increase by 140% and 160%, respectively. With Mixed Flow lead concentrations at remote Tap Mun (0.07 $\mu g\ m^{-3}$) similar to that at urban Shenzhen (0.08 $\mu g\ m^{-3}$), particulate lead in Hong Kong vicinity appears to be regionally controlled.

4.4 Correlative Analysis

One simple and useful approach to looking at the influence of local versus regional sources is to correlate pairs of sites. Figures 11a-d show examples of the information obtained by comparing two sites in Hong Kong situated in developed areas (Central/Western and Tung Chung) with a site located in an undeveloped region (Tap Mun). It is seen that S and K levels appear to have similar characteristics at both the rural and urban sites, having high correlation ($R^2 > 0.76$) and comparable concentrations. This strong relationship suggests that the Hong Kong area is affected regionally by exterior sources for both species. Sulfur, usually found as a sulfate ion in particulate matter, is typically associated with the combustion of coal burning while K is often linked with biomass burning (Watson et al., 2001), although incineration has also been suggested as another important source of K in the Pearl River Delta (Louie et al., 2005). In comparison, Na and Ni show very little relationship among the sites in Hong Kong ($R^2 < 0.23$), indicating that local sources (oceanic and fuel oil, respectively) may be important in controlling their levels.

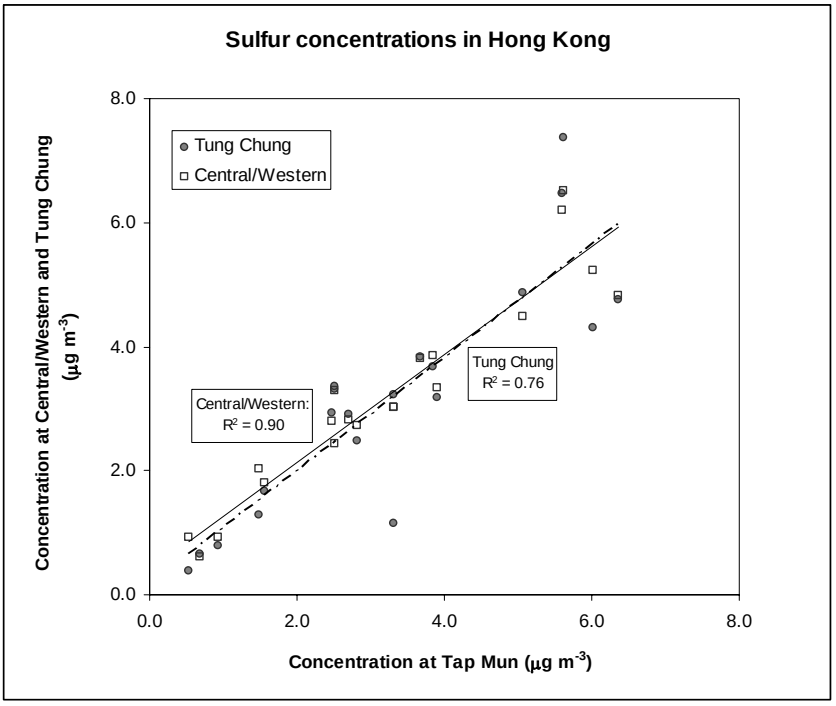

Figure 11a. Sulfur measured at the Hong Kong background site, Tap Mun, compared with the more developed sites in Hong Kong, Central/Western and Tung Chung.

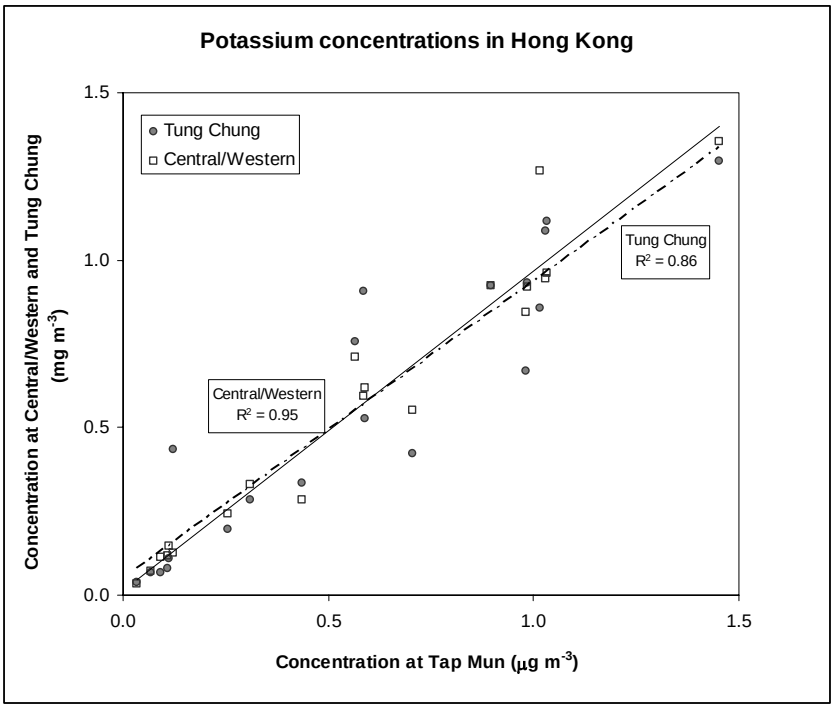

Figure 11b. Potassium measured at rural Tap Mun, compared with Central/Western and Tung Chung.

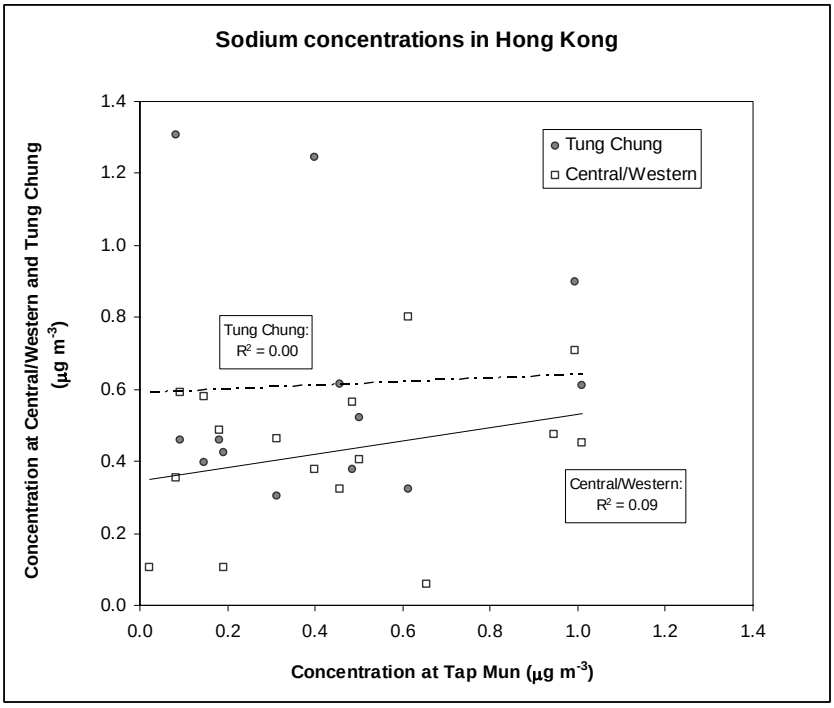

Figure 11c. Sodium measured at rural Tap Mun, compared with Central/Western and Tung Chung.

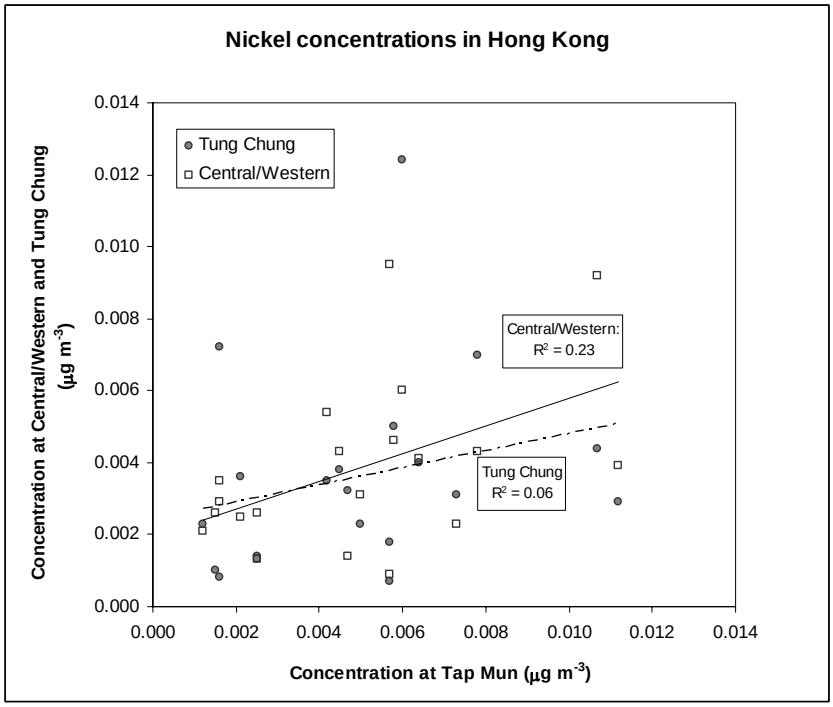

Figure 11d. Nickel measured at rural Tap Mun, compared with Central/Western and Tung Chung.

This analysis of correlative characteristics was extended to all 24 elements, with the inter-site Pearson correlation coefficients displayed in Figure 12. Based upon this analysis, 11 of the 24 elements (Al, Si, S, K, Ca, Mn, Fe, Zn, Br, Rb, Pb) exhibit strong inter-site correlation for the Hong Kong sites (average Pearson r > 0.8) and thus appear to be controlled by sources outside of Hong Kong. In contrast, the remaining species (Na, Cl, V, Cr, Co, Ni, Cu, As, Se, Sr, Sn, Tl, EC) appear to be influenced to varying degrees by local natural and anthropogenic sources.

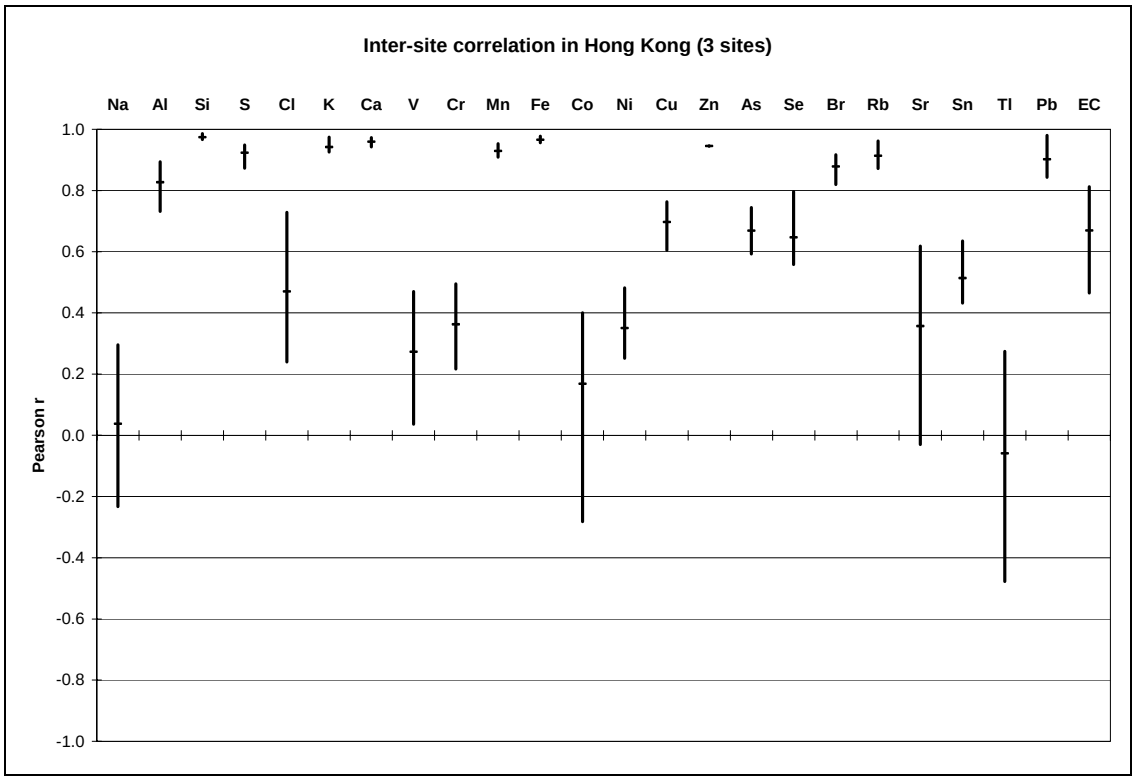

Figure 12. Pearson correlation coefficient calculated between pairings of Hong Kong sites Tap Mun, Tung Chung, and Central/Western. Markers denote the average of the three correlations, with bars stretching from maximum to minimum correlation coefficient.

While high correlation between sites in Hong Kong may be due to transport of external emissions into the Hong Kong area, the strong relationship between sites could also be

induced by a locally distributed source that undergoes similar patterns among sites due to meteorology. However, additional evidence of equal element magnitudes points to an external source impacting the Hong Kong area equally. To further test that the 11 highly correlated elements (Al, Si, S, K, Ca, Mn, Fe, Zn, Br, Rb, Pb) are controlled by sources exterior to Hong Kong, a linear least squares fit was calculated for these species, using the rural Hong Kong site, Tap Mun, as an independent predictor of concentrations at the two Hong Kong sites in developed locations (Central/Western and Tung Chung). It can be seen in Table 6 that the linear fit for each species has a calculated slope in the range of 0.7-1.1, with the significance of the slope represented by t-values well-exceeding 2.0. In addition, the calculated intercept is shown to be minor to negligible for each species. This demonstrates how concentrations of the selected species increase and decrease in a nearly equal fashion among the entire Hong Kong region, indicating that exterior sources influence the Hong Kong area as a whole.

Table 6 Least-squares fit of developed sites in Hong Kong versus rural Tap Mun

	Tung Chung vs. Tap Mun						Central and Western vs. Tap Mun					
Species	Slope[a]		t[b]	Intercept		t	Slope		t	Intercept		t
Al	0.86	±0.39	4.6	0.010	±0.043	0.5	1.07	±0.27	8.5	0.010	±0.030	0.7
Si	0.84	±0.11	16.0	0.018	±0.049	0.8	0.91	±0.08	24.7	0.028	±0.035	1.7
K	0.89	±0.18	10.4	0.052	±0.127	0.9	0.96	±0.11	18.3	0.013	±0.078	0.4
Ca	1.00	±0.18	12.0	0.014	±0.021	1.4	0.97	±0.12	17.7	0.025	±0.014	3.9
Mn	0.96	±0.19	10.4	0.001	±0.003	1.3	0.95	±0.15	13.3	0.003	±0.002	3.3
Fe	1.02	±0.14	15.3	0.021	±0.024	1.9	0.93	±0.14	13.8	0.041	±0.024	3.6
Zn	0.94	±0.16	12.2	0.006	±0.037	0.3	0.79	±0.13	12.5	0.047	±0.031	3.2
Rb	0.80	±0.25	6.9	0.001	±0.002	0.9	0.81	±0.12	14.5	0.000	±0.001	0.2
S	0.91	±0.25	7.6	0.163	±0.093	0.4	0.87	±0.15	12.6	0.406	±0.536	1.6
Br	0.66	±0.23	6.1	0.002	±0.002	2.2	0.86	±0.21	8.7	0.001	±0.002	1.9
Pb	0.80	±0.26	6.5	0.009	±0.021	0.9	0.80	±0.08	20.3	0.005	±0.007	1.7

[a]Value is the calculated best-fit slope or intercept ± the parameters 95% confidence interval, using the Tap Mun concentrations of each element as the independent variable.
[b]The t-value is the estimated regression coefficient divided by its standard error.

The next step of analysis was to determine whether sources of the 11 species are located within the Pearl River Delta or at a further distance from Hong Kong. Correlating the levels of Hong Kong sites against potential nearby source areas (sites in developed areas of Guangdong province - Shenzhen, Zhongshan, and Guangzhou) provides useful information about source location. High correlation with nearby developed areas in Guangdong province would indicate that long-distance transport is the dominant mechanism controlling a species throughout the entire region, while low correlation indicates a local source area is important. Figures 13a-c show the correlation of the selected species (Al, Si, S, K, Ca, Mn, Fe, Zn, Br, Rb, and Pb) for pairings of the Hong Kong sites with Shenzhen, Zhongshan, and Guangzhou, respectively. In Figure 13a, it appears that Shenzhen has a close relationship with Hong Kong for nearly all species, with high correlation (average Pearson $r > 8.0$) for 8 species (Si, S, K, Ca, Fe, Zn, Rb, Pb) and moderate correlation (average Pearson $r > 6.0$) for 2 others (Al and Mn). However, Br appears to have a weaker relationship (average $r = 0.43$). The pairing of Hong Kong and Zhongshan (Figure 13b) also has a moderate to strong relationship for 9 species (Al, Si, S, K, Ca, Mn, Fe, Rb, Pb), while Zn and Br stand out for low correlation. Finally, correlating Hong Kong with Guangzhou leads to no correlation for 8 species (Al, Si, K, Ca, Mn, Fe, Rb, and Pb), with moderate positive correlation for S and Br, and moderate negative correlation for Zn. The low correlation of the 8 species between Hong Kong and Guangzhou combined with the regional maximum average concentration of each species recorded at Guangzhou points to this rapidly industrializing area as a major source area of both crustal material (Al, Si, Ca, and Fe) and anthropogenic species (K, Mn, Rb, Pb).

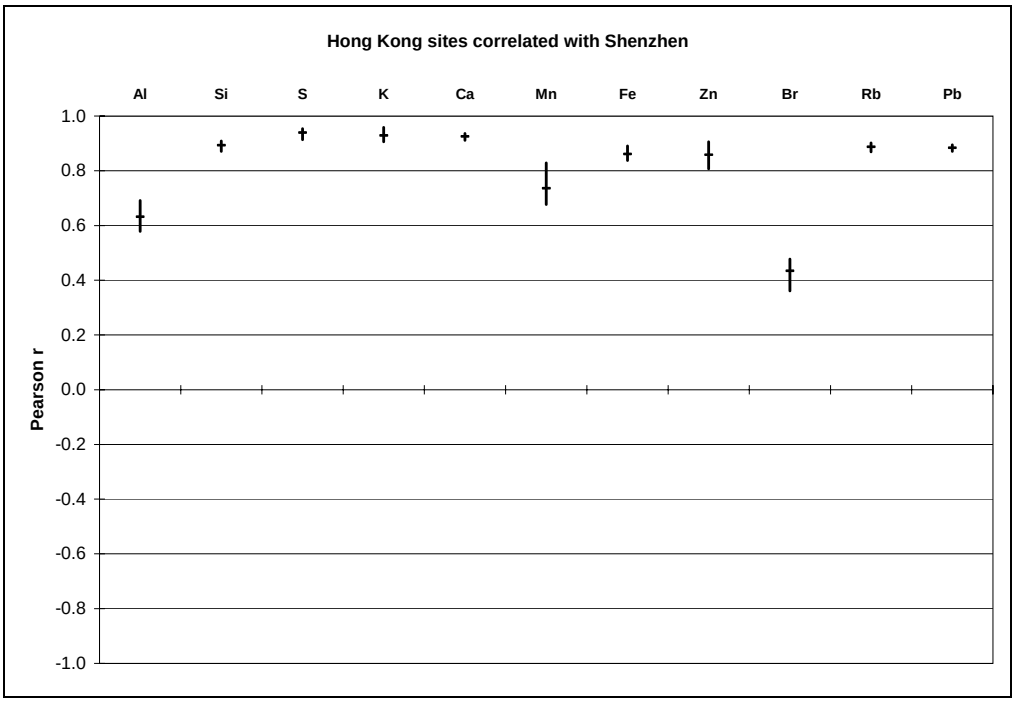

Figure 13a. Pearson correlation coefficient calculated between pairings of Hong Kong sites Tap Mun, Tung Chung, and Central/Western with Shenzhen, located immediately north of the Hong Kong Special Administrative Region.

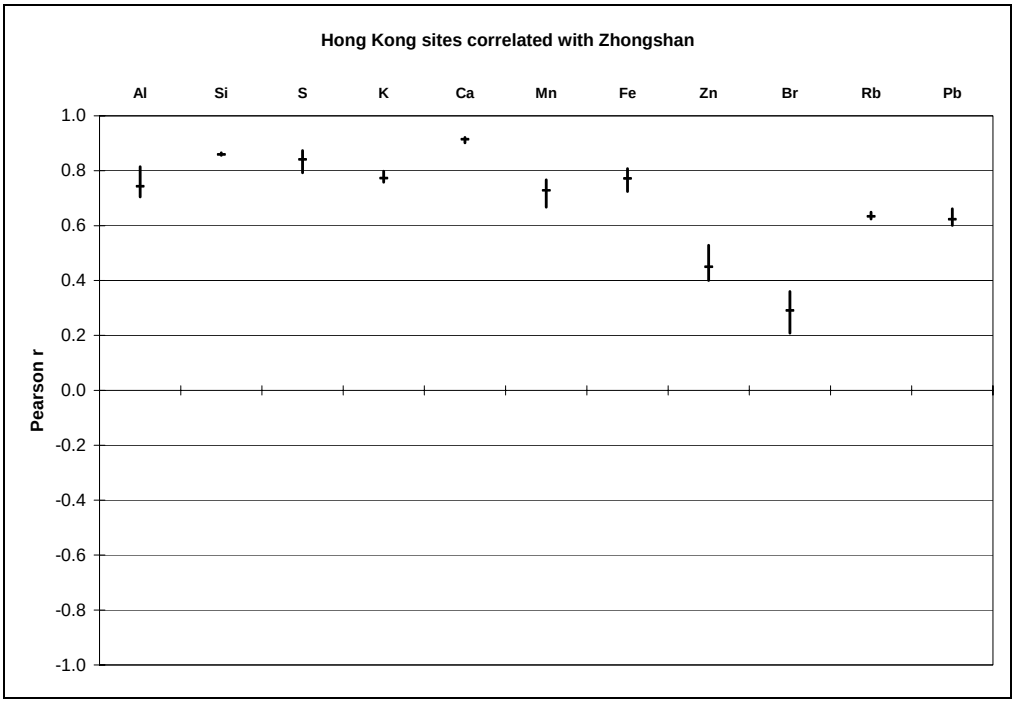

Figure 13b. Pearson correlation coefficient calculated between pairings of Hong Kong sites Tap Mun, Tung Chung, and Central/Western with Zhongshan, located west of the Hong Kong Special Administrative Region.

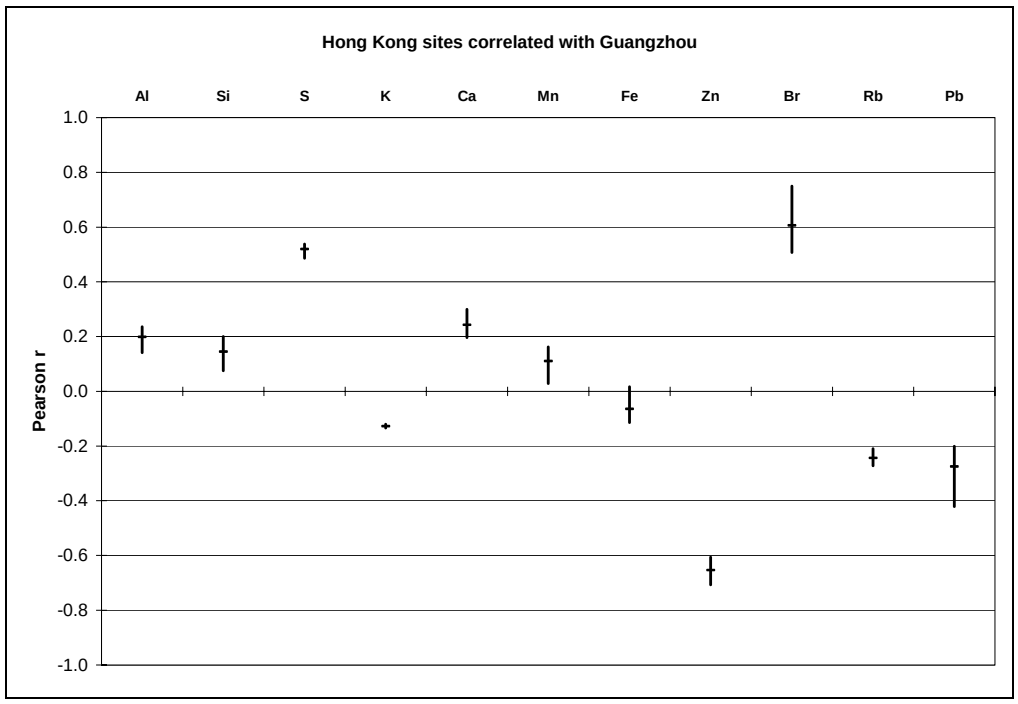

Figure 13c. Pearson correlation coefficient calculated between pairings of Hong Kong sites Tap Mun, Tung Chung, and Central/Western with Guangzhou, located northwest of the Hong Kong Special Administrative Region.

The varying relationship of Br and Zn for pairings of Hong Kong sites with Guangzhou, Zhongshan, and Shenzhen points to sources in the Guangdong province influencing the Hong Kong area. The strong positive correlation of Zn at Shenzhen, no correlation at Zhongshan, and moderately negative correlation at Guangzhou indicates a possible source area located south of Guangzhou and near Zhongshan. In addition, the source location of Br is perplexing, having the maximum concentration observed at rural northern site, Conghua, yet also poor correlation for Hong Kong sites paired with Shenzhen and Zhongshan. One previous study linked Hong Kong's bromide levels with vehicular sources and road dust (Lee et al., 1999), although incineration has also been suggested as another potentially important source for the region (Louie et al., 2005). Clearly, further research is needed to evaluate the source characteristics of Br in the Pearl

River Delta. Finally, the moderate to high correlation of S (average Pearson r of 0.52 to 0.94) between Hong Kong and the three developed sites in Guangdong supports the meteorological case studies which described region-wide increases in sulfate levels during northerly flow, although local sources of S are also expected. Given that sulfate is a significant component of $PM_{2.5}$ throughout the region, sources outside of the Pearl River Delta region may be an important factor influencing overall $PM_{2.5}$ concentrations in the area.

4.5 Factor Analysis

After having established that all three Hong Kong sites and to a major extent, Shenzhen, are influenced by external sources for 11 species (Al, Si, S, K, Ca, Mn, Fe, Zn, Br, Rb, and Pb), statistical relationships between these species can point to source types. Combining data for the three Hong Kong sites and Shenzhen, Principal Components Analysis was performed using a statistical software package (SPSS 12.0). Shown in Table 7, two factors were found that represented 81% of the total variance, with one factor displaying crustal characteristics (Al, Si, Ca, and Fe) while the second has a mix of urban and industrial activities (K, Mn, Zn, Rb, and Pb). While the former grouping is unsurprising, as Al, Si, Ca, and Fe exhibited similarly low crustal enrichment factors, the latter clustering of elements may not be easily explained as originating from the same source. For example, K is often used as a common tracer for biomass burning (Watson et al., 2001), while Pb has a multitude of non-biomass burning sources including fossil fuel combustion and metallurgy (Nriagu and Pacyna, 1988). A likely explanation for the clustering of these anthropogenic elements is a similar origin and/or co-located sources at

a distance from Hong Kong, resulting in a general anthropogenic pollution signature observed in the Hong Kong area.

Table 7. Principle Components Analysis of measurements made at sites in Hong Kong (Tap Mun, Tung Chung, Central/Western), and Shenzhen

	Component[a]	
	1	2
Al	.249	**.912**
Si	.456	**.865**
S	.499	.227
K	**.826**	.486
Ca	.315	**.898**
Mn	**.749**	.553
Fe	.562	**.790**
Zn	**.895**	.323
Br	.462	.429
Rb	**.903**	.301
Pb	**.928**	.303
% Variance	44.3%	37.0%

[a]Rotation method: Varimax with Kaiser Normalization.

CHAPTER 5: CONCLUSIONS AND RECOMMENDATIONS

5.1 Conclusions

Development of an effective fine particulate management plan in the Pearl River Delta has been hindered by a lack of information about the regional nature of $PM_{2.5}$, with regional chemical composition, influential source areas, and meteorological impacts not well known. To assess fine particulate pollution throughout the PRD, simultaneous 24-hour filter measurements were conducted at seven sites during October 2002, December 2002, March 2003, and June 2003. From the concentrations and variability of $PM_{2.5}$ species throughout the region, the following conclusions were drawn:

$PM_{2.5}$ overall concentration and composition:

- $PM_{2.5}$ concentrations at all sites in the region far exceed the United States National Ambient Air Quality Standard of 15 $\mu g\ m^{-3}$ (annual average) and World Health Organization Air Quality Guideline of 10 $\mu g\ m^{-3}$ (annual average), with levels in Hong Kong ranging from 29-34 $\mu g\ m^{-3}$ and even higher average concentrations in Guangdong ranging from 37-71 $\mu g\ m^{-3}$.
- The chemical make-up of the fine particulate matter is similar among the seven sites, with organic mass and sulfate dominating fine particulate mass at 24-35% and 21-32%, respectively. Other measured species include crustal matter (7-13%), ammonium (6-8%), elemental carbon (3-8%), and nitrate (1-6%). The unaccounted portion of $PM_{2.5}$ mass ranges from 10-21%. This fraction of $PM_{2.5}$ may be due to water mass associated with the particulate matter, underestimation of the crustal mass

from elemental concentrations, and/or an underestimation of the mass of organic compounds.

Source information from meteorology case studies:

- Comparison of $PM_{2.5}$ levels at sites immediately upwind and downwind of Guangzhou during northerly and southerly flow conditions indicates an estimated contribution of 18-34 $\mu g\ m^{-3}$ to downwind $PM_{2.5}$ by sources in the vicinity of Guangzhou city. A gradient effect was observed, with the most extreme increases in fine particulate matter during northerly winds occurring at Zhongshan, located close to Guangzhou, and lesser change observed at the more distant sites.
- Sulfate, related to the burning of coal, has a high regional background level estimated at 6-8 $\mu g\ m^{-3}$, over half of the total measured sulfate. Analysis of sulfate concentrations at sites upwind and downwind of Guangzhou indicates a direct input of 5-6 $\mu g\ m^{-3}$ from sources near Guangzhou city.
- Guangzhou also stands out as a prominent regional source of organic mass (OM), with observed increases of 8.5-14.5 $\mu g\ m^{-3}$ at sites immediately downwind and a disproportionate elevation in organic mass at the Guangzhou site during stagnant conditions. Local OM sources are also evident in the Hong Kong region, with rural Tap Mun consistently lower than urban Central/Western.
- Regional levels of elemental carbon (EC) are highest during all flow conditions at urban Shenzhen and Guangzhou. Local sources of EC are evident within Hong Kong, with more developed sites at Tung Chung and Central/Western having nearly double the EC concentrations measured at rural Tap Mun.

- The distribution of potassium (biomass burning) and lead (industrial sources, combustion of fossil fuels) indicate significant sources in northern area of the delta influencing concentrations downwind. The regional distribution of potassium points to sources in the vicinity of both Guangzhou and Conghua, with strikingly high levels observed at Conghua during southerly flow. Regional levels of lead appear to be controlled by sources in the vicinity of Guangzhou.

Source information from analysis of element enrichment and correlation:

- Local emissions in Hong Kong appear to contribute to local $PM_{2.5}$ element concentrations. Significant differences in concentration among three Hong Kong sites were observed for a number of species (EC, Cl, V, Cr, Co, Cu, Sr, and Sn), which also indicates spatial variability in local population exposure. In addition, low ($r < 0.5$) or moderate ($0.5 < r < 0.8$) inter-site correlation supports the conclusion that Hong Kong is impacted by local sources for the above elements as well as several others (As, Ni, Na, Se, Tl).
- It appears that the heavily developed northern (Guangdong) section of the Pearl River Delta substantially influences regional air quality:
    - With elements initially grouped by their enrichment factors as primarily crustal, oceanic, or anthropogenic origin, it was found that Guangdong sites had generally much higher concentrations of both crustal and anthropogenic elements in relation to sites in Hong Kong.
    - The high inter-site correlation ($r > 0.8$) of certain elements (Al, Si, S, K, Ca, Mn, Fe, Zn, Br, Rb, Pb) and their similar magnitude of concentration

throughout Hong Kong points to region-wide impacts by sources external to the city. This subgroup of elements were studied using Principal Components Analysis and 9 were found to group as a crustal identity (Al, Si, Ca, and Fe) and an anthropogenic pollution signature (K, Mn, Zn, Rb, Pb) potentially linked by co-located industrial activities, such as biomass burning and incinerator emissions.

  - Correlative analysis extended to include source areas in Guangdong suggests that Guangzhou is a regionally important source area of crustal species and most of the clustered anthropogenic elements (K, Mn, Rb, Pb), with Zn appearing to be controlled by a source area between Guangzhou and Zhongshan.

- The moderate to high inter-site correlation of S in all analyses supports the influence of long-distance transport into the Pearl River Delta, although local sources are also expected to contribute to regional concentrations.

5.2 Policy Implications

Environmental pollution in the Pearl River Delta Region of China is particularly challenging to govern on a region-wide scale. Since Hong Kong was incorporated into China in 1997, it was granted status as a Special Administrative Region and is under the "one country, 2 governments" system until 2047. Under this political framework, Hong Kong has a fairly autonomous political and economic system that extends to self-governship in environmental affairs. Thus, although close neighbors, the Hong Kong Special Administrative Region and Guangdong Province have different air quality

standards and different means of enforcement. Neither region currently regulates $PM_{2.5}$. Daily and annual limits for PM_{10} in Hong Kong are 180 $\mu g\ m^{-3}$ and 55 $\mu g\ m^{-3}$, respectively. Guangdong has regulations particular to two separate emission classes, nonindustrial regions (150 $\mu g\ m^{-3}$ daily, 100 $\mu g\ m^{-3}$ annual average) and industrial regions (250 $\mu g\ m^{-3}$ daily, 150 $\mu g\ m^{-3}$ annual average) (CH2M HILL, 2002). The ability to regulate emissions in the region is further complicated by vast socioeconomic and industrial differences between the two populations. In Hong Kong, the average income is ~$16,500, while in the neighboring city of Guangzhou (located in Guangdong) the average income is ~$7,500 (Asiaweek, 2000). In addition, Hong Kong is mainly a service industry while Guangdong has an economy fueled by manufacturing. While it would be politically easier to continue managing the two regions as separate entities, our findings indicate that the two diverse parts of China will need to work together to improve regional air quality.

Overall, our results suggest that fine particulate pollution in the Pearl River Delta Region of China can be greatly improved by targeting emissions inside the region, both within the Hong Kong Special Administrative Region and in neighboring Guangdong Province. The heavily developed Guangzhou vicinity, located in Guangdong, appears to be an important emissions area that substantially influences downwind $PM_{2.5}$ concentrations. Management of emissions (biomass burning, fossil fuel combustion, and dust) in the Guangzhou vicinity would have strong positive impacts on air quality at nearby regions, including the city of Hong Kong. In addition, it appears that air quality in the city of Hong Kong can be improved by locally reducing emissions from vehicles and shipping.

A need to address emissions on an even larger scale is suggested by our observation that nearly half of the measured sulfate may be transported into the region. With coal burning as a common source of sulfur dioxide and consequent secondary sulfate in particulate matter, it is likely that the intense growth of coal-based power in China is impacting air quality on a national scale. Further research would be needed to evaluate the characteristics of the larger-scale sulfur pollution in China and its role in the Pearl River Delta.

5.3 Recommendations for Further Research

Particulate matter pollution in the Pearl River Delta Region of China is a challenging issue linking research disciplines such as sociology, economics, atmospheric science, epidemiology, agriculture, and engineering. To fully understand air quality in the Pearl River Delta and the best strategies for its improvement, continuing research is needed in each of these areas. Addressing the specific focus of this thesis, suggestions for further research in the atmospheric science arena are provided here:

- **Determine spatial variability in source impacts and population exposure**

Closely linked with this study, expanded (spatially and temporally) field measurement of fine particulate matter in this region would provide a great deal of policy-relevant information. The limited number of measurements presented by this thesis illustrates spatially variable $PM_{2.5}$ concentrations, suggesting equally variable population exposure and location-specific source impacts. A greater number of sampling locations, particularly in high concentration areas such as the Guangzhou vicinity, would better

capture the state of particulate pollution and its associated impacts. In addition, sustaining sampling over a longer period of time would provide a higher number of data points and more sophisticated analytical tools (e.g. Positive Matrix Factorization) could be applied to derive site-specific source information. Also, extending sampling would allow for an improved understanding of the connection between particulate pollution and local human health impacts.

- **Characterize regional emissions magnitude, source locations, and source profiles**

Emissions of fine particles and gaseous precursors are only crudely known in the Pearl River Delta Region. Source profiles of major sources in the region are unknown, including coal burning, biomass burning, shipping fuel combustion, and vehicular emissions. Not only would these source profiles be useful in defining an emissions inventory, they would also support higher accuracy in applying receptor modeling analyses (e.g. chemical mass balance model) to apportion fine particulate pollution to sources. While some emission inventory estimates have been calculated, these are unfortunately not without controversy. For examples, recent NO_x emission estimates in China were reported to be in disagreement with satellite-derived NO_x (Akimoto et al., 2006), adding doubt to emissions reported for other types of air pollutants in China. As China's energy appetite continues to grow with increasing individual vehicle ownership and booming industrial growth, precise and up-to-date emissions inventories are needed to accurately model and forecast regional air quality.

- **Analyze linkage between unique episodes and regional air quality**

While long-term sampling of air quality is useful in determining sources and population exposures, observing extreme air quality events (high and low) induced by emissions changes can provide unique information. One period of time that would be very interesting to study would be April-May 2003, during the Severe Acute Respiratory Syndrome (SARS) outbreak that was centered in Guangdong and Hong Kong. The SARS episode ended up significantly altering population dynamics during this time period as residents sought to lessen exposure by avoiding public areas. In addition, the World Health Organization issued an international advisory on 12 April 2003 that suggested all non-essential travel to the region be postponed, causing a significant drop in air traffic and tourism. This major event likely caused an alteration of related emissions such as vehicular and aircraft transport, restaurant emissions, and shipping traffic. To our knowledge, no $PM_{2.5}$ measurements are available covering that time period, but it would be highly interesting to study related species (e.g. NO_x, CO, PM_{10}) that are routinely sampled by regional environmental protection departments and relate the changes in anthropogenic sources with the resulting ambient concentrations.

An additional reoccurring event that may provide insight on air quality impacts is the Chinese New Year. During this annual celebration, manufacturing in China often shuts down for a week or more. It would be interesting to evaluate the short-term effects of reduced emissions on particulate matter composition and concentrations. In addition, epidemiological factors, such as hospital admissions or personal exposure, would be very

interesting to assess during the Chinese New Year in comparison with other times of the year.

- **Evaluate long-distance transport of particulate matter in China**

While this thesis focuses primarily on pollution transport within the Pearl River Delta Region, in all likelihood a much greater spatial scale is involved both in generating particulate matter and in receiving pollution generated by the PRD. Our research suggests that the sulfate component of particulate matter, most likely produced by coal burning, has a spatial scale extending beyond the PRD. Also, past studies have found that airborne dust in China can be heavily impacted by long-distance transport from Asian dust storms occurring in northwest China (Tsai and Chen, 2006; Wang et al., 2006). As cities within and near China struggle to meet air quality health standards, it is crucial to understand the long-distance impacts of emitting sources in China on both background levels and episodic events.

PART 2: PARTICULATE MATTER ON THE GREENLAND ICE SHEET

CHAPTER 6: INTRODUCTION

6.1 Foreword

Part II of this thesis focuses on carbonaceous particulates measured in the air and snow on the Greenland Ice Sheet, providing an extended version of the following publications:

(1) Hagler, G.S.W, Bergin, M.H., Smith, E.A., Anderson, C., Dibb, J.E., Steig, E.J. Particulate and water-soluble carbon measured in recent snow at Summit, Greenland, *Geophysical Research Letters,* in review.

(2). Hagler, G.S.W, Bergin, M.H., Smith, E.A. A summer time series of particulate carbon in the air and surface snow on the Greenland Ice Sheet. *Journal of Geophysical Research-Atmospheres,* in preparation.

(3). Hagler, G.S.W, Bergin, M.H., Smith, E.A., Dibb, J.E, Town, M. Analysis of camp impact on atmospheric and snow carbonaceous particulate measurements at Summit, Greenland. *Atmospheric Environment,* in preparation.

6.2 Background on the Greenland Ice Sheet

The Greenland Ice Sheet is arguably the most pristine region of the Northern Hemisphere, covering over 80% of sparsely inhabited Greenland (population: ~60,000) with 1.7 million km^2 of ice. It is valued as both a major agent in modern global climate and for its frozen archive of atmospheric history dating up to 100,000 ybp (years before present) (Bender et al., 1994; Meese et al., 1997). In addition, located far from any

biogenic or anthropogenic emissions, the air above the Greenland Ice Sheet may be considered as the hemispheric background for atmospheric pollutants.

6.2.1 Climate Change and Ice Loss

While the global surface average temperature warmed by 0.6 °C (±0.2 C) during the 20th century (IPCC, 2001), the Greenland Ice Sheet has been observed to have experienced 2.2 times the global temperature increase over the time period of 1974-2005 (Chylek and Lohmann, 2005) which is in agreement with global climate models predicting Greenland's faster temperature increase of 1.2-3 times the global mean (IPCC, 2001). The local warming measured on the Greenland Ice Sheet translates to observations of a gradual loss of ice, with the modeled ice sheet mass balance estimated at -76 $km^3\ y^{-1}$, leading to a 2.2 mm sea level rise (contributing 15% of global sea level rise) during 1991-2000 (Box et al., 2004). A second modeling study over a longer period of time found an overall mass balance of -22 $km^3\ y^{-1}$ in 1961-1990 and -36 $km^3\ y^{-1}$ for 1998-2003, with melting during the past 6 years contributing 0.15 mm y^{-1} to global sea level rise (Hanna et al., 2005). Finally, a recent study reported laser altimeter measurements of accelerating mass loss in recent years, with mass loss in 1999-2004 (57-105 Gt y^{-1}) much higher than in 1993-1999 (4-50 Gt y^{-1}) (Thomas et al., 2006). It appears that the progressive melting of the Greenland Ice Sheet is not a futuristic fear, but a present-day event.

Since the mid-1980s, black carbon (or soot) entrapped in snow has been highlighted for its potential to lower surface albedo and contribute to local warming in snow-covered regions, also resulting in a net positive forcing on global climate (Clarke and Noone, 1985; Twohy et al., 1989). There have been several recent modeling efforts aimed at

quantifying the climate impact of black carbon in the Arctic. One study tested quadrupling fossil fuel black carbon emissions and found that the Arctic had proportionally greater warming than at lower latitudes, explained by an ice melting/surface albedo feedback mechanism (Roberts and Jones, 2004). Another study assessed the climatic impact of black carbon lowering snow and sea ice albedo, estimating a Northern Hemisphere climate forcing of +0.3 W m^{-2} and finding that the snow/ice albedo forcing was twice as effective in altering global surface air temperatures as the same given CO_2 forcing (Hansen and Nazarenko, 2004). Additionally, a similar study found that, when accounting for the snow/ice albedo impacts of fossil fuel and biofuel soot (black and organic carbon) in a global climate model, a 10-year near-surface temperature response was estimated at +0.27K, with black carbon in snow/ice accounting for ~0.06 K of the total response (Jacobson, 2004). It is clear that black carbon transported to the pristine Arctic is capable of significantly impacting both local and global surface temperatures.

6.2.2 Archival of Atmospheric History

Pioneering ice core research on the Greenland Ice Sheet took place in the late 1960s and early 1970s, successfully dating a ~1400 meter ice core via isotopes of oxygen (Dansgaard et al., 1969) and evaluating anthropogenic impacts on heavy metals by comparing surface snow samples with dated samples from the walls of deep ice shafts (Weiss et al., 1971a; Weiss et al., 1971b). Forty years of research has since followed those early studies, measuring the ice core record of a wide variety of species and determining related background information, such as the transport pathways of pollutants to the Arctic and the physical properties of archival in the ice sheet.

A number of ice core studies on the Greenland Ice Sheet have detected heightened levels of atmospheric species related to human activities. The oldest anthropogenic emissions (lead and silver) detected in Greenland ice cores thus far date back to 500 B.C. from Roman and Greek mining/smelting operations (Hong et al., 1994). More recent human industrial activities are also reflected in the buried Greenland ice, such as the significant increase in lead observed during 1750-1998, with the phasing out of leaded gasoline in the 1970s reflected in a >75% decline in annual lead flux to the ice sheet (McConnell et al., 2002). Also, ice core records reveal that non-sea-salt sulfate archived concentrations tripled from 1900-1910 to the 1980s and nitrate doubled since 1955 (Mayewski et al., 1986). Human-driven emissions were also detectable in the sulfur isotopic signature, comparing a preindustrial period (14^{th} to 18^{th} century) with 1872-1969 (Patris et al., 2002). Specific episodes in human history are also found to leave a record in the glacial ice, such as the measured pulse of deposited ^{36}Cl in ice core layers in the 1950s to1970s resulting from marine nuclear tests that took place in the 1950s (Elmore et al., 1982) and ^{134}Cs and ^{137}Cs in the Greenland snow pack were linked to the 1986 Chernobyl accident (Davidson et al., 1987). It appears that the Greenland Ice Sheet holds a wealth of historical information related to anthropogenic emissions.

Atmospheric impurities associated with natural events such as volcanic eruptions, forest fires, and dust storms are also tracked in ice cores from the Greenland Ice Sheet. Major sulfate spikes are associated with volcanic activity occurring from 7000 B.C. to recent times (Zielinski et al., 1994). High episodic levels of black carbon, organic species, and

ammonia have also been associated with biomass burning (Cachier and Pertuisot, 1994; Chylek et al., 1995; Legrand et al., 1992; Masclet et al., 1995; Whitlow et al., 1994). Finally, major dust events are also reflected in the ice cores on the Greenland Ice Sheet, including an apparent record of the United States dust bowl disaster that occurred in the 1930s (Donarummo et al., 2003).

6.2.3 Modern Origin of Pollutants Reaching the Greenland Ice Sheet

Several studies have investigated the origin of atmospheric pollution transported to the Greenland Ice Sheet through meteorological modeling and chemical signatures. Back-trajectory analysis of air masses reaching Summit, Greenland over 1946-1989 found longest 10-day trajectories in wintertime, with the majority of wintertime air parcels transported from Asia and Europe. Shortest 10-day trajectories occurred during summertime, with nearly half originating over North America (Kahl et al., 1997). Through chemical analysis of dust in shallow snow depths, Northwest Asia has been pointed out as the likely main source area of recent (post-1987) mineral dust deposits in Greenland snow (Bory et al., 2003; Bory et al., 2002; Drab et al., 2002). Looking in particular at sources of carbonaceous particulates reaching the pristine Arctic, a recent study used a general circulation model to determine that 30% of Arctic soot is transported from industrial and biofuel emissions in south Asia, while North America, Europe, and Russia each produce 10-15% of Arctic soot. Biomass burning, mostly at northern latitudes, was also found to contribute a significant portion of soot (28%) (Koch and Hansen, 2005). It appears that modeling studies and analysis of minerals in the snow/ice are in agreement that the Greenland Ice Sheet is regularly exposed to natural and anthropogenic atmospheric particulate matter generated thousands of kilometers away.

6.3 Carbonaceous Particulate Matter and the Greenland Ice Sheet

Organic (OC) and elemental carbon (EC) in air, snow, and ice on the Greenland Ice Sheet are of interest for their potential usefulness as chemical signatures of anthropogenic and biogenic pollution. Past research has found that the ambient particulate organic fraction contains numerous compounds, many of which are stable in the atmosphere and can fingerprint source types such as biomass burning, coal combustion, and vehicular transport (Schauer et al., 1996; Simoneit et al., 1999). Outside of its utility as a combustion tracer, EC in the air and surface snow is also of interest for its capability to alter the radiative balance of the ice sheet. Finally, recent research points to the possibility that particulate organic species may participate in active chemistry after deposition to the Greenland Ice Sheet, which has implications for ice core research and atmospheric chemistry.

6.3.1 Atmospheric Carbonaceous Particulate Matter

While gas-phase organics have been measured in numerous field studies on the Greenland Ice Sheet (Dassau et al., 2002; Dibb and Arsenault, 2002; Dibb et al., 1994; Ford et al., 2002; Hutterli et al., 1999; Jacobi et al., 2002), very few measurements of particulate carbon compounds have been reported. One field study measured particulate oxalate at Summit, Greenland (the highest point of the Greenland Ice Sheet) from 1992-1995 and linked high concentration spikes to biomass burning pollution (Jaffrezo et al., 1998). Also, ^{14}C was measured on filter samples covering 5 days in August, 1994 and described a high one-day concentration spike linked to biomass burning activity in

Canada (Currie et al, 2005). In addition, black carbon was also measured at Summit and found to hit intensely high levels (up to 600 ng m^{-3} from the 2003-2006 annual average of ~15 ng m^{-3}) during the 2004 Alaskan and Canadian forest fires (Stohl et al., 2006). To the author's knowledge, there are no other reported measurements of particulate carbonaceous species in the Greenland atmosphere. The quite limited information on atmospheric carbonaceous particulate matter on the Greenland Ice Sheet underlines the need for further research.

6.3.2 Archival and Post-Depositional Processing in Snow

A number of recent research studies sought to use carbonaceous species entrapped in glacial snow/ice to interpret recent and long-term history on the Greenland Ice Sheet. Black carbon and total carbon were sampled in a 300-meter core and in surface snow, with authors noting that the surprisingly little change in black carbon concentrations since pre-industrial times may be due to emissions from forest fires before the industrial era (Cachier and Pertuisot, 1994). Another group measured black carbon in the GISP2 ice core and found that major peaks in 320-330 AD correlated with spikes in ammonium, indicating that the high black carbon levels were linked to forest fires. This second study also noted that the surface snow concentration (1989-1990) was at similar levels as the 320-330 AD period (Chylek et al., 1995). More recent measurements (3-5 m snow pits) sampled at higher temporal resolution for ^{14}C (Slater et al., 2002) and polycyclic aromatic hydrocarbons (PAHs) (Jaffrezo et al., 1994; Masclet et al., 2000; Slater et al., 2002). The ^{14}C measurements in 1994 indicated that fossil fuel combustion was a major source of carbonaceous particulate matter in the fall and spring while biomass burning and fossil fuel combustion equally impacted summertime concentrations (Slater et al., 2002).

Although seasonality and correlations with sulfate were consistently observed among the three studies measuring PAHs, one group noticed significant depletion (90%) of benzopyrene in a 3 meter snow pit and suggested that post-depositional processes may alter the record of organics in snow (Jaffrezo et al., 1994).

A major focus of recent research has been to better understand the linkage between atmospheric and snow-phase species, investigating the major modes of deposition and assessing post-depositional processes that may impact the glacial archive. The first step, transfer of atmospheric carbonaceous particulates to the snow pack, is unfortunately not as clear-cut as one would hope. Although associated with perennial snow cover, the Greenland Ice Sheet is a desert climate with a low snow accumulation rate (~65 cm per year) that inconsistently varies with seasons (Dibb and Fahnestock, 2004). In addition, there are several possible modes of deposition to the surface of the ice sheet – dry deposition and wet deposition by snow or fog. While a modeling study found wet deposition to be the main mechanism (accounting for 98%) of depositing black carbon to surfaces globally (Jacobson, 2004), a previous study discerning deposition rates to the Greenland Ice Sheet for ^{134}Cs and ^{137}Cs from the Chernobyl disaster (D_p ~0.2 to 0.7 μm) calculated dry deposition to contribute 25-50% of the radioactive cesium measured during a relatively dry period of time (Davidson et al., 1987). In addition, a past study of atmospheric ions during a summer season on the Greenland Ice Sheet found fog and dry deposition to contribute 13-32% and 5-23% of deposited ions, respectively (Bergin et al., 1995). Given the sparse precipitation over the Greenland Ice Sheet, intermittent summertime fogs that develop during stagnant conditions, and unknown composition of

carbonaceous species reaching Greenland, it is difficult to predict the dominant air-to-snow transfer mechanisms for carbonaceous species and in situ measurements are needed.

After atmospheric carbonaceous species transfer to the ice sheet by wet or dry deposition, they are expected to concentrate in the quasi-liquid layer believed to exist at the air-snow interface (Cho et al., 2002; Jacobi et al., 2004). Past studies reveal that, once in the snow pack, carbonaceous species may be impacted by post-depositional air-to-snow partitioning and photochemical processes. Gaseous organics may partition to the snow surface and enhance snow-phase organic concentrations, although the science of organic gas-to-snow partitioning is yet undeveloped. Estimates of snow-vapor phase partitioning coefficients have found that Henry's law does not fit observed partitioning; rather, linear free energy relationships provide a better fit (Roth et al., 2004). In addition, partitioning coefficients for formaldehyde were found to vary at below freezing temperatures (-5 to -35 °C) (Burkhart et al., 2002). Outside of temperature and pressure-dependent partitioning, other physical parameters that may be important are diffusion of gases through the firn pore space and snow grain metamorphosis. The ice sheet structure is generally characterized into three zones, the uppermost convective zone (0 to 10s of cm in depth) where strong winds have been detected at 15 cm below the snow surface (Albert and Shultz, 2002), the diffusive zone located below and extending to the pore close-off depth (~50-110 meters below the surface), and finally the nondiffusive zone (Sowers et al., 1992). In addition to the diffusion of gases through the snow pore space, snow grain size can potentially play an important role in air-to-snow partitioning. Given

the assumption that organics reside primarily in a quasi-liquid layer on the surface of snow and ice grains, the growth of snow grains after deposition (Sowers et al., 1992) can lead to lower overall surface area and potentially induce degassing from the snow. A recent study in the Norwegian Arctic found a strong association between their concentrations of PCBs and organochlorine pesticides with snow density (Herbert et al., 2005). It is likely that snow density change also impacts air-to-snow partitioning of organics in Greenland snow.

Numerous studies have recently sought to determine whether snow-phase contaminants undergo post-depositional photochemical reactions. The suggestion that photolysis may be occurring originated in the surprisingly high concentrations of organic gases (formaldehyde, formic acid, acetic acid) measured in the snow pore space and in the air above the snowpack (Dibb and Arsenault, 2002; Dibb et al., 1994; Hutterli et al., 1999; Jacobi et al., 2002). These observations led to field and laboratory studies seeking to detect and characterize the occurrence of photochemistry in snow and ice. Shading experiments on the Greenland Ice Sheet isolated sunlight as the driving force in generating alkenes and ethyl iodide in the snow pack (Swanson et al., 2002). Laboratory-created frozen mixtures of aromatics (notably at much higher concentrations than typical environmental conditions) were found to substantially degrade on the order of hours to days at both the snow surface and at 10 cm below the snow on Spitsbergen Island, located in the Arctic (Klan et al., 2003). Laboratory studies have found that ambient snow can produce formaldehyde and acetaldehyde upon UV irradiation (Grannas et al., 2004) and that oxidation of aromatics mixed with hydrogen peroxide can occur at

temperatures of -20 to -180 °C (Dolinova et al., 2006). Several studies have looked into the formation of the highly reactive hydroxyl radical in snow, a likely agent in photo-degradation of snow-phase organics. Laboratory studies suggest that frozen hydrogen peroxide photolysis produces a significant portion of the hydroxyl radical in snow (Chu and Anastasio, 2005). Field measurements during summertime at Summit, Greenland measured the hydroxyl radical at surprisingly high levels, comparable with concentrations observed in the tropical marine boundary layer (Sjostedt et al., 2007). With shallow e-folding depths (~ 4-11 cm) of actinic flux on the Greenland Ice Sheet (Galbavy et al., 2006), it is expected that photochemical reactions only occur near the surface of the snow pack. Given the apparent active photochemistry observed during sunlit conditions in the Arctic and in laboratory conditions, it is hypothesized that snow-phase organics (particulate and water-soluble) degrade in sunlit surface snow on the Greenland Ice Sheet and produce a flux of organic gases emerging from the snow pack.

6.4 Research Objectives

The nature of carbonaceous particulate matter on the Greenland Ice Sheet is currently not well understood, with only limited measurements available for species entrapped in the snow and no direct measurements made of organic and elemental carbon in the atmosphere above the ice sheet. Also, it is a current open question whether carbonaceous particulates are well-preserved after deposition to the snowpack, providing the opportunity for their use as tracers of atmospheric history in ice cores.

To provide information on the levels and chemical stability of carbonaceous particulate matter on the Greenland Ice Sheet, two field campaigns to the Greenland Ice Sheet took place in 2005 and 2006. For comparison purposes, measurements were also taken at the remote Niwot Ridge in Colorado in the winter of 2006. This area of Colorado was selected for its distance from sources, high-elevation location (similar elevation as Summit, Greenland), long-lasting snow coverage, and for the likelihood that higher air and snow concentrations would exist and allow for additional analyses.

The objectives of the study are to:

1. Quantify the levels of carbonaceous particulate matter and related species in the air and snow on the Greenland Ice Sheet
2. Determine whether carbonaceous particulate matter undergoes chemical alteration after deposition to snow.
3. If post-depositional processing is occurring, determine potential mechanisms controlling the chemical alteration.

CHAPTER 7: METHODS

7.1 Field Sites and Sampling Overview

7.1.1 Summit, Greenland

Two field campaigns took place to measure carbonaceous particulate matter on the Greenland Ice Sheet. The first was a short field mission during July 2005 to test our ability to measure carbonaceous species and also to provide samples for co-researchers at the University of Wisconsin-Madison. The second campaign was an 8-week set of measurements from 29 May-20 July 2006, with simultaneous field sampling conducted by our project partners at the University of Wisconsin-Madison and the University of New Hampshire.

Sampling in the summers of 2005 and 2006 took place near Summit Camp, located at the highest point of the Greenland Ice Sheet (72° N, 38° W, elevation 3200 m). Figure 14 provides a map of the Summit's location on the ice sheet and Figure 15 is a photo of Summit, Camp.

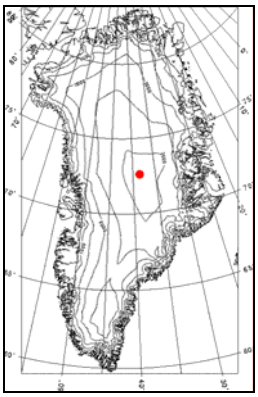

Figure 14. Location of Summit, Greenland (source: zero.eng.ucmerced.edu)

Figure 15. A view of Summit, Greenland taken from the Swiss Tower, located in the clean air sector. To the left are the living quarters (yellow tents) and heated kitchen structure ("Big House"). On the right side are the heated laboratory ("Green House") and various camp equipment. A Twin Otter can be seen taking off in flight near the horizon on the right side of the photo.

The 2005 set of field measurements were taken near the Swiss Tower as shown in Figure 16. During 2005, the influence of camp activity was found to significantly impact the atmospheric measurement of the particulate absorption coefficient. A complete coverage of those observations is provided in Appendix C. To avoid camp contamination during the 2006 campaign, sampling was moved to a satellite location about 1 km from the main camp and accessed during the sampling period by foot. In addition, integrated atmospheric filter measurements were controlled by a sector control system which cut off sampling during low winds (<0.5 m/s) or during winds from the camp direction. The sector control system included an anemometer, wind vane, and a datalogger linked to a

switched power strip. The computer code loaded onto the sector control datalogger is provided in Appendix C.

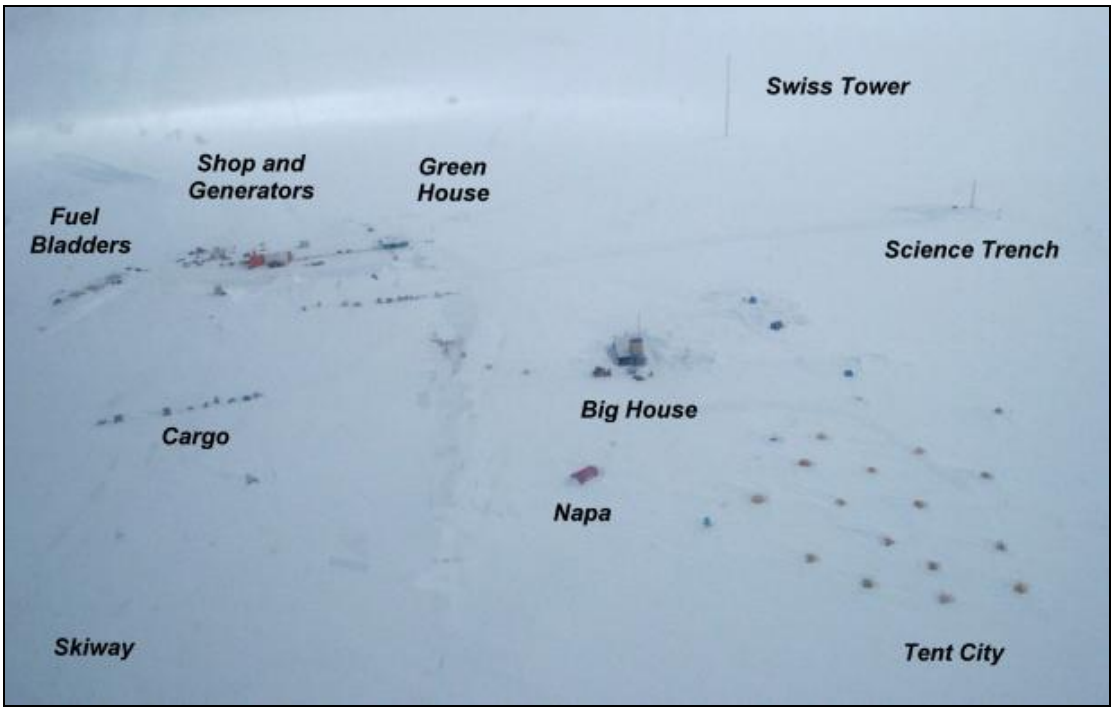

Figure 16. Spatial layout of Summit Camp (source: summitcamp.org)

An overview of the various measurements made at Summit, Greenland during the 2005 pilot sampling trip and the more extensive 2006 field season is provided (Table 8). The measured atmospheric species included filter-based measurement of particulate water-insoluble organic carbon (WIOC), particulate elemental carbon (EC), and particulate water-soluble organic carbon (WSOC). Optical measurements on the Greenland Ice Sheet included the absorption coefficient, calculated on a time basis of minutes to hours, and particle size-resolved number count measured every 1 minute. The carbonaceous particulate and water-soluble species were also measured in surface snow and in snow pits, along with major ions (Na^+, K^+, NH_4^+, Mg^{2+}, Ca^{2+}, Cl^-, NO_3^-, SO_4^{2-}), and water-

isotopes ($\delta^{18}O$ or $\delta^{2}H$). The laboratory and field sampling procedures associated with these measurements are described in detail in sections 7.2 and 7.3.

Table 8. Description of field sampling at Summit, Greenland

Sampling	Snow/Air	Summer 2005: July	Summer 2006: May-July
Snow pit (3 m):WIOC, EC, WSOC, major ions, isotopes ($\delta^{18}O$ or $\delta^{2}H$)	Snow	X	X
Daily surface snow: WIOC, EC	Snow	X	X
Hourly surface snow: WSOC	Snow		X
Distant snow pits (1 m): WIOC, EC	Snow		X
Absorption coefficient (σ_{ap})	Air	X	X
Particle size and count	Air		X
Integrated filters: WIOC,WSOC, EC	Air		X

7.1.2. Niwot Ridge, Colorado

Field measurements took place at the University of Colorado Mountain Research Station "Soddie Site" on Niwot Ridge, Colorado during January 5-11, 2006. The sampling site was located at coordinates 40º 02' 52" N, 105º 34' 15" W, elevation 3345 m and is shown in Figure 17. The sampling site was located near the tree line and accessed by foot (~3 mile trail and ~1500 vertical feet from base camp) during the sampling period. During the site set-up and break-down (and at other times during the winter season), a diesel-powered snow cat was driven to within 300 meters of the sampling site, with the remaining distance traveled by dragging equipment manually on sleds.

Figure 17. Location of Niwot Ridge, Colorado field campaign ("Soddie Site")

Given the higher concentrations of particulate species in the air and snow at Niwot Ridge, a greater variety of measurement techniques were employed. Additional measurements included snow-phase hydrophobic/hydrophilic WSOC and the atmospheric particulate scattering coefficient. A summary of the measurements conducted during the 2 week field campaign is provided in Table 9.

Table 9. Description of field sampling at Niwot Ridge, Colorado

Sampling	Snow/Air
Snow pit (1 m):WIOC, EC, WSOC, hydrophilic/hydrophobic WSOC, major ions	Snow
Daily surface snow: WIOC, EC	Snow
Hourly surface snow: WSOC, hydrophilic/hydrophobic WSOC	Snow
Particulate absorption coefficient (σ_{ap})	Air
Particulate scattering coefficient (σ_{sp})	Air
Particle size and count	Air
Integrated filters: WIOC,WSOC, EC	Air

7.2 Field Sampling and Instrumentation

7.2.1 Surface Snow Sampling

In all field campaigns, surface snow (approximately the top 1-3 cm of snow) was collected at time increments ranging from 1– 24 hours. On the Greenland Ice Sheet, each sample was collected at a distance approximately ½ km away from the satellite site, further into the clean air sector. On the Niwot Ridge, surface snow samples were collected in a clearing surrounded by sporadic coniferous trees – unfortunately, conducting sampling at altitudes above the tree line was unfeasible. Great care was taken to prevent contamination during all snow sampling. Operators faced into the wind, moved progressively upwind during subsequent sampling, and wore low-particulate vinyl gloves for all sampling. Snow samples were carefully collected using a glass scraper into 250 mL (WSOC) and 1 L (WIOC and EC) Kaptclean^{TM} glass sample jars with Teflon-lined plastic lids (Cole Parmer: EW-34605-70). The glass scraper and sample jars were cleaned by rinsing in ultrapure DI water and heated to 550° C for 12 hours. Lids were sonicated in ultrapure low-TOC DI water for 20 minutes and dried in an ISO Class 5* (Class 100) clean hood (Envirco Corp #10557). Prior to sampling, laboratory tests were performed to determine the effectiveness of the cleaning and are provided in Appendix C. After cleaning, sample bottles were tightly capped, externally rinsed with DI water, dried in the laminar flow hood, and sealed in Ziploc bags. Due to the high volume of carbon samples in the 2006 Greenland field campaign, sample jars were often recycled after in-field analysis by rinsing in ultrapure deionized water in-field and drying face-down in a clean hood. Laboratory tests found negligible carbon addition by the sample bottles.

7.2.2 Snow Pit Sampling

Snow pits, ranging in depth from 1-3 meters, were dug and sampled at all field campaigns to trace the recent history of deposited carbonaceous particulate matter. Snow pits were dug by researchers wearing full clean room apparel, using DI-rinsed shovels and saws that had no paint markings. Snow pits were oriented so that the researcher was facing into the wind while sampling. To prevent any contamination to samples by the digging process, a pre-cleaned glass scraper was used to scrape away ~5 cm of snow from the exposed face of the wall prior to sampling. Samples were collected by pushing sample jars into the snow pit wall. Samples for carbonaceous species were collected in precleaned glass jars, with the cleaning process for these samples described above in section 7.2.1. Snow pit ion samples were collected in pre-cleaned HDPE bottles and isotope ($\delta^{18}O$ or $\delta^{2}H$) sample volumes (20 mL) were aliquotted from WIOC/EC samples.

Snow pit samples were collected at increments of 5-10 cm, with replicate samples taken periodically in each snow pit. Given the large volume (5-10 L) needed for the carbonaceous particulate measurement, duplicates were collected by alternating collection of 1 L samples across the snow pit face to avoid issues with spatial variability in concentration. An image of a snow pit collected at Summit, Greenland is provided below (Figure 18). After sampling, snow-filled sample jars were immediately packed into insulated boxes and kept at a below-freezing temperature until later laboratory processing and analysis.

Figure 18. Sampling a 1 meter snow pit located 20 km south of Summit, Greenland in 2006. On the right side of the pit are depth markers (10 cm).

7.2.3 Atmospheric Sampling

Atmospheric samples included integrated filter samples (24-80 hours of run time) and real-time sampling of particulate optical properties. Integrated samples for the measurement of particulate elemental and organic carbon (EC, WIOC, WSOC) were collected on 25 mm quartz fiber filters (Pall Corp: #2500 QAT-UP, 25 mm) in stainless steel filter holders (Pall Corp: #1209). In Colorado, filter samples had mass flow rates of 13.1 lpm measured with a NIST traceable dry gas meter (ID #C-0701), with the nominal 16.7 lpm flow rate (set by a critical orifice) reduced by lower air pressure at high altitude. An approximate 3.0 μm D_{50} size cut was performed using a $PM_{2.5}$ cyclone rated for 16.7 lpm (URG-2000-30EH). In Greenland (Summer 2006 only), filter samples were collected at a mass flow rate of 18.1 lpm downwind of 16.7 $PM_{2.5}$ cyclones, yielding an approximate 2.3 μm D_{50} size cut. In both Colorado and Greenland, field blanks were

taken by loading a sample filter into a filter holder, unloading, and analyzing alongside the ambient samples.

Optical atmospheric measurements included particulate absorption (σ_{ap}) using a Particle Soot Absorption Photometer (PSAP), and particle size-resolved number count using a LASAIR optical particle counter. Additionally, the higher atmospheric particulate concentrations at Niwot Ridge allowed for the measurement of particulate dry scattering (σ_{sp}) via a nephelometer. To remove moisture prior to sampling in the nephelometer, the incoming sample air stream passed through a membrane-lined tube with an opposing air flow of low relative humidity (stripped of moisture by passing the air through a silica gel column). A view of the optical instrumentation set-up for the Niwot Ridge campaign is provided in Figure 19.

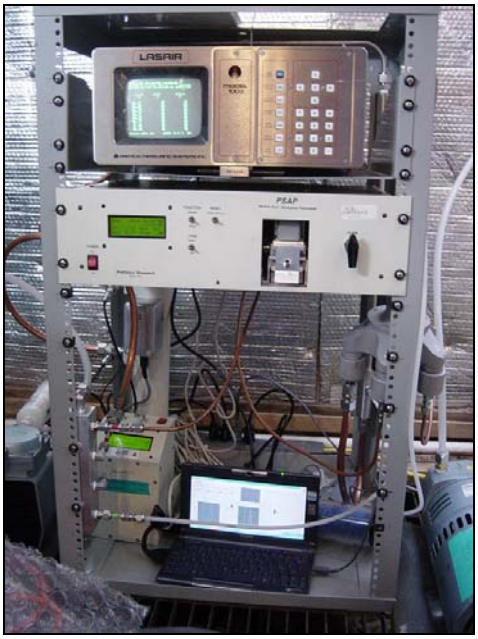

Figure 19. Instrumentation used during the Niwot Ridge, Colorado field campaign, including LASAIR (top), PSAP (below LASAIR), nephelometer (bottom left), and computer datalogger (bottom center).

The operation of the LASAIR and nephelometer is via laser-beam scattering of airborne particles, producing essentially instantaneous measurements that are reported as 1-minute averages. Given that the nephelometer has greater instrumental noise than the LASAIR, it has a higher detection limit for measuring ambient particulate samples and thus could not be used on the Greenland Ice Sheet. The PSAP, however, operates by accumulating particles on a filter and calculating absorption from a gradual laser (λ = 565 nm) transmittance drop with time. Thus, the PSAP collection mechanism can allow for variable time periods of measurement and is suitable for measurement on the pristine Greenland Ice Sheet.

The LASAIR instrument measures particle number concentration in a series of size bins: 0.1-0.2 μm, 0.2-0.3 μm, 0.3-0.4 μm, 0.4-0.5 μm, 0.5-0.7 μm, 0.7-1.0 μm, and 1.0-2.0 μm. This data was used to approximate $PM_{0.1\text{-}1.0}$, assuming a diameter at the midpoint of the size bin and a particle density of 1 g cm^{-3}. The calculation is provided below and a copy of the computer code (IGOR) is provided in Appendix C:

$$PM_{0.1\text{–}1.0} = \sum_i \frac{\frac{4}{3}\pi r_i^3 \cdot \rho_p \cdot C_i}{Q \cdot t}$$ for bins (i) covering 0.1 – 1.0 μm, ρ_p is particle density, C_i is the number count, Q is the flow rate, and t is the sample time interval.

Given the low particulate concentrations at Niwot Ridge and on the Greenland Ice Sheet, σ_{ap} was calculated on a varying time increment (minutes to hours) based on requiring a transmittance drop of 0.003. The transmittance drop requirement was set to balance the desire for high-frequency samples and avoid erroneous measurements from instrument

noise. Calculation of the absorption coefficient is as follows and the associated computer code is provided in Appendix C, including an empirical manufacturer calibration found to properly correct for filter media biases at transmittance levels > 0.7 (Bond et al., 1999):

$$\sigma_{ap,i}{}' = \frac{A}{Q \cdot t_i} \ln\left(\frac{I_o}{I}\right)$$

$$\sigma_{ap,i} = \frac{\sigma_{ap,i}{}'}{2\left(0.5398 \cdot \left(\frac{I_o + I}{2}\right) + 0.355\right)}$$

where A is the impacted filter area, Q is the flow rate, t_i is the time period of the sample measurement, and I_o/I represent the initial/final transmittance through the filter.

For optical measurements conducted on the Greenland Ice Sheet in 2006, an additional program was developed to filter out time periods flagged for camp contamination by the sector control system. The computer code used to filter the LASAIR and PSAP datasets is also provided in Appendix C. Camp contamination was not a concern at Niwot Ridge, given the ~3 mile distance and 1500' altitude change from the base camp to the sampling site.

7.3 Laboratory Analyses

7.3.1 Snow Samples

Collection of particulate WIOC and EC was performed by melting and weighing 10 L of snow, followed by filtering through quartz fiber filters and drying in pre-fired aluminum-lined Petri dishes under a clean hood. Although the quartz fiber filters are rated at a nominal pore size of 700 nm, liquid-filtration particle collection efficiencies of 95% or higher have been previously reported (Ducret and Cachier, 1992; Lavanchy et al., 1999), explained by the tortuous pathway through the filter media. Lavanchy et al. (1999) used a gravimetric approach to observe the collection efficiency, while Ducret and Cachier (1992) measured particles collected on a 100 nm filter after passing water samples through a quartz fiber filter. Thus, it can be roughly estimated that the quartz fiber filters capture 95% of particles greater than 100 nm, while the collection-efficiency of smaller particles is currently unknown. After filtration, all filter samples were kept at below-freezing temperatures until later analysis at the Georgia Institute of Technology. WIOC and EC were quantified using a Sunset Laboratory carbon analyzer following the NIOSH protocol of thermal evolution and combustion (Birch and Cary, 1996). Any contamination due to handling was investigated by collecting frequent laboratory blanks, which involved placing a quartz fiber filter on the filtration flask, rinsing with 50 mL of ultrapure water, then allowing to dry alongside ambient samples in the clean hood. To ensure the analyzer's accuracy, sucrose standards were regularly run at concentrations from 5.0 μgC cm^{-2} to 25 μgC cm^{-2}, covering the range measured in the snow samples.

WSOC samples were melted and measured using a Sievers 900 UV-oxidation-based carbon analyzer with an in-line quartz fiber filter as the operationally-defined split between WSOC and WIOC. Reliable detection of very low levels of WSOC (<40 μg C kg^{-1}) was achieved by preacidying samples using phosphoric acid (~20 μl, 85% H_3PO_4) to lessen the potentially interfering signal of inorganic carbon. Laboratory tests were performed prior to analysis to determine no additional background WSOC was added by the pre-acidification step. For further description on the preacidification process, please refer to Appendix C. In addition, WSOC standards (potassium hydrogen phthalate, 100 – 300 μg C kg^{-1}) were routinely run to monitor the performance of the carbon analyzer.

Additional WSOC analysis for the Niwot Ridge snow samples included measuring the hydrophobic/hydrophilic fractions via XAD-8 column separation. This technique was recently developed to study atmospheric particulate WSOC and has been described in recent literature (Sullivan and Weber, 2006a). Briefly, the hydrophobic/hydrophilic WSOC fractions are determined by passing a melted and filtered snow sample through an XAD-8 column at a pH of 2 (with HCl added prior to column extraction), with hydrophilic WSOC defined as the fraction of WSOC that penetrates the XAD-8 column and quantified using the Sievers 900 carbon analyzer. The hydrophilic portion of WSOC appears to include short-chained (<4-5 carbon atoms) carbonyls and aliphatic carboxylic acids, amines, and saccharides, while the hydrophobic portion contains longer-chained (>3-4 carbon atoms) carbonyls and aliphatic carboxylic acids, aromatic acids, phenols, organic nitrates, and cyclic acids (Sullivan and Weber, 2006a). While hydrophobic bases also appear to penetrate the XAD-8 resin and are quantified as hydrophilic WSOC, past

research has suggested the contribution of hydrophobic bases is <1% for atmospheric aerosols (Sullivan and Weber, 2006b).

Major ions (Na^+, K^+, NH_4^+, Mg^{2+}, Ca^{2+}, Cl^-, NO_3^-, SO_4^{2-}) were measured at the University of New Hampshire by ion chromatography. Isotopes of water used for dating ($\delta^{18}O$ or δ^2H) were measured at the University of Washington by mass spectrometry with Cr reduction of H_2O. Water-isotopes in the environment include a combination of the isotopes of their individual elements, including ^{16}O (99.76%), ^{17}O (0.04%), ^{18}O (0.2%), ^1H (99.98%), and ^2H/deuterium (0.16%). After evaporation, water vapor will condense to form precipitation, with higher enrichment in heavier isotopes (^{18}O, ^2H) occurring at warmer temperatures. Thus, paleoclimatology can use ratios of water-isotopes in snow and ice as a proxy for temperature and is a common method used in dating ice cores. Using the Standard Mean Ocean Water as a reference, isotope ratios are calculated as follows:

$$\delta^{18}O = \frac{\left(\frac{^{18}O}{^{16}O}\right)_{sample} - \left(\frac{^{18}O}{^{16}O}\right)_{SMOW}}{\left(\frac{^{18}O}{^{16}O}\right)_{SMOW}} * 10^3$$

$$\delta^2H \text{ or } \delta D = \frac{\left(\frac{^{2}H}{^{1}H}\right)_{sample} - \left(\frac{^{2}H}{^{1}H}\right)_{SMOW}}{\left(\frac{^{2}H}{^{1}H}\right)_{SMOW}} * 10^3$$

7.3.2 Integrated Filter Samples

Atmospheric filter samples were analyzed for particulate WIOC and EC using a Sunset Carbon Analyzer, using the thermal/optical transmittance technique (Birch and Cary, 1996). For a number of atmospheric filters, the extremely low EC concentrations required overlaying two filter punches in the Sunset Carbon Analyzer to achieve detectable mass. Prior tests were conducted to ensure that this would give accurate results and are provided in Appendix C. In addition, WSOC was quantified by placing a filter punch into 10 mL of ultrapure water, sonicating for 40 minutes, and then analyzing on the Sievers 900 carbon analyzer with an in-line quartz fiber filter. Given that the WSOC concentrations were high (>150 μg C kg^{-1}), pre-acidification using phosphoric acid was unnecessary and this step was not used in analysis. Field blanks were also analyzed along with the ambient samples for WIOC, EC, and WSOC.

CHAPTER 8: RESULTS AND DISCUSSION

8.1 Foreword

This section describes results from the 2006 field campaigns to the Greenland Ice Sheet (sections 8.2-8.4) and Niwot Ridge, Colorado (section 8.5). The 2005 field campaign to Summit, Greenland was a short-term pilot study to develop our measurement techniques. Results from the 2005 field campaign were used to initially assess the importance of camp impact on atmospheric measurements of carbonaceous particulate matter (Appendix C) and to determine the expected concentration range of snow-phase carbonaceous species. Snow-phase results from the 2005 field campaign are provided in Appendix D.

8.2 Organic Carbon Record in Snow on the Greenland Ice Sheet

8.2.1 Concentrations and Dating of Snow Pit Samples

Concentrations of particulate and water-soluble carbonaceous species in the 3-meter snow pit are shown in Figure 20, with δ^2H, calcium (Ca^{2+}), potassium (K^+), and sulfate (SO_4^{2-}) also provided for reference. Past summer layers are shaded in Figure 20 and were estimated by the seasonal temperature-dependent fluctuations in δ^2H (Figure 20d) and using Ca^{2+} (Figure 20e) as a known springtime marker (Dibb et al., 2007). However, isolating the 2005 summer period was challenging due to a noisier δ^2H signal. An additional calculation of a secondary summer marker, the ratio of Cl^-/Na^+, was performed (shown in Appendix D) and, using all three data sets, the layer 50-70 cm was isolated as the most reasonable selection for Summer 2005.

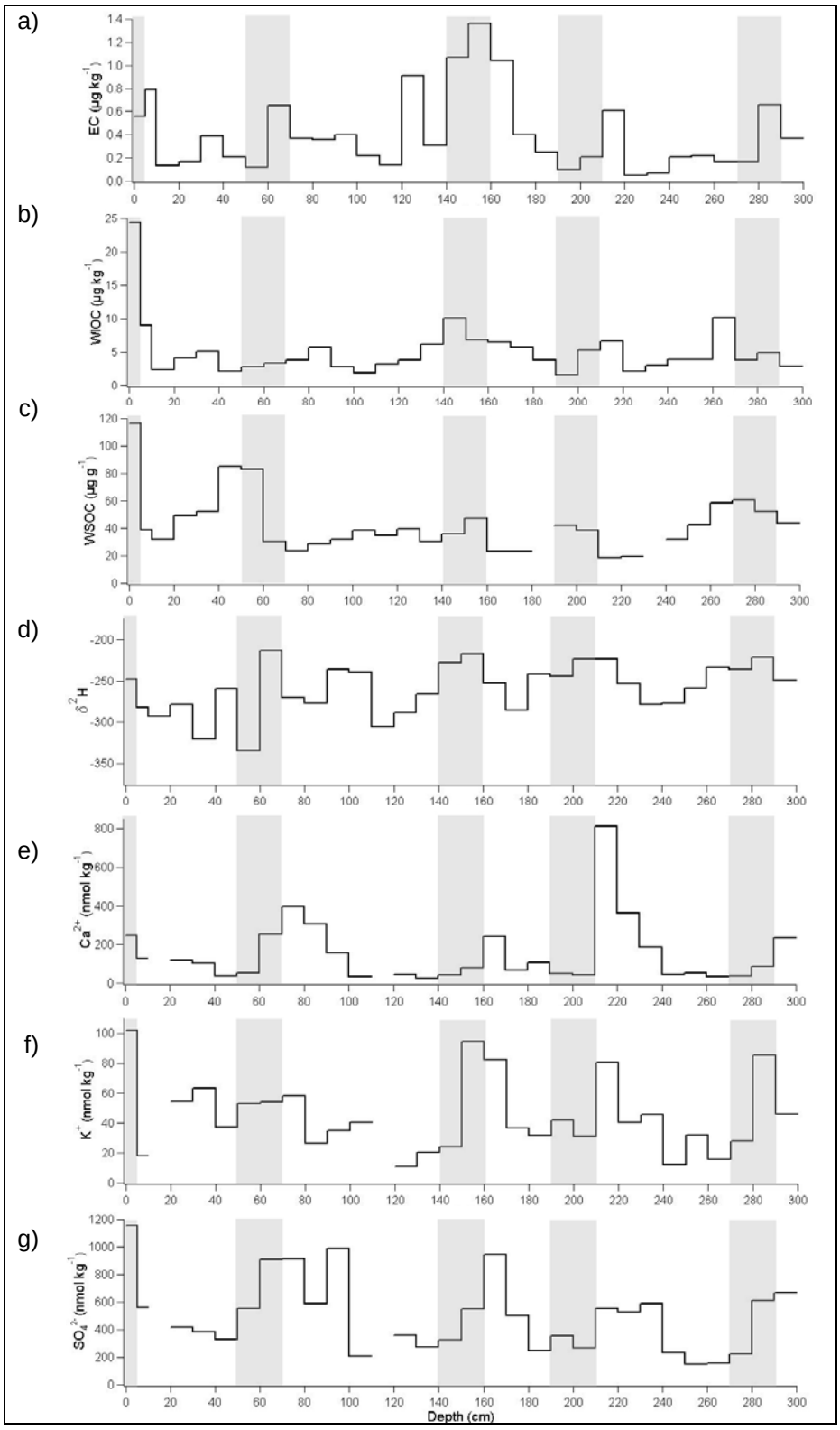

Figure 20. 3-meter snow pit profiles of elemental carbon(a), water-insoluble organic carbon(b), water-soluble organic carbon(c), deuterium ratio(d), calcium ion(e), potassium ion(f), and sulfate ion(g). Estimated summer periods are shaded.

Given the large sampling increments (10 cm) in the snow pit, the past summer months can not be as precisely isolated as with smaller-increment sampling (e.g. 3 cm), a limitation imposed by the large volume of snow required to measure particulate carbonaceous species. Thus, the isolated past summer layers do not represent a precise series of days, but rather isolate a snow layer that appears to have deposited during past summer months (May to August). Past summer layers selected were 50-70 cm (2005), 140-160 cm (2004), 190-210 cm (2003), and 270-290 cm (2002).

Particulate elemental (EC) and water-insoluble organic carbon (WIOC) were detectable at all levels of the 3-meter snow pit as shown in Figure 20a-b. Duplicates at 50, 100, 150, 200, and 250 cm had an average difference of 2.1 $\mu g\ kg^{-1}$ for WIOC and 0.20 $\mu g\ kg^{-1}$ for EC. Numerous field blanks (quartz fiber filters placed in the filtration apparatus, rinsed with 50 mL of ultrapure water, and allowed to dry alongside the sample filters) were found to have detectable WIOC (1.1 ± 0.49 $\mu g\ cm^2$ filter area) but no measurable EC (<0.01 $\mu g\ cm^2$). Thus, blank-correction was only performed for WIOC, with variability in the blanks adding minor uncertainty compared to the average snow pit sample loading of 7.4 $\mu g\ cm^2$ filter area. From 5-300 cm in depth, approximate 4-year average WIOC and EC concentrations were 4.6 $\mu g\ kg^{-1}$ snow (range 1.7-10.7 $\mu g\ kg^{-1}$) and 0.4 $\mu g\ kg^{-1}$ (range 0.1-1.4 $\mu g\ kg^{-1}$), respectively.

8.2.2 Comparison With Past Measurements

To our knowledge, no previous measurements of EC and WIOC on the Greenland Ice Sheet have been made using the same analytical procedure, which prevents direct comparison. A rough comparison with past optical measurements of black carbon (BC)

in recent snow on the Greenland Ice Sheet puts our measured EC concentrations on the lower end of previously measured BC of 1-4 μg kg^{-1} in 1988-1989 snow (Cachier and Pertuisot, 1994) and 1.4-2.7 μg kg^{-1} in 1989-1990 snow (Chylek et al., 1995). Comparison with previously measured EC by an alternative thermal method finds our levels well below reported values of 4.2-30.1 μg kg^{-1} in 1994-1996 snow, although the authors mention that possible artifacts in their analysis may have induced the higher observed concentrations (Slater et al., 2002). Very limited measurements are available for comparison with WIOC, including a solitary measurement of 78 μg kg^{-1} for surface snow at Summit in 2001 (Grannas et al., 2004) and total particulate carbon (including BC) measured by coulometric analysis of 18-35 μg kg^{-1} in 1988-1989 snow (Cachier and Pertuisot, 1994). Our WIOC sample range (1.7-10.7 μg kg^{-1}) is significantly lower, although direct comparison is again difficult due to different analytical techniques.

Water-soluble organic carbon in the 3-meter snow pit is shown in Figure 20c. Prior analysis of spatial variability in snow concentrations, taking 4 sets of 5 co-located samples, determined a relatively constant standard deviation of 24 μg kg^{-1} for sample sets averaging 88-112 μg kg^{-1}. The variability in side-by-side measurements is expected to be lower for snow pit replicates in comparison to surface snow, given the higher likelihood of human error in collecting homogenous surface snow layers. Based upon this, two layers (180-190 cm, 230-240 cm) of the 3-meter pit were flagged for contamination concerns and removed from analysis due to duplicate differences exceeding 2σ (48 μg kg^{-1}). Excluding these two layers, the 5 cm-300 cm average WSOC concentration was found to be 40.5 μg kg^{-1} (ranging 18.3-84.9 μg kg^{-1}) and duplicates at approximately

every layer had an average difference of 7.9 μg kg^{-1}. This WSOC observed range is on the lower end of 30-320 μg kg^{-1} reported using a similar analytical process for a 2.3 m snow pit in 1984 near Dye 3, Greenland (Twickler et al., 1986), the difference in location and time likely playing a major role in the dissimilarity of measured WSOC. A much higher level of WSOC (~480 μg kg^{-1}) was quantified in a Summit surface sample in 2001, although a difference in analytical methods and the lack of multiple measurements limits comparison (Grannas et al., 2004).

8.2.3 Trends Observed in Snow Pit Carbonaceous Species

As seen in Figure 20, all carbonaceous species appear to oscillate seasonally, with higher levels observed in the late-spring or summer and lowest levels in the winter. Sulfate and potassium (Figures 20f and 20g) have similar spring/summer maxima, which may be a combination of meteorology and source types (biomass burning and fossil fuel combustion) related to the carbonaceous species. An observed prominent summer maximum in EC in 2004 is likely linked to emissions from major forest fires in Alaska and Canada (Stohl et al., 2006). Potassium, a common indicator of biomass burning, is also seen to have maximum snow pit concentrations during this period. Averaging over the buried snow pit layers (5-300 cm, with layers 180 cm and 230 cm excluded), it appears WSOC makes up the vast majority (88%) of carbonaceous species in Greenland Snow, with substantially lower fractions in WIOC (11%) and EC (1%). The particulate-phase ratio of WIOC/EC (11:1) is similar to atmospheric particulate OC/EC ratios at background sites in the Northern Hemisphere (Carrico et al., 2003a; Lee et al., 2001; Tanner et al., 2004). However, adding the WSOC fraction leads to an extremely high ratio of total OC/EC (99:1) compared with typical atmospheric carbonaceous particulate

matter. These results suggest either the oxidation of EC (which is usually considered inert) or, possibly, that gaseous organics are a source of OC in Greenland snow.

In order to determine whether buried snow pit layers are representative of surface deposition, previous summer layers (50-70 cm, 140-160 cm, 190-210 cm, and 270-290 cm) were selected for approximate comparison with surface snow collected daily throughout the summer campaign. As shown in Table 10, WSOC and WIOC are at higher concentrations in the surface layer than in lower layers, with past summer concentrations averaging 56% and 59% lower than the surface, respectively. In contrast, the buried summer layers have average EC only 10% lower than the 2006 summer snow. Assuming EC is conserved after deposition and acts as a tracer for the original levels WSOC and WIOC, an EC-corrected loss of ~46-49% can be estimated for the organic fraction after deposition. It is interesting that while the concentration of EC in 2004 is more than double its 2006 surface snow level, WSOC and WIOC in 2004 are still substantially lower than their 2006 average. Assuming biomass-burning emissions in the summer of 2004 were the major source of the buried EC (Stohl et al., 2006), one would expect similarly high OC levels in the 2004 snow; thus, it appears there was a substantial loss in the particulate and water-soluble OC record. However, while EC is at consistently higher ratios-to-surface relative to WSOC and WIOC in 2002, 2004, and 2005, year 2003 stands out as an exception with all three species within similar ratio range. Given that 2003 also has the lowest EC concentrations (all other years are over a factor of 2 higher), this observation may be explained by a different combination of sources impacting carbonaceous particulate matter reaching the Greenland Ice Sheet in 2003. For example,

air masses reaching Summit may have contained carbonaceous particulate matter mainly from high OC/low EC sources, such as the gas-to-particle conversion of plant emissions.

Table 10. Comparison of surface snow with buried summer snow layers

	WSOC		WIOC		EC	
Time period	C ($\mu g\ kg^{-1}$)	Ratio to surface	C ($\mu g\ kg^{-1}$)	Ratio to surface	C ($\mu g\ kg^{-1}$)	Ratio to surface
Surface (5/30-7/20/06)	111.1	1.00	11.9	1.00	0.60	1.00
Summer 2005	56.9	0.51	3.1	0.26	0.39	0.64
Summer 2004	41.6	0.37	8.4	0.71	1.21	2.02
Summer 2003	40.3	0.36	3.5	0.29	0.16	0.26
Summer 2002	56.4	0.51	4.4	0.37	0.41	0.69

Given the higher frequency (every 4-6 hours) surface snow sampling for WSOC that took place from 12 June to 20 July 2006, it is possible to compare average daily maximum/minimum concentrations with buried summer layers to provide upper and lower estimates of loss. Average daily maximum (129.8 $\mu g\ kg^{-1}$) and minimum (72.6 $\mu g\ kg^{-1}$) surface WSOC concentrations for this period correlate to an average WSOC difference in the buried summer layers of 62% (52% EC-corrected) and 33% (23% EC-corrected), respectively. Since the relative contribution of wet and dry deposition to snow for WSOC has yet to be explored, the daily maximum can be considered as either fresh deposition prior to degradation and/or the upper end of a temperature-dependent cycle. Similarly, the averaged daily minimum WSOC can be understood as either partially or fully-degraded WSOC and/or the lower end of a temperature-dependent cycle. The fact that the average daily minimum WSOC is significantly higher than aged summer layers implies that post-depositional processes, such as photochemical reactions, play a role in depleting organics in the snow pack.

8.3 Time Series of Organic and Elemental Carbon on the Greenland Ice Sheet

8.3.1 Atmospheric Concentrations and Transport

A summary of atmospheric OC, EC, WSOC, σ_{ap}, and $PM_{0.1\text{-}1.0}$ is provided in Table 11, with a time series representing over 50 days of sampling shown in Figure 21. Additional information provided in Figure 21 includes plots of particle number concentration and the estimated origin of the sampled air mass as determined by clustering of 10-day back-trajectories. Isobaric 10-day back-trajectories were calculated for each sampling day and clustered with the Hybrid Single-Particle Lagrangian Integrated Trajectory (HYSPLIT) model (Draxler and Rolph, 2003) using FNL reanalysis data of the NCEP/GDAS meteorological model output. With the exception of one day (10 June 2006), all sampling days were fit to four clusters, with the clustered mean trajectories shown in Figure 22. The majority (71%) of sampling days had 10-day trajectories constrained to the area near the Greenland Ice Sheet (cluster 2) or from the northeastern part of North America (cluster 1), with only a few sampling days represented by longer trajectories arriving from over Alaska (cluster 3) or the Asian continent (cluster 4). Our findings agree with prior results from a long-term analysis of 10-day back-trajectories reaching Summit, Greenland that observed summertime trajectories to have generally shorter paths and a large fraction (46%) to originate over North America (Kahl et al., 1997).

Table 11. Concentrations of atmospheric species at Summit, Greenland during Summer 2006

Species	Sampling	Dates	Averaging period	Concentration	Units
OC	filter collection	27 May-20 July	80 hours	63 ± 28	ng m^{-3}
EC	filter collection	27 May-20 July	80 hours	8 ± 5	ng m^{-3}
WSOC	filter collection	27 May-20 July	80 hours	55 ± 29	ng m^{-3}
$PM_{0.1\text{-}1.0}$	OPC	28 May-18 July	1 minute	177 ± 162	ng m^{-3}
σ_{ap}	PSAP	28 May-18 July	minutes to hours	0.15 ± 0.13	Mm^{-1}

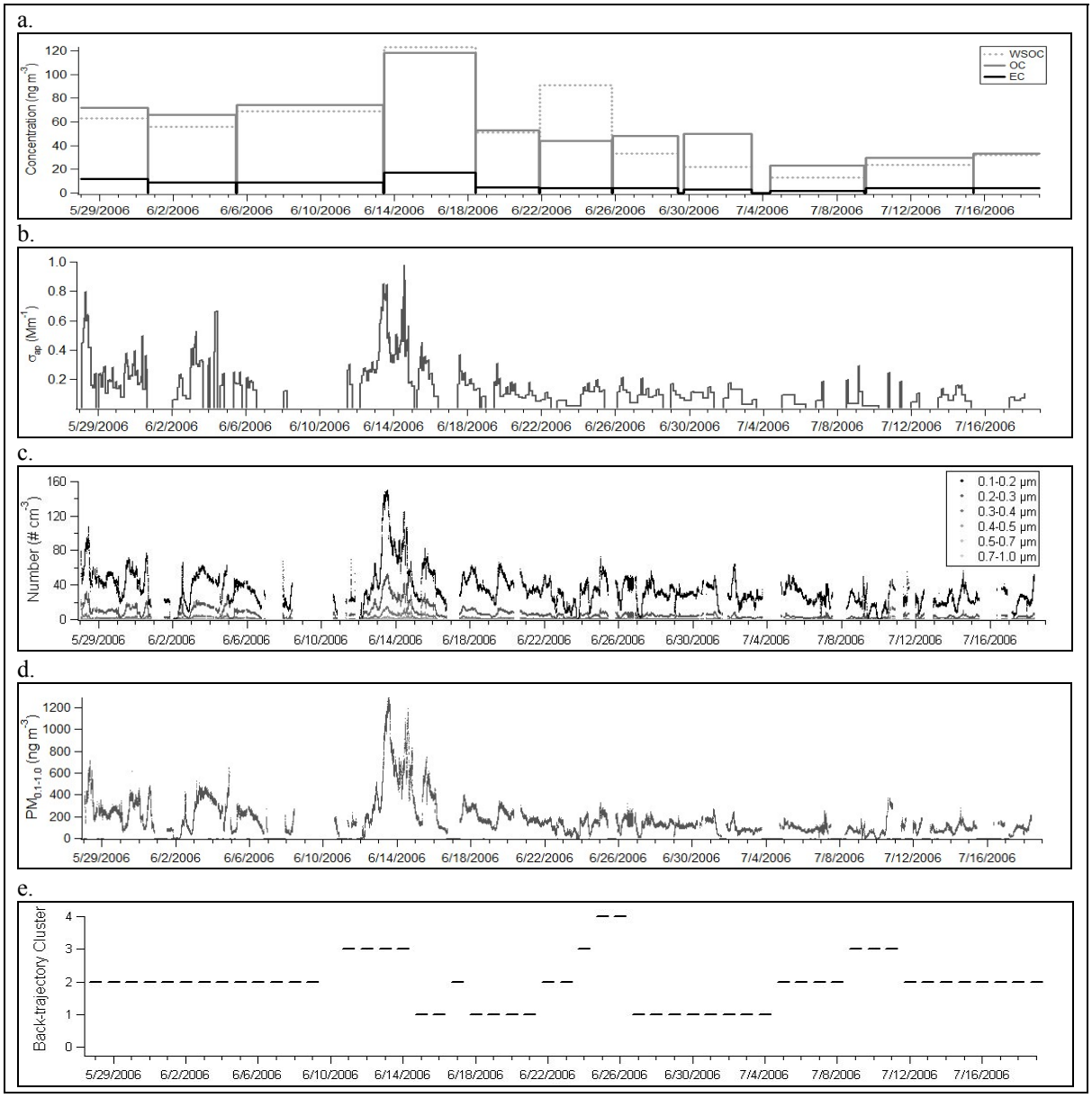

Figure 21. A time series of particulate measurements in the atmosphere of Summit, Greenland during Summer 2006, including carbonaceous particulate matter (a) the absorption coefficient (b), number concentration (c), $PM_{0.1\text{-}1.0}$ (d), and each sampling day's associated back-trajectory cluster (e).

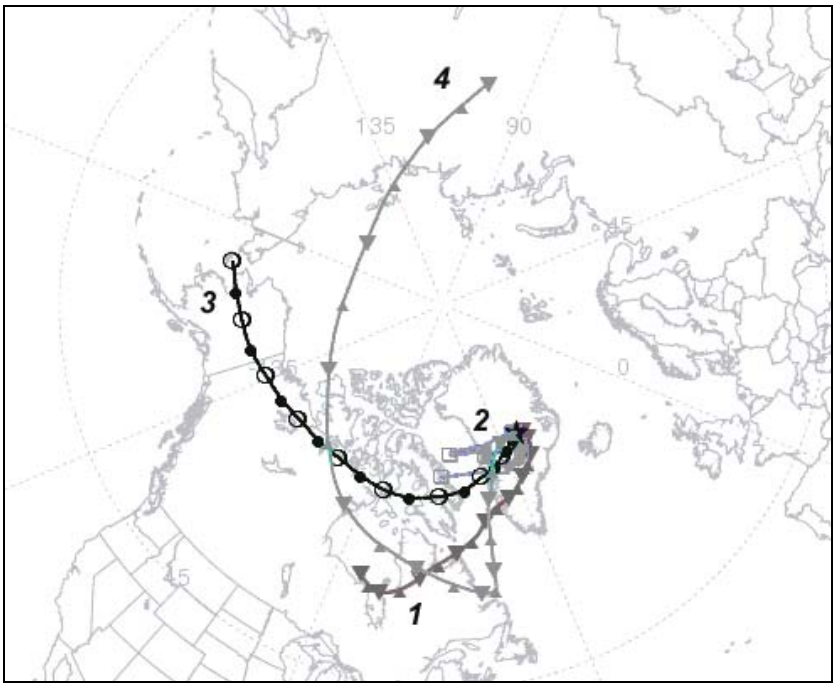

Figure 22. Mean clustered 10-day back trajectories for 28 May 2006 – 19 July 2006. Each cluster contains a varying number of sampling days, with 27% of the days in cluster #1, 54% in cluster #2, 15% in cluster #3, and 4% in cluster #4.

Filter-based concentrations during the first four measurement periods (representing 27 May 2006 to 18 June 1006) were high enough to allow for duplicate measurement of OC and EC. Duplicates were found to be very close for OC (averaging 8 ng m^{-3} or 11%) but had higher difference for EC (averaging 4 ng m^{-3} or 36%). Given that OC makes up the majority (~90%) of the particulate carbon mass measured at Summit, a small difference in the analytical split point between OC and EC for two duplicates results in a magnified change in EC. WSOC duplicates were found to be within close range (averaging 1 ng m^{-3} or 2%), although variability in blanks contributes to higher uncertainty (2-3 ng m^{-3} or contributing 2-17% uncertainty dependent on the sample concentration). WSOC constitutes a large fraction of the particulate OC (Figure 21a). While the fifth sampling period (initiated late on 21 June 2006) has WSOC values within range of other

atmospheric samples, the WSOC/OC fraction is far greater than 1.0 and outside of the uncertainty estimated in the measurement. It is expected that there may have been either an underestimation of OC or overestimation of WSOC, with WSOC contamination also a possible issue for this sample. Excluding this time period, it is seen that WSOC constitutes, on average, 81±19% of OC in Summit carbonaceous particulate matter. For the first three periods, where WSOC and OC were measured directly from the same filter and duplicates were available, WSOC/OC has an even higher average of 0.89 (WSOC/OC duplicates ranging 0.84-0.99 throughout the three periods).

To our knowledge, no prior Summit data is available to directly compare with our measured levels of atmospheric particulate OC, WSOC, and EC. However, measurements made using the same collection and analytical methods are available for other locations in the Northern Hemisphere and may add perspective to our results. The OC, WSOC, and EC values determined for Summit, Greenland were much less than the 211 ng m^{-3}, 123 ng m^{-3}, and 20 ng m^{-3}, respectively, observed using identical measurement techniques at a remote high altitude (3345 m) site in the Colorado Rocky Mountains in January, 2006. Given the high altitude location of both Summit, Greenland and Niwot Ridge, Colorado, these concentrations likely represent the free troposphere. In addition to the absolute concentration comparison, the WSOC/OC ratio in Colorado is 0.52 on average, much lower than average WSOC/OC observed at Summit, Greenland. The WSOC/OC at Summit, Greenland was also much higher than past measurements reported in urban areas, such as Tokyo, Japan (monthly average WSOC/OC of 0.20-0.35) (Miyazaki et al., 2006) and St. Louis, USA (monthly average WSOC/OC of 0.31-0.64)

(Sullivan et al., 2004), both studies which used similar analytical techniques as this study although modified for higher frequency sampling. The substantially higher WSOC/OC observed at Summit, Greenland suggests the oxidation of primary organic carbon aerosol during transport and/or the significant contribution of secondary organic aerosol to particulate carbon mass. This result also suggests that water-based collection of WSOC (such as a mist-chamber or Particle-Into-Liquid Sampler) would be well-suited for the study of OC on the Greenland Ice Sheet.

Atmospheric OC and EC appear to be very highly correlated ($r = 0.94$), indicating common sources and/or source locations (Figure 23). Although well-correlated, the OC/EC ratio appears to have a wide range (6.4-16.2, average = 10), with generally higher ratios at lower EC concentrations. While the combination of high OC-EC correlation and highly water-soluble OC points to processed combustion emissions, the inconsistent OC/EC ratio suggests that the nature of emissions reaching Summit and degree of secondary organic aerosol formation likely varied throughout the summer. Only limited past research adds to our understanding of the nature of atmospheric particulate OC at Summit. One study described secondary particulate OC at Summit during a Canadian biomass burning event in 1994, reporting enhanced levels of particulate carboxylates at Summit relative to that of fresh biomass burning emissions (Dibb et al., 1996). Additionally, while gas/particle partitioning appeared to occur on an hourly basis concurrent with our atmospheric sampling (Anderson et al., 2007), the high correlation between OC and EC suggests that the multiday integrated filter samples appear to preserve the broader signal of emissions transported to the Greenland Ice Sheet.

After averaging σ_{ap} over the extended filtering time periods, an extremely high correlation was observed between the σ_{ap} and EC (r = 0.95) (Figure 24). Dividing average σ_{ap} by average EC results in an average estimated mass absorption cross-section (E_{ap}) of 24 m^2 g^{-1}. Equivalently, assuming a black carbon (BC) absorption cross-section of 10 m^2 g^{-1} (λ = 565 nm) leads to BC/EC slope of 2.4. Estimated E_{ap} at Summit, Greenland is similar to the 18.3 m^2 g^{-1} found in Atlanta, Georgia using identical measurement techniques (Carrico et al., 2003b). However, as observed in the Atlanta study (Carrico et al., 2003b) and described in a recent review of light absorbing carbon (Bond and Bergstrom, 2006), the estimation of E_{ap} varies depending the technique used to estimate EC mass. In addition, it is possible that other absorbing species besides EC, such as dust or absorbing organics, can contribute to the absorption value.

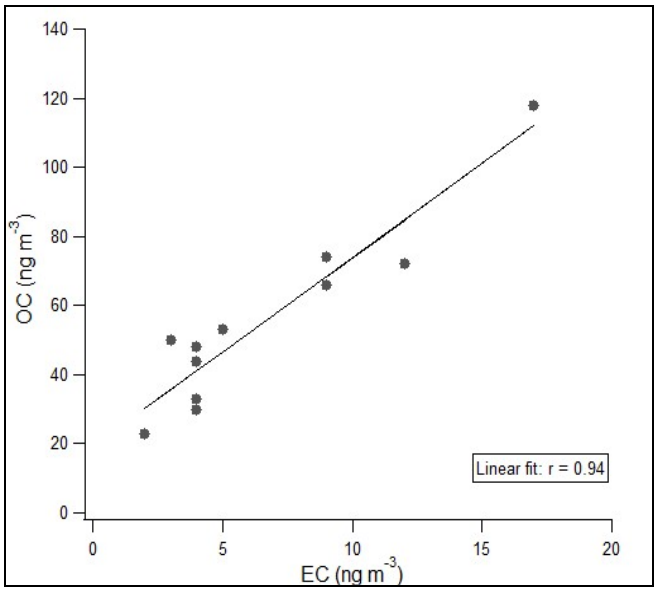

Figure 23. Relationship between atmospheric elemental carbon (EC) and organic carbon (OC).

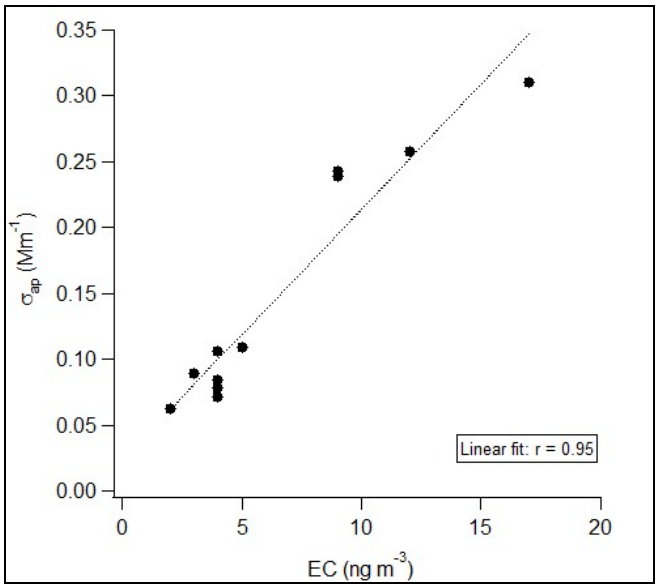

Figure 24. Relationship between atmospheric elemental carbon (EC) and the absorption coefficient (σ_{ap}).

As seen in Figure 21, the time period of June 13-14 stands out for the significant sustained increase observed in every measured aerosol property. During the filter sampling period covering most of this episode (June 13-18), OC and EC are higher than their summertime averages by 87% and 113%, respectively. Given that the integrated filter sampling did not perfectly line up with the high concentration episode, this is likely an underestimate of the actual increase. The higher frequency measurement of σ_{ap} and $PM_{0.1\text{-}1.0}$ found levels during 13-14 June at 197% and 290% higher than their summertime averages, respectively. Given that EC and σ_{ap} were seen to greatly increase, it is expected that some form of combustion emissions were transported to Summit, Greenland. The air mass pathways are displayed in Figure 25, with HYSPLIT-calculated trajectories displayed starting every 12 hours. It appears that the air mass tracked a path from northern Alaska/western Canada. Fire records from Canada (Canadian Forest

Service, 2006) indicate that active fires (155,000 acres) were occurring during the time period when back-trajectories passed over the region.

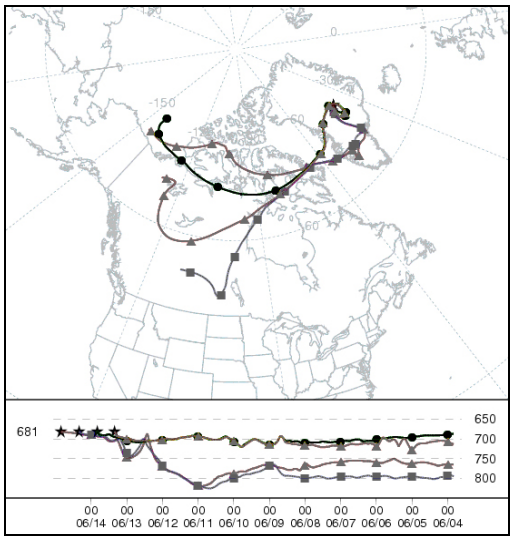

Figure 25. 10-day back-trajectories and pressure altitude (hPa) during the high particulate matter concentrations observed on June 13th and 14th, 2006.

8.3.2 Surface Snow Concentrations

The average surface snow concentrations of water-soluble organic carbon (WSOC), water-insoluble organic carbon (WIOC), and elemental carbon (EC) have been previously discussed to compare with a 3 meter snow pit (section 8.2) and are provided in Table 12 for reference. In addition, a time series of the measured surface snow concentrations are presented in Figure 26, as well as precipitation (snowfall and fog) as noted during each of our snow sample collections and including weather logs from science technicians at the research site. On average, duplicates (N = 18) for WIOC and EC in the surface snow were within 40% (3.5 µg kg^{-1}) and 36% (0.1 µg kg^{-1}), respectively. The more frequent collection of duplicates (N = 216) for WSOC had an average agreement of 34% (29.1 µg kg^{-1}). The agreement between surface snow

duplicates is less than what was observed in the 3 meter snow pit (section 8.2), likely due to the greater difficulty in collecting a uniform surface snow layer.

Concentrations of all snow-phase carbonaceous species (WSOC, WIOC, and EC) are observed to vary throughout the summer, with precipitation events appearing to occur either immediately prior or during spikes in concentrations (Figure 26). Unlike the prominent maxima observed in atmospheric particulate matter concentrations during June 13-14, WSOC, WIOC, and EC are found to have their individual maximum concentrations roughly a week prior. For high WIOC and EC concentrations occurring on June 2nd and June 8th, it is interesting to note that fog appears to be the dominant wet deposition mechanism. Surface snow WSOC also appears to have concentration spikes associated with fogs, with major increases on June 12th and June 18th occurring after isolated fog episodes (i.e. no snowfall had occurred for several days). Previous research has also found fog-based deposition to be important in the flux of ions to the Greenland Ice Sheet (Bergin et al., 1995).

Snowfall, in isolation from fog episodes, also appears to contribute to higher surface snow concentrations, such as on June 2nd (WIOC, EC), June 15th (WSOC, WIOC), July 4th (EC), and July 15th (WSOC). However, it should be noted that the occurrence of snowfall or fog does not always lead to a concentration spike in surface snow concentrations. As discussed in a model developed to link atmospheric and snow concentrations of aerosol species (Bergin et al., 1995), a number of factors impact the wet deposition flux of particulate species to snow, including the current atmospheric

particulate matter concentration and the properties of each snow/fog event (scavenging ratio, duration, intensity, and atmospheric height).

Table 12. Concentrations of snow-phase species at Summit, Greenland during Summer 2006

Species	Measurement	Dates	Frequency	Concentration	Units
WSOC	UV-oxidation	31 May-20 July	4-24 hours	111.1 ± 45.5	μg kg^{-1}
WIOC	Thermal/optical	29 May-20 July	24 hours	11.9 ± 7.1	μg kg^{-1}
EC	Thermal/optical	29 May-20 July	24 hours	0.6 ± 0.4	μg kg^{-1}

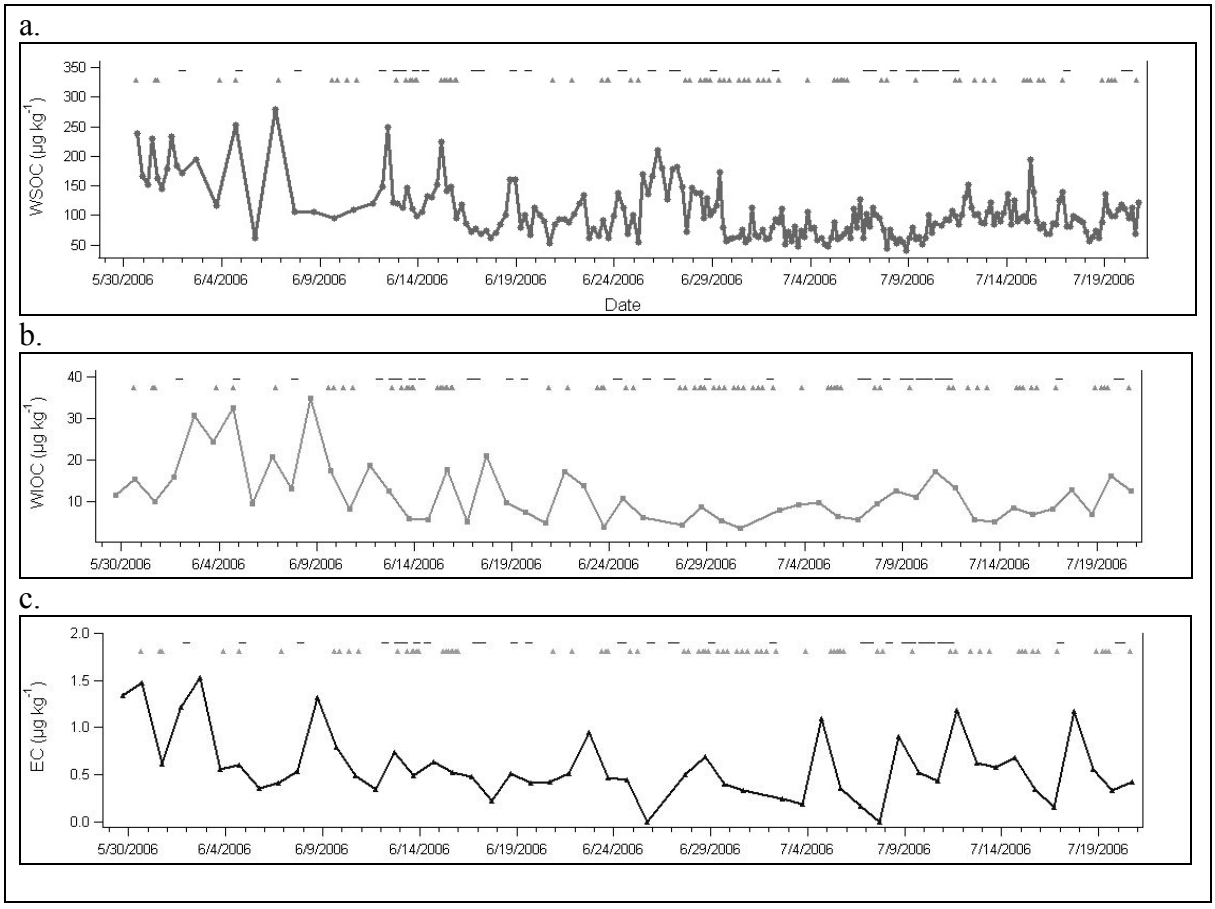

Figure 26. A time series of snow-phase water-soluble organic carbon (a), water-insoluble organic carbon (b), and elemental carbon (c). Observations of snow (triangle markers) and fog (dash markers) are indicated.

Given the small snow volume (250 mL) needed for WSOC measurement, higher frequency (every 4-6 hours) WSOC sampling was consistently performed starting 12 June 2006 and provides information on concentration changes on a shorter time basis. One major observation is that WSOC concentrations did appear to vary on a 4-6 hour time basis (Figure 26). In addition, precipitation events (in particular, fog) mostly occurred during the coldest part of the day (approximately between 23:00 – 06:00 local time) and led to frequent WSOC spikes in the early morning. For example, on July 15-16, WSOC was measured to be 95 $\mu g\ kg^{-1}$ at 17:00 (July 15th), rising to a maximum of 195 $\mu g\ kg^{-1}$ at 05:00 (July 16th), and then dropping to 90 $\mu g\ kg^{-1}$ by 17:00 (July 16th). If measuring only at 17:00, an undulation of ~100 $\mu g\ kg^{-1}$ (>100% increase and drop off) would have been missed. Considering the variability among WSOC duplicates (~34% or 29 $\mu g\ kg^{-1}$), this ~100 $\mu g\ kg^{-1}$ concentration increase/decrease appears to represent a real concentration change that occurred on a sub-24 hour time basis.

As pointed out in the analysis of a 3 meter snow pit (section 8.2), there is a likelihood that the surface snow WIOC and WSOC concentrations measured are influenced by photochemical processes. In addition, temperature-dependent air-snow partitioning may also play a substantial role in modifying snow-phase concentrations of organics, particularly that of WSOC. Given that precipitation events often coincide with low temperatures, it is difficult to separate the ensuing decrease of concentrations by photochemical degradation and temperature-dependent partitioning. One simple comparison would be to look at several days with and without the occurrence of wet deposition. Looking at the sampling period with continuous 4-hour sampling (27 June

2006 – 20 July 2006), a 24-hour dry period occurred over 17:00 July 2nd - 17:00 July 3rd. WSOC was found to oscillate from a minimum of 48 μg kg^{-1} to 82 μg kg^{-1} (difference of 40 μg kg^{-1}). Another 24-hour period without precipitation was 17:00 July 13th - 17:00 July 14th, where WSOC varied from a minimum of 90 μg kg^{-1} to a maximum of 136 μg kg^{-1} (difference of 46 μg kg^{-1}). Finally, the longest stretch of time with no precipitation took place during 05:00 July 17th - 17:00 July 18th, where snow concentrations ranged from 57 to 99 μg kg^{-1} (difference of 42 μg kg^{-1}). For all periods of time, no consistent diurnal pattern in WSOC concentration was observed. Given that some concentration change may be due to spatial variability in surface snow concentrations and our ability to precisely collect the identical layer of surface snow (i.e. WSOC duplicate difference of 29.1 μg kg^{-1}), it is suggested that the average value of ±43 μg kg^{-1} is an upper limit on the impact of air-snow temperature-dependent partitioning on WSOC concentrations.

Looking in detail at a few days with precipitation-linked concentration spikes may provide insight into the impact of post-depositional processes. For example, an evening fog occurred on June 25th, with maximum surface snow concentrations (211 μg kg^{-1}) observed following the fog event and then dropping by 40% to 127 μg kg^{-1} within the following 8 hours. Another example is July 15th, which had a maximum WSOC concentration after snowfall of 195 μg kg^{-1} and then fell by 54% to 90 μg kg^{-1} within the next 8 hours. That the change in concentration for both days was significantly greater than 43 μg kg^{-1} points to a factor outside of temperature-dependent air-snow partitioning causing a net loss in surface snow concentrations. At this point it is difficult to determine whether the greater loss is due to outgassing of freshly deposited snow/fog or linked to

post-depositional processes, such as photolysis. This supports our 3-meter snow pit analysis, which found substantial loss of organic carbon in the snowpack record (section 8.2), but the time scale of this loss is yet uncertain.

In addition to the apparent net loss of organic compounds from the snow pack, it may be possible that photochemical processes may cause a transfer of organic mass from WSOC to WIOC or vice versa. To investigate the possible transfer between carbon fractions, 24-hour concentration change was calculated for WSOC and WIOC for each sampling day (ex. $\Delta WSOC = WSOC_{t+1} - WSOC_t$). Given that WSOC is sampled at a higher frequency, only samples taken at 17:00 (simultaneous with WIOC samples) were included in this analysis. Plotted in Figure 27, it can be seen that the majority of cases fall into the first (positive ΔWSOC, positive ΔWIOC) and third quadrant (negative ΔWSOC, negative ΔWIOC). Only a small number of cases (9 out of 39 data points) appear to fit the case where there is an opposing change in WSOC and WIOC, and even fewer cases have opposing change exceeding sampling uncertainty. In addition, there is a wide degree of scatter and in a number of cases, one species changes substantially while the other has zero change in concentration. Overall, it appears that the relationship between WSOC and WIOC is weak. However, it should be noted that this analysis is likely hindered by the fact that only a 24 hour change is available for analysis and that it is likely that any evening/morning concentration spikes from wet deposition may have already been substantially processed by the time of WIOC and EC sample collection at 17:00.

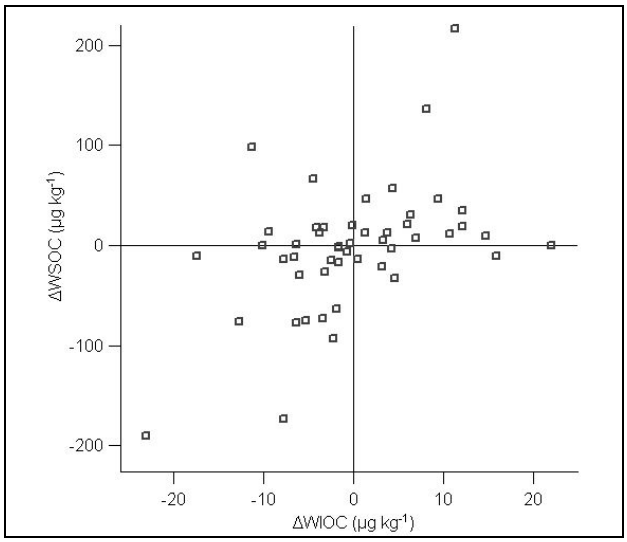

Figure 27. 24-hour change in surface snow WSOC compared with 24-hour change in surface-snow WIOC

8.3.3 Comparison of Air and Snow

While it is highly interesting to directly compare our measured time series of carbonaceous species in the air and snow, a number of caveats need to be taken into consideration prior to making conclusions. First, our atmospheric measurements were either shut off or were filtered for time periods potentially impacted by camp emissions. Unfortunately, there is no possible sector control system to prevent emissions from impacting snow concentrations. Next, while we used identical filter media and analytical instrumentation in processing atmospheric and snow-phase WSOC, WIOC, and EC, there are fundamental differences in the air and snow sampling techniques. All atmospheric filter samples were collected downstream of a $PM_{2.5}$ cyclone and WSOC was extracted off of the filters. For snow-phase samples, liquid filtration through a quartz-fiber filter was used to separate insoluble species (WIOC and EC) and soluble species (WSOC) prior to analysis. In addition to possible differences in collection in air vs. liquid filtration, snow-phase EC and WIOC also do not have an upper size-cut and may include

particulates larger than 2.3 μm. Finally, probably the most significant caveat is that snow concentrations are highly dependent on the occurrence of deposition (dry or wet) and related factors affecting the magnitude of flux to snow (Bergin et al., 1995), as well as the potential occurrence of post-depositional processing.

Despite the numerous hurdles to overcome in interpreting air vs. snow concentrations, there may still be useful information in the comparison. The high-frequency snow-phase sampling of WSOC is displayed in Figure 28 along with atmospheric $PM_{0.1\text{-}1.0}$ that was averaged over identical time periods. In a number of periods, it appears that snow-phase WSOC increases while $PM_{0.1\text{-}1.0}$ decreases (e.g. June 15th, June 18th, and June 22nd). However, it is inconsistent, with some major spikes in snow-phase WSOC (e.g. June 12th and July 16th) occurring with no simultaneous decrease in $PM_{0.1\text{-}1.0}$. As mentioned earlier, snow concentrations of WSOC may also be influenced by a temperature-based partitioning of gaseous organics to the snow.

Assuming for a moment that all snow-phase particulate matter is derived from deposited atmospheric particulate matter, it would be expected that the carbon balance between the various carbon species (WSOC, WIOC, EC) would be similar in the air and snow. However, it appears that this is not the case, as atmospheric WIOC and EC was at an approximate 1:1 ratio compared with 11:1 in snow (Figure 29). This may suggest that WIOC is formed in the snow through polymerization of water-soluble organic molecules. However, the enhanced WIOC relative to EC in the snow may also be linked to other factors, such as preferential deposition or differences between air/snow measurement.

Additionally, total OC to EC in the atmosphere is roughly 8:1 while in the surface snow it is 205:1. Similar to the high total OC/EC ratio observed in the 3 meter snow pit (section 8.2), it appears that the snow concentrations do not mimic the atmosphere levels. While there are numerous reasons for expected differences in the air and snow concentrations, the extreme enhancement of organics (WSOC and WIOC) in the snow pack supports the idea that gaseous organics are a secondary source of OC in snow.

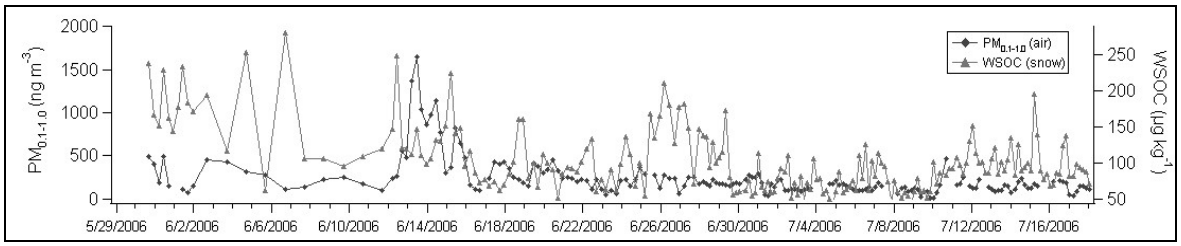

Figure 28. Comparison of atmospheric $PM_{0.1\text{-}1.0}$ concentrations versus surface snow WSOC.

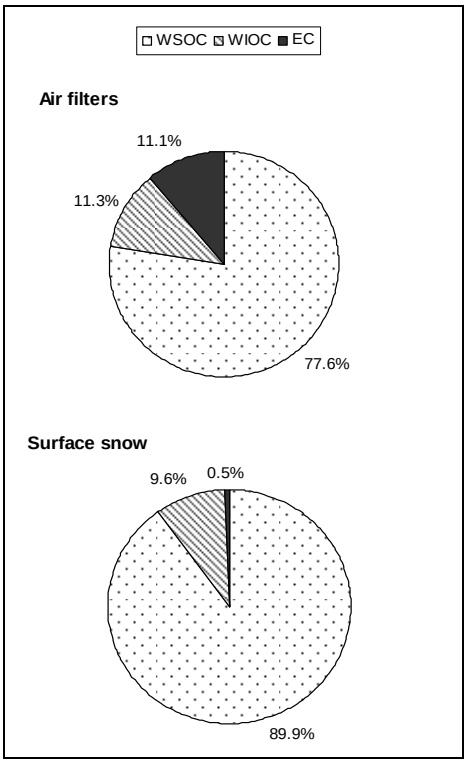

Figure 29. Comparison of carbon balance in air samples and surface snow.

8.4 Investigation of Camp Contamination at Summit, Greenland

After observing several unexpected concentration spikes in ambient particulate matter measurements during the short-term 2005 field study on the Greenland Ice Sheet (see Appendix C), great emphasis was placed on minimizing any contamination to 2006 samples from local camp emissions. Our sampling site was moved to a distance about 1 km from base camp and a sector control system was put in place to flag/shut-down sampling during stagnant periods or when winds were arriving from base camp regions. In addition to these preventative actions, we also sought to investigate and record the impact of camp on both atmospheric and snow concentrations. As Summit, Greenland continues to host year-round field measurements, these results will hopefully support improved accuracy in sampling a pristine environment that is unfortunately not free of local anthropogenic emissions.

8.4.1 Camp Emissions and Atmospheric Samples

During the 2006 campaign, wind speed and direction were monitored at 10-minute increments at our satellite monitoring location and are displayed in Figure 30. From the vantage point of the remote sampling site located south of the base camp, we estimated wind direction >288° or <45° to cover camp emission locations (mainly, heavy equipment grooming the "ski-way" and the camp generator). During a nearly month-long time period with no incoming flights and thus no ski-way grooming occurring NW of the sampling site, the NW wind direction limit was increased to >315°. In addition, "stagnant" conditions were defined as wind speeds <0.5 m/s. Given the occurrence of either poor wind direction or stagnation, the sector control system flagged the time period and shut down integrated filter sampling.

As seen in Figure 30, winds were dominated by southerly winds during the sampling period, hitting >315°/<45° limits for only ~16% of the summer or ~24% with wind direction limits expanded (>288°/<45°) to include ski-way traffic. In addition, Figure 30 shows that the majority of wind speeds falling between 2-8 m/s. Throughout the entire summer, stagnant conditions (wind speed <0.5 m/s) were rare (<5% of the summer).

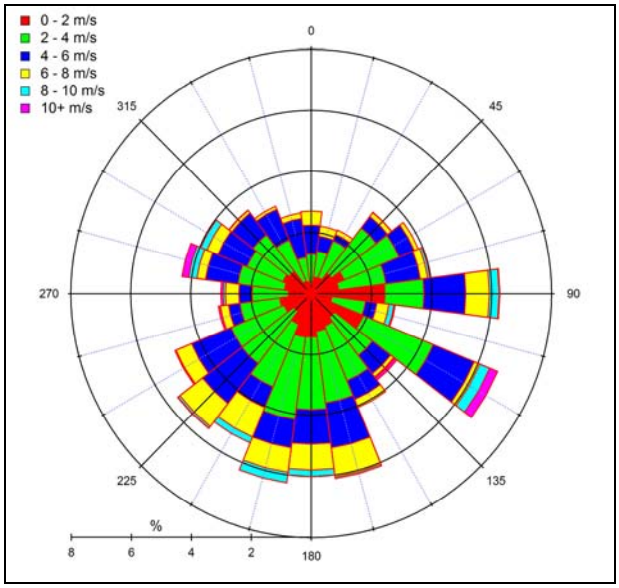

Figure 30. Wind patterns observed during 26 May 2006 – 18 July 2006.

Altogether, sector control flagged 21% of the sampling time during 26 May – 18 July 2006. As shown in Figure 31, the time periods flagged for contamination concern (Figure 31a) are often associated with brief extreme spikes in the absorption coefficient (Figure 31b) reaching up to 30 Mm^{-1}, 2000% higher than the summertime average of 0.15 Mm^{-1}. It is clear that controlling sampling for camp winds is extremely important when measuring ambient carbonaceous particulate matter. Additionally, it is also apparent in Figure 31 that our sector control criteria captured every major spike and thus our atmospheric measurements are likely free from significant contamination.

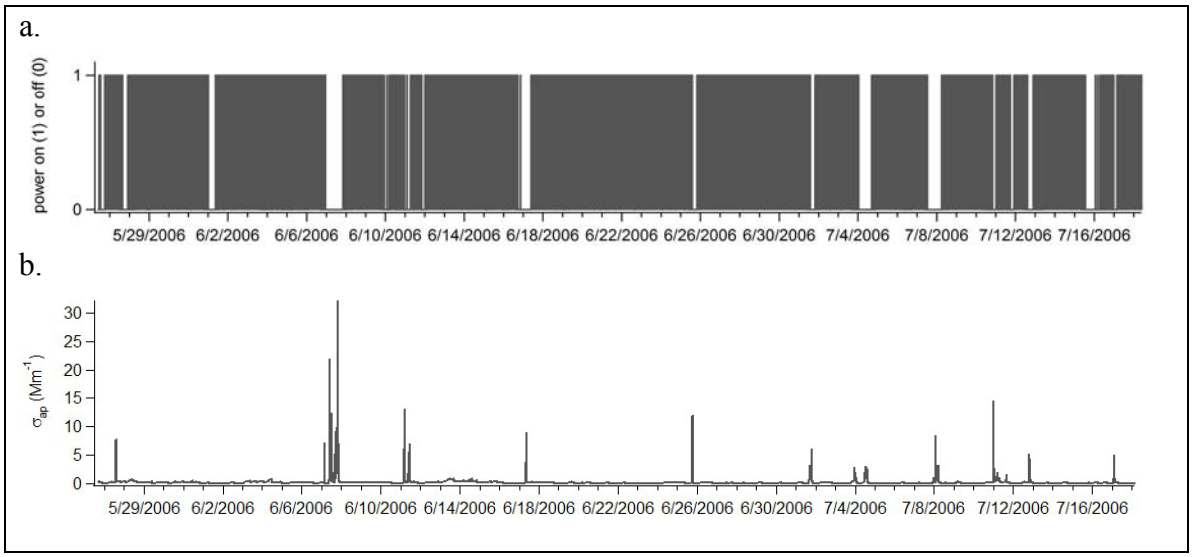

Figure 31. Sector control power on/off (a) and the unfiltered measurement of the absorption coefficient (b).

Using long-running wind measurements at Summit conducted by ETH Zürich – Institute for Atmospheric and Climate Science, it is possible to understand the year-to-year variability in camp wind patterns. Shown in Figure 32, hourly-collected wind data for spring through fall months (wintertime data collection was limited due to wind vane issues at T < -35°C) for the years 2003-2005. Each wind rose displays the frequency of observation (%) at a given angle and is shaded according to wind speed. As seen in Figure 32, it appears that there is no major monthly trend in wind patterns, although in general it appears that southerly winds dominate. As with summer 2006, it appears that low wind speeds (<0.5 m/s) are a rare event, occurring only 2.5%, 1.7%, and 1.9% of the time during 2003 (June to Oct), 2004 (May to Oct), and 2005 (May to Oct), respectively. Wind directions covering camp emission locations (<45° or >315°), were a more common event, occurring 11.9%, 10.0%, and 14.3% of the time during 2003, 2004, and 2005, respectively. These results suggest that long-term air monitoring at Summit Camp would be able to obtain data at least ~85% of the time with sector control in place.

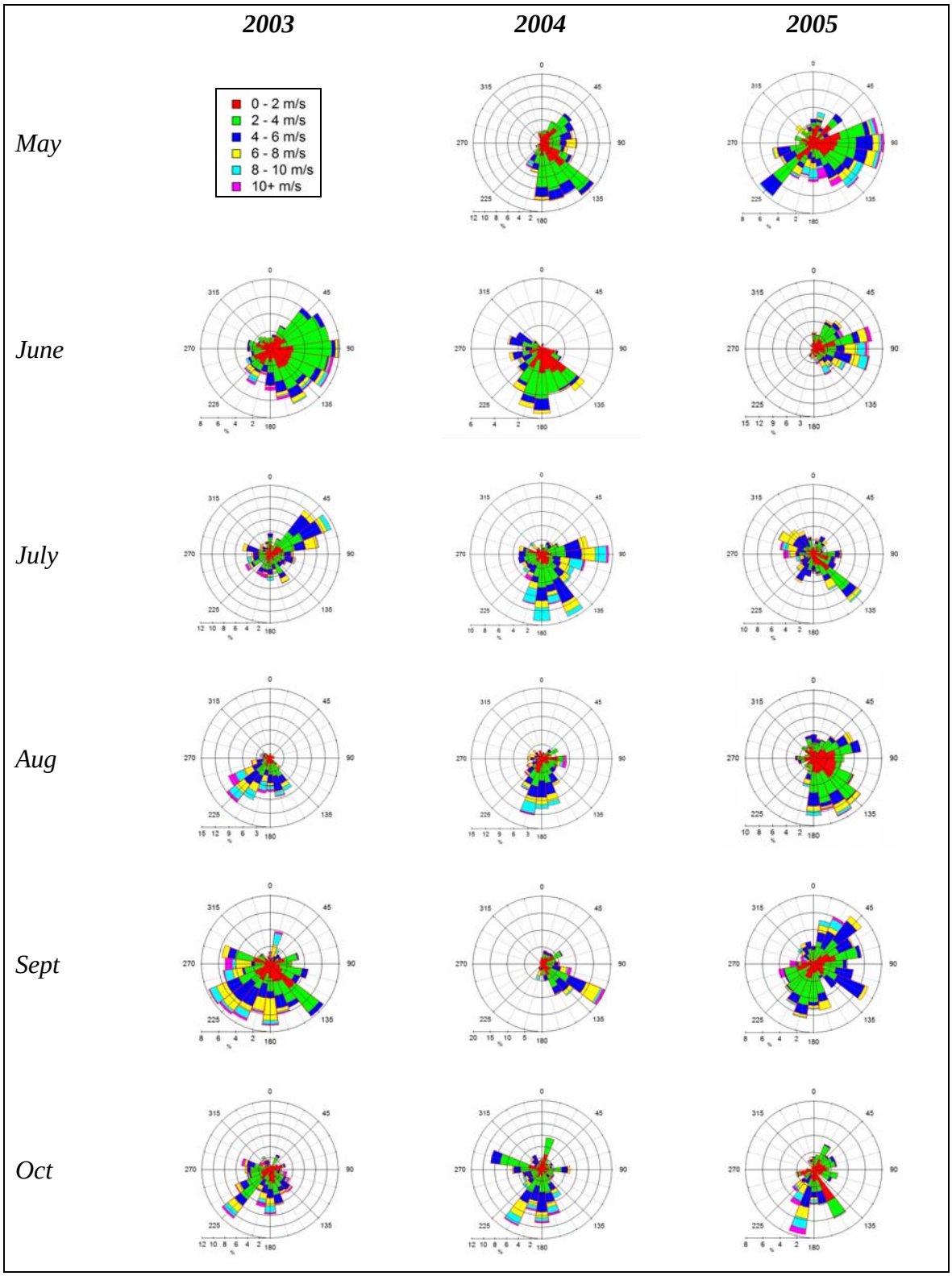

Figure 32. Wind direction and speed during 2003-2005 at Summit, Greenland

8.4.2 Impact of Camp Emissions on Snow Concentrations

While it seems to be feasible to avoid camp contamination in atmospheric samples by adding in a sector control system, there is unfortunately not similar method available to prevent the deposition of camp emissions to surface snow. To minimize snow contamination, camp staff members eliminate all possible emissions (e.g. snowmobile traffic and usage of heavy equipment) during northerly winds. However, the camp electricity depends on continuous use of a diesel generator. In addition, flights to the research site take place independent of wind direction. It is of concern that these emissions may impact measurements made of carbonaceous particulate matter in modern (post- 1989) snow.

In order to understand the possible footprint of Summit Camp on surrounding snow, a series of 1-meter snow pits were dug and sampled in the clean air sector of Summit and at distances up to 20 km north and south of camp. A description of the 6 snow pits sampled is provided in Table 13. At all sites, WIOC and EC were sampled at 20 cm increments, with duplicates taken at 2-3 layers.

Table 13. 1-meter snow pit locations near Summit, Greenland

Snow pit description	Date sampled	Coordinates
20 km North of Summit	26 June 2006	N72˚ 44', W38˚ 12'
10 km North of Summit	25 June 2006	N72˚ 40', W38˚ 26'
Summit Camp I, in clean air sector	20 June 2006	N72˚ 34', W38˚ 27'
Summit Camp II, in clean air sector	22 June 2006	N72˚ 34', W38˚ 27'
10 km South of Summit	29 June 2006	N72˚ 30', W38˚ 40'
20 km South of Summit	3 July 2006	N72˚ 24', W38˚ 39'

As the sampling was coarse (5 layers total per pit) and given the possibility of spatially variable snow accumulation, the snow pits are compared for total average concentration rather than comparing the snow pit profiles (profiles are provided in Appendix D). As shown in Figure 33, it is immediately apparent that the snow pits near camp (Summit I and II) appear to be elevated both WIOC and EC in comparison with the snow pits at a distance from camp. On average, the two Summit snow pits are 52% (1.16 $\mu g\ kg^{-1}$) and 82% (0.13 $\mu g\ kg^{-1}$) higher than the remote snow pits for WIOC and EC, respectively. This substantial difference is concerning and suggests that future snow pit sampling should be performed at distances from Summit. It is interesting that snow pits at 20 km are not substantially lower in concentration than those at 10 km, suggesting that the footprint of Summit is confined to within 10 km. In addition, it is also of note that the snow pits north of the research site are not higher (in fact, are slightly lower) than those south of Summit camp, suggesting that the higher camp emissions during southerly winds do not translate to long-distance impacts on snow concentrations.

Assuming camp emissions contribute a constant fraction to the nearby snow, our presented snow pit concentrations (section 8.1) and surface snow levels (section 8.2) can be readjusted by 1.16 $\mu g\ kg^{-1}$ for WIOC and 0.13 $\mu g\ kg^{-1}$ for EC, which would lower the averages but preserve the fluctuations. However, it is difficult at this point to determine whether this is an appropriate assumption to make, as the impact of camp on snow in the "clean air" sector is likely dependent on the co-occurrence of precipitation and wind direction. Also, it is likely that camp contamination is highly spatially variable. As seen in the sector control observations (Figure 31), there are a number of periods flagged for

camp contamination that did not experience spikes in σ_{ap}; and, when spikes did occur, they were not at a consistent concentration.

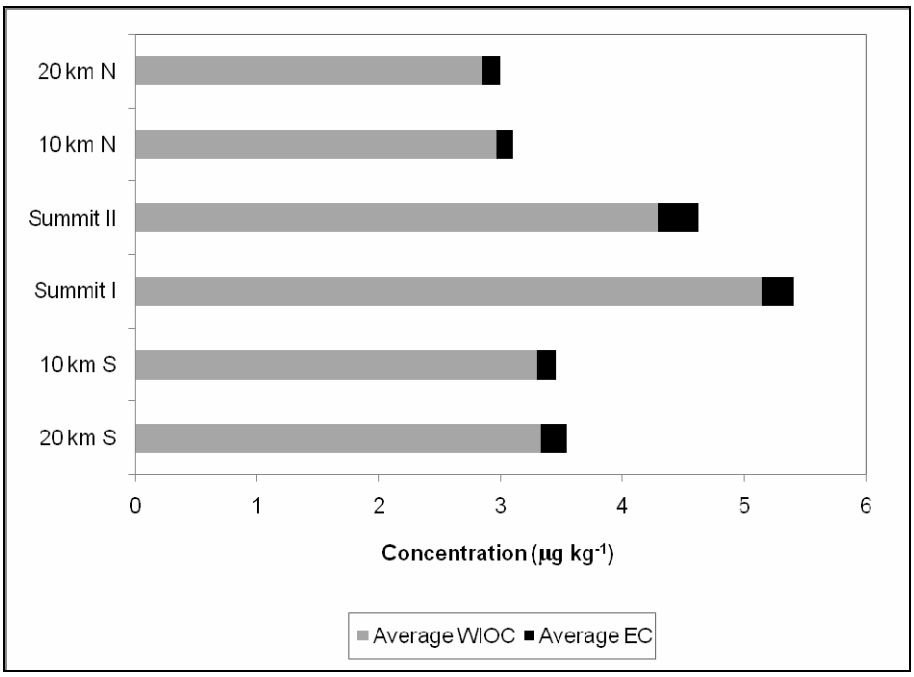

Figure 33. Comparison of average snow pit concentrations in 1 meter snow pits located near and far from Summit Camp.

8.5 Related Measurements at Niwot Ridge, Colorado

As described in the Chapter 7, a short field campaign took place in January 2006 to measure carbonaceous particulate species on Niwot Ridge in the Colorado Rocky Mountains. Removed from any emitting sources, this sampling site represents another remote, high-altitude (3345 m) location in the Northern Hemisphere and serves as an interesting comparison to the Greenland Ice Sheet.

8.5.1 Atmospheric Concentrations

Atmospheric sampling took place for one week and included identical measurements made on the Greenland Ice Sheet – filter-based collection of OC/EC/WSOC, σ_{ap}, and particle size-resolved number concentration (N, $PM_{0.1\text{-}1.0}$). In addition, the higher particulate concentrations measured at Niwot Ridge allowed for the measurement of the particulate scattering coefficient (σ_{sp}) using a nephelometer, also allowing the calculation of the single-scattering albedo ($\omega = \sigma_{sp} / \sigma_{ext}$). The week-long average values are presented in Table 14 and the time series is shown in Figure 34.

To the author's knowledge, these are the first measurements of the major particulate matter carbon fractions (OC, WSOC, EC) and optical properties (σ_{ap}, σ_{sp}, ω, N) made on Niwot Ridge, Colorado or at any high-altitude site in the Rocky Mountains, for that matter. One previous study measured a number of specific particulate organic molecules in the summertime of 1996 at Niwot Ridge, although there is unfortunately no direct overlap with our measurements to allow comparison (Veltkamp, 1996).

Table 14. Measured atmospheric species at Niwot Ridge during January 2006

Species	Sampling	Averaging period	Concentration	Units
OC	filter collection	24-48 hours	208 ± 0.104	ng m^{-3}
EC	filter collection	24-48 hours	20 ± 0.001	ng m^{-3}
WSOC	filter collection	24-48 hours	122 ± 0.054	ng m^{-3}
$PM_{0.1\text{-}1.0}$	OPC	1 minute	248 ± 0.172	ng m^{-3}
σ_{ap}	PSAP	minutes to hours	0.34 ± 0.23	Mm^{-1}
σ_{sp}	Nephelometer	1 minute	2.03 ± 1.51	Mm^{-1}
ω	calculated value	minutes to hours	0.85 ± 0.05	

On average, it can be seen that the levels of atmospheric particulate matter at Niwot Ridge are significantly higher than what was observed at Summit, Greenland, likely due to the closer proximity of Niwot Ridge to emitting sources (e.g. plant emissions, vehicular traffic). For the integrated filter samples, the relatively short sampling period (24-48 hr compared with 80 hr at Summit) led to the need to use two filter punches to quantify OC and EC mass. Thus, no duplicates are available to confirm the measured concentrations and there is more uncertainty in the WSOC/OC ratio. One measurement period found WSOC/OC > 1, suggesting an overestimation of WSOC or underestimation of OC. Excluding this time period, the average WSOC/OC ratio is 0.52 (down from 0.69 with all samples included), much lower than that observed at Summit, Greenland (average WSOC/OC = 0.81).

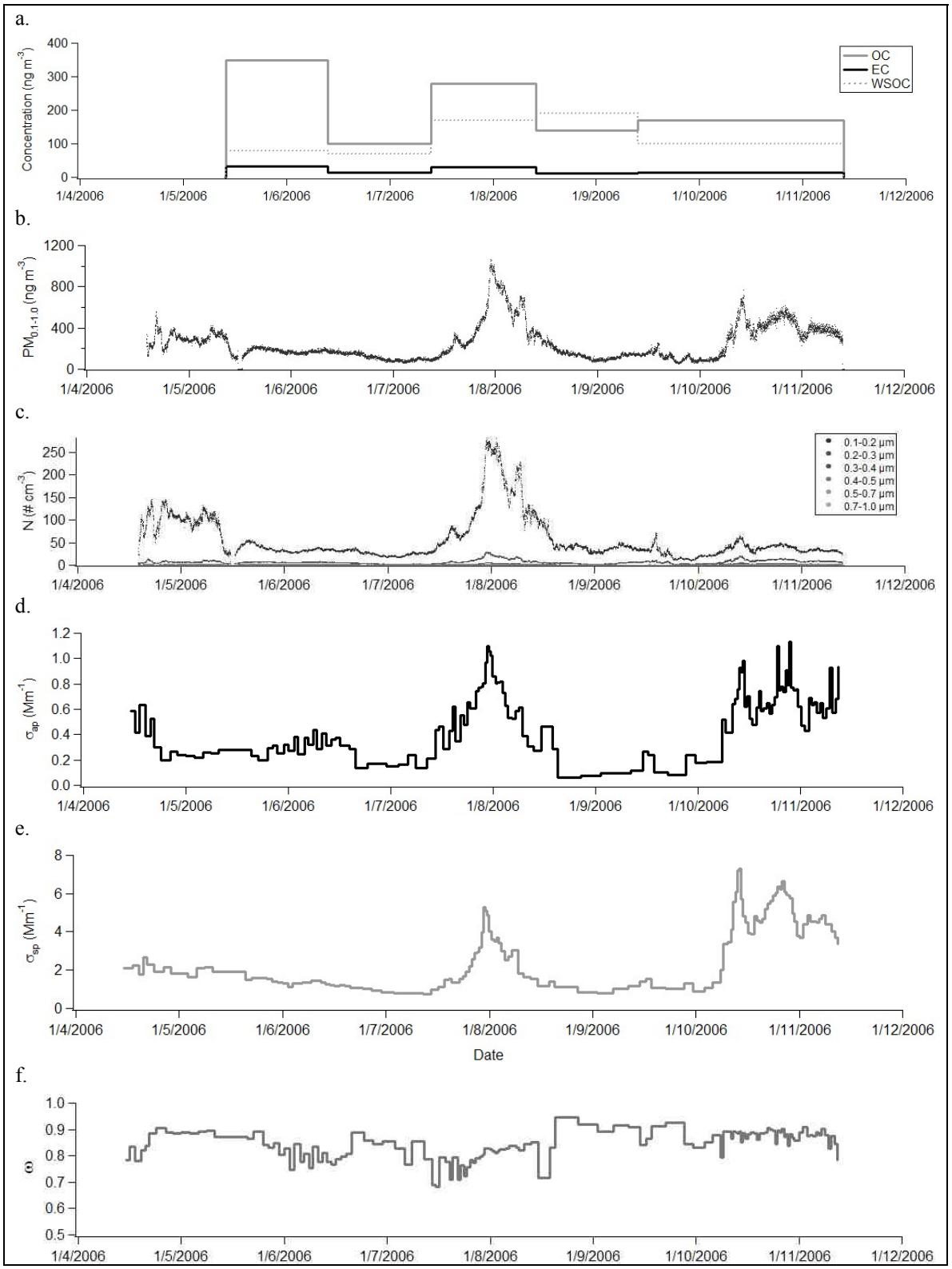

Figure 34. A time series of atmospheric particulate matter species at Niwot Ridge, Colorado, including carbonaceous particulate matter (a), $PM_{0.1\text{-}1.0}$ (b), number concentration (c), particulate absorption coefficient (d), particulate scattering coefficient (e), and single-scattering albedo (f)

As shown in Figure 35, it can be seen that the particulate scattering and absorbing are highly correlated, suggesting similar particle composition and mixing state throughout the measurement period. In addition, it can be seen that all measurements observe a similar increases in concentration during the evening of January 8th and late on January 10th. The decrease in concentrations during the early morning of January 9th is likely due to the occurrence of heavy snowfall. The dry aerosol single-scattering albedo, displayed in Figure 34, ranged from 0.68 to 0.95 throughout the measurement period.

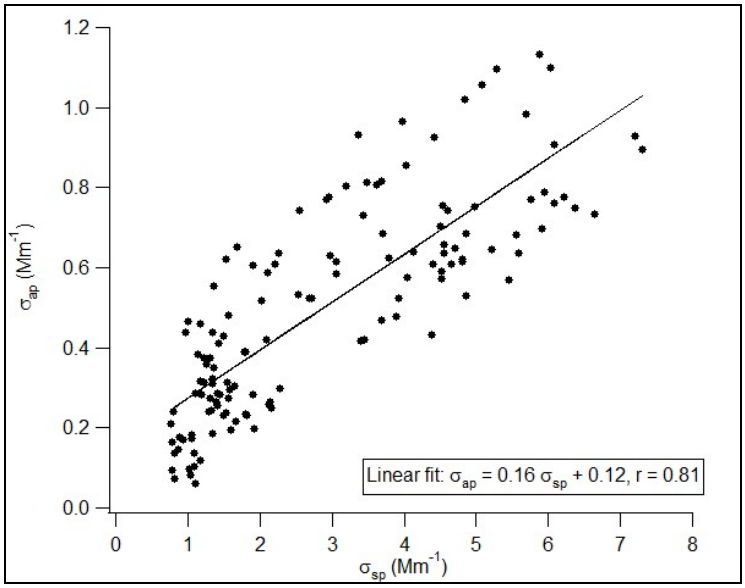

Figure 35. Relationship between ambient particulate absorption and scattering at Niwot Ridge, Colorado

8.5.2 Snow Concentrations

Snow-phase water-soluble organic carbon (WSOC) was measured in a 1 meter snow and in surface snow, as shown in Figure 36 and 37. In addition, the higher concentration of WSOC at Niwot Ridge allowed for the additional detection of the WSOC hydrophilic fraction, defined as the portion of WSOC that penetrates through an XAD-8 column at a pH of 2 (Sullivan and Weber, 2006a). The particulate carbonaceous species (WIOC and EC) were not measurable due to the occurrence of plant debris in the large-volume (5 L) snow samples. The challenging mountainous conditions made it unfortunately impossible at the time to monitor above the tree-line. Thus, only snow-phase WSOC concentrations are available for comparison with Summit data. WSOC concentrations averaged 212 μg kg^{-1} (142 μg kg^{-1} hydrophilic) in the 1 m snow pit and 235 μg kg^{-1} (172 μg kg^{-1} hydrophilic) in surface snow samples, nearly twice as high as the summertime surface snow WSOC average on the Greenland Ice Sheet. Duplicates of WSOC and hydrophilic WSOC were taken at every level of the 1 meter snow pit with an average difference of 30.3 μg kg^{-1} (14% of average) and 17.7 μg kg^{-1} (12% of average), respectively.

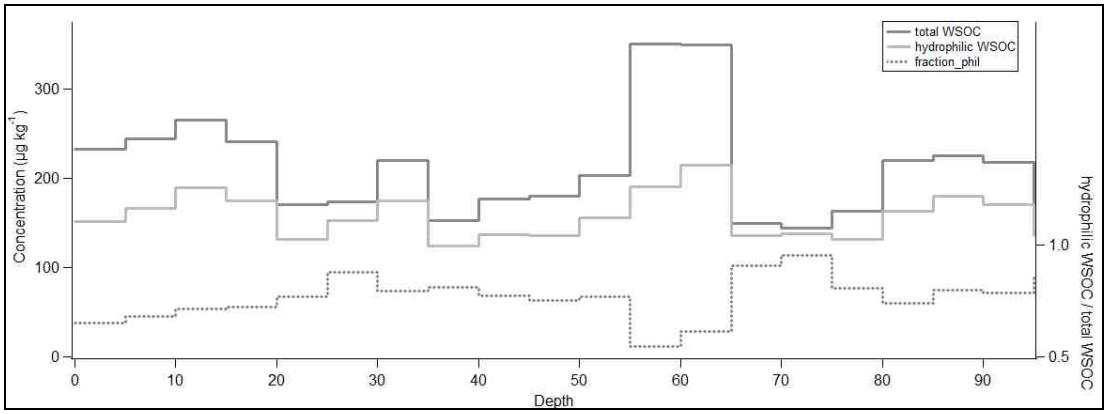

Figure 36. Water-soluble organic carbon measured at 5 cm increments in a 1 meter snow pit at Niwot Ridge, Colorado

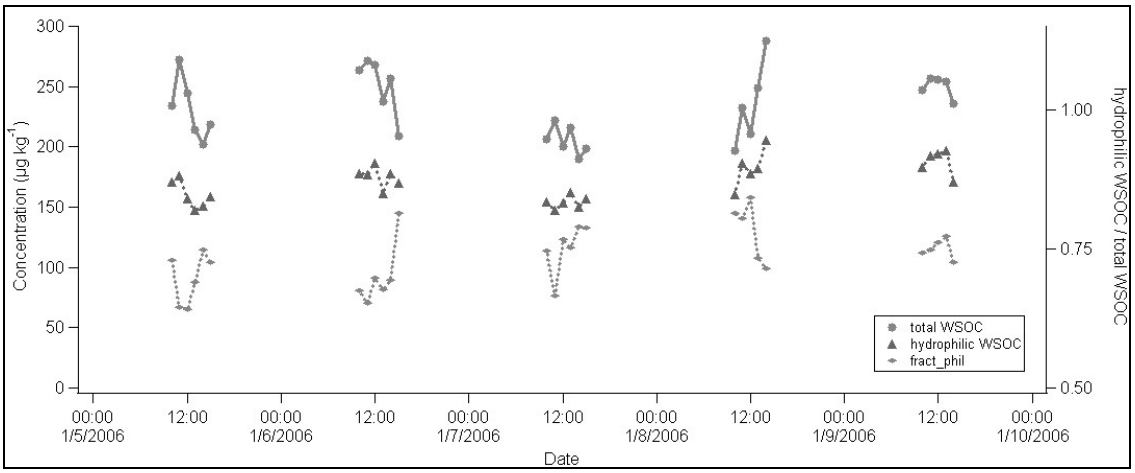

Figure 37. Water-soluble organic carbon in surface snow measured hourly starting at 10:00 am at Niwot Ridge, Colorado

The snowpack at Niwot Ridge has a number of physical differences to consider before comparing with the Greenland Ice Sheet. The Niwot Ridge area experiences springtime snow melt, thus the concentrations measured represent only snow accumulated in the winter of 2005/2006. In addition, Niwot Ridge receives significantly greater snowfall, with >1 m of snowfall in the winter season compared with a typical 0.65 m year-long accumulation on the Greenland Ice Sheet. Another major factor to consider are the sporadic coniferous trees located surrounding the snow fields sampled at Niwot Ridge – in addition to deposited atmospheric species, the sampled snow may have a secondary contribution from the nearby vegetation. Finally, the snowpack at Niwot Ridge sits on top of soil and rock, while the highest point of the Greenland Ice Sheet is >3000 m above bedrock. Thus, there is a greater chance that bacteria contained in the soil may digest snow-phase carbonaceous species at Niwot Ridge.

The fraction of hydrophilic WSOC/total WSOC is plotted in both Figure 36 and Figure 37. An interesting trend is noticeable in both plots, with the hydrophilic fraction appearing to vary opposite the total WSOC concentration. A correlation was performed between the hydrophilic fraction and total WSOC for both the surface snow and the snow pit, shown in Figure 38. A strong negative linear relationship ($r = -0.81$) was observed between the hydrophilic fraction and total WSOC in the snow pit, while a weaker relationship ($r = -0.58$) was seen in the surface snow. The stronger relationship in the snow pit is likely due to the higher range of WSOC concentration measured (144-351 $\mu g\ kg^{-1}$ vs. 148-206 $\mu g\ kg^{-1}$ in surface snow). One possible conclusion from this observed trend is that the higher concentrations of WSOC in the snowpack are essentially "fresh" snow layers that were not exposed to post-depositional oxidative processes, thus higher total WSOC concentrations and a lower hydrophilic fraction. This situation could occur during periods of high snow accumulation, where a freshly deposited snow layer is buried quickly by additional snow and thus not exposed to photochemical reactions. Likewise, the low WSOC/high hydrophilic fraction may indicate the state of aged snow that has undergone oxidation, leading to a net loss of WSOC from the snow pack and a shift towards more hydrophilic organic compounds.

An alternative possibility is that the trend of enhancement of the hydrophilic WSOC fraction with lower WSOC is merely a coincidence, that the buried WSOC characteristics are simply representative of the particulate matter in the atmosphere. However, the hydrophilic WSOC/total WSOC levels (ranging 0.55-0.95) in the snowpack were higher than the past reported values for atmospheric particulate matter (hydrophilic WSOC/total

WSOC values ranging 0.49-0.65) in St. Louis, Missouri (Sullivan and Weber, 2006), suggesting that post-depositional processes alter snow-phase particulate matter. It should be noted, however, that the composition of particulate WSOC at Niwot Ridge may be quite different than at St. Louis. Finally, it appears that the short period of surface snow measurements track with the snow pit samples (Figure 38) and were likely from a consistent source type, suggesting that post-depositional processes do indeed impact snow-phase WSOC properties. Given the lack of information on WSOC hydrophobicity in the atmosphere at Niwot Ridge, the unknown-degree of bioactivity impacting WSOC in the snowpack, and that nearby vegetation may also impact snow-phase concentrations, these results are considered preliminary and further study is recommended.

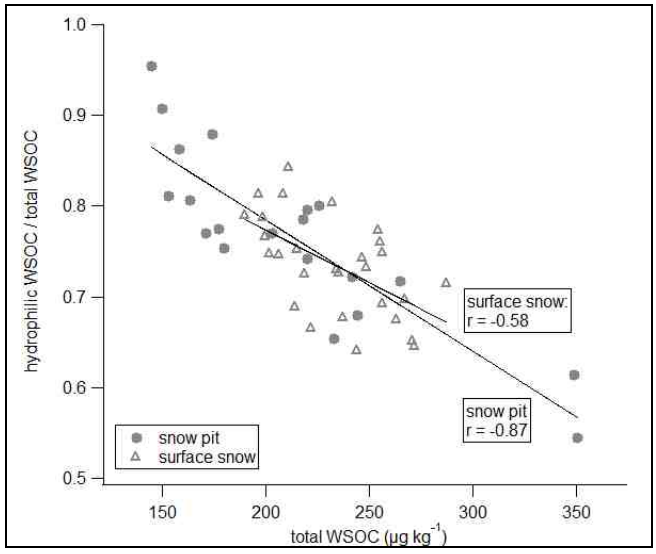

Figure 38. Relationship between the fraction of WSOC that is hydrophilic and total WSOC

CHAPTER 9: CONCLUSIONS AND RECOMMENDATIONS

9.1 Conclusions

Part II of this thesis focuses on studying atmospheric carbonaceous particulate pollution at what is possibly the most pristine location in the Northern Hemisphere – the Greenland Ice Sheet. Carbonaceous particulate matter (organic and elemental carbon) is a present-day concern for its potential warming influence in the air above the ice sheet and in lowering the reflectivity of the ice sheet after deposition to surface snow. In addition, the organic fraction of carbonaceous particulate matter consists of thousands of organic compounds, some of which have been found to be stable in the atmosphere and useful as source signatures (Schauer et al., 1996). These species may also serve as historical markers of atmospheric emissions in ice cores. However, post-depositional processing may alter the original form of deposited organic carbon and complicate the linkage between the frozen archive and the atmosphere.

To better understand the nature of carbonaceous particulate matter in the air and snow on the Greenland Ice Sheet, numerous field measurements were conducted during the summer of 2006 at Summit, Greenland. In addition, field studies were conducted in January 2006 at the high-altitude and remote Niwot Ridge, Colorado to provide a reference point to particulate matter concentrations measured at Summit. The results of these field campaigns are summarized and commented on below.

Atmospheric Carbonaceous Particulate Matter Concentrations

- 10-day back-trajectories calculated for the measurement period (20 May 2006 – 19 July 2006) show that the majority (71%) of sampling days had 10-day trajectories constrained to the area near the Greenland Ice Sheet or from the northeastern part of North America, with only a few sampling days represented by longer trajectories arriving from over northwestern North America or the Asian continent.
- Measurement of atmospheric particulate carbon on the Greenland Ice Sheet found WSOC (average of 55 ng m^{-3}) to constitute over 80% of particulate OC (average of 63 ng m^{-3}), suggesting that atmospheric organic compounds reaching the Greenland Ice Sheet in summer are highly oxidized. WSOC and OC concentrations were nearly twice as high at Niwot Ridge and had a lower fraction WSOC/OC (52%).
- Atmospheric EC on the Greenland Ice Sheet (average of 8 ng m^{-3}) was found to highly correlate with atmospheric OC ($r = 0.94$). Atmospheric EC was also well-correlated with the σ_{ap} ($r = 0.95$) and had a calculated mass-absorption cross-section of 24 m^2 g^{-1}, although other species may also contribute to light absorption (e.g. dust or organic molecules).
- A high pollution event occurred on June 13-14 at Summit, Greenland, with short-term measurements of σ_{ap} and $PM_{0.1\text{-}1.0}$ averaging 197% and 290% higher than their summertime averages, respectively. The increase in σ_{ap} and EC during this time period suggests that the pollution episode was combustion-related. Isobaric 10-day back-trajectories during this time period indicate that the air mass tracked from Alaska/western Canada over northern Canada to Summit. Fire records show sizable forest fires (~155,000 acres burning) were occurring in Canada in early June.

Snow-Phase Carbonaceous Concentrations and Trends

- Measurements of WSOC, WIOC, and EC in a 3-meter snow pit on the Greenland Ice Sheet, representing over 4 years of snow fall, find that WSOC makes up the majority (40.5 μg kg^{-1} or 88%) of the measured carbonaceous species, followed by WIOC (4.6 μg kg^{-1} or 11%) and EC (0.4 μg kg^{-1} or 1%). Seasonal cycles were observed for all three species, with maximum concentrations in spring/summer. Similar seasonal patterns were observed in K^+ and SO_4^-, which are known to be co-produced with carbonaceous species in biomass burning and fossil fuel combustion, respectively.
- Comparison of summer surface snow concentrations at Summit, Greenland in 2006 with past summer snow pit layers (2002-2005) found, on average, snow pit levels much lower in WSOC (56%) and WIOC (59%), while only a minor difference (10%) is seen for EC. The apparent substantial loss of WSOC and WIOC in aged snow suggests that post-depositional processes, such as photochemical reactions, need to be considered in linking ice core records of organics to atmospheric concentrations.
- Analysis of ~50 day time series of surface snow concentrations (WSOC, WIOC, EC) at Summit, Greenland find significant day-to-day variability in concentrations, with all concentration spikes appearing to coincide with a wet deposition (fog or snowfall) event. The higher-frequency (every 4-6 hours) measurement of WSOC in the surface snow yielded substantial decreases (e.g. 54% loss in 8 hours on July 15th) in snow-phase WSOC after a deposition-related concentration spike. These losses appear to be outside of the possible variability in concentration due air-to-snow partitioning behavior.

- On a 24 hour basis, it appears that WSOC and WIOC in Greenland surface snow both tend to increase or decrease together, suggesting that the transfer of organic compounds between the two carbon fractions has only a minor effect on day to day concentration change. However, this analysis is limited changes occurring over 24 hours and may miss detecting any movement of organic molecules between WSOC and WIOC that occurs on a shorter time basis.
- Higher concentrations of WSOC at Niwot Ridge, Colorado, allowed for further analysis of hydrophilic WSOC, defined as the fraction of WSOC that remains after passing through an XAD-8 column. In a 1-meter snow pit, a strong negative relationship was found between total WSOC and the hydrophilic WSOC/total WSOC fraction. Additionally, a weaker relationship was observed during a short period of surface snow measurements at Niwot Ridge. These preliminary results suggest that post-depositional processes may cause chemical alteration to snow-phase WSOC after deposition.

Comparison of Air and Snow Carbonaceous Species

- Comparing air to surface snow concentrations, a large difference was observed between the WSOC, WIOC (or OC minus WSOC), and EC balance in air (77.6%, 11.6% , and 11.3%, respectively) and snow (89.9%, 9.6%, and 0.5%, respectively). While some dissimilarity was expected due to differences in measurement, the much higher OC/EC ratio in snow suggests the uptake of gaseous organics by snow.

Impact of Camp Emissions at Summit, Greenland

- Atmospheric sampling of the absorption coefficient combined with wind monitoring found that camp activity can have major short-term impacts on atmospheric carbonaceous particulate matter. During the summer 2006 field campaign, wind patterns (direction and/or speed) were found to cause atmospheric contamination concerns for 21% of the ~2 month time period.
- Wind data extended to cover spring to fall months for 2003-2005 indicate that low winds are rare (~2% of the time), while wind directions covering camp emission locations are more common (~12% of the time). It appears that, over the long run, atmospheric sampling with sector control at Summit, Greenland would be able to obtain data a vast majority of the time.
- Camp impact on snow measurements was assessed by sampling a series of 6 1-meter snow pits at varying distances from Summit, Greenland. Snow pit samples illustrate that snow-phase WIOC and EC near to the base camp are significantly higher than at sites located 10 or 20 km from camp. No decrease in concentration was observed at 20 km relative to 10 km, suggesting that a distance of 10 km is sufficient to avoid an impact from camp activity.

9.2 Recommendations for Further Research

While atmospheric particulate matter is well-understood in many developed locations in the Northern Hemisphere, the enormous difficulty in field sampling on the Greenland Ice Sheet has resulted in a current knowledge gap about the nature of particulate matter in this pristine and remote region. Thus, this thesis presents a number of "first-ever" measurements of particulate matter in the air and snow on the Greenland Ice Sheet. A great deal of further research is needed to understand the current trends of carbonaceous particulate matter in the atmosphere over the Greenland Ice Sheet and to evaluate the capability of using carbonaceous species as tracers in ice cores. Several recommendations for further research are provided below.

- **Characterize major carbonaceous source types and source regions impacting the Greenland Ice Sheet**

Currently, the major source types and source regions impacting atmospheric carbonaceous particulate matter on the Greenland Ice Sheet are not well known. An ideal approach to better understand the transport of emissions to the Greenland Ice Sheet would be a pairing of transport modeling and long-term monitoring of atmospheric particulate matter at Summit, Greenland. Field measurements of particulate matter species linked to specific sources (including trace organic compounds, ions, and elements) would provide information on the origin of particulate matter pollution reaching the Greenland Ice Sheet. However, a recent attempt in continuing atmospheric filter sampling throughout winter by Georgia Tech/University of Wisconsin has demonstrated the extreme difficulty in maintaining atmospheric sampling in this

challenging environment (i.e. temperatures < -50 °C, high wind speeds, drifting snow, and limited access to resources). It was found that durable plastic wind sensors would crack under the combination of extremely low temperatures and high winds. In addition, maintaining carbon brush motors on a high-volume sampler was found to be very difficult in the winter conditions. Finally, another major issue was snow blowing into the sampler, depositing onto filter samples and obstructing the inlet. More rugged sampling equipment (ie. full-metal wind sensors, brushless motors) and designing a sampler inlet to avoid snow intake may improve our ability to perform winterover sampling.

- **Determine major modes of carbonaceous particulate matter deposition to snow**

The transfer of atmospheric carbonaceous species to surface snow leads to short-term impacts on the surface albedo and long-term archival of atmospheric components in Greenland snow/ice. In order to model the linkage between air and snow, it is essential to understand the relative importance of wet (snowfall, fog) and dry deposition on atmospheric and snow concentrations. Direct measurement of precipitation would be a challenging task, particularly with the analytical limitations for particulate WIOC and EC. Additionally, the uptake and release of organics by snow would be difficult to quantify in-situ. It is likely that specialized techniques would need to be developed in order to make these valuable field measurements.

- **Additional investigation of organic carbon post-depositional processing**

One major finding of this thesis research is that snow-phase organic carbon appears to substantially degrade after initial deposition, likely due to photochemical processes. A

major open question is the role of snow-phase organic carbon in the cycling of reactive species (e.g. hydroxyl radical) in the air and snow pack on the Greenland Ice Sheet. Other unknowns regarding snow-phase organic carbon reactivity include the depth to which post-depositional processes occur, the major products generated, and the rates of oxidative processing after initial deposition. Additionally, it would be highly valuable to determine whether certain organic compounds remain inert to photochemical reactions after deposition and thus are potential candidates for use in ice core research. This topic of study encompasses a wide array of potential research projects, from laboratory studies to in situ measurements on the Greenland Ice Sheet.

APPENDIX A: CHINA – FIELD DOCUMENTATION

A.1 Field Operating Procedures for RAAS $PM_{2.5}$ Samplers in the Pearl River Delta Study – English version, Authored by Lynn Salmon

Sampler Set-up

Air monitoring will be conducted at seven locations in Hong Kong and the Pearl River Delta region of China beginning in October, 2002. Each station has been designated using a two letter identifying code and a site number that will be placed on all sample labels. The codes are:

TM1 - Tap Mun

TC2 - Tung Chung

CW3 - Central and Western

SZ4 - Shenzhen

GZ5 - Guangzhou

CH6 - Conghua

ZS7 - Zhongshan

Andersen PM2.5 speciation samplers will be used at the first five stations, and Caltech Gray Box PM2.5 ambient samplers will be used at the remaining two sites. Each sampler contains 4 filter holders for collecting fine particle samples located inside the cabinet. There are two quartz fiber filters for collecting organic particles. The other two filters are teflon membrane filters used for aerosol mass, ionic species (Cl^-, $SO_4^=$, NO_3^-, NH_4^+), and trace metals determinations. These filter holders are labelled: Quartz 1, Teflon 2, Teflon 3, and Quartz 4.

Each sampler will work using one pump connected to a manifold with critical orifices for flow control. The samplers have been wired to run on 220V power and will be calibrated during initial field placement.

A notebook and tool box have been provided with each sampler. The notebook contains a copy of these instructions and log sheets (one for each sampling event) that need to be filled out each time samples are loaded and unloaded. An example log sheet is provided at the beginning. The tool box contains the basic needs for filter changing and correcting minor problems with the sampler. Two pairs of tweezers are provided wrapped in annealed aluminum foil. Care to keep the tweezers clean should be exercised. Spare filter cassettes, o-rings, and a spare filter holder are provided for changing any that become soiled. There is also a cassette loader tool for opening filter cassettes. In addition, the tool box contains external flow measuring devices and other useful tools.

More explicit details for loading and unloading filter samples are provided on the next pages.

Site: TM1 Filter Set ID: TM1-021003
Tap Mun

START Date: _____ Time: _____
STOP Date: _____ Time: _____
Duration: _____

	Before Run		After Run	
Filter Holder	Filter ID # (FID)	Initial Flow Rates (L/m)	Avg flow L/m	Vol m3
Quartz 1				
Teflon 2				
Teflon 3				
Quartz 4				

After Run record values below:

	Avg	Min	Max	Comments:
Amb. Temp				
Bar. Pres.				
% RH				

Filter samples

The filters are pre-packaged in individual petri dishes which should be stored in the laboratory before use. Collected samples should be transported from the field in a cooler or ice chest with "blue ice" and stored in the freezer immediately upon return to the laboratory to minimize loss of volatile materials.

Each sample is given a label in the form:

$$TM1 - Q1 - 021003$$

where TM1 is the site label (TM1, TC2, CW3, SZ4, GZ5, CH6, or ZS7); Q1 is the filter holder label (Q1, T2, T3, or Q4); and 021003 is the sampling period given as year month day (YYMMDD). The corresponding dates for each sampling event are recorded on the log sheets.

One filter set includes 4 filters in petri dishes:

(Q1) Quartz fiber filter, in foil lined petri dish

(T2) Teflon membrane filter

(T3) Teflon membrane filter

(Q4) Quartz fiber filter, in foil lined petri dish

When loading filters, the most important thing is to make sure the correct filter is loaded into the correct holder. Each filter will have a designation (e.g., Q1) on the petri dish and the filter holders are labelled similarly (e.g., Quartz 1).

Do not use any filter with a hole or other imperfection. If a filter is dropped on the ground while loading, do not use it. In either case, take a spare filter from the set of spares provided and write the sample label on the spare filter petri dish. Cross out the label on the original problem filter and write BAD on it to avoid mistaken use in the future.

Each filter sample also has a unique 5 digit filter ID number (FID) on the petri dish. This number is specific for the individual filter. When using spare filters, make sure the original number stays with the filter. These ID numbers should also be written on the daily event log sheets.

All filters should be loaded maintaining the same side up that is currently up in the petri dish, and filters should be handled only using tweezers, never touched with bare hands. Putting down a clean piece of aluminum foil as a work surface on top of the sampler is helpful during loading and unloading samples.

Details for loading filter samples:

The filter holders are located downstream of a cyclone for collecting fine particles. The filter holders will be left in the sampler between sampling periods with the empty filter cassettes inside. They should be completely assembled and connected so that the interior remains clean when not in use. The filter holders are connected to critical flow orifices on the manifold at the bottom of the sampler. Typical flow rates through each filter holder are: Q1 - 16.7 lpm; T2 - 7.3 lpm; T3 - 7.3 lpm; Q4 - 16.7 lpm.

Steps for filter loading:

1. Set out a piece of clean aluminum foil on top of the sampler as a work surface.
2. Get items needed for filter load: tweezers, cassette loader tool, and 4 petri dishes with filters to be loaded.
3. Beginning with the first filter holder. Unscrew the black hand ring in the middle of the filter holder and remove the white filter cassette. Place the cassette on the clean foil work surface.
4. Loosely reconnect the filter holder so the interior remains clean while loading the filter into the cassette. Do not set anything down on a dirty surface.
5. Open the cassette using the aluminum cassette loader tool. Handle only on the edges, and take care not to touch the interior with fingers.
6. Using tweezers, take a filter from the correct petri dish and load it into the filter cassette and carefully push the top of the filter cassette on to close.
7. Place the loaded filter cassette back into the correct filter holder and tighten.
8. Repeat steps 3-7 for each of the other 3 filter holders.
9. Leave empty petri dishes in the sampler to collect filters after the run.
10. Program the sampling event and record details like the FID numbers on the log sheet as described below.

Programming an event to run:

1. Go to the >>>>Main Menu<<<< on the programming screen. Use the Cancel key to return to the previous menu until >>>>Main Menu<<<< is reached.
2. Use the arrow key "V" to select "Events>" and press enter.
3. Use the arrow key to select "Add Event>" and press enter.
4. Use the arrow key to select "Manual Event" and press enter.
5. Event Start Date: change the date that appears automatically to be the current date that sampler should start on. Date is given in Month - Day - Year (MMDDYY) format.
6. Event Start Time: enter the time sampling should begin (e.g., 9:00).
7. Event Duration 24:00 24 hours, press enter.
8. Enter Filter Set ID (SID). This will be the site number followed by the date as given on the top of the event log sheet. (e.g., 1-021003).
9. Enter Filter ID (FID1): 5-digit number from petri dish
10. Enter Filter ID (FID2): 5-digit number from petri dish
11. Enter Filter ID (FID3): 5-digit number from petri dish
12. Enter Filter ID (FID4): 5-digit number from petri dish

Wait for the sampler to start at 9:00 am. Once it is running check the initial flow rates are in the correct range.

1. Press the Cancel button to get to the >>>>Main Menu<<<<.
2. Use arrow key to select "Events>" and press enter.
3. Use arrow key to select "View Event>" and press enter.
4. You will see a screen with the header "Status: Executing"
5. Use the arrow key to page through the status screens and verify the settings are correct.
6. Record the current values for Flow 1, Flow 2, Flow 3, and Flow 4 on the event log sheet under Initial Flow rates (L/m).
7. If the instrument is operating correctly. Close the cabinet door and leave the instrument to run overnight.

Details for unloading filter samples:

After the sample run has ended, verify correct operation and record average values on the log sheet as follows:

1. Press the Cancel button to get to the >>>>Main Menu<<<<.
2. Use arrow key to select "Events>" and press enter.
3. Use arrow key to select "View Event>" and press enter.
4. Choose the event last run and press enter.
5. You will see a screen with the header "Status: Completed"
6. Use the arrow key to page through the status screens and record information onto the log sheet. Use the Actual Information for START - Date - Time and STOP - Date - Time.
7. Record the Duration of the run (should be 24 hours unless there was a problem).
8. Use the arrow key to page through status screens and record the Ambient Temp: Avg, Min and Max values.
9. Record the Barometric Pressure: Avg, Min and Max values.
10. Record the Humidity: Avg, Min and Max values.
11. For each flow record the Avg. Flow and volume of air sampled on the log sheet.
12. Record any problems that occured while sampling in the comments section. Continue comments on the back of the log sheet or on addition pages if necessary. Also, note down what weather conditions were like on the day the samplers were run (i.e., windy, rain, etc.)

Steps for filter unloading:

1. Set out a piece of clean aluminum foil on top of the sampler as a work surface.
2. Get items needed for filter unloading: tweezers, cassette loader tool, and 4 empty petri dishes.
3. Beginning with the first filter holder. Unscrew the black hand ring in the middle of the filter holder and remove the white filter cassette. Place the cassette on the clean foil work surface.
4. Loosely reconnect the filter holder so the interior remains clean while loading the filter into the cassette. Do not set anything down on a dirty surface.
5. Open the cassette using the aluminum cassette loader tool. Handle only on the edges, and take care not to touch the interior with fingers.
6. Using tweezers, carefully remove the sampled filter from the cassette and place it into the correct petri dish. Touch the filter only with tweezers and only near the edges of the filter.
7. Close the cassette and place the empty filter cassette back into the filter holder and tighten.
8. Repeat steps 3-7 to unload each of the other 3 filter holders.
9. Wrap Teflon tape around the edge of each petri dish, pulling it tight to seal. Make sure to hold the dish upright while doing this.
10. Transport to lab in cooler with "blue ice" and store frozen until time for sample shipment for analysis.
11. Download data using data link.

Sampling Schedule

Samples will be collected during four seasons beginning in October, 2002. Subsequent sampling will occur during December, 2002, March, 2003 and June, 2003. During each month there will be five 24-hour samples and one field blank collected. Sampling dates will be (see Figure 1):

October, 2002 Sampling Dates: 3, 9, 15 21, 27

December, 2002 Sampling Dates: 5, 11, 17, 23, 29

March, 2003 Sampling Dates: 4, 10, 16, 22, 28

June, 2003 Sampling Dates: 2, 8, 14, 20, 26

On each sampling day samples will be loaded in the morning allowing sufficient time to start samplers running at 9:00 am. Sample timers will be set to turn samplers off after 24 hours at which time operators will unload samples.

A field blank is a set of samples that are taken to the field and loaded normally and then immediately removed without running the sampler. The field blank should be taken on the last sampling day of each month of sampling. Field blank designations are: 0210FB - October, 0212FB - December, 0303FB - March, and 0306FB - June.

Sampler Problems/Trouble Shooting

If there is a problem with the electronics in the sampler, samples can be taken in manual operation mode. For manual operation use the pump bypass cord provided in the tool box. The pump bypass cord will enable the pump to be powered directly without progamming the instrument. In this mode, the sampler can be turned on and off by plugging/unplugging the power to the pump.

If manual operation is used, the flow rates through the filter holders should be measured using an external flowmeter provided. Flows should be checked initially when the sampler is first started, and final flows should be checked again 24 hours later before the sample is removed. An alternative log sheet is provided should manual operation be necessary. See Figure 3.

An adapter is provided to measure flows using the external flowmeter. To measure the flow with the external flowmeter, disconnect each filter holder one-at-a-time by unscrewing the top white plastic disc. Attach the flowmeter adapter to the top of the filter holder and hold the flowmeter vertically while reading the flow. There are two balls inside the glass tube on the flow meter (black and silver). Read the number nearest to the center of each ball and record the reading. For example, 103B/60S would be 103 black ball and 60 silver ball. A calibration page will be provided with each flowmeter to convert the ball readings to lpm.

Calibration and Maintenance

Sampler flow rates will be calibrated using a dry gas test meter when the equipment is set up by Caltech and Georgia Tech personnel. It should not be necessary to recalibrate the instruments during the course of the year sampling study.

Each month before the beginning of a new set of samples. Flow rates will be checked with the external flow meter provided to verify that the instrument calibration is valid.

Samplers were thoroughly cleaned with hexane and methanol before being brought to the field. It should not be necessary to dissasemble and clean the equipment during the course of the year sampling study. However, care should be taken to keep the filter holders closed and all sampling lines connected between sampling months so that the parts remain as clean as possible.

At the start of each sampling month, the large particle collection cup at the bottom of each cyclone should be emptied. This cup unscrews and any large particles collected can be discarded. There are two cyclones per sampler.

Filter cassettes should be inspected for cleanliness at the start of each sampling month. Spares are provided should any need to be replaced.

At the end of each sampling month. Download all data from the unit using the Datalink and software provided. The data in the datalink unit should be transferred to a computer and emailed to lynn@thesalmons.org.

A.2 Field Operating Procedures for RAAS $PM_{2.5}$ Samplers in the Pearl River Delta Study – Chinese version, authored by Lynn Salmon, translated by Yang Qiang

简介（Introduction）：

对香港和珠江三角洲七个采样点的空气监测从 2002 年 10 月开始。每一个采样点的代码用两个字母和一个数字表示。这些代码是：

TM1－Tap Mun

TC2－Tung Chung

CW3－Central and Western

SZ4－深圳

GZ5－广州

CH6－从化

ZS7－中山

安德森采样器（Thermo Andersen PM2.5 speciation sampler）将安置在前 5 个站，灰色采样器（Caltech Gray Box PM2.5 ambient samplers）（安德森采样器的原型）安置在后两个站。每一个采样器内有 4 个采集细粒子的采样头。两个放置放石英膜（Quartz）来采集有机粒子。两个放置特氟龙膜（Teflon）来测定气溶胶的质量浓度、离子分析（Cl－，SO4＝，NO3－，NH4＝）和微量金属分析。这些采样头被标示：Quartz 1，Teflon 2，Teflon3 和 Quartz4。

每一个采样器有一个泵（pump）和几个流量能严格控制的限流孔（orifice）。采样器工作在 220V 电压下，采样流量在安置前将被标定。

每一个采样器都附带一个笔记本和一个工具箱。笔记本包括一份操作程序介绍和记录纸（log sheets）（每次采用一张），每次装膜和取膜时都需要填写采样记录纸。每个采样点都有一份带有参考流量的采样记录纸的示例。工具箱包含换膜需要的基本工具和采样器维护的一些常用工具。两个用烧过的铝箔包好的镊子（tweezers）。这两个镊子需要保持干净。备用的采样夹（cassettes）、O 型圈（O-rings）和采样头（filter holder），这些备用物品在采样器中的变脏时可以更换。还包括一个打开采用夹的工具（cassette loder tool）。另外，工具箱里还有一个手动测量流量的器械和其他相关的工具。

更详细的放膜和取膜的介绍见下一页。

采样膜（Filter samples）

预先包放在有盖培养皿的采样膜在采样前需要保存在实验室里。采样膜需要在有“蓝冰”（blue ice）的冷却器或者冰箱里运输，到达实验室后需要立即存放在冰箱里以减少挥发性物质的损失。

每一个采样膜都有一个如下形式的标签：

TM1-Q1-021002

TM1 是采样点的标识（TM1,TC2,CW3,SZ4,GZ5,CH6 或 ZS7）；Q1 是采样头的标识（Q1,T2,T3 或 Q4）；021002 是以年月日的形式给出的采样时间。每一次采样的相应采样日期在记录在记录纸上。

一套膜包含 4 个放置在有盖培养皿里的采样膜：

（Q1）石英膜，放置在用铝箔包裹的培养皿里

（T2）特氟龙膜

（T3）特氟龙膜

（Q4）石英膜，放置在用铝箔包裹的培养皿里

当放置采样膜时，最重要的是把不同的采样膜放在正确的采样头里。每一个采样膜在培养皿上都有一个名称（如，Q1），在采样头上也有一个相近的标识（如，Quartz 1）。

不要使用有孔或者有其他缺陷的采样膜。在采样过程中，如果采样膜掉在地上，请不要使用。出现上面的情况时，启用备用的采样膜，并在备用膜的培养皿盖子上写上相同的标签。划掉原来膜的盖子上的标识并且写上 BAD 以防以后误拿。换下的膜需要保存起来和其他的采样膜一起寄回。

在培养皿的盖子上，每一个采样膜都有一个唯一的 5 位数的膜 ID 数字（FID）。每一张膜都有自己的 ID 数字。这些 ID 数字需要记录在每次采样的记录纸上。

当使用备用的采样膜时，请确认膜在它原来的培养皿里并在培养皿的盖子上写上采样点的代号和采样日期。不要改变备用膜的 ID 数字。

当放膜时，膜向上一面需要和膜在培养皿中一致。采样膜只能用镊子取放，千万不要用手或者手套触摸。操作人员需要带上手套当安放采用夹时。在采样器的顶部铺放干净的铝箔作为操作台。放膜和取膜时不能在采样器附近吸烟。

放膜具体操作细节（**Details for loading filter samples**）：

采样头安置在旋风切割头（cyclone）后来收集细粒子。在采样间隔期间，带有空的采样夹的采样头将被留在采样器里。在不用时，他们必须装配完好以保证内部干净。采样头和几个设置在采样器底部流量能严格控制的限流孔相连。通过每一个采样头的流量近似为：Q1-16.7 升/分；T2-7.3 升/分；T3-7.3 升/分；Q4-16.7 升/分。每一个采样器都会给一个标定过的参比流量。操作人员在放膜时需要确认流量在可以接受的范围。

放膜时间最好接近采样开始时间以尽可能的减少污染。严格说来，膜应在采样开始前 12 小时之内放置。如果不能在这个时间内达到采样点，可以作为例外处理。

只有经过培训被授权的操作人员才可以放/取膜。在每一个采样月期间，采样器和操作人员至少要被审计一次，以确认操作程序是否正确。参看审查检查表（Audit Checklist）。

放膜操作步骤（**Steps for filter loading**）：

1. 在采样器顶部放一张烧过的干净的铝箔作为操作台。在采样期间需要时可以更换铝箔。
2. 取出放膜需要的物品：镊子，放置采样夹的工具，手套和 4 个装有将被安放的膜的培养皿。
3. 打开采样器的门（门可能比较脏），戴上干净的一次性手套。不要用手套触摸脏东西。如果手套被弄脏了，需要更换新的干净的手套然后继续操作。
4. 从第一个采样头开始。拧开在采样头中间的黑色的手可以握住的盖子，取出里面的白色的采样夹。把采样夹放在干净的铝箔工作台上。
5. 简单的重新装好采样头，以保证在向采样夹中放膜时采样头内部清洁。不要放任何东西在脏的地方。
6. 用铝制采样夹器打开采样夹。取放膜时只能接触采样夹边缘，注意不要触摸采样夹内部。

7. 用镊子取一个正确的采样膜放在采样夹中。注意只能用镊子接触采样膜的边缘。
8. 用采样夹器施加一个均匀的压力，小心的压采样器的顶部闭合采样夹。检查装好的采样膜是否平展的处于采样夹的中心。如果采样膜有皱纹或者不平整，打开采样夹，再次用采样夹压紧，采样膜将会光滑平整。如果采样膜不能平整，可以用备用膜进行替换。
9. 把采样夹放回正确的采样头并且拧紧，采样夹的不锈钢面朝下，放有采样膜的一面向上。
10. 重复 3-9，放置另外 3 个采样膜。
11. 把空的培养皿放在采样器内，以便采样后收集采样膜，摘掉（throw away）手套。
12. 设置采样程序，在记录纸上记录详细的资料，例如 FID，也可以记录下需要什么配件。

采样程序设置（Programming an event to run）：

1. 首先需要到>>>Main Menu<<<界面。按 Cancel 键直至出现>>>Main Menu<<<界面。
2. 按上下键选择“Events>”，按 Enter。
3. 按上下键选择“Add Event>”，按 Enter。
4. 按上下键选择“Manual Event>”，按 Enter。
5. 设置采样开始日期（Event Start Date）：将自动显示在显示屏上的日期改成实际需要的采样开始日期。以月－日－年的形式（MMDDYY）输入，按 Enter。
6. 设置采样开始时间（Event Start Time）：输入采样开始时间（如在 12：00am 开始，输入 0000），按 Enter。
7. 采样持续时间（Event Duration）：24：00，表示持续 24 小时，按 Enter。
8. 输入一套采样膜的 ID（SID）（Filter Set ID）：这个数字由采样点的顺序号再加上记录纸上的采样日期组成。（例如，1-021002）
9. 输入采样膜 ID（FID1）：培养皿上的五位数。
10. 输入采样膜 ID（FID2）：培养皿上的五位数。
11. 输入采样膜 ID（FID3）：培养皿上的五位数。
12. 输入采样膜 ID（FID4）：培养皿上的五位数。
13. 在记录纸上的 INITIAL 栏记下放膜日期、时间，人员签名。

开始时的流量检查（Initial flow rate check）

在一起显示屏上检查安德森（Andersen）电子流速传感器（electronic flow sensors）给出的流量，同时用流量计（rotameter）检查流量。确认流速在参比流速（Reference Flow Sheet）范围内。

1. 按 Cancel 键直至出现>>>Main Menu<<<界面。
2. 用上下键选择“Maintenance>”，按 Enter。
3. 进入 Maintenance 菜单，用上下键选中“Yes”，按 Enter。
4. 用上下键选择“Diagnostics>”，按 Enter。
5. 用上下键选择“Flow Valves”，按 Enter。
6. 此时，显示屏上将会显示三列数字。最后一列是流速值。等待约 15 秒让流速稳定。在记录纸上 Initial Flow Rates，Andersen（L/m）一栏记录下初始流速：Quartz 1＝Q1a，Teflon 2＝Q2a，Teflon 3＝Q3a，Quartz 4＝Q4a。
7. 用流量计测定流速。测定流速时，每次拧开一个采样头上的白色塑料盖，套上测定流速时需要的附件（adapter），然后连接上流量计。读取流量时，要保持流量计竖直。流量

计有两个颜色分别为黑色和银灰色的小球（black and silver），读取每个小球中心所指示的读数，记录在 Initial Flow Rates，Rotameter（ball）栏下。同时记录下流量计的代号（Rotameter ID）。

8. 按 Cancel 键关掉泵。
9. 与参比流速进行对比。Andersen 值在参比值+-2%范围内。流量计值在参比值+-10%的范围内。
10. 如果流速在允许范围内，关上采样器的门，让采样器按设定的时间工作一天。如果有问题，参看解决问题指南部分（Trouble shooting section），或者向求助人员列表（contact help list）上的人员请求帮助。

中途检查（Middle flow check）

在采样器运行的 24 小时内至少需要中途检查一次，以确定采样器工作是否正常。

1. 按 Cancel 直至出现>>>Main Menu<<<界面。
2. 用上下键选中“Events>”，按 Enter。
3. 用上下键选中“View Event>”，按 Enter。
4. 选中 current event，按 Enter。
5. 将会出现一个以“Status：Executing”开始的显示屏。
6. 用上下键翻页检查设置是否正确。
7. 在 Middle Flow Rates，Andersen（L/m）一栏记录下当时的流量数值。Flow1，Flow2，Flow3 和 Flow4。
8. 用流量计检查流速是否正确。拧开采样头下部的白色圆环，按放膜时的方法判断流量是否正确。
9. 如果采样器工作正常，关上采样器的门，让采样器继续运转。如果有问题，参看解决问题指南部分（Trouble shooting section），或者向求助人员列表（contact help list）上的人员请求帮助。
10. 记下中途检查的日期、时间，并在 middle operator 一栏签名。同时记录下当时的天气情况（如，有风，下雨等）。

取膜的具体操作（Details for unloading filter samples）：

采样结束后，采样膜应尽可能早的取出。采样结束后，样品在野外停留的时间应不超过 16 小时。如果不能在这个时间内达到采样点，可以作为例外处理。向求助人员列表上的人员请求同意在 16 小时之外取膜。

采样结束后，在记录纸上按如下操作记录平均流速：

1. 按 Cancel 键直至出现>>>Main Menu<<<界面。
2. 用上下键选中“Events>”，按 Enter。
3. 用上下键选中“View Event>”，按 Enter。
4. 选择希望记录的日期，按 Enter。
5. 显示屏将会显示“Status：Completed”。
6. 用上下键翻页并在记录纸上记录详细的信息。记录采样实际开始/结束的日期和时间（Actual Information for START-Date-Time and STOP-Date-Time）。
7. 记录采样持续时间（如果在采样过程中没有其他的问题，采样持续时间应该是 24 小时）。

8. 用上下键翻页，记录采样温度：平均值，最大、最小值（Ambient Temp：Avg，Min and Max values）。
9. 记录采样气压：平均值，最大、最小值（Barometric Pressure：Avg，Min and Max values）。
10. 记录采样湿度：平均值，最大、最小值（Humidity：Avg，Min and Max values）。
11. 记录每一个采样通道的平均流速（Avg. Flow）和采集空气体积（Vol，m3）。
12. 在评论（comments section）记录采样过程中发现的任何问题。当记录纸不够用时，可以写在记录纸的背面或者加纸。
13. 在 END 一栏记录下取膜的日期、时间，并写下操作人员的名字。

取膜具体步骤（Steps for filter unloading）

1. 在采样器的顶部放置一张干净的铝箔作为操作台。
2. 准备好取膜需要的物品：镊子，采样夹器和 4 个空的培养皿。
3. 打开采样器的门，戴上干净的手套。不要用手套触摸任何脏东西。如果不小心弄脏了手套，取下脏的手套换上干净的手套在继续。
4. 从采样头开始。拧开采样头中间的黑色圆环，取出采样头中白色的采样夹。把采样夹放在干净的铝箔上。
5. 轻轻的拧好采样头以在当从采样夹中取膜时能保持采样头内部干净。不要在脏的地方放任何东西。
6. 用铝制采样夹器打开采样夹。用手拿采样头的边缘部分，要注意不要用手碰采样夹的中间部分。
7. 用镊子小心的从采样夹中取出采样膜，放入正确的培养皿中。只能用镊子接触采样膜的边缘部分。
8. 盖上培养皿的盖子，把培养皿放置在不易碰到的地方。
9. 关上采样夹，把空的采样夹放回采样头并拧紧。
10. 重复 3-9，取出另外 3 个采样膜。
11. 用特氟龙胶带（Teflon tape）密封培养皿，注意要稍微用力拉带子使其密封。在操作过程中要保持培养皿竖直。
12. 将采样膜放入有“蓝冰”的制冷器中。
13. 用数据下载器（DataLink）下载数据（参加下）。
14. 取下数据下载器，关掉（OFF）仪器。
15. 每次采样后，把采样膜、数据下载器和记录纸带回实验室。参加样品保存/运输部分（Sample handling/shipping）。

下载数据（Downloading data with DataLink）

1. 把数据下载器（DataLink）插入采样器中的 RS-232 端口（RS-232 port）。此时，数据下载器的绿灯会亮。
2. 按 Cancel 键直至出现>>>Main Menu<<<界面。
3. 用上下键选中“Data Transfer>”，按 Enter。
4. 用上下键选中“Transmit All”，按 Enter。显示屏将会显示“Data Log Transmission in Progress”，下载器的绿灯将会闪烁。
5. 整个数据传输过程将会持续几分钟。等数据传输完成后，从采样器 RS-232 端口上取下

下载器。

样品保存/运输（Sample Handling/Shipping）

如前所述，在每次野外采样结束时，样品都要求立即放入带有“蓝冰”的制冷器中。在香港，这些样品在取膜当天将被送给 HKEPD 的 Wan Chai。操作人员也应数据下载器送到 HKEPD。数据将会被下载至 HKPED 的电脑内，然后会及时的 email 给 lynn@thesalmons.org 和 gwillis.ce02@gtalumni.org，以便数据在下次采样开始之前得到检查。

每次采样后，HKEPD 会传真采样记录给 Lynn Salmon 1(626)395-2940。采样的原始记录将会保存在 HKEPD。每个采样月结束后，采样膜和记录纸都会被提交给 Jian Yu。记录纸的复印件将会保存在野外记录本中。

在 HKEPD，采样膜将会保存在冷冻条件下（-4℃或者更低）。在每个采样月末，Dr. Jian Yu 将从 HKEPD 取走 采样膜，保留在 HKUST 分析的膜，将其余的膜在 10 天之内寄给 Caltech 的 Lynn Salmon。

在 PRD，采样膜将会保存在制定实验室的冰箱里。野外采集的样品需要在样品收集的当天放在制冷器里送至制定的实验室。操作人员在每次采样结束后应将数据下载器和记录纸送到指定的实验室，数据将被下载然后 email，记录纸要求传真给 Lynn Salmon。

在每个采样月末，PRD 采样点的样品将被送至由北大监测的深圳采样点（冷冻）。深圳点收到样品后要求在一周之内送给 HKUST 的 Jian Yu。Dr. Yu 将对样品进行分类，将其余的样品和香港的样品一起寄给 Caltech。样品要求要在有“蓝冰”的密封的箱子里邮寄。使用 Fedex 或其他的快递方式。

采样日程（Sampling Schedule）

采样将会从 2002 年 10 月开始，持续 4 个季节。接下来的采样时间依次是：2002 年 12 月，2003 年 3 月和 2003 年 6 月。在每一个采样月内，都有 5 个 24 小时的采样样品和一个野外操作空白。采样的日期是（见日历）：

2002 年 10 月：2，8，14，20，26

2002 年 12 月：1，7，13，19，25

2003 年 3 月：1，7，13，19，25

2003 年 6 月：5，11，17，23，29

采样膜在采样日期的前一天放置。定时器（Timers）用来自动打开采样器并在 24 小时采样结束后关掉采样器。采样结束后，操作人员将取下采样膜，将其立即放至有蓝冰的制冷器中。

如果采样点不能在采样前/后一天之内到达，应采取一些特殊的措施。如果出现这种情况，请向求助人员列表上的人员请求帮助。

野外空白（Field Blank）

野外空白是带至野外的一套完整的采样膜。按正确的操作放好膜后，不用运行采样器，几分钟后取出。野外空白在每个采样月的最后一次采样后进行。野外空白的标识是：0210FB-October，0212FB-December，0303FB-March，0306FB-June。

常见问题/解决办法（Sampler Problems/Trouble Shooting）

如果采样器的电子元件出现问题，可以用手动的方式运行采样器。工具箱里有一根备用的电源线（bypass cord）可以让采样器的泵在手动的方式下运行。这个电源线可以不用设置采样程序而直接让泵运转。在这种方式下，可以通过插/拔电源插头来开/关泵。

在手动操作状态下，只能用流量计来测定通过采样头的流量。流量需要在采样器开始工作时测定，在采样器运行过程中至少需要测定一次流量。在取膜时需要做最后一次的流量检查。

一个专门的器件用来辅助流量计测定流量。在测定流速时，每次拧开一个采样头上的白色塑料盖，套上测定流速时需要的附件（adapter），然后连接上流量计。读取流量时，要保持流量计竖直。流量计有两个颜色分别为黑色和银灰色的小球（black and silver），读取每个小球中心所指示的读数。如果黑球超出了量程，只是记录银灰色小球所指示的数值。

如果出现其他的问题，可以向求助人员列表上的人求助。

如果出现了一些不能采样的影响因素，需要另外采样来（an additional “make-up”sample）补齐缺少的数据。例如，如果是电源或者程序设置导致在某一个采样点不能采样，这个采样点在采样日期的后一天将采一次样进行补齐。如果更严重的情况，比如台风影响了整个采样区域，一次补做的采样将在这个采样月月末进行。如果需要补做采样，请向求助人员列表上的人员询问具体的采样日期。

标定和维护（Calibration and Maintenance）

在野外采样前，当采样器在 Caltech 和 Georgia Tech 组装时，使用干气体流量计（dry gas meter）标定流量。因此，除非发生流量严重偏离参比流量的情况，在这一年的采样过程中不必要对采样器再进行标定。如果有有关标定的任何问题，向求助人员询问，将再次标定。

采样器在野外使用前用正己烷和甲醇彻底清洗过。在这一年的采样过程中不必拆卸清洗仪器。但是，必须小心的保证采样头和采样管路的密闭，以保证采样器尽可能的干净。

在每个采样月开始的时候，每个旋风切割头（cyclone）底部的大颗粒物收集器（large particle collection）都要求被清空。这部分器械可以被拧下来，里面的大颗粒物可以被清空。每个采样器有两个切割头。

每次采样开始前，需要检查采样夹清洁与否。如果发现有被污染，请换用备用采样夹。脏的采样夹需要用甲醇清洗，用干净的高质量的纸巾擦干，保存在工具箱里备用。

每次野外采样前，需要检查采样夹器是否干净。如果被污染，需要用甲醇清洗，然后用干净的高质量的纸巾擦干。

A.3 Quality Control and Quality Assurance Audit, authored by Gayle Hagler

AUDIT CHECKLIST

SITE: _____
DATE:_____
AUDITOR:_____
OPERATOR: _____

Sampler Appearance

YES	NO	
		Is the outside of the sampler undamaged?
		Is the inside of the sampler neat and clean?
		Are any fans blocked by items left in the sampler?
		Are there any incidents of operators smoking around the sampler?
		Are all necessary supplies in tool box?
		Is the power cord secure and undamaged?

Loading/Unloading Filters:

YES	NO	
		Are operators wearing clean gloves when touching the filter cassettes?
		Are tweezers kept clean, wrapped in clean foil?
		Are operators using only tweezers to touch filters?
		Are operators keeping aluminum cassette loader clean – placing it on aluminum foil during use and storing in a clean plastic bag?
		Are filters being loaded properly into the cassettes?
		Are cassettes being loaded properly into the filter holders?
		Are operators placing any portion of the filter holders on a dirty surface during loading/unloading?
		Are filter holders hand-tightened prior to starting a sampling event?
		Are operators taking care to place filter into correct petri dish after event is finished?
		Are all samples in petri dishes sealed with Teflon tape?

Running an event and flow checks:

YES	NO	
		Are filters loaded and unloaded within the set time-frame?
		Are operators programming an event correctly?
		Are the sampling events being done on the correct dates?
		Are operators doing the initial, middle, and final checks for each sampling event?
		Are operators performing the Rotameter and Andersen flow checks properly?
		Given a problem in operation, do the operators know who to contact for help?

Data acquisition and sample transportation:

YES	NO	
		Are the log sheets being filled out completely and accurately?
		Are operators obtaining data using the Datalink device for each event and bringing it to the appropriate person?
		Are the sampled filters transported in coolers?

COMMENTS:

APPENDIX B: CHINA – ADDITIONAL DATA AND ANALYSES

B.1 Meteorological observations during the Pearl River Delta, China field campaign

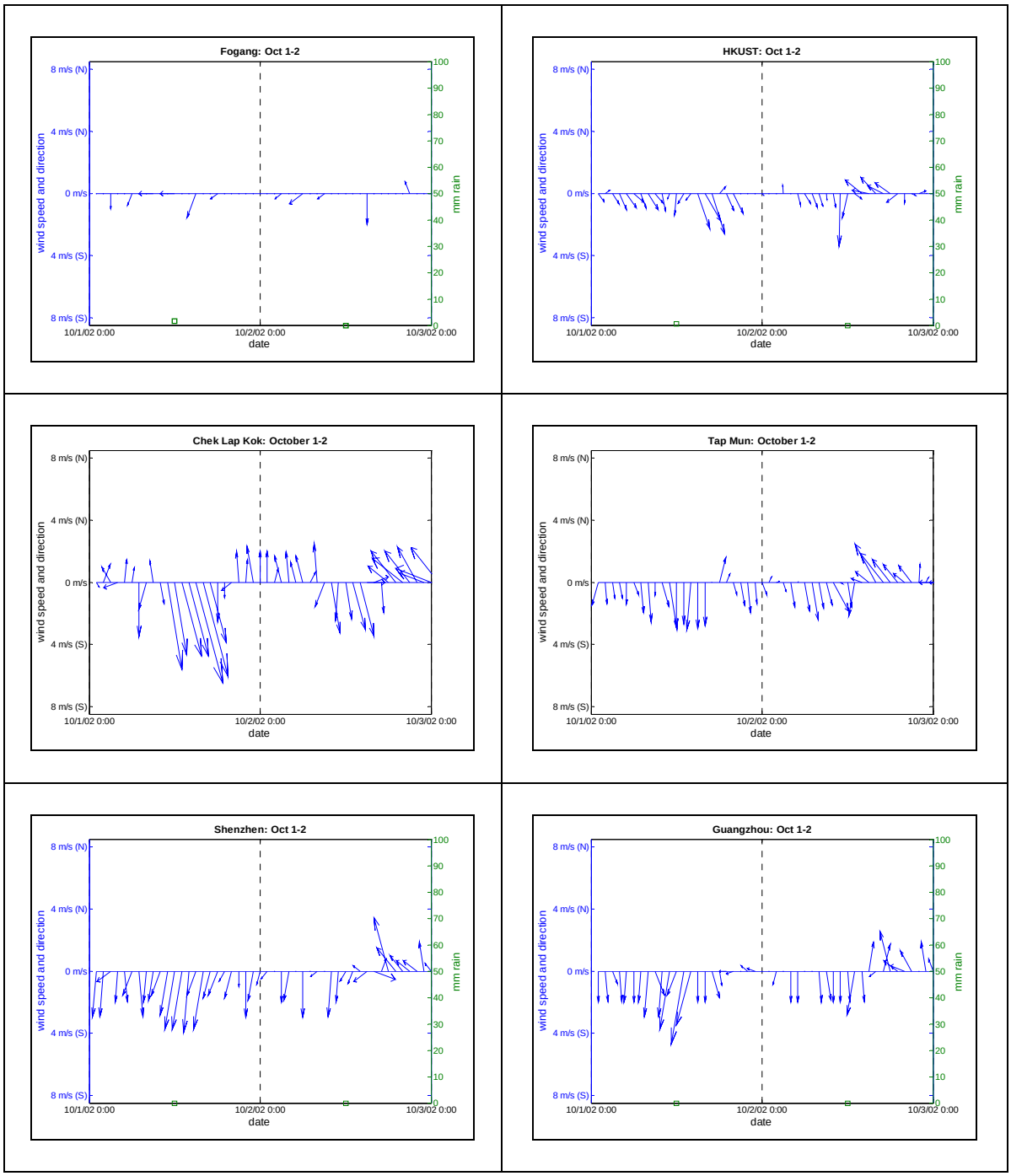

Figure B.1. Hourly wind vectors and 24-hour rainfall at six meteorological sites in the Pearl River Delta on 10/1/2002-10/2/2002.

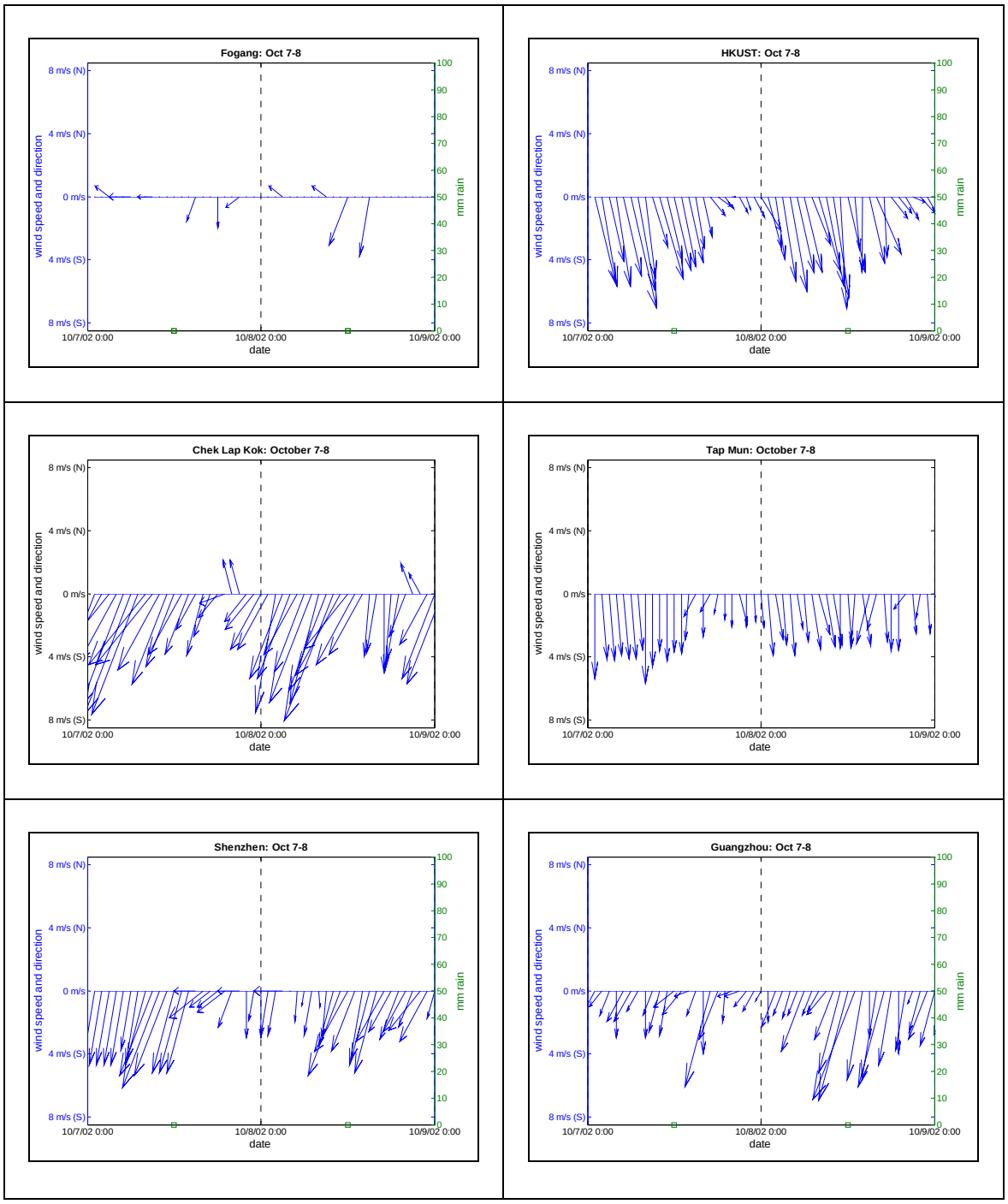

Figure B.2 Hourly wind vectors and 24-hour rainfall at six meteorological sites in the Pearl River Delta on 10/7/2002-10/8/2002.

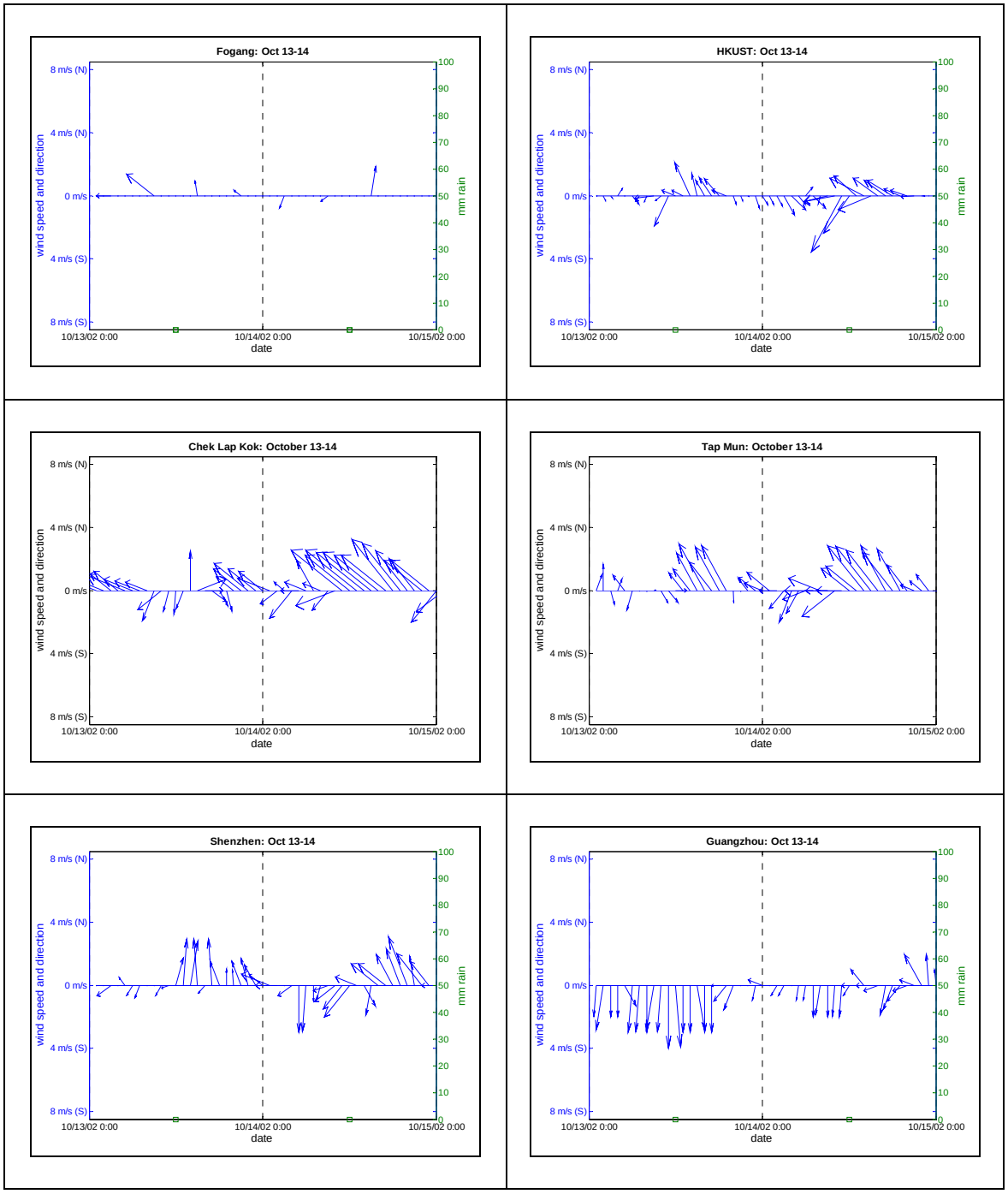

Figure B.3 Hourly wind vectors and 24-hour rainfall at six meteorological sites in the Pearl River Delta on 10/13/2002-10/14/2002.

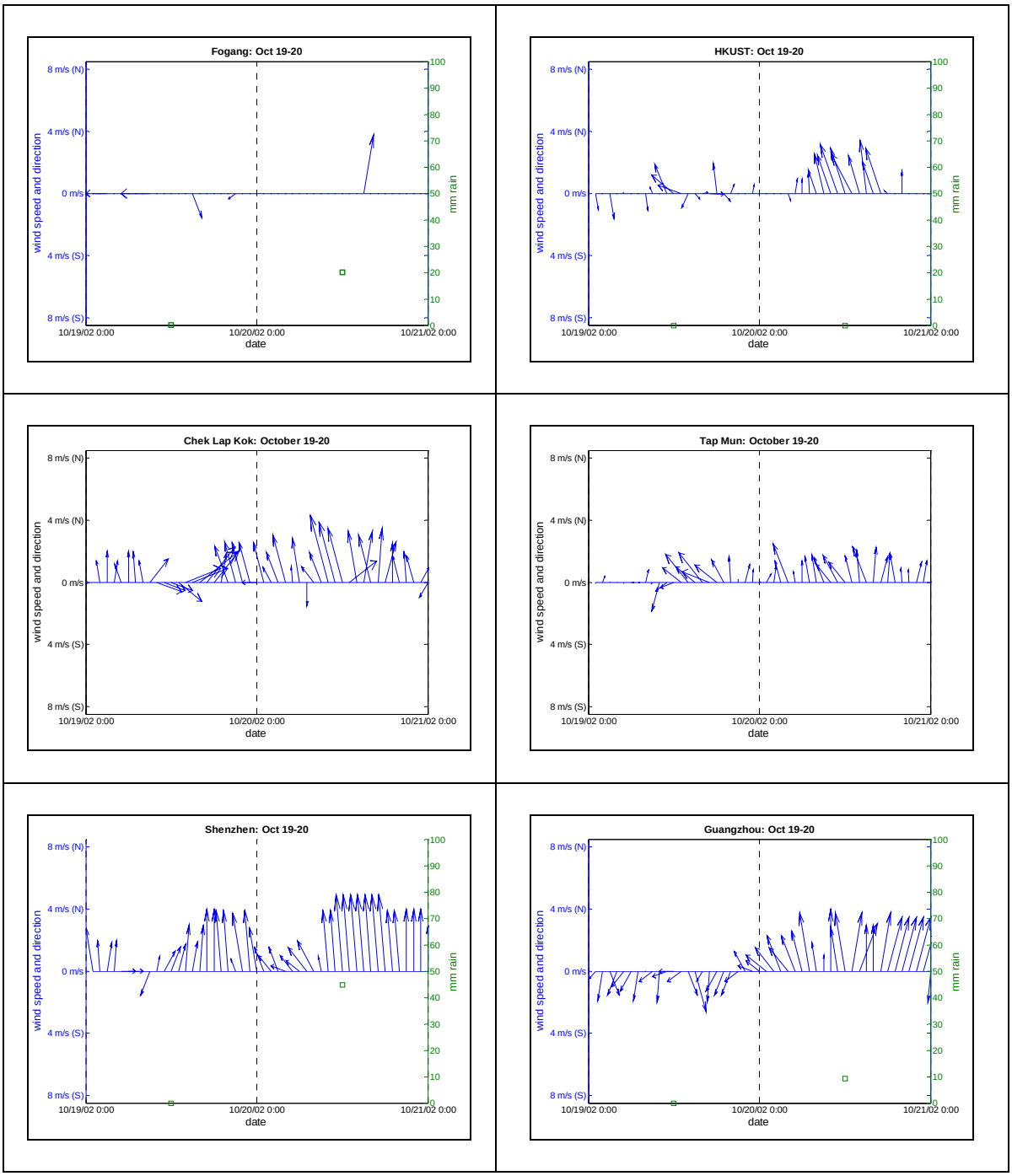

Figure B.4 Hourly wind vectors and 24-hour rainfall at six meteorological sites in the Pearl River Delta on 10/19/2002-10/20/2002.

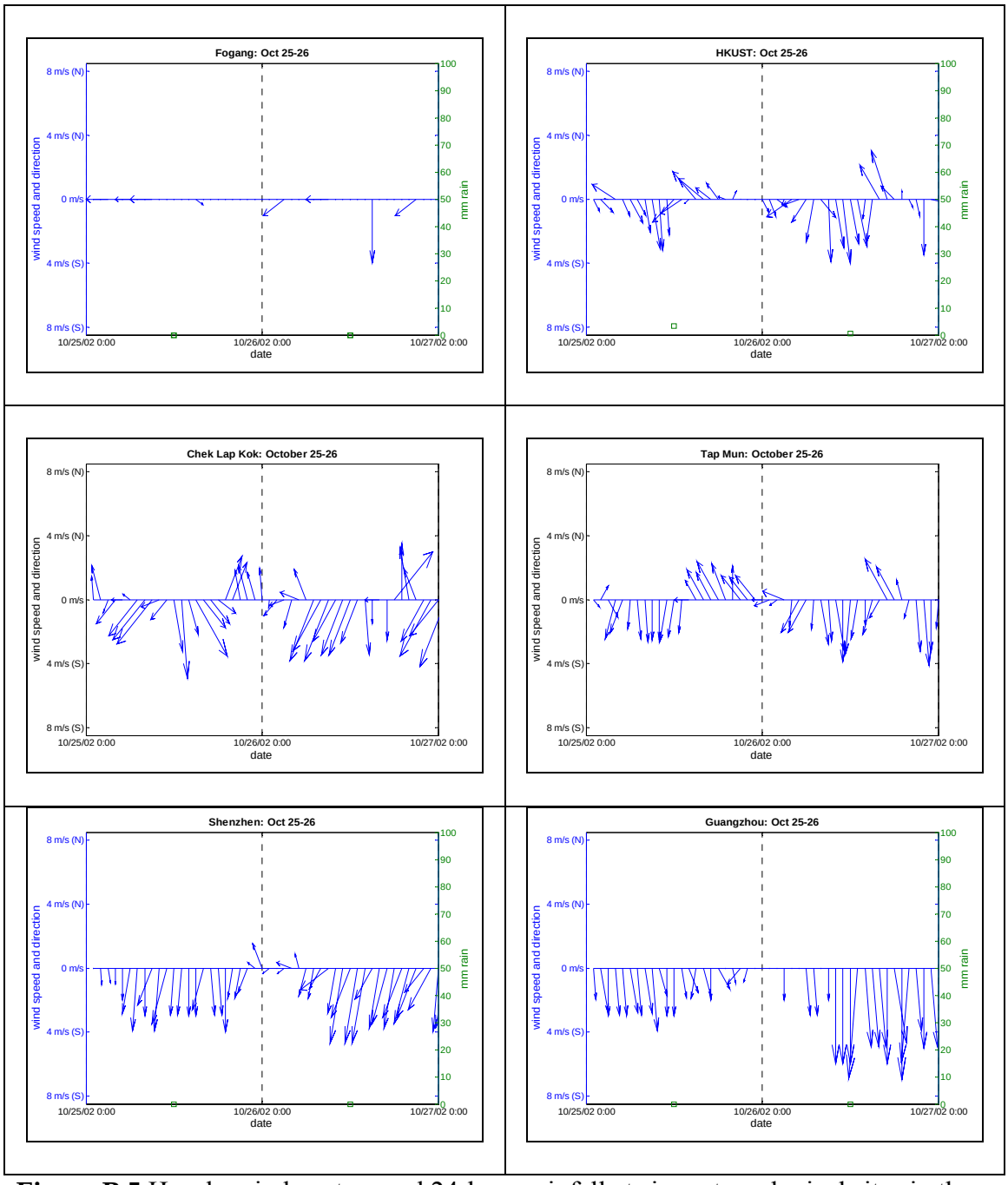

Figure B.5 Hourly wind vectors and 24-hour rainfall at six meteorological sites in the Pearl River Delta on 10/25/2002-10/26/2002

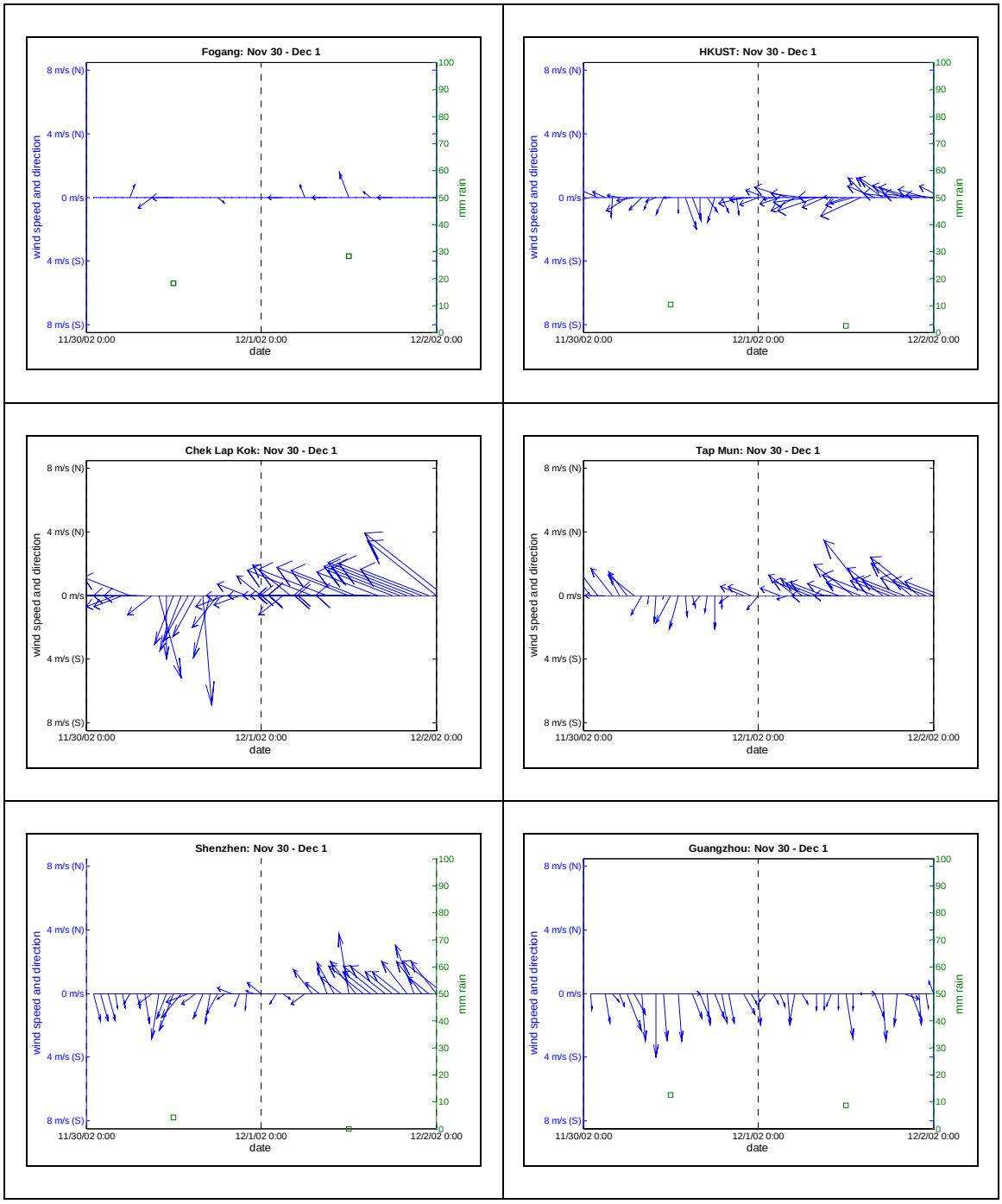

Figure B.6. Hourly wind vectors and 24-hour rainfall at six meteorological sites in the Pearl River Delta on 11/30/2002-12/1/2002.

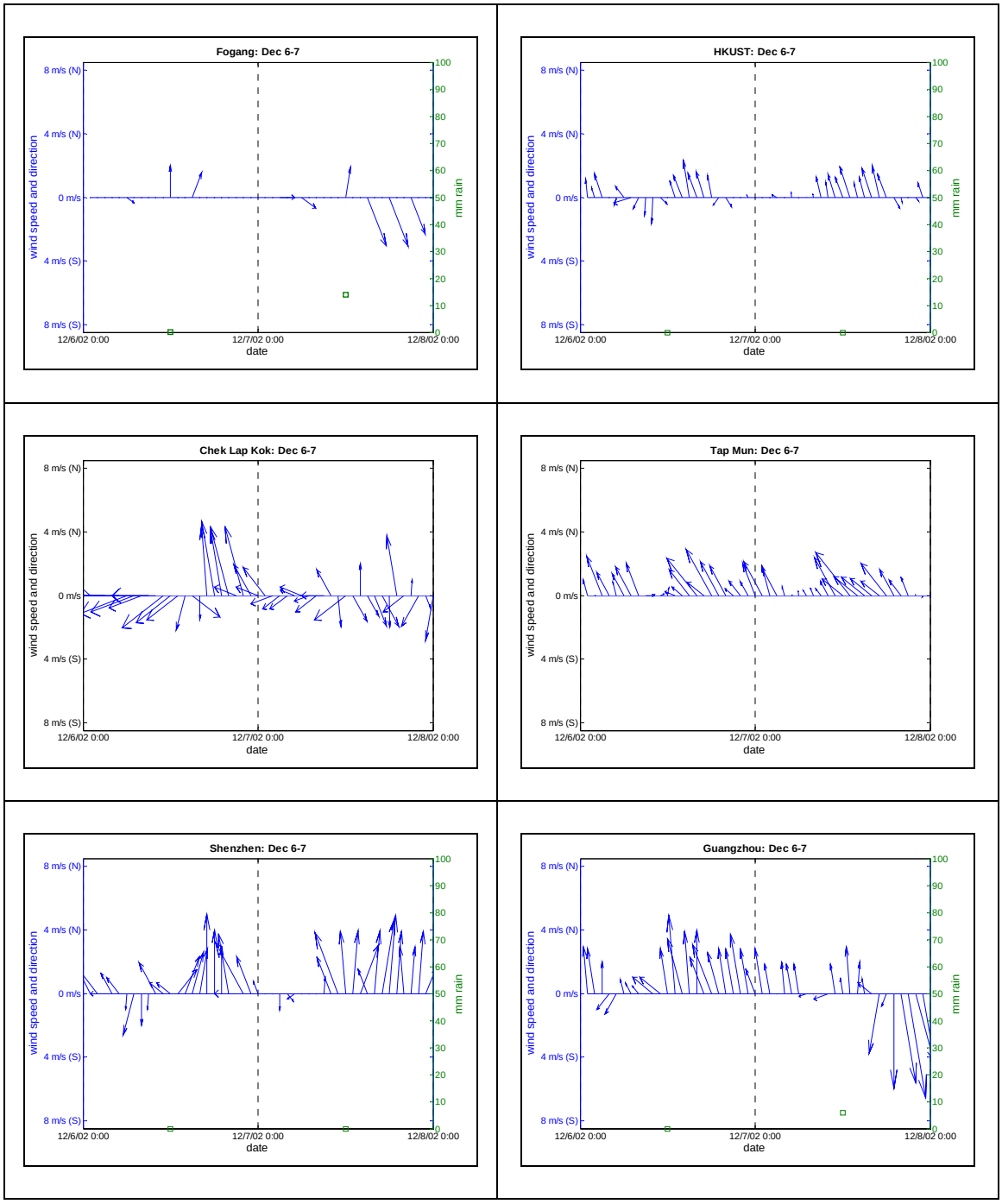

Figure B.7. Hourly wind vectors and 24-hour rainfall at six meteorological sites in the Pearl River Delta on 12/6/2002-12/7/2002.

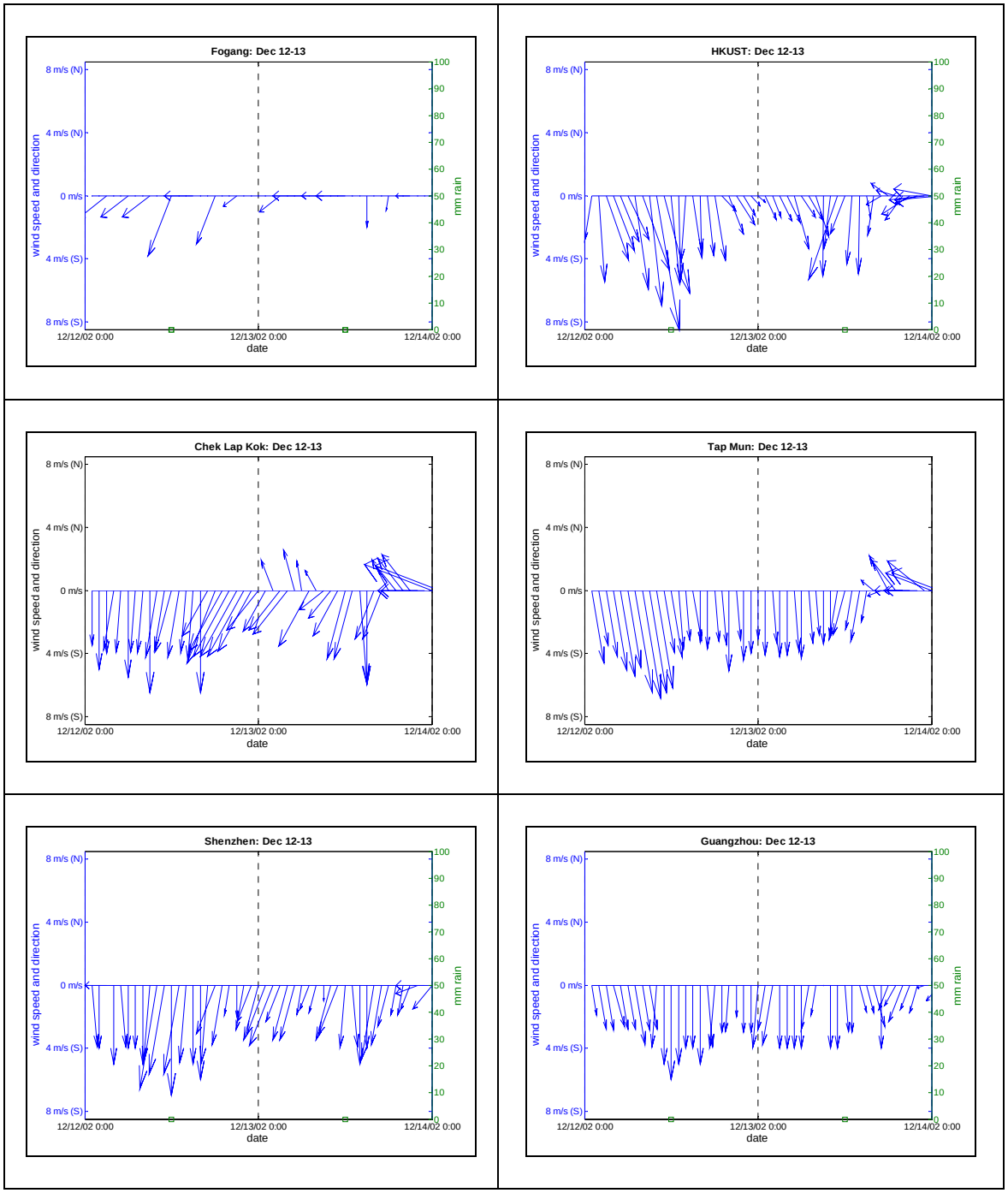

Figure B.8. Hourly wind vectors and 24-hour rainfall at six meteorological sites in the Pearl River Delta on 12/12/2002-12/13/2002.

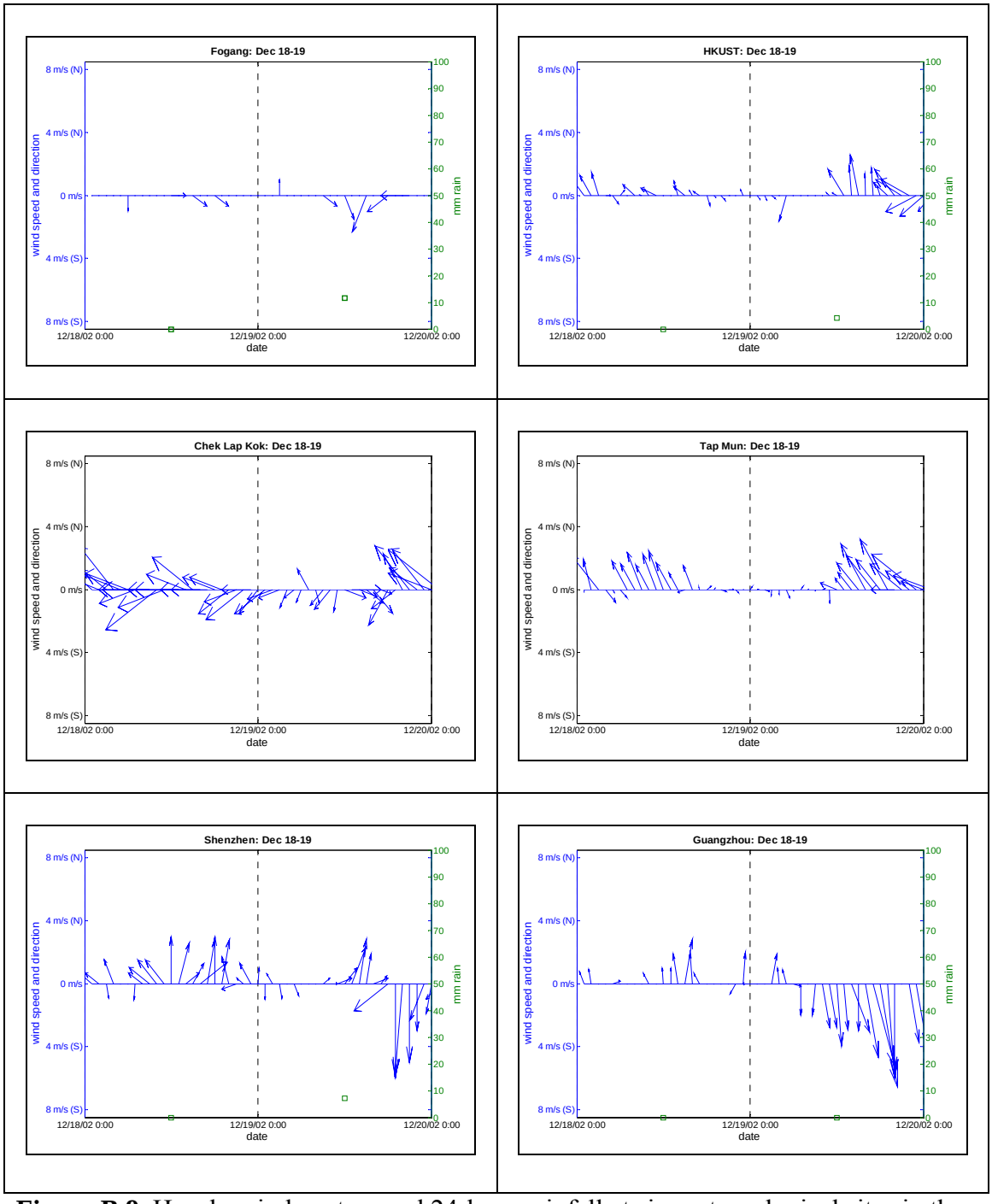

Figure B.9. Hourly wind vectors and 24-hour rainfall at six meteorological sites in the Pearl River Delta on 12/18/2002-12/19/2002.

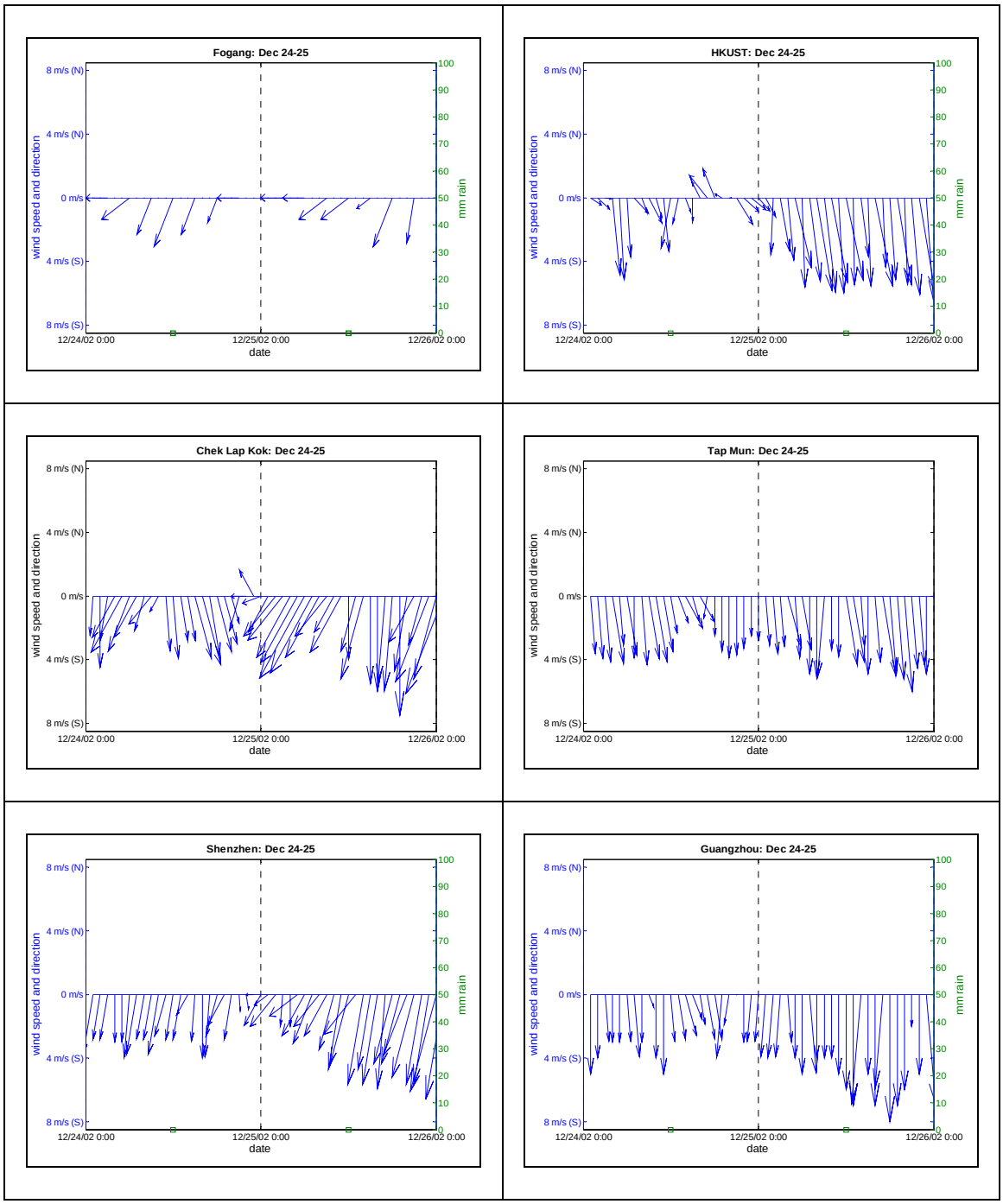

Figure B.10. Hourly wind vectors and 24-hour rainfall at six meteorological sites in the Pearl River Delta on 12/24/2002-12/25/2002.

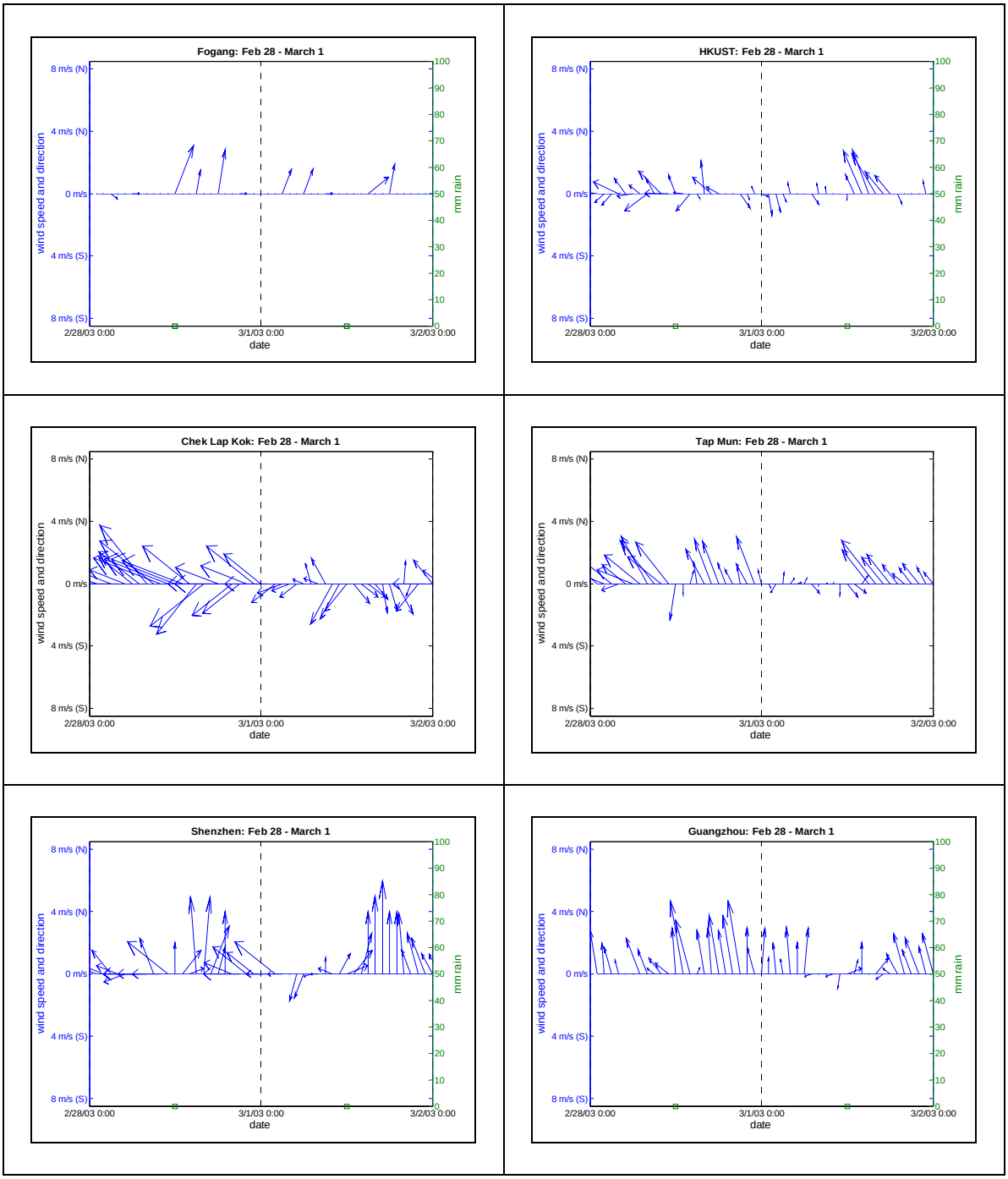

Figure B.11. Hourly wind vectors and 24-hour rainfall at six meteorological sites in the Pearl River Delta on 2/28/2003-3/1/2003.

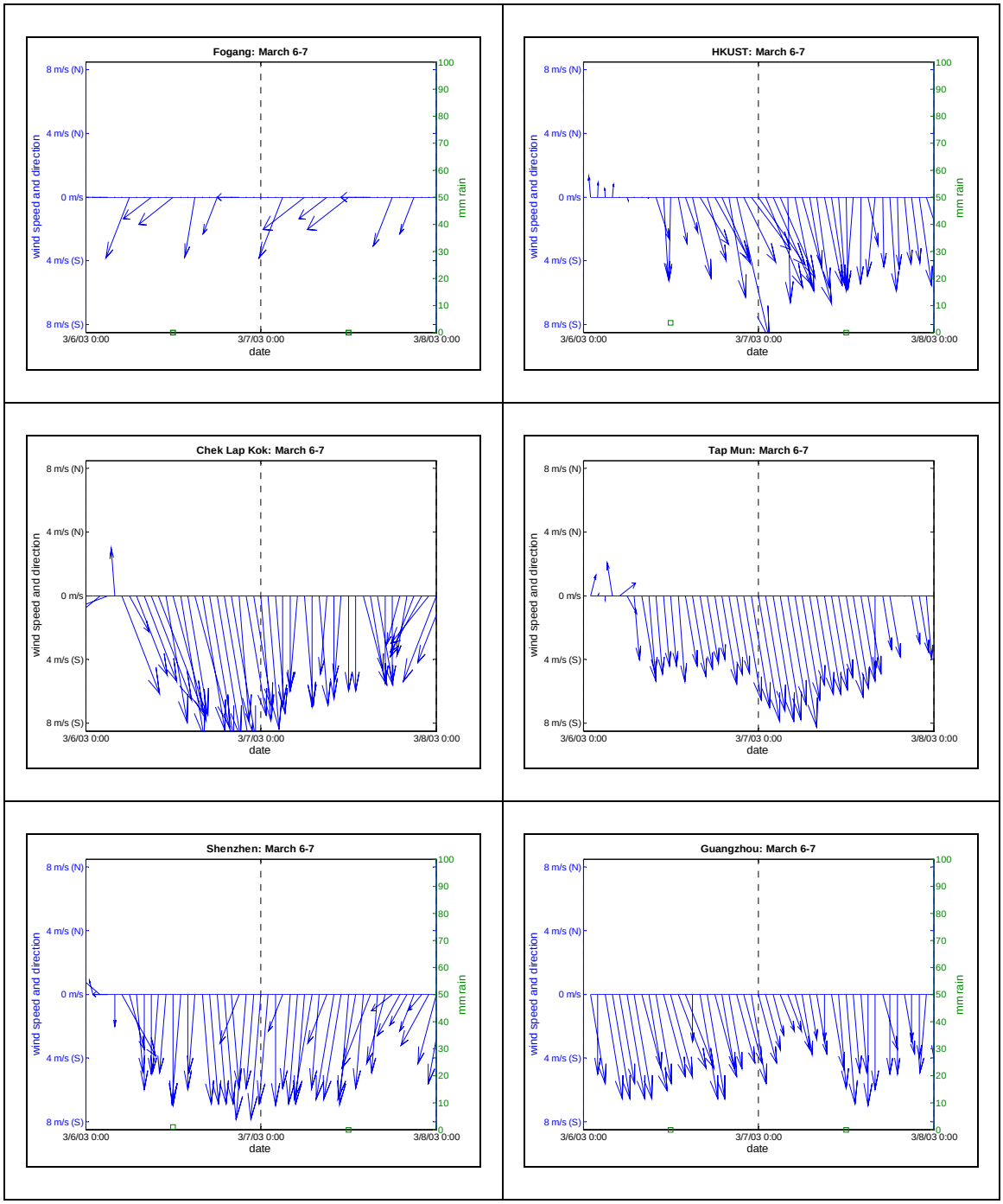

Figure B.12. Hourly wind vectors and 24-hour rainfall at six meteorological sites in the Pearl River Delta on 3/6/2003-3/7/2003.

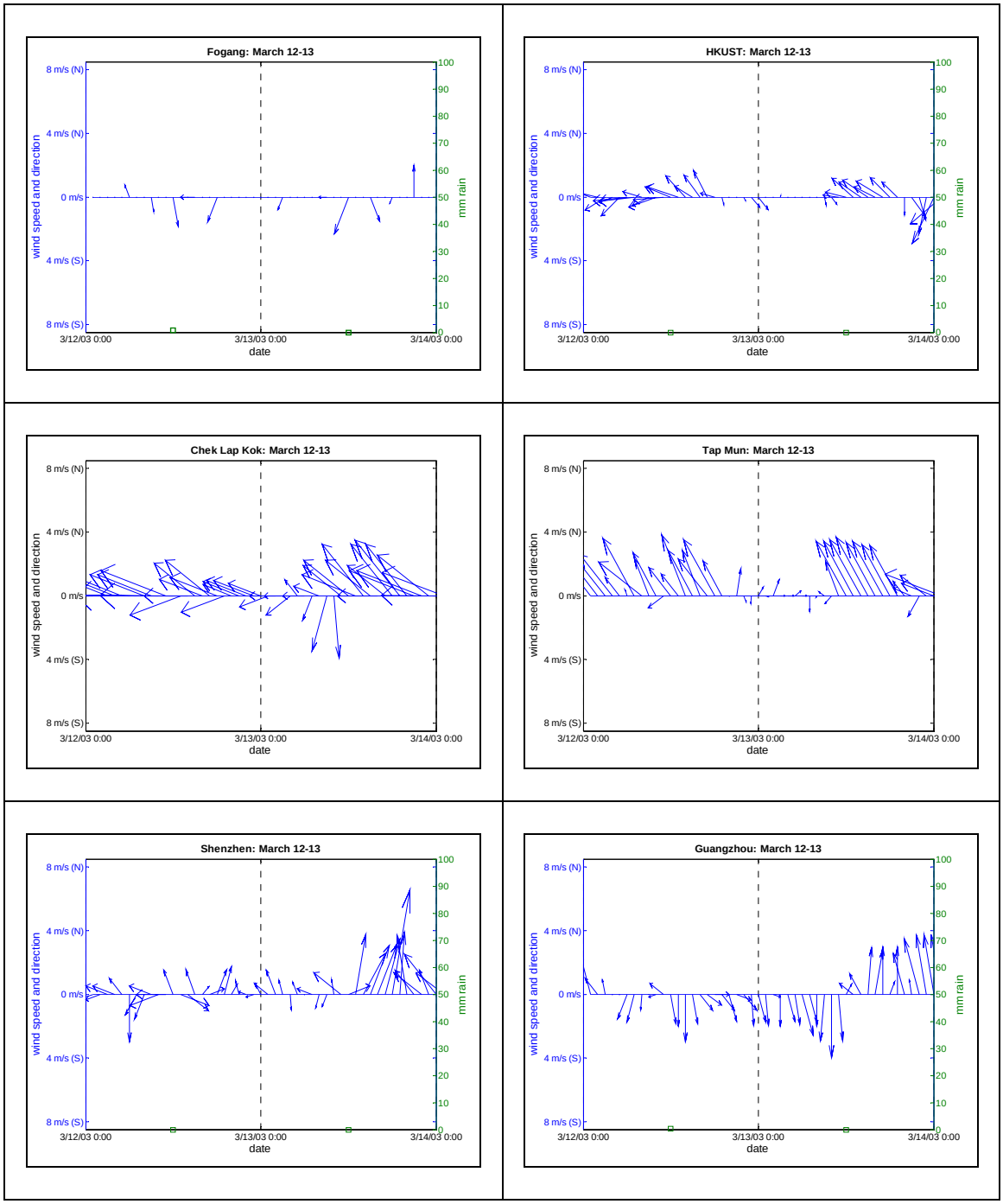

Figure B.13. Hourly wind vectors and 24-hour rainfall at six meteorological sites in the Pearl River Delta on 3/12/2003-3/13/2003.

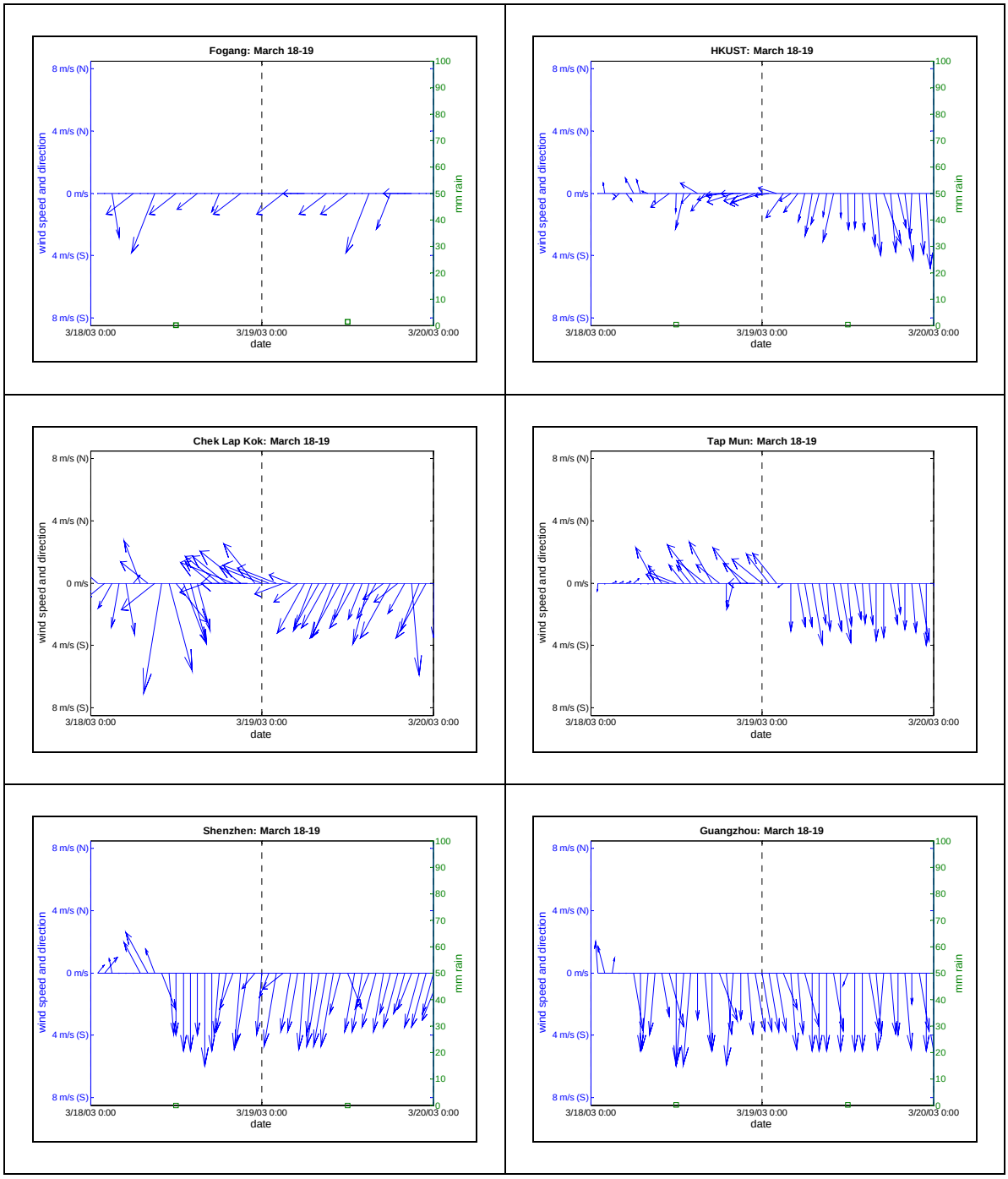

Figure B.14. Hourly wind vectors and 24-hour rainfall at six meteorological sites in the Pearl River Delta on 3/18/2003-3/19/2003.

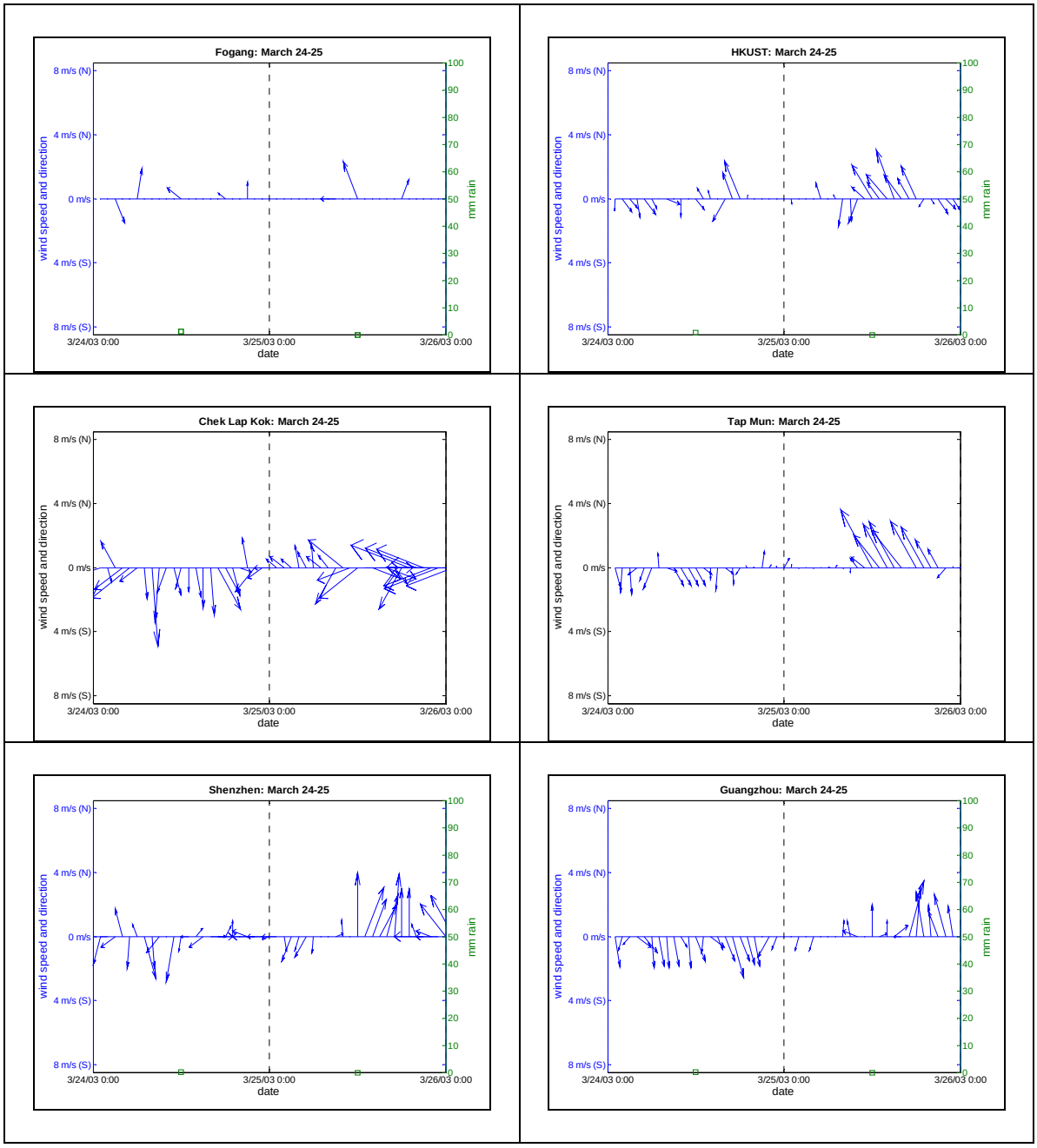

Figure B.15. Hourly wind vectors and 24-hour rainfall at six meteorological sites in the Pearl River Delta on 3/24/2003-3/25/2003.

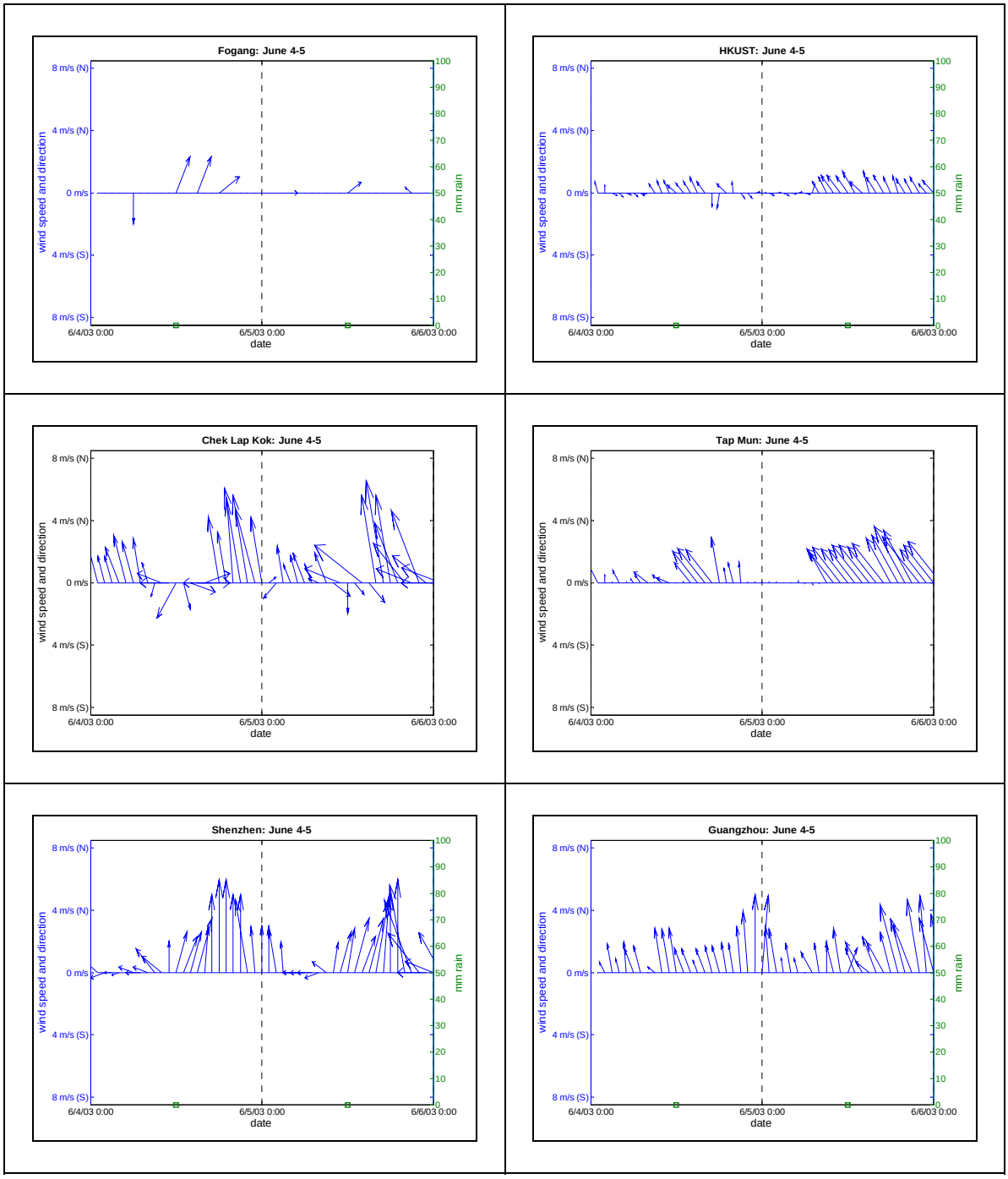

Figure B.16. Hourly wind vectors and 24-hour rainfall at six meteorological sites in the Pearl River Delta on 6/4/2003-6/5/2003.

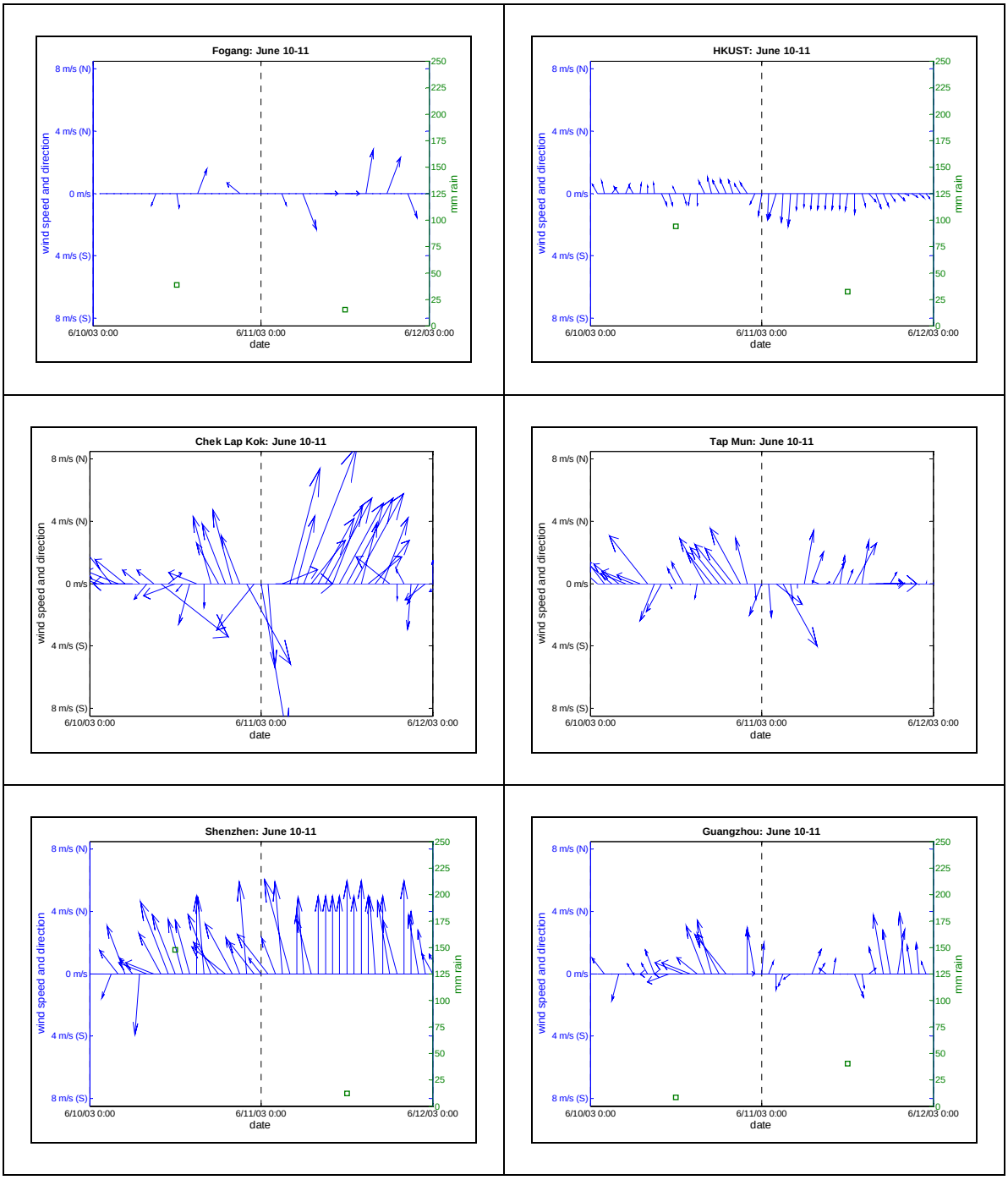

Figure B.17. Hourly wind vectors and 24-hour rainfall at six meteorological sites in the Pearl River Delta on 6/10/2003-6/11/2003.

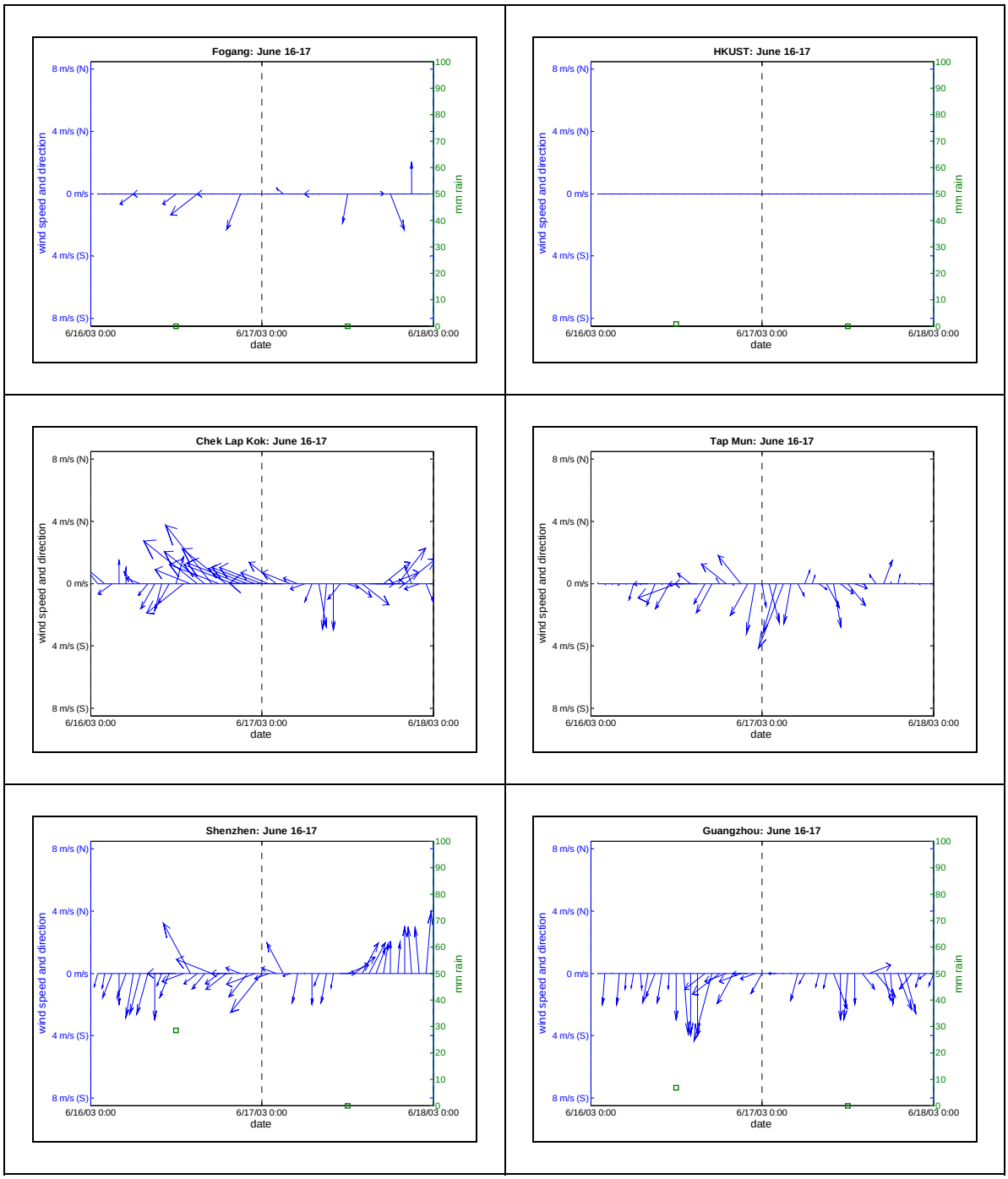

Figure B.18. Hourly wind vectors and 24-hour rainfall at six meteorological sites in the Pearl River Delta on 6/16/2003-6/17/2003.

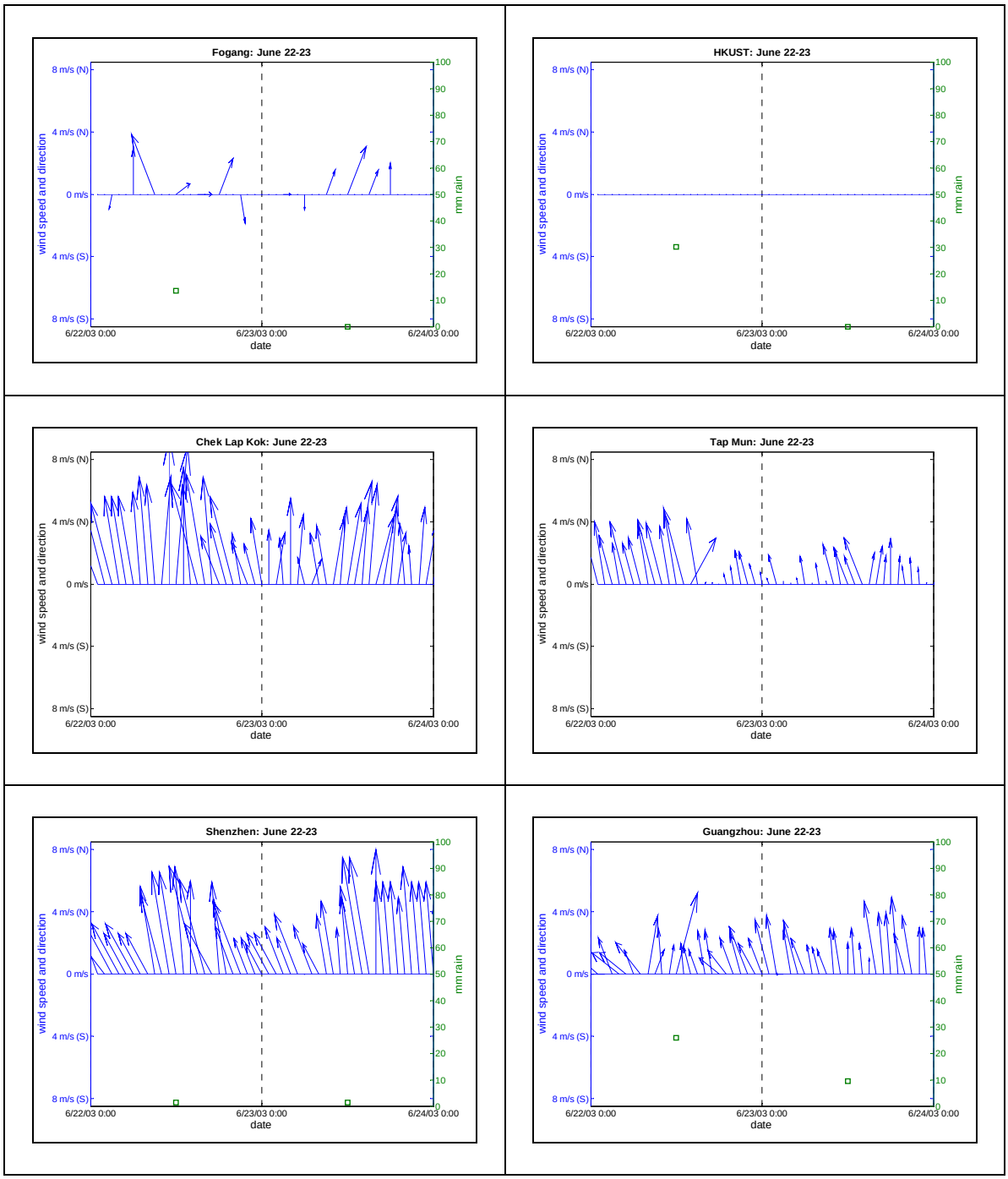

Figure B.19. Hourly wind vectors and 24-hour rainfall at six meteorological sites in the Pearl River Delta on 6/22/2003-6/23/2003.

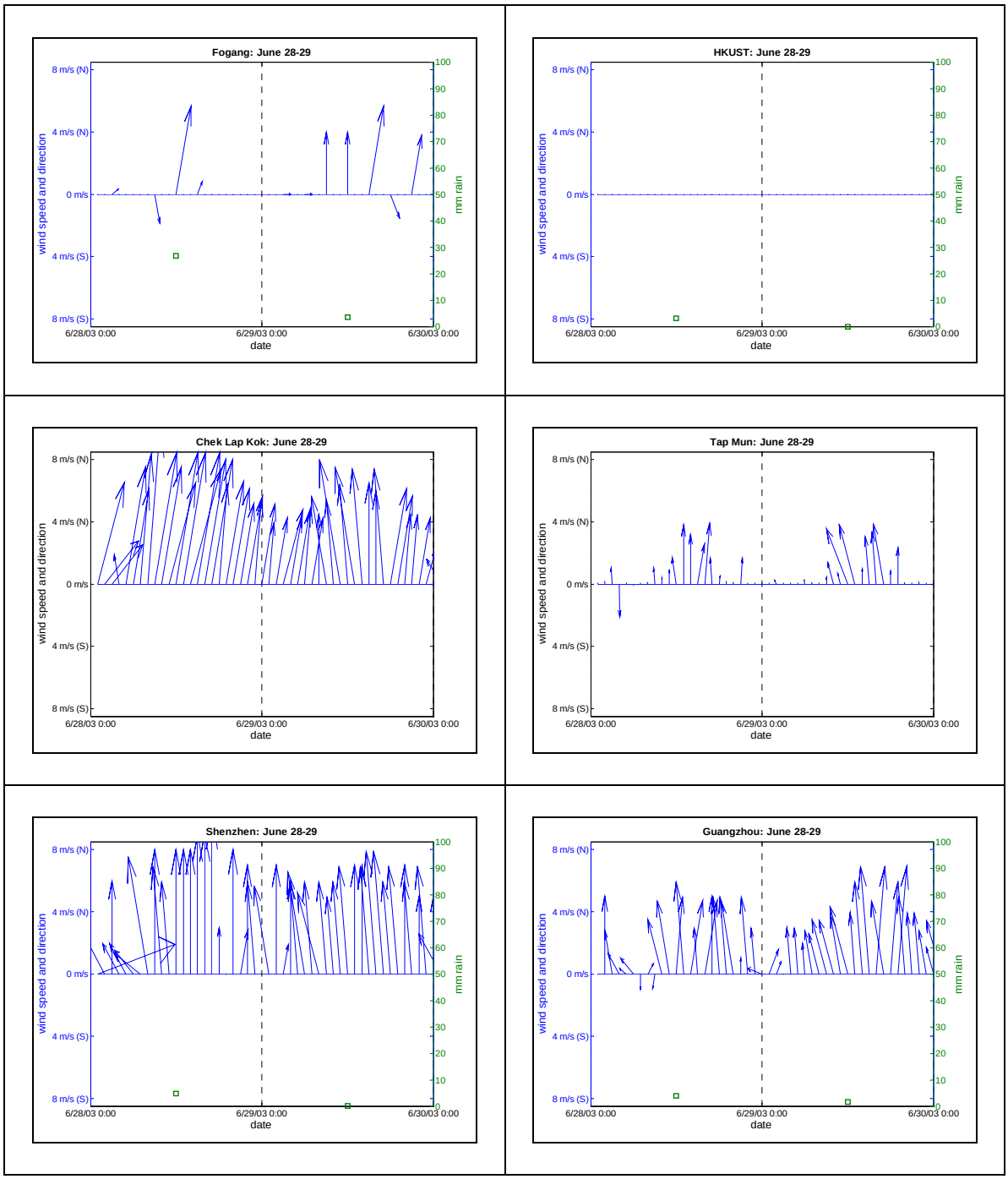

Figure B.20 Hourly wind vectors and 24-hour rainfall at six meteorological sites in the Pearl River Delta on 6/28/2003-6/29/2003

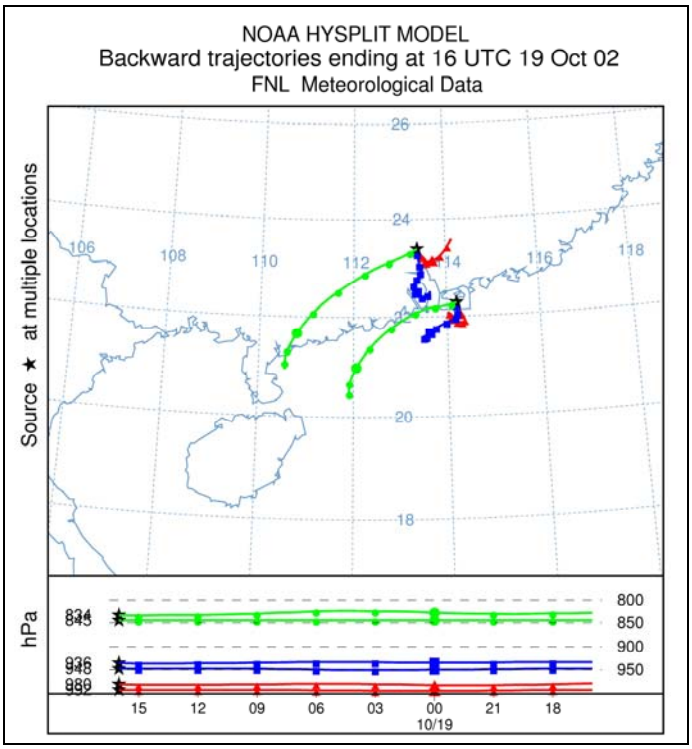

Figure B.21 24 hour back-trajectory of air parcels reaching sites Tap Mun and Conghua on 0000 local time, October 20th, 2002.

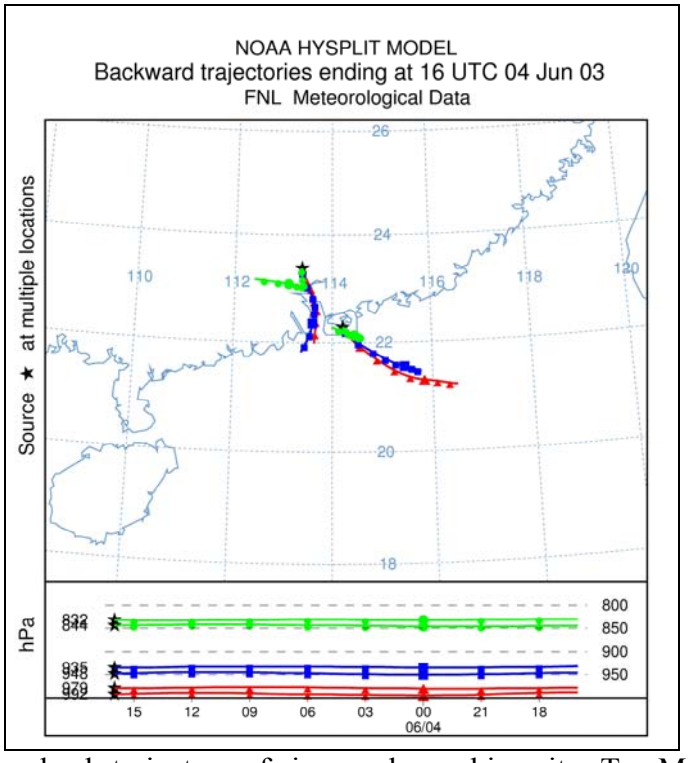

Figure B.22 24 hour back-trajectory of air parcels reaching sites Tap Mun and Conghua on 0000 local time, June 5th, 2003

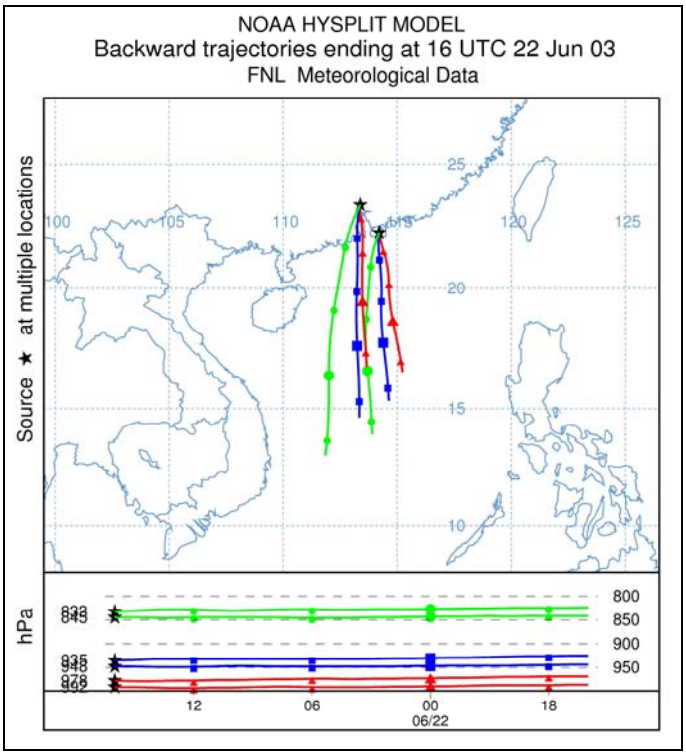

Figure B.23 24 hour back-trajectory of air parcels reaching sites Tap Mun and Conghua on 0000 local time, June 23rd, 2003

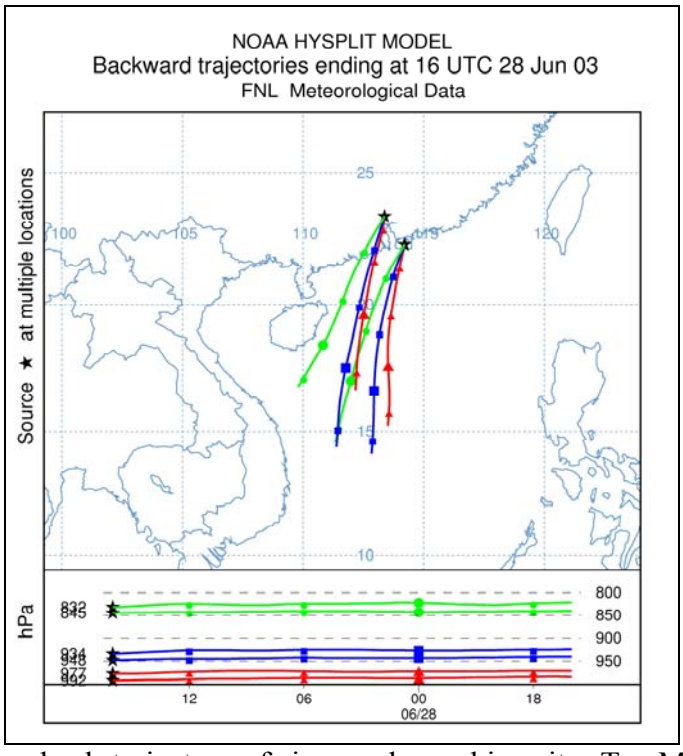

Figure B.24 24 hour back-trajectory of air parcels reaching sites Tap Mun and Conghua on 0000 local time, June 29th, 2003

B.2 Mass and Carbon Data ($\mu g\ m^{-3}$)

Site	Date	Mass	Organics (OC *1.4)	Elemental Carbon
CH6	20021002	25.57 ± 0.66	10.18 ± 0.73	1.16 ± 0.20
CH6	20021008	35.19 ± 0.88	11.56 ± 0.85	1.40 ± 0.25
CH6	20021014	50.19 ± 0.94	18.10 ± 1.18	1.93 ± 0.23
CH6	20021020	37.00 ± 0.78	12.94 ± 0.88	1.93 ± 0.23
CH6	20021026	28.76 ± 0.69	9.18 ± 0.67	1.12 ± 0.19
CH6	20021201	18.10 ± 0.88	8.61 ± 0.63	1.68 ± 0.21
CH6	20021207	32.27 ± 0.97	9.84 ± 0.70	1.59 ± 0.21
CH6	20021213	26.60 ± 0.93	10.68 ± 0.74	1.35 ± 0.20
CH6	20021219	46.27 ± 1.10	19.43 ± 1.25	2.02 ± 0.23
CH6	20021225	18.16 ± 0.88	6.09 ± 0.49	0.77 ± 0.17
CH6	20030301	68.47 ± 1.26	23.27 ± 1.47	2.18 ± 0.25
CH6	20030307	26.05 ± 1.03	8.90 ± 0.73	0.58 ± 0.24
CH6	20030313	71.44 ± 1.30	23.97 ± 1.51	2.15 ± 0.25
CH6	20030319	no data	no data	no data
CH6	20030325	36.59 ± 0.88	11.51 ± 0.81	1.13 ± 0.20
CH6	20030605	80.19 ± 1.61	26.18 ± 1.62	1.91 ± 0.23
CH6	20030611	29.37 ± 1.12	8.27 ± 0.62	1.26 ± 0.20
CH6	20030617	27.11 ± 1.10	9.60 ± 0.69	0.72 ± 0.17
CH6	20030623	23.60 ± 1.08	7.25 ± 0.56	0.97 ± 0.19
CH6	20030629	18.61 ± 1.06	5.47 ± 0.46	0.95 ± 0.18
CW3	20021002	34.52 ± 0.88	10.12 ± 0.71	4.34 ± 0.35
CW3	20021008	46.81 ± 1.01	16.35 ± 1.06	2.21 ± 0.23
CW3	20021014	19.03 ± 0.76	4.97 ± 0.42	1.23 ± 0.19
CW3	20021020	13.07 ± 0.73	2.18 ± 0.27	0.75 ± 0.16
CW3	20021026	37.27 ± 0.91	11.44 ± 0.78	1.47 ± 0.20
CW3	20021201	36.76 ± 1.27	8.40 ± 0.62	1.45 ± 0.20
CW3	20021207	32.44 ± 1.24	11.31 ± 0.78	2.70 ± 0.26
CW3	20021213	34.22 ± 1.25	10.63 ± 0.74	2.39 ± 0.25
CW3	20021219	51.46 ± 1.39	13.55 ± 0.91	3.23 ± 0.29
CW3	20021225	33.72 ± 1.25	11.17 ± 0.77	2.39 ± 0.25
CW3	20030301	40.09 ± 1.05	11.38 ± 0.78	3.05 ± 0.28
CW3	20030307	30.93 ± 0.97	11.12 ± 0.77	2.16 ± 0.24
CW3	20030313	35.50 ± 1.01	8.90 ± 0.64	1.07 ± 0.18
CW3	20030319	34.65 ± 1.00	8.55 ± 0.63	0.90 ± 0.18
CW3	20030325	55.77 ± 1.21	12.38 ± 0.84	2.08 ± 0.23
CW3	20030605	52.86 ± 1.56	9.62 ± 0.69	1.24 ± 0.19
CW3	20030611	20.15 ± 1.37	3.86 ± 0.36	2.35 ± 0.24
CW3	20030617	55.24 ± 1.58	15.78 ± 1.02	2.02 ± 0.23
CW3	20030623	13.58 ± 1.35	2.04 ± 0.27	0.66 ± 0.16
CW3	20030629	8.22 ± 1.34	1.50 ± 0.24	0.46 ± 0.15
GZ5	20021002	84.76 ± 1.50	41.71 ± 2.49	4.49 ± 0.35
GZ5	20021008	54.49 ± 1.10	21.53 ± 1.34	4.35 ± 0.34
GZ5	20021014	102.46 ± 1.74	44.94 ± 2.67	5.99 ± 0.43
GZ5	20021020	43.06 ± 0.97	14.25 ± 0.94	3.53 ± 0.30
GZ5	20021026	46.43 ± 1.01	18.90 ± 1.20	4.84 ± 0.37

Site	Date	Mass	Organics (OC *1.4)	Elemental Carbon
GZ5	20021201	100.69 ± 1.94	45.58 ± 2.70	6.55 ± 0.46
GZ5	20021207	84.63 ± 1.74	27.54 ± 1.68	3.92 ± 0.32
GZ5	20021213	49.80 ± 1.38	19.39 ± 1.22	5.91 ± 0.43
GZ5	20021219	96.17 ± 1.88	31.33 ± 1.90	7.28 ± 0.50
GZ5	20021225	30.76 ± 1.24	11.13 ± 0.76	2.83 ± 0.26
GZ5	20030301	84.49 ± 1.57	24.25 ± 1.50	4.29 ± 0.34
GZ5	20030307	41.75 ± 1.08	13.55 ± 0.90	2.45 ± 0.24
GZ5	20030313	116.25 ± 2.01	34.71 ± 2.10	4.66 ± 0.36
GZ5	20030319	32.63 ± 1.00	9.02 ± 0.64	2.71 ± 0.26
GZ5	20030325	122.06 ± 2.08	37.42 ± 2.25	8.35 ± 0.57
GZ5	20030605	74.95 ± 1.76	21.01 ± 1.32	1.69 ± 0.20
GZ5	20030611	77.76 ± 1.79	22.57 ± 1.40	3.02 ± 0.27
GZ5	20030617	98.59 ± 2.02	29.85 ± 1.82	3.16 ± 0.28
GZ5	20030623	44.11 ± 1.48	14.07 ± 0.92	4.83 ± 0.37
GZ5	20030629	25.97 ± 1.38	9.51 ± 0.67	2.54 ± 0.25
SZ4	20021002	55.95 ± 1.11	26.95 ± 1.67	5.34 ± 0.41
SZ4	20021008	69.83 ± 1.29	28.31 ± 1.75	5.42 ± 0.41
SZ4	20021014	26.17 ± 0.80	10.19 ± 0.73	3.27 ± 0.30
SZ4	20021020	17.98 ± 0.75	4.09 ± 0.38	2.25 ± 0.24
SZ4	20021026	43.88 ± 0.97	17.00 ± 1.11	4.02 ± 0.34
SZ4	20021201	34.05 ± 1.25	8.30 ± 0.62	1.52 ± 0.21
SZ4	20021207	30.14 ± 1.22	10.25 ± 0.73	3.92 ± 0.33
SZ4	20021213	59.74 ± 3.44	22.11 ± 1.68	5.46 ± 0.66
SZ4	20021221	70.29 ± 3.64	26.05 ± 1.92	10.73 ± 0.95
SZ4	20021225	39.68 ± 1.29	13.89 ± 0.92	2.93 ± 0.28
SZ4	20030102	94.19 ± 1.85	27.93 ± 1.72	4.78 ± 0.38
SZ4	20030301	53.13 ± 1.19	14.90 ± 0.99	2.75 ± 0.28
SZ4	20030307	40.17 ± 1.06	13.16 ± 0.90	2.19 ± 0.25
SZ4	20030313	56.78 ± 1.23	18.33 ± 1.19	5.16 ± 0.41
SZ4	20030319	50.42 ± 1.16	16.84 ± 1.11	3.89 ± 0.34
SZ4	20030325	72.57 ± 1.42	21.83 ± 1.39	5.80 ± 0.44
SZ4	20030605	59.41 ± 1.61	13.03 ± 0.88	1.51 ± 0.21
SZ4	20030611	33.90 ± 1.42	11.00 ± 0.77	6.26 ± 0.46
SZ4	20030617	57.16 ± 1.59	16.56 ± 1.08	2.27 ± 0.24
SZ4	20030623	12.89 ± 1.33	3.56 ± 0.35	1.35 ± 0.20
SZ4	20030629	11.38 ± 1.33	2.34 ± 0.29	0.94 ± 0.18
TC2	20021002	35.48 ± 0.87	13.94 ± 0.92	3.59 ± 0.31
TC2	20021008	43.96 ± 0.96	15.48 ± 1.01	2.58 ± 0.25
TC2	20021014	20.81 ± 0.75	8.33 ± 0.60	0.96 ± 0.17
TC2	20021020	9.26 ± 0.69	1.72 ± 0.25	0.86 ± 0.17
TC2	20021026	36.15 ± 0.88	13.29 ± 0.88	2.13 ± 0.23
TC2	20021201	29.33 ± 1.20	6.29 ± 0.49	1.24 ± 0.18
TC2	20021207	15.52 ± 1.13	3.61 ± 0.34	2.48 ± 0.24
TC2	20021213	37.26 ± 1.25	13.52 ± 0.90	2.93 ± 0.27
TC2	20021219	37.76 ± 1.25	10.88 ± 0.74	2.70 ± 0.25
TC2	20021225	36.09 ± 1.24	12.95 ± 0.87	3.47 ± 0.30
TC2	20030301	34.84 ± 1.01	7.06 ± 0.53	2.06 ± 0.23
TC2	20030307	40.60 ± 1.07	11.90 ± 0.81	1.90 ± 0.22
TC2	20030313	33.46 ± 1.00	7.48 ± 0.56	1.65 ± 0.21

Site	Date	Mass	Organics (OC *1.4)	Elemental Carbon
TC2	20030319	45.87 ± 1.12	10.63 ± 0.74	2.09 ± 0.23
TC2	20030325	44.84 ± 1.11	11.09 ± 0.76	2.98 ± 0.27
TC2	20030605	58.34 ± 1.61	9.39 ± 0.66	1.08 ± 0.18
TC2	20030611	13.63 ± 1.35	2.67 ± 0.29	2.21 ± 0.23
TC2	20030617	55.75 ± 1.59	13.75 ± 0.91	2.24 ± 0.23
TC2	20030623	11.89 ± 1.34	1.40 ± 0.22	0.40 ± 0.15
TC2	20030629	8.92 ± 1.34	1.19 ± 0.21	0.24 ± 0.14
TM1	20021002	24.78 ± 0.81	8.55 ± 0.63	0.97 ± 0.18
TM1	20021008	48.63 ± 1.03	15.72 ± 1.04	1.80 ± 0.22
TM1	20021014	15.78 ± 0.75	2.87 ± 0.32	0.37 ± 0.16
TM1	20021020	10.85 ± 0.73	3.37 ± 0.34	0.41 ± 0.16
TM1	20021026	29.06 ± 0.84	9.70 ± 0.69	0.89 ± 0.18
TM1	20021201	31.65 ± 1.23	6.45 ± 0.50	0.99 ± 0.18
TM1	20021207	23.12 ± 1.19	4.00 ± 0.38	0.41 ± 0.16
TM1	20021213	31.49 ± 1.23	8.95 ± 0.64	1.60 ± 0.21
TM1	20021219	44.65 ± 1.33	10.00 ± 0.70	1.29 ± 0.19
TM1	20021225	30.62 ± 1.23	9.34 ± 0.67	1.27 ± 0.19
TM1	20030301	29.94 ± 0.99	3.95 ± 0.38	0.40 ± 0.16
TM1	20030307	20.40 ± 0.93	5.85 ± 0.48	0.50 ± 0.16
TM1	20030313	32.88 ± 1.01	5.63 ± 0.46	0.64 ± 0.17
TM1	20030319	27.30 ± 0.97	6.71 ± 0.53	0.74 ± 0.17
TM1	20030325	53.94 ± 1.21	11.41 ± 0.78	1.17 ± 0.19
TM1	20030605	44.13 ± 1.49	7.31 ± 0.56	0.54 ± 0.16
TM1	20030611	11.67 ± 1.34	2.28 ± 0.28	0.98 ± 0.18
TM1	20030617	47.00 ± 1.52	12.39 ± 0.84	1.21 ± 0.19
TM1	20030623	10.75 ± 1.34	1.30 ± 0.24	0.10 ± 0.14
TM1	20030629	6.18 ± 1.33	1.36 ± 0.24	0.15 ± 0.15
ZS7	20021002	no data	no data	no data
ZS7	20021008	79.55 ± 1.35	30.41 ± 1.85	3.21 ± 0.28
ZS7	20021014	43.92 ± 0.87	21.74 ± 1.36	2.51 ± 0.25
ZS7	20021020	13.95 ± 0.58	4.96 ± 0.42	1.72 ± 0.21
ZS7	20021026	32.29 ± 0.74	8.15 ± 0.59	0.97 ± 0.17
ZS7	20021201	62.12 ± 1.29	22.22 ± 1.39	3.85 ± 0.32
ZS7	20021207	30.87 ± 0.98	9.66 ± 0.67	2.56 ± 0.25
ZS7	20021213	69.89 ± 1.38	32.51 ± 1.97	4.46 ± 0.35
ZS7	20021219	78.64 ± 1.49	23.56 ± 1.46	4.87 ± 0.37
ZS7	20021225	50.82 ± 1.16	18.09 ± 1.15	3.99 ± 0.32
ZS7	20030301	44.98 ± 0.97	12.57 ± 0.85	1.71 ± 0.22
ZS7	20030307	41.96 ± 0.94	14.15 ± 0.95	1.65 ± 0.22
ZS7	20030313	51.42 ± 1.05	17.56 ± 1.13	3.34 ± 0.31
ZS7	20030319	57.35 ± 1.12	11.56 ± 0.80	1.92 ± 0.23
ZS7	20030325	81.40 ± 1.44	23.25 ± 1.46	3.76 ± 0.33
ZS7	20030605	52.65 ± 1.34	8.46 ± 0.62	1.29 ± 0.19
ZS7	20030611	15.93 ± 1.09	4.00 ± 0.36	2.12 ± 0.23
ZS7	20030617	55.22 ± 1.37	12.29 ± 0.83	1.43 ± 0.20
ZS7	20030623	10.74 ± 1.09	2.66 ± 0.29	1.18 ± 0.19
ZS7	20030629	9.49 ± 1.07	1.60 ± 0.24	0.97 ± 0.17

B.3 Ions Data ($\mu g\ m^{-3}$)

Site	Date	Chloride	Nitrate	Sulfate	Ammonium
CH6	20021002	0.02 ± 0.04	0.19 ± 0.04	6.95 ± 0.22	1.75 ± 0.05
CH6	20021008	0.20 ± 0.05	0.47 ± 0.05	7.92 ± 0.35	2.36 ± 0.08
CH6	20021014	0.05 ± 0.10	0.23 ± 0.05	13.31 ± 1.01	2.61 ± 0.09
CH6	20021020	0.01 ± 0.04	0.20 ± 0.04	12.11 ± 1.02	2.46 ± 0.16
CH6	20021026	0.06 ± 0.04	0.36 ± 0.04	8.66 ± 0.30	1.93 ± 0.06
CH6	20021201	0.05 ± 0.04	0.22 ± 0.04	2.34 ± 0.18	0.62 ± 0.04
CH6	20021207	0.05 ± 0.04	0.22 ± 0.04	10.84 ± 0.92	2.32 ± 0.14
CH6	20021213	0.02 ± 0.04	0.33 ± 0.04	6.86 ± 0.22	1.49 ± 0.11
CH6	20021219	0.01 ± 0.04	0.32 ± 0.04	11.28 ± 0.36	2.51 ± 0.17
CH6	20021225	0.00 ± 0.03	0.05 ± 0.04	7.27 ± 0.70	1.77 ± 0.11
CH6	20030301	0.12 ± 0.05	0.65 ± 0.05	22.11 ± 1.57	4.98 ± 0.18
CH6	20030307	0.01 ± 0.05	0.11 ± 0.06	9.01 ± 0.27	2.22 ± 0.07
CH6	20030313	0.04 ± 0.05	0.67 ± 0.05	18.21 ± 1.47	3.29 ± 0.22
CH6	20030319	no data	no data	no data	no data
CH6	20030325	0.02 ± 0.04	0.88 ± 0.05	8.99 ± 0.32	2.00 ± 0.07
CH6	20030605	0.02 ± 0.05	0.44 ± 0.05	23.02 ± 1.64	5.63 ± 0.26
CH6	20030611	0.00 ± 0.03	0.13 ± 0.04	8.04 ± 0.29	1.82 ± 0.06
CH6	20030617	0.01 ± 0.04	0.06 ± 0.04	6.97 ± 0.28	1.81 ± 0.06
CH6	20030623	0.02 ± 0.04	0.32 ± 0.04	8.14 ± 0.69	1.67 ± 0.08
CH6	20030629	0.05 ± 0.04	0.37 ± 0.04	6.14 ± 0.21	1.52 ± 0.05
CW3	20021002	0.02 ± 0.05	0.42 ± 0.05	8.36 ± 0.28	1.58 ± 0.06
CW3	20021008	0.09 ± 0.05	0.75 ± 0.06	10.02 ± 0.37	2.47 ± 0.08
CW3	20021014	0.49 ± 0.09	1.50 ± 0.10	5.46 ± 0.24	1.16 ± 0.05
CW3	20021020	0.00 ± 0.04	0.18 ± 0.05	5.99 ± 0.25	1.98 ± 0.06
CW3	20021026	0.05 ± 0.05	0.65 ± 0.06	11.20 ± 0.39	3.87 ± 0.11
CW3	20021201	0.71 ± 0.05	1.80 ± 0.07	11.22 ± 0.94	3.19 ± 0.15
CW3	20021207	0.11 ± 0.05	1.42 ± 0.07	9.85 ± 0.92	2.45 ± 0.14
CW3	20021213	0.10 ± 0.05	1.09 ± 0.07	8.19 ± 0.28	1.96 ± 0.14
CW3	20021219	0.25 ± 0.05	2.44 ± 0.09	15.98 ± 1.36	4.04 ± 0.21
CW3	20021225	0.06 ± 0.05	1.00 ± 0.07	9.02 ± 0.29	2.24 ± 0.14
CW3	20030301	0.13 ± 0.05	1.23 ± 0.06	12.29 ± 0.41	2.97 ± 0.14
CW3	20030307	0.04 ± 0.05	1.19 ± 0.07	6.87 ± 0.27	2.41 ± 0.07
CW3	20030313	0.25 ± 0.05	1.82 ± 0.08	8.06 ± 0.28	2.75 ± 0.09
CW3	20030319	0.07 ± 0.05	1.54 ± 0.08	9.12 ± 0.37	2.64 ± 0.09
CW3	20030325	0.09 ± 0.05	2.02 ± 0.08	13.39 ± 0.42	3.69 ± 0.15
CW3	20030605	0.03 ± 0.05	0.22 ± 0.05	16.94 ± 1.32	3.85 ± 0.15
CW3	20030611	0.32 ± 0.05	0.33 ± 0.05	2.34 ± 0.23	0.56 ± 0.05
CW3	20030617	0.01 ± 0.05	0.25 ± 0.05	17.06 ± 1.32	4.33 ± 0.16
CW3	20030623	0.23 ± 0.05	0.30 ± 0.05	2.65 ± 0.23	0.64 ± 0.05
CW3	20030629	0.31 ± 0.05	0.32 ± 0.05	1.67 ± 0.08	0.39 ± 0.04
GZ5	20021002	0.29 ± 0.06	4.83 ± 0.17	15.39 ± 0.52	4.36 ± 0.13
GZ5	20021008	0.09 ± 0.05	0.97 ± 0.06	11.08 ± 0.39	2.91 ± 0.09
GZ5	20021014	0.17 ± 0.06	2.55 ± 0.11	22.57 ± 1.75	4.21 ± 0.27
GZ5	20021020	0.39 ± 0.05	0.76 ± 0.06	10.42 ± 0.38	2.96 ± 0.09
GZ5	20021026	0.05 ± 0.05	0.49 ± 0.06	11.38 ± 0.39	3.75 ± 0.10
GZ5	20021201	3.02 ± 0.19	4.10 ± 0.13	13.06 ± 0.52	4.73 ± 0.29

Site	Date	Chloride	Nitrate	Sulfate	Ammonium
GZ5	20021207	1.57 ± 0.07	7.43 ± 0.22	19.00 ± 0.60	5.94 ± 0.30
GZ5	20021213	0.31 ± 0.05	2.36 ± 0.09	9.22 ± 0.37	2.31 ± 0.20
GZ5	20021219	2.77 ± 0.19	9.00 ± 0.31	20.24 ± 1.89	7.62 ± 0.32
GZ5	20021225	0.08 ± 0.05	1.02 ± 0.07	8.50 ± 0.29	2.09 ± 0.19
GZ5	20030301	0.91 ± 0.06	5.80 ± 0.20	23.24 ± 0.81	6.51 ± 0.23
GZ5	20030307	0.18 ± 0.05	1.54 ± 0.09	10.98 ± 0.52	3.76 ± 0.11
GZ5	20030313	1.06 ± 0.07	13.43 ± 0.40	21.30 ± 0.61	7.46 ± 0.39
GZ5	20030319	0.50 ± 0.05	4.17 ± 0.15	5.48 ± 0.25	2.73 ± 0.08
GZ5	20030325	0.51 ± 0.07	10.70 ± 0.29	20.47 ± 0.64	8.76 ± 0.57
GZ5	20030605	0.03 ± 0.06	0.81 ± 0.06	20.91 ± 1.79	6.97 ± 0.23
GZ5	20030611	1.08 ± 0.06	3.86 ± 0.12	14.13 ± 0.43	3.70 ± 0.19
GZ5	20030617	1.06 ± 0.06	5.01 ± 0.16	22.58 ± 1.31	6.03 ± 0.22
GZ5	20030623	0.39 ± 0.05	0.87 ± 0.06	9.04 ± 0.36	2.02 ± 0.08
GZ5	20030629	0.12 ± 0.05	0.41 ± 0.05	5.20 ± 0.24	1.33 ± 0.05
SZ4	20021002	0.68 ± 0.18	2.44 ± 0.18	9.68 ± 0.49	2.35 ± 0.08
SZ4	20021008	0.23 ± 0.06	1.34 ± 0.07	13.17 ± 0.49	4.21 ± 0.12
SZ4	20021014	0.03 ± 0.05	0.48 ± 0.05	5.58 ± 0.45	0.88 ± 0.05
SZ4	20021020	0.03 ± 0.05	0.36 ± 0.05	5.29 ± 0.24	1.71 ± 0.06
SZ4	20021026	0.08 ± 0.05	0.54 ± 0.05	10.16 ± 0.37	3.25 ± 0.10
SZ4	20021201	0.58 ± 0.05	2.07 ± 0.10	11.05 ± 0.94	3.25 ± 0.12
SZ4	20021207	0.30 ± 0.05	1.19 ± 0.07	7.92 ± 0.28	2.71 ± 0.08
SZ4	20021213	0.35 ± 0.14	4.25 ± 0.22	9.84 ± 0.71	3.98 ± 0.16
SZ4	20021221	1.05 ± 0.14	4.71 ± 0.24	8.18 ± 0.74	4.07 ± 0.17
SZ4	20021225	0.22 ± 0.05	1.97 ± 0.08	9.30 ± 0.32	2.60 ± 0.16
SZ4	20030102	1.08 ± 0.06	6.78 ± 0.24	24.53 ± 0.84	7.17 ± 0.39
SZ4	20030301	0.28 ± 0.05	3.42 ± 0.16	15.47 ± 0.58	4.22 ± 0.16
SZ4	20030307	0.26 ± 0.05	2.87 ± 0.10	8.43 ± 0.36	3.39 ± 0.10
SZ4	20030313	0.55 ± 0.06	3.43 ± 0.14	9.30 ± 0.38	3.66 ± 0.10
SZ4	20030319	0.95 ± 0.06	3.87 ± 0.12	7.37 ± 0.27	3.63 ± 0.10
SZ4	20030325	0.40 ± 0.06	4.49 ± 0.14	12.23 ± 0.38	4.65 ± 0.13
SZ4	20030605	0.21 ± 0.05	1.39 ± 0.08	16.76 ± 0.97	4.46 ± 0.16
SZ4	20030611	0.21 ± 0.05	1.23 ± 0.06	3.82 ± 0.24	1.02 ± 0.07
SZ4	20030617	0.01 ± 0.05	0.85 ± 0.06	16.67 ± 0.96	4.34 ± 0.16
SZ4	20030623	0.21 ± 0.05	0.45 ± 0.05	2.46 ± 0.23	0.68 ± 0.05
SZ4	20030629	0.30 ± 0.04	0.44 ± 0.05	1.74 ± 0.07	0.43 ± 0.04
TC2	20021002	0.00 ± 0.03	0.23 ± 0.05	8.92 ± 0.35	2.45 ± 0.08
TC2	20021008	0.09 ± 0.05	0.74 ± 0.05	9.82 ± 0.36	3.04 ± 0.09
TC2	20021014	0.13 ± 0.05	1.10 ± 0.07	5.33 ± 0.24	1.12 ± 0.05
TC2	20021020	0.00 ± 0.03	0.18 ± 0.05	4.00 ± 0.23	1.29 ± 0.05
TC2	20021026	0.02 ± 0.05	0.26 ± 0.05	11.24 ± 0.39	3.55 ± 0.10
TC2	20021201	0.12 ± 0.05	0.75 ± 0.05	11.39 ± 0.92	3.47 ± 0.12
TC2	20021207	0.09 ± 0.05	0.54 ± 0.05	3.61 ± 0.16	1.12 ± 0.05
TC2	20021213	0.11 ± 0.05	1.51 ± 0.08	7.93 ± 0.33	2.45 ± 0.19
TC2	20021219	0.02 ± 0.05	0.65 ± 0.05	13.60 ± 1.19	3.20 ± 0.19
TC2	20021225	0.08 ± 0.05	1.72 ± 0.07	8.91 ± 0.29	2.42 ± 0.14
TC2	20030301	0.00 ± 0.04	0.37 ± 0.05	13.23 ± 0.43	3.28 ± 0.10
TC2	20030307	0.12 ± 0.05	2.74 ± 0.11	10.16 ± 0.38	3.58 ± 0.10
TC2	20030313	0.05 ± 0.05	1.09 ± 0.07	7.99 ± 0.24	2.00 ± 0.06
TC2	20030319	0.19 ± 0.05	2.64 ± 0.10	9.66 ± 0.38	3.66 ± 0.10

Site	Date	Chloride	Nitrate	Sulfate	Ammonium
TC2	20030325	0.02 ± 0.05	0.35 ± 0.06	11.84 ± 0.34	3.15 ± 0.10
TC2	20030605	0.00 ± 0.04	0.15 ± 0.05	19.15 ± 0.53	4.05 ± 0.15
TC2	20030611	0.16 ± 0.05	0.23 ± 0.05	1.05 ± 0.07	0.39 ± 0.04
TC2	20030617	0.00 ± 0.05	0.10 ± 0.05	19.07 ± 1.65	4.26 ± 0.16
TC2	20030623	0.26 ± 0.05	0.29 ± 0.05	2.27 ± 0.23	0.63 ± 0.05
TC2	20030629	0.34 ± 0.05	0.35 ± 0.05	1.58 ± 0.08	0.35 ± 0.04
TM1	20021002	0.00 ± 0.04	0.18 ± 0.05	7.96 ± 0.28	1.74 ± 0.06
TM1	20021008	0.03 ± 0.05	0.54 ± 0.06	12.01 ± 0.41	3.76 ± 0.10
TM1	20021014	0.55 ± 0.09	0.90 ± 0.05	5.40 ± 0.25	1.27 ± 0.05
TM1	20021020	0.01 ± 0.05	0.21 ± 0.05	4.47 ± 0.24	1.40 ± 0.05
TM1	20021026	0.02 ± 0.05	0.27 ± 0.05	11.22 ± 0.93	2.44 ± 0.14
TM1	20021201	0.19 ± 0.05	0.69 ± 0.05	11.51 ± 0.94	2.61 ± 0.15
TM1	20021207	0.02 ± 0.05	0.15 ± 0.05	9.52 ± 0.30	2.21 ± 0.14
TM1	20021213	0.09 ± 0.05	0.63 ± 0.05	8.47 ± 0.29	1.95 ± 0.14
TM1	20021219	0.03 ± 0.05	0.38 ± 0.05	17.15 ± 1.23	3.80 ± 0.19
TM1	20021225	0.02 ± 0.05	0.44 ± 0.05	9.37 ± 0.30	2.11 ± 0.18
TM1	20030301	0.02 ± 0.05	0.20 ± 0.05	13.19 ± 1.00	3.01 ± 0.12
TM1	20030307	0.02 ± 0.05	0.30 ± 0.05	6.77 ± 0.28	2.15 ± 0.07
TM1	20030313	0.15 ± 0.05	1.00 ± 0.07	7.64 ± 0.28	2.23 ± 0.07
TM1	20030319	0.05 ± 0.05	0.89 ± 0.07	6.90 ± 0.27	1.92 ± 0.06
TM1	20030325	0.01 ± 0.05	0.83 ± 0.06	16.03 ± 1.38	5.21 ± 0.29
TM1	20030605	0.01 ± 0.05	0.17 ± 0.05	15.13 ± 0.56	3.36 ± 0.10
TM1	20030611	0.19 ± 0.05	0.26 ± 0.05	1.41 ± 0.08	0.32 ± 0.04
TM1	20030617	0.02 ± 0.05	0.22 ± 0.05	15.08 ± 1.32	3.58 ± 0.15
TM1	20030623	0.16 ± 0.04	0.27 ± 0.05	2.60 ± 0.17	0.75 ± 0.05
TM1	20030629	0.28 ± 0.05	0.39 ± 0.05	1.73 ± 0.08	0.43 ± 0.04
ZS7	20021002	no data	no data	no data	no data
ZS7	20021008	0.25 ± 0.04	1.46 ± 0.08	17.91 ± 1.34	3.15 ± 0.20
ZS7	20021014	0.06 ± 0.04	0.51 ± 0.04	10.41 ± 0.99	2.22 ± 0.11
ZS7	20021020	0.00 ± 0.03	0.17 ± 0.04	5.07 ± 0.20	1.76 ± 0.05
ZS7	20021026	0.07 ± 0.04	0.59 ± 0.04	13.52 ± 1.02	3.04 ± 0.16
ZS7	20021201	0.92 ± 0.05	2.28 ± 0.09	15.20 ± 1.38	4.38 ± 0.22
ZS7	20021207	0.19 ± 0.04	0.70 ± 0.04	9.00 ± 0.28	2.31 ± 0.14
ZS7	20021213	0.44 ± 0.05	4.44 ± 0.15	13.69 ± 0.44	3.63 ± 0.22
ZS7	20021219	0.88 ± 0.05	4.50 ± 0.15	19.86 ± 1.40	5.51 ± 0.23
ZS7	20021225	0.72 ± 0.04	2.45 ± 0.10	10.85 ± 1.03	4.09 ± 0.22
ZS7	20030301	0.06 ± 0.04	0.67 ± 0.05	15.58 ± 0.50	3.58 ± 0.13
ZS7	20030307	0.25 ± 0.04	2.22 ± 0.08	10.69 ± 0.35	2.97 ± 0.16
ZS7	20030313	0.21 ± 0.04	1.81 ± 0.07	12.23 ± 1.06	3.23 ± 0.09
ZS7	20030319	1.62 ± 0.06	4.78 ± 0.16	11.46 ± 0.42	4.16 ± 0.23
ZS7	20030325	0.25 ± 0.05	5.67 ± 0.15	15.70 ± 1.04	5.10 ± 0.24
ZS7	20030605	0.01 ± 0.04	0.12 ± 0.04	17.87 ± 1.56	5.88 ± 0.16
ZS7	20030611	0.08 ± 0.04	0.35 ± 0.04	1.92 ± 0.18	0.60 ± 0.04
ZS7	20030617	0.04 ± 0.04	0.15 ± 0.04	20.18 ± 1.17	4.71 ± 0.14
ZS7	20030623	0.04 ± 0.04	0.44 ± 0.04	3.24 ± 0.12	0.98 ± 0.04
ZS7	20030629	0.19 ± 0.04	0.58 ± 0.04	2.15 ± 0.18	0.39 ± 0.04

B.4 Elements Data from XRF Analysis (μg m^{-3})

Site	Date	Aluminum	Silicon	Sulfur	Potassium	Calcium
CH6	021002	.1486 ± .0125	.4731 ± .0094	2.7330 ± .0145	1.3265 ± .0097	.1462 ± .0075
CH6	021008	.4184 ± .0210	1.2628 ± .0164	3.1397 ± .0150	1.2336 ± .0108	.4391 ± .0085
CH6	021014	.1932 ± .0164	.8062 ± .0125	5.2043 ± .0213	2.1338 ± .0123	.2957 ± .0117
CH6	021020	.2140 ± .0147	.5947 ± .0109	4.7960 ± .0175	1.5445 ± .0104	.1633 ± .0086
CH6	021026	.1499 ± .0160	.4633 ± .0098	3.5746 ± .0153	1.3152 ± .0098	.1987 ± .0077
CH6	021201	.0489 ± .0154	.3321 ± .0079	.9795 ± .0087	.6886 ± .0069	.0688 ± .0043
CH6	021207	.1715 ± .0131	.3859 ± .0090	4.2145 ± .0168	1.5733 ± .0106	.1217 ± .0086
CH6	021213	.1158 ± .0122	.4731 ± .0093	2.6126 ± .0132	1.0616 ± .0086	.1248 ± .0063
CH6	021219	.1419 ± .0166	.6394 ± .0108	4.7442 ± .0195	1.6452 ± .0108	.2131 ± .0092
CH6	021225	.0400 ± .0132	.1867 ± .0066	2.9521 ± .0129	.5877 ± .0066	.0569 ± .0039
CH6	030301	.2261 ± .0169	.7740 ± .0129	7.5054 ± .0248	1.9270 ± .0120	.2740 ± .0107
CH6	030307	.0760 ± .0139	.1999 ± .0085	3.0822 ± .0161	.5079 ± .0077	.1163 ± .0046
CH6	030313	.2265 ± .0364	1.0654 ± .0168	7.5020 ± .0332	3.8482 ± .0190	.3482 ± .0204
CH6	030319	.0437 ± .0113	.0622 ± .0046	.7716 ± .0091	.5564 ± .0072	.0350 ± .0039
CH6	030325	.0659 ± .0127	.3967 ± .0091	3.0393 ± .0175	1.4956 ± .0109	.1457 ± .0085
CH6	030605	.2464 ± .0163	.7454 ± .0124	8.3378 ± .0230	2.9424 ± .0146	.3041 ± .0157
CH6	030611	.1514 ± .0130	.5332 ± .0100	3.1424 ± .0142	1.5912 ± .0106	.1509 ± .0088
CH6	030617	.0962 ± .0114	.3294 ± .0083	2.4016 ± .0122	.7732 ± .0077	.0985 ± .0050
CH6	030623	.1083 ± .0111	.2376 ± .0074	2.9166 ± .0129	.9713 ± .0085	.1947 ± .0062
CH6	030629	.0851 ± .0104	.1897 ± .0068	2.1439 ± .0112	1.0106 ± .0086	.1244 ± .0061
CW3	021002	.1438 ± .0143	.3746 ± .0102	2.7897 ± .0149	1.2643 ± .0112	.0998 ± .0074
CW3	021008	.3728 ± .0221	1.2282 ± .0170	3.3273 ± .0164	1.3536 ± .0117	.3962 ± .0090
CW3	021014	.0776 ± .0116	.1811 ± .0074	1.7948 ± .0116	.1241 ± .0041	.0629 ± .0029
CW3	021020	.0254 ± .0322	.0880 ± .0062	2.0284 ± .0118	.1151 ± .0037	.0274 ± .0025
CW3	021026	.1034 ± .0146	.4358 ± .0108	3.8564 ± .0172	.9189 ± .0096	.1359 ± .0061
CW3	021201	.1260 ± .0147	.3878 ± .0102	3.8166 ± .0173	.6196 ± .0078	.1114 ± .0048
CW3	021207	.0133 ± .0368	.0843 ± .0067	3.0187 ± .0145	.1119 ± .0037	.0855 ± .0032
CW3	021213	.0947 ± .0152	.6158 ± .0124	2.7180 ± .0152	.9630 ± .0098	.1694 ± .0065
CW3	021219	.0478 ± .0158	.3519 ± .0108	5.2222 ± .0192	.5501 ± .0075	.1545 ± .0048
CW3	021225	.1307 ± .0134	.3101 ± .0092	3.0154 ± .0152	.9454 ± .0095	.0865 ± .0059
CW3	030301	.0578 ± .0153	.2675 ± .0107	4.4951 ± .0205	.3310 ± .0068	.1286 ± .0045
CW3	030307	.0791 ± .0137	.2558 ± .0096	2.4327 ± .0159	.5918 ± .0089	.0960 ± .0051
CW3	030313	.1392 ± .0143	.3275 ± .0106	2.8241 ± .0167	.2424 ± .0057	.1351 ± .0045
CW3	030319	.0274 ± .0378	.1945 ± .0090	3.2811 ± .0174	.2837 ± .0061	.0774 ± .0040
CW3	030325	.0885 ± .0165	.4535 ± .0127	4.8150 ± .0220	.8445 ± .0102	.1124 ± .0061
CW3	030605	.1348 ± .0177	.4019 ± .0125	6.5196 ± .0237	.7111 ± .0093	.1307 ± .0057
CW3	030611	.1527 ± .0138	.3804 ± .0106	.9250 ± .0096	.1481 ± .0049	.1006 ± .0038
CW3	030617	.1711 ± .0175	.5748 ± .0136	6.1889 ± .0233	.9222 ± .0106	.1549 ± .0066
CW3	030623	.0484 ± .0102	.0459 ± .0055	.9198 ± .0096	.0693 ± .0034	.0340 ± .0030
CW3	030629	.0677 ± .0087	.0295 ± .0046	.6023 ± .0080	.0328 ± .0027	.0236 ± .0028
GZ5	021002	.1246 ± .0203	.7483 ± .0144	4.9076 ± .0219	1.5931 ± .0128	.2551 ± .0096
GZ5	021008	.3110 ± .0213	1.1017 ± .0164	3.6290 ± .0176	1.4964 ± .0124	.4762 ± .0099
GZ5	021014	.4392 ± .0271	1.5859 ± .0204	7.2203 ± .0318	3.6537 ± .0190	.6511 ± .0199
GZ5	021020	.1798 ± .0184	.7159 ± .0136	3.2560 ± .0206	.6502 ± .0081	.1795 ± .0054
GZ5	021026	.1294 ± .0171	.5262 ± .0123	3.7721 ± .0184	1.2472 ± .0112	.1967 ± .0078
GZ5	021201	.2375 ± .0237	1.7231 ± .0199	4.4609 ± .0311	1.8709 ± .0134	.3828 ± .0112

Site	Date	Aluminum	Silicon	Sulfur	Potassium	Calcium
GZ5	021207	.3155 ± .0228	1.0784 ± .0168	5.6245 ± .0276	2.6627 ± .0160	.6379 ± .0153
GZ5	021213	.0472 ± .0485	.6163 ± .0127	3.0175 ± .0174	1.5383 ± .0121	.3739 ± .0096
GZ5	021219	.1543 ± .0212	1.0012 ± .0161	6.1834 ± .0279	1.7502 ± .0130	.3052 ± .0104
GZ5	021225	.1553 ± .0139	.3592 ± .0089	2.6693 ± .0164	.9117 ± .0094	.1302 ± .0060
GZ5	030301	.3221 ± .0248	.9767 ± .0183	7.8793 ± .0308	1.1305 ± .0119	.3058 ± .0084
GZ5	030307	.0851 ± .0158	.4352 ± .0123	3.8104 ± .0216	1.0529 ± .0114	.1773 ± .0074
GZ5	030313	.1606 ± .0257	.9773 ± .0189	7.1005 ± .0339	3.0627 ± .0196	.3335 ± .0171
GZ5	030319	.0672 ± .0182	.2063 ± .0095	1.7195 ± .0146	.6463 ± .0090	.0747 ± .0051
GZ5	030325	.2302 ± .0222	.9482 ± .0180	7.0612 ± .0326	2.2558 ± .0166	.3461 ± .0132
GZ5	030605	.1952 ± .0218	.7553 ± .0161	7.9344 ± .0270	1.1596 ± .0117	.2563 ± .0081
GZ5	030611	.5392 ± .0257	1.2273 ± .0194	5.0244 ± .0270	1.7005 ± .0141	.3146 ± .0106
GZ5	030617	.5602 ± .0287	1.5177 ± .0221	7.3795 ± .0351	3.0925 ± .0192	.5728 ± .0177
GZ5	030623	.1990 ± .0200	.6159 ± .0145	3.2001 ± .0246	1.5802 ± .0138	.2500 ± .0098
GZ5	030629	.1669 ± .0156	.4147 ± .0119	1.9394 ± .0172	.3589 ± .0067	.1648 ± .0049
SZ4	021002	.2134 ± .0178	.8022 ± .0140	3.1175 ± .0171	1.1761 ± .0108	.2157 ± .0076
SZ4	021008	.4123 ± .0250	1.6406 ± .0195	4.2942 ± .0199	1.7432 ± .0130	.8209 ± .0118
SZ4	021014	.1001 ± .0139	.3636 ± .0096	1.8536 ± .0116	.3294 ± .0058	.1195 ± .0039
SZ4	021020	.2087 ± .0169	.5172 ± .0112	1.8109 ± .0112	.1964 ± .0046	.1772 ± .0040
SZ4	021026	.1975 ± .0181	.6698 ± .0132	3.3776 ± .0171	1.2287 ± .0110	.2039 ± .0078
SZ4	021201	.0813 ± .0142	.3547 ± .0100	3.4527 ± .0162	.5476 ± .0073	.1196 ± .0045
SZ4	021207	.1752 ± .0152	.3868 ± .0101	2.4230 ± .0133	.2809 ± .0056	.1510 ± .0041
SZ4	021213	.2225 ± .0410	1.0646 ± .0307	3.6887 ± .0346	1.6176 ± .0245	.5394 ± .0161
SZ4	021221	.3118 ± .0422	1.0322 ± .0322	3.2912 ± .0367	1.7452 ± .0254	.2954 ± .0151
SZ4	021225	.0940 ± .0152	.4533 ± .0112	3.0868 ± .0163	1.0040 ± .0098	.1328 ± .0064
SZ4	030102	.2006 ± .0225	.8220 ± .0151	7.3367 ± .0249	1.8153 ± .0132	.2936 ± .0106
SZ4	030301	.2281 ± .0196	.5850 ± .0142	5.6226 ± .0231	.4934 ± .0081	.1985 ± .0055
SZ4	030307	.0970 ± .0155	.4297 ± .0123	2.9686 ± .0191	.9836 ± .0111	.1665 ± .0070
SZ4	030313	.2830 ± .0198	.7564 ± .0148	3.3267 ± .0185	.5995 ± .0087	.2413 ± .0061
SZ4	030319	.0638 ± .0165	.4441 ± .0122	2.6345 ± .0179	.8165 ± .0102	.2137 ± .0067
SZ4	030325	.2188 ± .0194	.7870 ± .0155	4.4336 ± .0224	1.1145 ± .0117	.2478 ± .0080
SZ4	030605	.1188 ± .0190	.4806 ± .0137	6.5368 ± .0237	.7648 ± .0096	.1900 ± .0062
SZ4	030611	.0504 ± .0142	.3738 ± .0105	1.5938 ± .0124	.3766 ± .0068	.1259 ± .0046
SZ4	030617	.1616 ± .0187	.5921 ± .0142	6.4291 ± .0236	.9437 ± .0106	.1939 ± .0069
SZ4	030623	.0253 ± .0357	.1139 ± .0067	.9322 ± .0095	.1780 ± .0049	.0549 ± .0034
SZ4	030629	.0165 ± .0321	.0928 ± .0063	.6167 ± .0081	.1467 ± .0045	.0698 ± .0035
TC2	021002	.0674 ± .0137	.3914 ± .0103	2.9214 ± .0148	.8559 ± .0090	.0998 ± .0056
TC2	021008	.3667 ± .0193	1.1652 ± .0158	3.1667 ± .0155	1.2956 ± .0111	.4082 ± .0087
TC2	021014	.0560 ± .0112	.1260 ± .0066	1.6738 ± .0109	.4364 ± .0065	.0456 ± .0036
TC2	021020	.0326 ± .0085	.0568 ± .0048	1.2901 ± .0092	.0800 ± .0034	.0153 ± .0022
TC2	021026	.0811 ± .0136	.3593 ± .0099	3.6639 ± .0163	.9328 ± .0094	.1022 ± .0059
TC2	021201	.0281 ± .0414	.3049 ± .0094	3.8304 ± .0163	.5245 ± .0071	.0888 ± .0042
TC2	021207	.0313 ± .0085	.0785 ± .0051	1.1554 ± .0091	.0650 ± .0032	.0598 ± .0027
TC2	021213	.0922 ± .0139	.4775 ± .0108	2.4743 ± .0144	1.1160 ± .0102	.1211 ± .0068
TC2	021219	.0489 ± .0147	.2795 ± .0096	4.2934 ± .0166	.4215 ± .0064	.1393 ± .0043
TC2	021225	.0720 ± .0134	.3730 ± .0103	3.2197 ± .0162	1.0877 ± .0102	.0901 ± .0065
TC2	030301	.1233 ± .0145	.2178 ± .0096	4.8587 ± .0207	.2861 ± .0062	.1069 ± .0043
TC2	030307	.1294 ± .0152	.3752 ± .0116	3.3074 ± .0196	.9069 ± .0107	.1253 ± .0065
TC2	030313	.0803 ± .0151	.2571 ± .0103	2.9152 ± .0164	.1958 ± .0056	.1248 ± .0043
TC2	030319	.0212 ± .0407	.2163 ± .0093	3.3586 ± .0182	.3352 ± .0067	.0719 ± .0041

Site	Date	Aluminum	Silicon	Sulfur	Potassium	Calcium
TC2	030325	.0844 ± .0150	.3238 ± .0113	4.7483 ± .0212	.6686 ± .0094	.0758 ± .0052
TC2	030605	.1096 ± .0182	.4193 ± .0134	7.3606 ± .0253	.7566 ± .0096	.1806 ± .0062
TC2	030611	.0673 ± .0136	.2782 ± .0093	.3859 ± .0067	.1101 ± .0041	.0955 ± .0038
TC2	030617	.1629 ± .0183	.4987 ± .0135	6.4754 ± .0237	.9247 ± .0106	.1404 ± .0065
TC2	030623	.0427 ± .0094	.0151 ± .0154	.7951 ± .0093	.0678 ± .0034	.0235 ± .0028
TC2	030629	.0346 ± .0099	.0438 ± .0050	.6530 ± .0082	.0367 ± .0028	.0316 ± .0029
TM1	021002	.0786 ± .0136	.4031 ± .0104	2.4690 ± .0142	1.0158 ± .0100	.0970 ± .0063
TM1	021008	.3087 ± .0222	1.3257 ± .0175	3.9066 ± .0174	1.4514 ± .0120	.3764 ± .0093
TM1	021014	.0636 ± .0109	.1563 ± .0068	1.5535 ± .0109	.1217 ± .0039	.0495 ± .0029
TM1	021020	.0259 ± .0304	.0556 ± .0054	1.4829 ± .0101	.1104 ± .0036	.0277 ± .0025
TM1	021026	.0960 ± .0162	.4435 ± .0116	3.8527 ± .0171	.9861 ± .0098	.1199 ± .0063
TM1	021201	.1659 ± .0135	.3547 ± .0100	3.6810 ± .0166	.5902 ± .0077	.0984 ± .0045
TM1	021207	.0513 ± .0099	.0706 ± .0055	3.3172 ± .0146	.0931 ± .0033	.0220 ± .0023
TM1	021213	.0649 ± .0152	.5601 ± .0118	2.8150 ± .0154	1.0314 ± .0099	.1284 ± .0065
TM1	021219	.0769 ± .0162	.4035 ± .0110	6.0108 ± .0201	.7048 ± .0084	.1492 ± .0053
TM1	021225	.0980 ± .0134	.3266 ± .0095	3.3100 ± .0157	1.0305 ± .0099	.0730 ± .0062
TM1	030301	.0289 ± .0446	.2144 ± .0101	5.0713 ± .0212	.3108 ± .0065	.0739 ± .0040
TM1	030307	.0283 ± .0406	.2543 ± .0097	2.5212 ± .0161	.5872 ± .0087	.0483 ± .0047
TM1	030313	.1021 ± .0149	.3277 ± .0109	2.7073 ± .0162	.2569 ± .0060	.1281 ± .0045
TM1	030319	.0433 ± .0136	.2186 ± .0094	2.5163 ± .0159	.4375 ± .0078	.0458 ± .0041
TM1	030325	.1169 ± .0179	.5709 ± .0140	6.3593 ± .0256	.9806 ± .0112	.0780 ± .0064
TM1	030605	.1452 ± .0165	.4530 ± .0122	5.6245 ± .0221	.5659 ± .0083	.1003 ± .0049
TM1	030611	.1045 ± .0138	.3294 ± .0096	.5298 ± .0076	.1110 ± .0044	.0706 ± .0035
TM1	030617	.1046 ± .0181	.4903 ± .0134	5.6094 ± .0222	.8949 ± .0105	.1329 ± .0065
TM1	030623	.0502 ± .0098	.0340 ± .0050	.9366 ± .0097	.0677 ± .0035	.0213 ± .0028
TM1	030629	.0279 ± .0282	.0394 ± .0047	.6780 ± .0083	.0330 ± .0027	.0225 ± .0028
ZS7	021008	.6394 ± .0261	2.2478 ± .0207	6.3557 ± .0280	4.1689 ± .0178	.8429 ± .0222
ZS7	021014	.1813 ± .0155	.6156 ± .0112	3.9676 ± .0155	1.0078 ± .0089	.1410 ± .0062
ZS7	021020	.0807 ± .0105	.2185 ± .0071	2.0774 ± .0105	.2004 ± .0040	.0572 ± .0025
ZS7	021026	.1277 ± .0139	.4727 ± .0100	5.1936 ± .0166	.6477 ± .0071	.1421 ± .0047
ZS7	021201	.1181 ± .0166	.7346 ± .0124	6.1011 ± .0208	.9498 ± .0084	.1345 ± .0058
ZS7	021207	.1513 ± .0137	.4176 ± .0097	3.5935 ± .0151	.5086 ± .0063	.1084 ± .0039
ZS7	021213	.2852 ± .0183	1.2607 ± .0151	4.7351 ± .0228	2.6532 ± .0139	.2839 ± .0142
ZS7	021219	.3770 ± .0204	1.2545 ± .0154	7.6061 ± .0239	1.4068 ± .0102	.2994 ± .0086
ZS7	021225	.1859 ± .0189	.8584 ± .0130	4.3201 ± .0231	2.0836 ± .0123	.2410 ± .0114
ZS7	030301	.1990 ± .0149	.5454 ± .0108	5.2831 ± .0177	.4484 ± .0087	.1843 ± .0044
ZS7	030307	.1751 ± .0157	.6346 ± .0114	3.6721 ± .0183	.8667 ± .0082	.1635 ± .0057
ZS7	030313	.2081 ± .0159	.6710 ± .0117	4.1224 ± .0161	.5583 ± .0068	.2017 ± .0048
ZS7	030319	.1057 ± .0162	.6486 ± .0116	3.8660 ± .0207	1.2461 ± .0100	.1845 ± .0074
ZS7	030325	.1845 ± .0150	.6473 ± .0113	5.2221 ± .0193	1.0810 ± .0092	.1270 ± .0065
ZS7	030605	.1757 ± .0145	.4207 ± .0100	5.5927 ± .0175	.6544 ± .0072	.1207 ± .0047
ZS7	030611	.1081 ± .0114	.4115 ± .0085	.7293 ± .0068	.1664 ± .0037	.0891 ± .0029
ZS7	030617	.2025 ± .0157	.5871 ± .0113	6.7480 ± .0198	.7773 ± .0079	.1271 ± .0052
ZS7	030623	.0596 ± .0086	.1407 ± .0056	1.1469 ± .0081	.0913 ± .0029	.0538 ± .0023
ZS7	030629	.0369 ± .0077	.0679 ± .0046	.6807 ± .0066	.0483 ± .0024	.0375 ± .0022

Site	Date	Titanium	Vanadium	Chromium	Manganese	Iron
CH6	021002	.0000 ± .0232	.0000 ± .0136	.0023 ± .0037	.0121 ± .0007	.1569 ± .0015
CH6	021008	.0361 ± .0090	.0037 ± .0115	.0094 ± .0008	.0207 ± .0008	.4427 ± .0029
CH6	021014	.0147 ± .0214	.0022 ± .0092	.0045 ± .0006	.0287 ± .0008	.3271 ± .0022
CH6	021020	.0224 ± .0068	.0234 ± .0030	.0060 ± .0007	.0123 ± .0006	.2132 ± .0018
CH6	021026	.0024 ± .0203	.0000 ± .0087	.0054 ± .0006	.0143 ± .0006	.2492 ± .0019
CH6	021201	.0057 ± .0188	.0005 ± .0081	.0100 ± .0006	.0187 ± .0007	.1888 ± .0016
CH6	021207	.0192 ± .0203	.0205 ± .0030	.0282 ± .0010	.0140 ± .0007	.3616 ± .0022
CH6	021213	.0000 ± .0203	.0000 ± .0087	.0071 ± .0006	.0192 ± .0007	.2154 ± .0018
CH6	021219	.0750 ± .0068	.0160 ± .0031	.0183 ± .0008	.0251 ± .0008	.4849 ± .0026
CH6	021225	.0035 ± .0200	.0020 ± .0086	.0127 ± .0007	.0088 ± .0005	.1723 ± .0016
CH6	030301	.0327 ± .0070	.0311 ± .0030	.0146 ± .0009	.0216 ± .0007	.3370 ± .0023
CH6	030307	.0062 ± .0283	.0020 ± .0115	.0232 ± .0010	.0095 ± .0007	.1670 ± .0019
CH6	030313	.0055 ± .0301	.0000 ± .0170	.0143 ± .0017	.0569 ± .0014	.8308 ± .0040
CH6	030319	.0000 ± .0280	.0000 ± .0161	.0016 ± .0046	.0023 ± .0007	.0674 ± .0012
CH6	030325	.0080 ± .0225	.0014 ± .0091	.0237 ± .0009	.0149 ± .0007	.2929 ± .0021
CH6	030605	.0076 ± .0254	.0218 ± .0050	.0087 ± .0015	.0161 ± .0008	.3180 ± .0022
CH6	030611	.0072 ± .0224	.0158 ± .0043	.0065 ± .0013	.0073 ± .0006	.1786 ± .0016
CH6	030617	.0062 ± .0224	.0004 ± .0090	.0137 ± .0007	.0139 ± .0006	.2179 ± .0018
CH6	030623	.0124 ± .0206	.0224 ± .0029	.0079 ± .0007	.0055 ± .0005	.1134 ± .0013
CH6	030629	.0119 ± .0222	.0232 ± .0031	.0069 ± .0007	.0043 ± .0004	.0875 ± .0012
CW3	021002	.0008 ± .0310	.0073 ± .0189	.0005 ± .0051	.0151 ± .0009	.1959 ± .0020
CW3	021008	.0252 ± .0317	.0000 ± .0193	.0000 ± .0053	.0231 ± .0011	.4844 ± .0031
CW3	021014	.0094 ± .0274	.0062 ± .0118	.0010 ± .0020	.0042 ± .0005	.0623 ± .0012
CW3	021020	.0000 ± .0293	.0037 ± .0126	.0000 ± .0020	.0022 ± .0005	.0332 ± .0010
CW3	021026	.0026 ± .0303	.0068 ± .0131	.0010 ± .0023	.0179 ± .0008	.1948 ± .0020
CW3	021201	.0000 ± .0281	.0025 ± .0121	.0023 ± .0007	.0168 ± .0008	.1487 ± .0018
CW3	021207	.0059 ± .0295	.0381 ± .0044	.0002 ± .0026	.0066 ± .0006	.1149 ± .0016
CW3	021213	.0000 ± .0287	.0002 ± .0124	.0021 ± .0022	.0188 ± .0008	.2059 ± .0021
CW3	021219	.0012 ± .0276	.0102 ± .0120	.0015 ± .0021	.0163 ± .0007	.1901 ± .0020
CW3	021225	.0076 ± .0270	.0066 ± .0116	.0019 ± .0021	.0137 ± .0007	.1951 ± .0020
CW3	030301	.0000 ± .0374	.0080 ± .0218	.0008 ± .0062	.0127 ± .0010	.2003 ± .0023
CW3	030307	.0000 ± .0364	.0000 ± .0148	.0016 ± .0026	.0159 ± .0009	.2242 ± .0024
CW3	030313	.0127 ± .0349	.0084 ± .0142	.0021 ± .0025	.0100 ± .0007	.1491 ± .0020
CW3	030319	.0000 ± .0358	.0078 ± .0146	.0015 ± .0025	.0142 ± .0008	.1453 ± .0020
CW3	030325	.0136 ± .0348	.0099 ± .0142	.0047 ± .0009	.0214 ± .0010	.2298 ± .0025
CW3	030605	.0000 ± .0381	.0000 ± .0225	.0000 ± .0064	.0110 ± .0010	.1872 ± .0022
CW3	030611	.0194 ± .0318	.0068 ± .0129	.0017 ± .0022	.0068 ± .0006	.1622 ± .0020
CW3	030617	.0091 ± .0361	.0066 ± .0207	.0012 ± .0058	.0193 ± .0011	.2353 ± .0025
CW3	030623	.0000 ± .0374	.0000 ± .0216	.0000 ± .0060	.0003 ± .0024	.0280 ± .0010
CW3	030629	.0000 ± .0358	.0068 ± .0146	.0018 ± .0024	.0003 ± .0014	.0150 ± .0009
GZ5	021002	.0305 ± .0306	.0335 ± .0045	.0016 ± .0027	.0249 ± .0009	.3518 ± .0027
GZ5	021008	.0389 ± .0101	.0197 ± .0044	.0017 ± .0024	.0291 ± .0010	.4940 ± .0031
GZ5	021014	.0458 ± .0104	.0582 ± .0047	.0051 ± .0011	.0428 ± .0012	.6634 ± .0037
GZ5	021020	.0336 ± .0093	.0387 ± .0042	.0054 ± .0010	.0334 ± .0010	.5308 ± .0033
GZ5	021026	.0202 ± .0295	.0138 ± .0043	.0026 ± .0008	.0301 ± .0010	.3364 ± .0026
GZ5	021201	.0770 ± .0092	.0399 ± .0042	.0075 ± .0012	.2547 ± .0026	2.0712 ± .0065

Site	Date	Titanium	Vanadium	Chromium	Manganese	Iron
GZ5	021207	.0563 ± .0102	.0499 ± .0063	.0064 ± .0018	.0261 ± .0011	.3956 ± .0028
GZ5	021213	.0183 ± .0305	.0134 ± .0184	.0000 ± .0050	.0245 ± .0010	.3193 ± .0025
GZ5	021219	.0303 ± .0311	.0308 ± .0064	.0021 ± .0054	.0374 ± .0012	.4669 ± .0030
GZ5	021225	.0000 ± .0274	.0024 ± .0118	.0005 ± .0020	.0174 ± .0008	.2169 ± .0021
GZ5	030301	.0160 ± .0400	.0472 ± .0077	.0024 ± .0067	.0368 ± .0014	.6447 ± .0040
GZ5	030307	.0029 ± .0397	.0000 ± .0228	.0000 ± .0064	.0264 ± .0013	.3486 ± .0030
GZ5	030313	.0243 ± .0423	.0280 ± .0083	.0076 ± .0024	.0633 ± .0017	.6188 ± .0040
GZ5	030319	.0010 ± .0383	.0031 ± .0219	.0003 ± .0061	.0175 ± .0011	.1756 ± .0022
GZ5	030325	.0433 ± .0120	.0432 ± .0051	.0057 ± .0011	.0493 ± .0014	.5710 ± .0038
GZ5	030605	.0411 ± .0113	.0379 ± .0048	.0044 ± .0010	.0265 ± .0010	.3628 ± .0030
GZ5	030611	.0529 ± .0112	.0975 ± .0050	.0070 ± .0015	.0385 ± .0012	.5164 ± .0035
GZ5	030617	.0089 ± .0437	.0623 ± .0085	.0042 ± .0076	.0460 ± .0016	.8291 ± .0045
GZ5	030623	.0425 ± .0121	.0585 ± .0052	.0046 ± .0012	.0438 ± .0013	.5435 ± .0036
GZ5	030629	.0224 ± .0329	.0383 ± .0046	.0008 ± .0027	.0197 ± .0009	.1756 ± .0021
SZ4	021002	.0267 ± .0285	.0304 ± .0042	.0025 ± .0026	.0233 ± .0009	.3326 ± .0026
SZ4	021008	.0381 ± .0104	.0554 ± .0066	.0008 ± .0057	.0340 ± .0012	.5919 ± .0034
SZ4	021014	.0127 ± .0293	.0133 ± .0042	.0003 ± .0021	.0079 ± .0006	.1176 ± .0016
SZ4	021020	.0126 ± .0275	.0107 ± .0119	.0010 ± .0020	.0070 ± .0006	.1663 ± .0018
SZ4	021026	.0307 ± .0102	.0242 ± .0045	.0020 ± .0026	.0216 ± .0009	.2719 ± .0024
SZ4	021201	.0127 ± .0264	.0093 ± .0114	.0016 ± .0020	.0167 ± .0007	.1540 ± .0018
SZ4	021207	.0166 ± .0275	.0216 ± .0040	.0013 ± .0023	.0100 ± .0006	.1658 ± .0018
SZ4	021213	.0299 ± .1078	.0097 ± .0617	.0009 ± .0172	.0471 ± .0031	.5019 ± .0062
SZ4	021221	.0613 ± .1008	.0485 ± .0138	.0107 ± .0026	.0475 ± .0025	.5114 ± .0063
SZ4	021225	.0218 ± .0280	.0274 ± .0041	.0033 ± .0008	.0206 ± .0008	.2099 ± .0021
SZ4	030102	.0373 ± .0093	.0223 ± .0041	.0042 ± .0008	.0391 ± .0010	.4174 ± .0028
SZ4	030301	.0106 ± .0350	.0319 ± .0049	.0027 ± .0029	.0263 ± .0010	.3422 ± .0029
SZ4	030307	.0113 ± .0370	.0096 ± .0215	.0036 ± .0062	.0262 ± .0012	.2620 ± .0026
SZ4	030313	.0232 ± .0387	.0147 ± .0224	.0017 ± .0063	.0340 ± .0013	.3817 ± .0031
SZ4	030319	.0379 ± .0120	.0289 ± .0050	.0037 ± .0010	.0273 ± .0011	.2613 ± .0026
SZ4	030325	.0060 ± .0379	.0264 ± .0053	.0036 ± .0010	.0377 ± .0012	.4292 ± .0033
SZ4	030605	.0215 ± .0349	.0177 ± .0048	.0027 ± .0009	.0174 ± .0009	.2693 ± .0026
SZ4	030611	.0132 ± .0371	.0065 ± .0218	.0000 ± .0062	.0233 ± .0012	.2691 ± .0026
SZ4	030617	.0000 ± .0393	.0274 ± .0075	.0023 ± .0063	.0350 ± .0013	.3460 ± .0029
SZ4	030623	.0000 ± .0380	.0000 ± .0218	.0000 ± .0060	.0075 ± .0010	.0851 ± .0016
SZ4	030629	.0060 ± .0336	.0028 ± .0136	.0003 ± .0021	.0108 ± .0007	.0938 ± .0016
TC2	021002	.0153 ± .0266	.0123 ± .0039	.0023 ± .0007	.0144 ± .0007	.2015 ± .0020
TC2	021008	.0378 ± .0093	.0051 ± .0120	.0009 ± .0021	.0235 ± .0009	.5068 ± .0031
TC2	021014	.0000 ± .0284	.0055 ± .0122	.0000 ± .0019	.0027 ± .0005	.0509 ± .0011
TC2	021020	.0024 ± .0262	.0031 ± .0112	.0002 ± .0018	.0020 ± .0004	.0207 ± .0008
TC2	021026	.0107 ± .0271	.0121 ± .0039	.0013 ± .0021	.0178 ± .0008	.1864 ± .0019
TC2	021201	.0137 ± .0252	.0109 ± .0109	.0022 ± .0007	.0135 ± .0007	.1288 ± .0016
TC2	021207	.0035 ± .0264	.0083 ± .0114	.0006 ± .0019	.0060 ± .0005	.0923 ± .0014
TC2	021213	.0160 ± .0284	.0094 ± .0123	.0018 ± .0022	.0175 ± .0008	.1999 ± .0020
TC2	021219	.0103 ± .0298	.0120 ± .0129	.0019 ± .0023	.0133 ± .0007	.1626 ± .0018
TC2	021225	.0170 ± .0270	.0095 ± .0116	.0011 ± .0021	.0171 ± .0007	.2129 ± .0020
TC2	030301	.0000 ± .0415	.0000 ± .0231	.0000 ± .0062	.0043 ± .0009	.1537 ± .0021
TC2	030307	.0000 ± .0371	.0095 ± .0153	.0028 ± .0009	.0213 ± .0010	.2685 ± .0027
TC2	030313	.0095 ± .0375	.0134 ± .0153	.0000 ± .0025	.0073 ± .0007	.1369 ± .0020
TC2	030319	.0000 ± .0413	.0000 ± .0229	.0000 ± .0062	.0102 ± .0010	.1751 ± .0022

Site	Date	Titanium	Vanadium	Chromium	Manganese	Iron
TC2	030325	.0124 ± .0364	.0221 ± .0050	.0018 ± .0027	.0159 ± .0009	.1843 ± .0022
TC2	030605	.0000 ± .0359	.0059 ± .0146	.0011 ± .0025	.0126 ± .0008	.1939 ± .0023
TC2	030611	.0132 ± .0357	.0022 ± .0145	.0012 ± .0023	.0038 ± .0006	.1262 ± .0019
TC2	030617	.0000 ± .0377	.0000 ± .0217	.0000 ± .0061	.0183 ± .0011	.2167 ± .0024
TC2	030623	.0002 ± .0332	.0022 ± .0134	.0010 ± .0021	.0010 ± .0014	.0132 ± .0008
TC2	030629	.0000 ± .0364	.0000 ± .0208	.0000 ± .0058	.0003 ± .0023	.0082 ± .0008
TM1	021002	.0107 ± .0294	.0139 ± .0043	.0004 ± .0022	.0123 ± .0007	.1662 ± .0019
TM1	021008	.0400 ± .0093	.0249 ± .0041	.0020 ± .0024	.0234 ± .0009	.4653 ± .0030
TM1	021014	.0036 ± .0290	.0054 ± .0125	.0000 ± .0020	.0021 ± .0005	.0322 ± .0010
TM1	021020	.0000 ± .0287	.0004 ± .0124	.0005 ± .0020	.0024 ± .0005	.0300 ± .0009
TM1	021026	.0157 ± .0306	.0270 ± .0045	.0006 ± .0025	.0160 ± .0008	.2012 ± .0021
TM1	021201	.0109 ± .0265	.0050 ± .0114	.0017 ± .0020	.0157 ± .0007	.1242 ± .0016
TM1	021207	.0030 ± .0271	.0206 ± .0039	.0008 ± .0021	.0014 ± .0004	.0189 ± .0008
TM1	021213	.0000 ± .0279	.0123 ± .0040	.0011 ± .0021	.0160 ± .0007	.1736 ± .0019
TM1	021219	.0127 ± .0267	.0141 ± .0039	.0025 ± .0007	.0155 ± .0007	.1405 ± .0017
TM1	021225	.0098 ± .0260	.0178 ± .0038	.0005 ± .0021	.0124 ± .0007	.1644 ± .0018
TM1	030301	.0000 ± .0378	.0124 ± .0216	.0001 ± .0060	.0065 ± .0009	.0882 ± .0016
TM1	030307	.0013 ± .0360	.0051 ± .0146	.0017 ± .0025	.0130 ± .0008	.1965 ± .0023
TM1	030313	.0000 ± .0416	.0000 ± .0236	.0000 ± .0065	.0031 ± .0010	.1062 ± .0018
TM1	030319	.0113 ± .0348	.0350 ± .0049	.0010 ± .0028	.0099 ± .0007	.1592 ± .0021
TM1	030325	.0000 ± .0370	.0000 ± .0216	.0000 ± .0061	.0180 ± .0011	.2272 ± .0025
TM1	030605	.0000 ± .0332	.0095 ± .0136	.0015 ± .0024	.0098 ± .0007	.1599 ± .0020
TM1	030611	.0125 ± .0344	.0049 ± .0140	.0010 ± .0023	.0038 ± .0006	.1143 ± .0018
TM1	030617	.0078 ± .0392	.0071 ± .0226	.0000 ± .0063	.0176 ± .0011	.1886 ± .0022
TM1	030623	.0010 ± .0346	.0040 ± .0140	.0005 ± .0022	.0009 ± .0014	.0087 ± .0008
TM1	030629	.0013 ± .0328	.0057 ± .0133	.0014 ± .0023	.0007 ± .0015	.0061 ± .0008
ZS7	021008	.0912 ± .0079	.0677 ± .0038	.0223 ± .0012	.0444 ± .0011	.8487 ± .0036
ZS7	021014	.0343 ± .0078	.0447 ± .0035	.0283 ± .0011	.0181 ± .0008	.3111 ± .0022
ZS7	021020	.0133 ± .0214	.0137 ± .0031	.0036 ± .0006	.0056 ± .0004	.0823 ± .0012
ZS7	021026	.0158 ± .0215	.0115 ± .0031	.0012 ± .0017	.0143 ± .0006	.1501 ± .0016
ZS7	021201	.0121 ± .0238	.0745 ± .0049	.0088 ± .0016	.0291 ± .0009	.3045 ± .0021
ZS7	021207	.0098 ± .0224	.0436 ± .0047	.0036 ± .0042	.0075 ± .0006	.1260 ± .0014
ZS7	021213	.0615 ± .0077	.0619 ± .0036	.0082 ± .0010	.0315 ± .0009	.3907 ± .0024
ZS7	021219	.0219 ± .0254	.0440 ± .0053	.0035 ± .0047	.0399 ± .0011	.4927 ± .0027
ZS7	021225	.0339 ± .0076	.0308 ± .0034	.0104 ± .0009	.0251 ± .0008	.3810 ± .0024
ZS7	030301	.0000 ± .0277	.0355 ± .0052	.0858 ± .0020	.0212 ± .0013	.5601 ± .0030
ZS7	030307	.0326 ± .0079	.0212 ± .0046	.0056 ± .0013	.0193 ± .0008	.2924 ± .0022
ZS7	030313	.0204 ± .0254	.0436 ± .0050	.0152 ± .0016	.0216 ± .0009	.3358 ± .0023
ZS7	030319	.0241 ± .0074	.0301 ± .0031	.0251 ± .0010	.0195 ± .0008	.3394 ± .0023
ZS7	030325	.0191 ± .0252	.0479 ± .0036	.0080 ± .0009	.0238 ± .0008	.2994 ± .0022
ZS7	030605	.0222 ± .0234	.0259 ± .0033	.0098 ± .0008	.0111 ± .0006	.2211 ± .0019
ZS7	030611	.0156 ± .0227	.0114 ± .0031	.0022 ± .0006	.0060 ± .0005	.1638 ± .0016
ZS7	030617	.0000 ± .0248	.0266 ± .0047	.0054 ± .0014	.0141 ± .0008	.2433 ± .0020
ZS7	030623	.0011 ± .0226	.0029 ± .0131	.0012 ± .0037	.0027 ± .0005	.0540 ± .0010
ZS7	030629	.0000 ± .0247	.0007 ± .0142	.0079 ± .0014	.0016 ± .0017	.0555 ± .0010

Site	Date	Cobalt	Nickle	Copper	Zinc	Gallium
CH6	021002	.0002 ± .0026	.0093 ± .0004	.0697 ± .0008	.2381 ± .0013	.0000 ± .0032
CH6	021008	.0030 ± .0068	.0146 ± .0005	.0146 ± .0005	.1251 ± .0011	.0000 ± .0034
CH6	021014	.0014 ± .0051	.0062 ± .0003	.0464 ± .0007	.6062 ± .0021	.0000 ± .0043
CH6	021020	.0013 ± .0034	.0154 ± .0004	.0148 ± .0004	.3600 ± .0016	.0001 ± .0032
CH6	021026	.0004 ± .0039	.0077 ± .0003	.0442 ± .0006	.3214 ± .0015	.0000 ± .0030
CH6	021201	.0012 ± .0030	.0110 ± .0004	.0592 ± .0007	.2269 ± .0012	.0000 ± .0026
CH6	021207	.0023 ± .0056	.0299 ± .0006	.0164 ± .0005	.1725 ± .0011	.0000 ± .0032
CH6	021213	.0013 ± .0034	.0090 ± .0003	.0374 ± .0006	.2741 ± .0014	.0000 ± .0029
CH6	021219	.0028 ± .0074	.0344 ± .0006	.0697 ± .0008	.3479 ± .0015	.0000 ± .0039
CH6	021225	.0011 ± .0028	.0150 ± .0004	.0847 ± .0008	.2018 ± .0012	.0000 ± .0027
CH6	030301	.0017 ± .0053	.0289 ± .0006	.0224 ± .0005	.3696 ± .0016	.0045 ± .0014
CH6	030307	.0016 ± .0029	.0331 ± .0007	.0463 ± .0008	.1204 ± .0012	.0000 ± .0036
CH6	030313	.0053 ± .0127	.0185 ± .0006	.2358 ± .0017	.9591 ± .0030	.0019 ± .0066
CH6	030319	.0011 ± .0015	.0099 ± .0004	.0713 ± .0009	.1814 ± .0013	.0000 ± .0033
CH6	030325	.0021 ± .0047	.0322 ± .0006	.0884 ± .0009	.5147 ± .0019	.0000 ± .0040
CH6	030605	.0017 ± .0050	.0328 ± .0006	.0222 ± .0005	.2930 ± .0014	.0029 ± .0037
CH6	030611	.0009 ± .0029	.0183 ± .0005	.0161 ± .0004	.2234 ± .0013	.0000 ± .0029
CH6	030617	.0021 ± .0035	.0250 ± .0005	.0264 ± .0006	.2768 ± .0014	.0000 ± .0029
CH6	030623	.0012 ± .0020	.0260 ± .0005	.0085 ± .0004	.0933 ± .0008	.0000 ± .0026
CH6	030629	.0002 ± .0017	.0174 ± .0005	.0065 ± .0004	.0830 ± .0008	.0000 ± .0026
CW3	021002	.0015 ± .0033	.0054 ± .0004	.0262 ± .0006	.3124 ± .0018	.0000 ± .0036
CW3	021008	.0013 ± .0075	.0009 ± .0010	.0081 ± .0005	.2714 ± .0016	.0000 ± .0037
CW3	021014	.0015 ± .0005	.0021 ± .0003	.0055 ± .0004	.0419 ± .0007	.0006 ± .0032
CW3	021020	.0008 ± .0012	.0026 ± .0003	.0044 ± .0004	.0297 ± .0007	.0000 ± .0033
CW3	021026	.0007 ± .0033	.0023 ± .0004	.0087 ± .0005	.3570 ± .0019	.0000 ± .0039
CW3	021201	.0011 ± .0026	.0025 ± .0003	.0155 ± .0005	.2560 ± .0016	.0000 ± .0035
CW3	021207	.0013 ± .0022	.0095 ± .0005	.0134 ± .0005	.0780 ± .0009	.0000 ± .0036
CW3	021213	.0013 ± .0034	.0031 ± .0003	.0131 ± .0005	.2897 ± .0017	.0000 ± .0035
CW3	021219	.0003 ± .0032	.0046 ± .0004	.0149 ± .0005	.1849 ± .0014	.0000 ± .0034
CW3	021225	.0011 ± .0032	.0014 ± .0003	.0083 ± .0005	.3323 ± .0018	.0000 ± .0034
CW3	030301	.0025 ± .0035	.0092 ± .0005	.0157 ± .0006	.1046 ± .0012	.0000 ± .0040
CW3	030307	.0013 ± .0039	.0029 ± .0004	.0111 ± .0006	.3324 ± .0020	.0000 ± .0043
CW3	030313	.0027 ± .0028	.0041 ± .0004	.0054 ± .0005	.1396 ± .0014	.0000 ± .0042
CW3	030319	.0020 ± .0028	.0039 ± .0004	.0080 ± .0005	.1521 ± .0014	.0010 ± .0043
CW3	030325	.0023 ± .0039	.0043 ± .0004	.0164 ± .0006	.3182 ± .0020	.0000 ± .0046
CW3	030605	.0010 ± .0033	.0043 ± .0004	.0136 ± .0006	.1614 ± .0014	.0000 ± .0041
CW3	030611	.0008 ± .0029	.0035 ± .0004	.0084 ± .0005	.0769 ± .0010	.0000 ± .0036
CW3	030617	.0030 ± .0040	.0060 ± .0005	.0171 ± .0006	.3098 ± .0019	.0000 ± .0040
CW3	030623	.0006 ± .0013	.0013 ± .0003	.0061 ± .0005	.0259 ± .0007	.0000 ± .0039
CW3	030629	.0004 ± .0012	.0026 ± .0004	.0053 ± .0005	.0113 ± .0006	.0000 ± .0040
GZ5	021002	.0016 ± .0056	.0068 ± .0004	.0273 ± .0007	.4161 ± .0020	.0000 ± .0046
GZ5	021008	.0026 ± .0076	.0028 ± .0004	.0220 ± .0006	.2029 ± .0014	.0000 ± .0040
GZ5	021014	.0023 ± .0101	.0212 ± .0006	.0426 ± .0008	.7493 ± .0027	.0012 ± .0065
GZ5	021020	.0007 ± .0082	.0117 ± .0005	.0233 ± .0007	1.1798 ± .0034	.0018 ± .0049
GZ5	021026	.0037 ± .0053	.0046 ± .0004	.0607 ± .0009	.2926 ± .0017	.0000 ± .0041
GZ5	021201	.0097 ± .0308	.0109 ± .0006	.0919 ± .0011	.7365 ± .0026	.0045 ± .0069

Site	Date	Cobalt	Nickle	Copper	Zinc	Gallium
GZ5	021207	.0026 ± .0062	.0176 ± .0006	.0320 ± .0007	.5322 ± .0022	.0009 ± .0057
GZ5	021213	.0011 ± .0050	.0051 ± .0004	.0242 ± .0006	.2766 ± .0016	.0000 ± .0039
GZ5	021219	.0052 ± .0072	.0127 ± .0005	.0447 ± .0008	.6318 ± .0024	.0000 ± .0057
GZ5	021225	.0011 ± .0036	.0033 ± .0003	.0624 ± .0009	.2486 ± .0015	.0000 ± .0039
GZ5	030301	.0054 ± .0101	.0207 ± .0007	.0416 ± .0009	.8373 ± .0032	.0039 ± .0055
GZ5	030307	.0012 ± .0056	.0015 ± .0004	.0399 ± .0009	.3183 ± .0020	.0000 ± .0049
GZ5	030313	.0037 ± .0097	.0179 ± .0007	.0930 ± .0013	.8010 ± .0031	.0003 ± .0069
GZ5	030319	.0011 ± .0031	.0026 ± .0004	.0776 ± .0011	.2678 ± .0018	.0025 ± .0045
GZ5	030325	.0058 ± .0090	.0185 ± .0007	.0446 ± .0009	.6055 ± .0027	.0032 ± .0064
GZ5	030605	.0027 ± .0059	.0144 ± .0006	.0179 ± .0007	.4979 ± .0024	.0000 ± .0046
GZ5	030611	.0024 ± .0081	.0281 ± .0008	.0308 ± .0008	1.2073 ± .0037	.0152 ± .0019
GZ5	030617	.0039 ± .0128	.0202 ± .0007	.0560 ± .0010	1.1344 ± .0036	.0000 ± .0073
GZ5	030623	.0039 ± .0085	.0131 ± .0006	.0199 ± .0007	.8393 ± .0031	.0000 ± .0060
GZ5	030629	.0012 ± .0031	.0087 ± .0005	.0133 ± .0006	.3296 ± .0020	.0000 ± .0047
SZ4	021002	.0018 ± .0052	.0078 ± .0004	.0293 ± .0007	.4364 ± .0020	.0000 ± .0040
SZ4	021008	.0039 ± .0090	.0155 ± .0005	.0184 ± .0006	.4933 ± .0022	.0000 ± .0041
SZ4	021014	.0011 ± .0022	.0036 ± .0004	.0065 ± .0005	.1068 ± .0011	.0000 ± .0034
SZ4	021020	.0011 ± .0028	.0032 ± .0003	.0028 ± .0004	.0780 ± .0009	.0000 ± .0032
SZ4	021026	.0010 ± .0044	.0062 ± .0004	.0126 ± .0006	.4652 ± .0021	.0000 ± .0041
SZ4	021201	.0004 ± .0026	.0030 ± .0003	.0116 ± .0005	.2041 ± .0014	.0029 ± .0033
SZ4	021207	.0011 ± .0028	.0074 ± .0004	.0103 ± .0005	.1689 ± .0013	.0000 ± .0033
SZ4	021213	.0045 ± .0090	.0089 ± .0012	.0241 ± .0016	.6778 ± .0049	.0022 ± .0115
SZ4	021221	.0056 ± .0092	.0145 ± .0013	.0275 ± .0016	.7306 ± .0052	.0101 ± .0125
SZ4	021225	.0000 ± .0035	.0077 ± .0004	.0067 ± .0005	.3621 ± .0018	.0000 ± .0038
SZ4	030102	.0018 ± .0065	.0072 ± .0004	.0267 ± .0006	.3728 ± .0019	.0000 ± .0042
SZ4	030301	.0009 ± .0055	.0128 ± .0005	.0196 ± .0007	.1847 ± .0015	.0000 ± .0041
SZ4	030307	.0013 ± .0044	.0064 ± .0005	.0085 ± .0006	.3960 ± .0022	.0054 ± .0015
SZ4	030313	.0021 ± .0061	.0090 ± .0005	.0122 ± .0006	.3210 ± .0020	.0005 ± .0042
SZ4	030319	.0035 ± .0044	.0098 ± .0005	.0165 ± .0007	.3481 ± .0021	.0000 ± .0044
SZ4	030325	.0012 ± .0068	.0110 ± .0006	.0196 ± .0007	.5532 ± .0026	.0031 ± .0050
SZ4	030605	.0001 ± .0044	.0064 ± .0005	.0076 ± .0005	.1718 ± .0015	.0009 ± .0041
SZ4	030611	.0012 ± .0044	.0151 ± .0006	.0085 ± .0005	.1048 ± .0012	.0028 ± .0039
SZ4	030617	.0030 ± .0056	.0153 ± .0006	.0127 ± .0006	.2890 ± .0019	.0000 ± .0043
SZ4	030623	.0017 ± .0019	.0018 ± .0004	.0023 ± .0004	.0253 ± .0007	.0020 ± .0040
SZ4	030629	.0007 ± .0020	.0004 ± .0010	.0013 ± .0004	.0112 ± .0005	.0007 ± .0038
TC2	021002	.0022 ± .0034	.0035 ± .0004	.0235 ± .0006	.3115 ± .0017	.0000 ± .0035
TC2	021008	.0026 ± .0078	.0007 ± .0009	.0120 ± .0005	.2838 ± .0016	.0000 ± .0036
TC2	021014	.0010 ± .0013	.0023 ± .0003	.0097 ± .0005	.0303 ± .0006	.0000 ± .0033
TC2	021020	.0002 ± .0010	.0014 ± .0003	.0131 ± .0005	.0135 ± .0005	.0000 ± .0030
TC2	021026	.0027 ± .0032	.0031 ± .0003	.0238 ± .0006	.4084 ± .0019	.0000 ± .0036
TC2	021201	.0021 ± .0023	.0036 ± .0003	.0138 ± .0005	.2101 ± .0014	.0030 ± .0032
TC2	021207	.0014 ± .0018	.0018 ± .0003	.0153 ± .0005	.0255 ± .0006	.0000 ± .0031
TC2	021213	.0009 ± .0033	.0023 ± .0003	.0151 ± .0005	.2735 ± .0016	.0000 ± .0037
TC2	021219	.0008 ± .0028	.0050 ± .0004	.0159 ± .0006	.1016 ± .0010	.0000 ± .0036
TC2	021225	.0012 ± .0035	.0032 ± .0003	.0135 ± .0005	.3921 ± .0019	.0000 ± .0036
TC2	030301	.0016 ± .0029	.0044 ± .0005	.0197 ± .0007	.0572 ± .0009	.0000 ± .0041
TC2	030307	.0035 ± .0045	.0072 ± .0005	.0148 ± .0007	.4213 ± .0023	.0000 ± .0046
TC2	030313	.0012 ± .0027	.0040 ± .0005	.0115 ± .0006	.0955 ± .0012	.0000 ± .0044
TC2	030319	.0025 ± .0032	.0029 ± .0004	.0167 ± .0006	.2080 ± .0016	.0000 ± .0044

Site	Date	Cobalt	Nickle	Copper	Zinc	Gallium
TC2	030325	.0019 ± .0033	.0070 ± .0005	.0193 ± .0007	.2210 ± .0017	.0037 ± .0046
TC2	030605	.0014 ± .0034	.0038 ± .0004	.0174 ± .0006	.1626 ± .0014	.0000 ± .0044
TC2	030611	.0004 ± .0024	.0008 ± .0011	.0116 ± .0006	.0104 ± .0006	.0023 ± .0043
TC2	030617	.0024 ± .0037	.0124 ± .0006	.0199 ± .0007	.2587 ± .0018	.0000 ± .0041
TC2	030623	.0004 ± .0011	.0013 ± .0003	.0084 ± .0005	.0021 ± .0004	.0007 ± .0038
TC2	030629	.0002 ± .0011	.0010 ± .0010	.0082 ± .0005	.0054 ± .0005	.0000 ± .0037
TM1	021002	.0009 ± .0029	.0042 ± .0004	.0128 ± .0005	.2958 ± .0017	.0000 ± .0038
TM1	021008	.0019 ± .0072	.0057 ± .0004	.0047 ± .0004	.2778 ± .0016	.0000 ± .0036
TM1	021014	.0005 ± .0012	.0012 ± .0003	.0000 ± .0011	.0194 ± .0006	.0000 ± .0033
TM1	021020	.0008 ± .0011	.0025 ± .0003	.0016 ± .0004	.0168 ± .0005	.0000 ± .0033
TM1	021026	.0013 ± .0034	.0073 ± .0004	.0042 ± .0005	.4250 ± .0020	.0000 ± .0040
TM1	021201	.0016 ± .0023	.0021 ± .0003	.0097 ± .0005	.2282 ± .0015	.0000 ± .0033
TM1	021207	.0006 ± .0010	.0057 ± .0004	.0017 ± .0003	.0193 ± .0005	.0016 ± .0030
TM1	021213	.0006 ± .0029	.0050 ± .0004	.0090 ± .0005	.2623 ± .0016	.0000 ± .0037
TM1	021219	.0014 ± .0025	.0058 ± .0004	.0077 ± .0004	.1265 ± .0011	.0000 ± .0033
TM1	021225	.0010 ± .0028	.0047 ± .0004	.0039 ± .0004	.2990 ± .0017	.0027 ± .0034
TM1	030301	.0005 ± .0019	.0107 ± .0005	.0069 ± .0005	.0571 ± .0009	.0000 ± .0040
TM1	030307	.0013 ± .0035	.0016 ± .0004	.0035 ± .0005	.3862 ± .0022	.0014 ± .0045
TM1	030313	.0007 ± .0022	.0064 ± .0005	.0033 ± .0005	.1236 ± .0013	.0000 ± .0041
TM1	030319	.0004 ± .0029	.0112 ± .0005	.0066 ± .0005	.2752 ± .0019	.0030 ± .0041
TM1	030325	.0006 ± .0039	.0078 ± .0005	.0160 ± .0006	.3810 ± .0022	.0000 ± .0047
TM1	030605	.0019 ± .0029	.0045 ± .0004	.0062 ± .0005	.1205 ± .0012	.0000 ± .0039
TM1	030611	.0010 ± .0023	.0016 ± .0004	.0014 ± .0004	.0162 ± .0006	.0000 ± .0039
TM1	030617	.0008 ± .0034	.0060 ± .0005	.0064 ± .0006	.2617 ± .0018	.0000 ± .0043
TM1	030623	.0004 ± .0011	.0025 ± .0004	.0009 ± .0012	.0022 ± .0004	.0004 ± .0040
TM1	030629	.0003 ± .0011	.0015 ± .0004	.0017 ± .0004	.0014 ± .0005	.0023 ± .0037
ZS7	021008	.0053 ± .0128	.0322 ± .0006	.0279 ± .0006	.5330 ± .0020	.0000 ± .0057
ZS7	021014	.0027 ± .0049	.0342 ± .0006	.0110 ± .0004	.2071 ± .0013	.0000 ± .0031
ZS7	021020	.0007 ± .0016	.0054 ± .0003	.0043 ± .0003	.0478 ± .0006	.0000 ± .0025
ZS7	021026	.0011 ± .0025	.0047 ± .0003	.0061 ± .0004	.1443 ± .0011	.0000 ± .0027
ZS7	021201	.0012 ± .0048	.0319 ± .0006	.0390 ± .0007	.8571 ± .0025	.0000 ± .0036
ZS7	021207	.0012 ± .0022	.0191 ± .0005	.0128 ± .0004	.2224 ± .0013	.0000 ± .0029
ZS7	021213	.0033 ± .0060	.0172 ± .0005	.0241 ± .0006	.4981 ± .0019	.0000 ± .0048
ZS7	021219	.0025 ± .0075	.0211 ± .0005	.0394 ± .0007	1.0221 ± .0027	.0000 ± .0043
ZS7	021225	.0025 ± .0059	.0192 ± .0005	.0281 ± .0006	.5911 ± .0020	.0000 ± .0049
ZS7	030301	.0073 ± .0086	.1125 ± .0011	.0192 ± .0006	.1488 ± .0011	.0004 ± .0028
ZS7	030307	.0015 ± .0046	.0166 ± .0005	.0491 ± .0007	.3023 ± .0015	.0032 ± .0036
ZS7	030313	.0026 ± .0053	.0292 ± .0006	.0180 ± .0005	.2771 ± .0015	.0000 ± .0029
ZS7	030319	.0045 ± .0054	.0375 ± .0007	.0452 ± .0007	.4472 ± .0018	.0028 ± .0042
ZS7	030325	.0018 ± .0048	.0236 ± .0006	.0194 ± .0005	.3744 ± .0017	.0000 ± .0035
ZS7	030605	.0019 ± .0036	.0231 ± .0005	.0096 ± .0004	.1486 ± .0011	.0000 ± .0029
ZS7	030611	.0009 ± .0027	.0044 ± .0003	.0031 ± .0003	.0417 ± .0006	.0000 ± .0027
ZS7	030617	.0023 ± .0039	.0166 ± .0005	.0169 ± .0005	.4574 ± .0018	.0000 ± .0030
ZS7	030623	.0004 ± .0012	.0039 ± .0003	.0030 ± .0003	.0312 ± .0005	.0000 ± .0024
ZS7	030629	.0009 ± .0013	.0107 ± .0004	.0024 ± .0003	.0072 ± .0004	.0000 ± .0025

Site	Date	Arsenic	Selenium	Bromine	Rubidium	Strontium
CH6	021002	.0065 ± .0267	.0011 ± .0003	.0021 ± .0023	.0110 ± .0004	.0050 ± .0004
CH6	021008	.0050 ± .0145	.0022 ± .0004	.0170 ± .0007	.0063 ± .0005	.0018 ± .0005
CH6	021014	.0305 ± .0436	.0037 ± .0004	.0196 ± .0014	.0197 ± .0006	.0003 ± .0012
CH6	021020	.0091 ± .0268	.0056 ± .0004	.0039 ± .0008	.0148 ± .0004	.0022 ± .0004
CH6	021026	.0123 ± .0235	.0029 ± .0003	.0617 ± .0010	.0110 ± .0009	.0006 ± .0011
CH6	021201	.0106 ± .0155	.0027 ± .0003	.0953 ± .0010	.0076 ± .0012	.0005 ± .0010
CH6	021207	.0130 ± .0283	.0035 ± .0004	.0213 ± .0009	.0161 ± .0005	.0010 ± .0011
CH6	021213	.0114 ± .0210	.0032 ± .0003	.0288 ± .0008	.0104 ± .0005	.0009 ± .0011
CH6	021219	.0171 ± .0390	.0055 ± .0004	.0699 ± .0014	.0163 ± .0010	.0004 ± .0011
CH6	021225	.0053 ± .0158	.0014 ± .0003	.0644 ± .0009	.0043 ± .0009	.0003 ± .0011
CH6	030301	.0119 ± .0481	.0060 ± .0004	.0155 ± .0013	.0195 ± .0006	.0046 ± .0004
CH6	030307	.0045 ± .0167	.0020 ± .0004	.0478 ± .0010	.0044 ± .0008	.0006 ± .0014
CH6	030313	.0360 ± .0791	.0061 ± .0006	.2502 ± .0027	.0361 ± .0032	.0022 ± .0005
CH6	030319	.0051 ± .0165	.0010 ± .0011	.0654 ± .0010	.0035 ± .0009	.0003 ± .0013
CH6	030325	.0082 ± .0386	.0023 ± .0004	.0396 ± .0012	.0160 ± .0007	.0000 ± .0012
CH6	030605	.0125 ± .0327	.0082 ± .0005	.0123 ± .0010	.0323 ± .0006	.0039 ± .0004
CH6	030611	.0139 ± .0205	.0069 ± .0004	.0000 ± .0019	.0165 ± .0005	.0012 ± .0004
CH6	030617	.0090 ± .0157	.0019 ± .0004	.0115 ± .0006	.0072 ± .0005	.0005 ± .0013
CH6	030623	.0010 ± .0126	.0016 ± .0003	.0072 ± .0005	.0099 ± .0004	.0014 ± .0004
CH6	030629	.0025 ± .0098	.0014 ± .0003	.0043 ± .0005	.0098 ± .0004	.0013 ± .0004
CW3	021002	.0043 ± .0164	.0020 ± .0004	.0057 ± .0006	.0072 ± .0005	.0131 ± .0006
CW3	021008	.0042 ± .0146	.0016 ± .0004	.0046 ± .0006	.0063 ± .0005	.0021 ± .0005
CW3	021014	.0002 ± .0033	.0009 ± .0011	.0091 ± .0004	.0006 ± .0013	.0008 ± .0014
CW3	021020	.0032 ± .0010	.0003 ± .0011	.0010 ± .0010	.0016 ± .0004	.0000 ± .0016
CW3	021026	.0067 ± .0159	.0015 ± .0004	.0040 ± .0006	.0078 ± .0005	.0000 ± .0017
CW3	021201	.0066 ± .0125	.0047 ± .0004	.0151 ± .0006	.0039 ± .0005	.0013 ± .0015
CW3	021207	.0002 ± .0034	.0005 ± .0012	.0058 ± .0004	.0013 ± .0013	.0008 ± .0017
CW3	021213	.0105 ± .0184	.0029 ± .0004	.0036 ± .0007	.0090 ± .0005	.0010 ± .0015
CW3	021219	.0011 ± .0108	.0033 ± .0004	.0118 ± .0006	.0040 ± .0005	.0017 ± .0005
CW3	021225	.0073 ± .0143	.0027 ± .0004	.0032 ± .0005	.0077 ± .0005	.0000 ± .0014
CW3	030301	.0000 ± .0060	.0017 ± .0005	.0106 ± .0006	.0010 ± .0016	.0025 ± .0006
CW3	030307	.0053 ± .0140	.0002 ± .0015	.0032 ± .0006	.0055 ± .0006	.0002 ± .0019
CW3	030313	.0000 ± .0064	.0013 ± .0014	.0163 ± .0006	.0009 ± .0017	.0018 ± .0018
CW3	030319	.0033 ± .0076	.0021 ± .0005	.0087 ± .0006	.0016 ± .0017	.0004 ± .0019
CW3	030325	.0078 ± .0235	.0043 ± .0005	.0073 ± .0008	.0066 ± .0006	.0020 ± .0006
CW3	030605	.0001 ± .0097	.0030 ± .0005	.0113 ± .0006	.0031 ± .0006	.0011 ± .0018
CW3	030611	.0002 ± .0031	.0007 ± .0012	.0041 ± .0004	.0001 ± .0014	.0019 ± .0005
CW3	030617	.0059 ± .0130	.0031 ± .0005	.0065 ± .0007	.0045 ± .0005	.0022 ± .0006
CW3	030623	.0004 ± .0031	.0007 ± .0014	.0034 ± .0004	.0008 ± .0016	.0000 ± .0018
CW3	030629	.0000 ± .0033	.0008 ± .0014	.0013 ± .0004	.0006 ± .0016	.0008 ± .0019
GZ5	021002	.0438 ± .0111	.0106 ± .0006	.0172 ± .0013	.0148 ± .0006	.0005 ± .0017
GZ5	021008	.0335 ± .0071	.0093 ± .0005	.0211 ± .0010	.0099 ± .0006	.0017 ± .0017
GZ5	021014	.0268 ± .0691	.0151 ± .0007	.0206 ± .0020	.0370 ± .0008	.0052 ± .0006
GZ5	021020	.0316 ± .0412	.0074 ± .0005	.0060 ± .0013	.0113 ± .0005	.0025 ± .0005
GZ5	021026	.0366 ± .0089	.0068 ± .0005	.0296 ± .0012	.0100 ± .0007	.0000 ± .0016
GZ5	021201	.0617 ± .0779	.0096 ± .0006	.0573 ± .0025	.0212 ± .0010	.0024 ± .0005

Site	Date	Arsenic	Selenium	Bromine	Rubidium	Strontium
GZ5	021207	.0372 ± .0580	.0070 ± .0006	.0189 ± .0018	.0254 ± .0007	.0053 ± .0006
GZ5	021213	.0183 ± .0289	.0054 ± .0005	.0154 ± .0010	.0150 ± .0006	.0021 ± .0005
GZ5	021219	.0422 ± .0557	.0115 ± .0006	.0348 ± .0018	.0162 ± .0008	.0017 ± .0017
GZ5	021225	.0158 ± .0274	.0034 ± .0004	.0498 ± .0011	.0082 ± .0008	.0000 ± .0015
GZ5	030301	.0172 ± .0434	.0086 ± .0007	.0195 ± .0014	.0092 ± .0007	.0044 ± .0007
GZ5	030307	.0333 ± .0109	.0055 ± .0006	.0069 ± .0012	.0118 ± .0007	.0000 ± .0019
GZ5	030313	.0553 ± .0675	.0102 ± .0008	.0881 ± .0023	.0288 ± .0015	.0028 ± .0007
GZ5	030319	.0193 ± .0197	.0037 ± .0005	.1071 ± .0015	.0045 ± .0015	.0000 ± .0018
GZ5	030325	.0345 ± .0638	.0138 ± .0008	.0146 ± .0019	.0231 ± .0008	.0023 ± .0007
GZ5	030605	.0110 ± .0250	.0084 ± .0006	.0115 ± .0009	.0080 ± .0006	.0038 ± .0006
GZ5	030611	.0427 ± .0521	.0285 ± .0008	.0176 ± .0017	.0162 ± .0007	.0064 ± .0006
GZ5	030617	.0618 ± .0767	.0494 ± .0011	.0100 ± .0023	.0343 ± .0010	.0043 ± .0008
GZ5	030623	.0344 ± .0561	.0083 ± .0007	.0196 ± .0018	.0175 ± .0008	.0025 ± .0007
GZ5	030629	.0244 ± .0338	.0053 ± .0005	.0013 ± .0033	.0029 ± .0005	.0015 ± .0017
SZ4	021002	.0128 ± .0251	.0041 ± .0005	.0227 ± .0009	.0104 ± .0006	.0012 ± .0016
SZ4	021008	.0140 ± .0287	.0054 ± .0005	.0393 ± .0011	.0115 ± .0007	.0023 ± .0005
SZ4	021014	.0036 ± .0055	.0012 ± .0004	.0095 ± .0005	.0016 ± .0004	.0009 ± .0016
SZ4	021020	.0000 ± .0037	.0015 ± .0004	.0019 ± .0003	.0031 ± .0004	.0015 ± .0005
SZ4	021026	.0119 ± .0223	.0030 ± .0005	.0084 ± .0008	.0106 ± .0006	.0007 ± .0018
SZ4	021201	.0040 ± .0112	.0039 ± .0004	.0120 ± .0006	.0035 ± .0004	.0009 ± .0014
SZ4	021207	.0024 ± .0076	.0008 ± .0011	.0066 ± .0005	.0034 ± .0004	.0011 ± .0015
SZ4	021213	.0146 ± .0376	.0063 ± .0014	.0104 ± .0016	.0137 ± .0016	.0003 ± .0049
SZ4	021221	.0183 ± .0546	.0078 ± .0014	.0644 ± .0025	.0191 ± .0019	.0008 ± .0051
SZ4	021225	.0113 ± .0208	.0017 ± .0004	.0090 ± .0008	.0094 ± .0005	.0002 ± .0016
SZ4	030102	.0197 ± .0307	.0070 ± .0005	.0652 ± .0013	.0129 ± .0010	.0026 ± .0005
SZ4	030301	.0007 ± .0099	.0028 ± .0005	.0192 ± .0007	.0020 ± .0006	.0016 ± .0018
SZ4	030307	.0134 ± .0269	.0034 ± .0005	.0059 ± .0009	.0106 ± .0006	.0000 ± .0017
SZ4	030313	.0040 ± .0120	.0018 ± .0005	.0210 ± .0008	.0028 ± .0006	.0029 ± .0006
SZ4	030319	.0073 ± .0200	.0022 ± .0005	.0248 ± .0009	.0069 ± .0007	.0005 ± .0018
SZ4	030325	.0112 ± .0280	.0053 ± .0006	.0168 ± .0010	.0076 ± .0007	.0003 ± .0020
SZ4	030605	.0052 ± .0094	.0028 ± .0005	.0116 ± .0007	.0053 ± .0006	.0026 ± .0006
SZ4	030611	.0024 ± .0063	.0005 ± .0013	.0090 ± .0005	.0022 ± .0005	.0012 ± .0018
SZ4	030617	.0070 ± .0147	.0036 ± .0005	.0087 ± .0007	.0067 ± .0006	.0014 ± .0019
SZ4	030623	.0015 ± .0034	.0000 ± .0013	.0025 ± .0004	.0010 ± .0015	.0004 ± .0018
SZ4	030629	.0000 ± .0032	.0001 ± .0013	.0017 ± .0004	.0007 ± .0015	.0011 ± .0018
TC2	021002	.0054 ± .0174	.0031 ± .0004	.0103 ± .0007	.0071 ± .0005	.0007 ± .0015
TC2	021008	.0077 ± .0150	.0029 ± .0004	.0050 ± .0006	.0087 ± .0005	.0022 ± .0005
TC2	021014	.0016 ± .0046	.0006 ± .0011	.0085 ± .0005	.0033 ± .0005	.0005 ± .0016
TC2	021020	.0000 ± .0027	.0007 ± .0010	.0009 ± .0003	.0011 ± .0011	.0002 ± .0014
TC2	021026	.0067 ± .0171	.0022 ± .0004	.0043 ± .0007	.0077 ± .0005	.0003 ± .0015
TC2	021201	.0034 ± .0110	.0033 ± .0004	.0133 ± .0006	.0035 ± .0004	.0011 ± .0013
TC2	021207	.0018 ± .0025	.0000 ± .0010	.0034 ± .0003	.0002 ± .0012	.0000 ± .0014
TC2	021213	.0112 ± .0184	.0024 ± .0004	.0034 ± .0007	.0090 ± .0005	.0000 ± .0016
TC2	021219	.0019 ± .0072	.0016 ± .0004	.0091 ± .0005	.0028 ± .0005	.0002 ± .0016
TC2	021225	.0067 ± .0201	.0024 ± .0004	.0035 ± .0007	.0093 ± .0005	.0004 ± .0014
TC2	030301	.0007 ± .0050	.0006 ± .0014	.0077 ± .0005	.0010 ± .0017	.0015 ± .0019
TC2	030307	.0080 ± .0257	.0030 ± .0005	.0037 ± .0009	.0072 ± .0006	.0003 ± .0019
TC2	030313	.0000 ± .0055	.0001 ± .0015	.0128 ± .0006	.0000 ± .0018	.0015 ± .0021
TC2	030319	.0005 ± .0105	.0014 ± .0014	.0071 ± .0006	.0017 ± .0017	.0000 ± .0018

Site	Date	Arsenic	Selenium	Bromine	Rubidium	Strontium
TC2	030325	.0067 ± .0181	.0022 ± .0005	.0067 ± .0007	.0050 ± .0006	.0003 ± .0019
TC2	030605	.0060 ± .0105	.0024 ± .0005	.0089 ± .0006	.0055 ± .0006	.0010 ± .0020
TC2	030611	.0009 ± .0034	.0004 ± .0014	.0024 ± .0004	.0015 ± .0017	.0000 ± .0019
TC2	030617	.0055 ± .0133	.0046 ± .0005	.0055 ± .0007	.0060 ± .0006	.0016 ± .0018
TC2	030623	.0000 ± .0030	.0001 ± .0012	.0017 ± .0004	.0001 ± .0014	.0004 ± .0017
TC2	030629	.0013 ± .0030	.0004 ± .0013	.0013 ± .0004	.0000 ± .0015	.0009 ± .0017
TM1	021002	.0084 ± .0185	.0024 ± .0004	.0038 ± .0007	.0090 ± .0005	.0000 ± .0016
TM1	021008	.0041 ± .0169	.0030 ± .0004	.0052 ± .0006	.0079 ± .0005	.0027 ± .0005
TM1	021014	.0017 ± .0030	.0005 ± .0011	.0072 ± .0004	.0005 ± .0013	.0009 ± .0016
TM1	021020	.0027 ± .0029	.0004 ± .0011	.0008 ± .0010	.0010 ± .0012	.0000 ± .0015
TM1	021026	.0065 ± .0187	.0019 ± .0005	.0043 ± .0007	.0091 ± .0005	.0000 ± .0018
TM1	021201	.0026 ± .0127	.0036 ± .0004	.0132 ± .0006	.0044 ± .0004	.0019 ± .0005
TM1	021207	.0000 ± .0039	.0012 ± .0003	.0028 ± .0003	.0011 ± .0004	.0004 ± .0013
TM1	021213	.0088 ± .0198	.0031 ± .0004	.0040 ± .0007	.0096 ± .0005	.0020 ± .0005
TM1	021219	.0068 ± .0121	.0034 ± .0004	.0105 ± .0006	.0037 ± .0004	.0014 ± .0015
TM1	021225	.0056 ± .0161	.0021 ± .0004	.0026 ± .0006	.0097 ± .0005	.0001 ± .0013
TM1	030301	.0007 ± .0057	.0014 ± .0005	.0077 ± .0005	.0020 ± .0006	.0011 ± .0018
TM1	030307	.0076 ± .0146	.0021 ± .0005	.0024 ± .0007	.0053 ± .0006	.0000 ± .0019
TM1	030313	.0023 ± .0065	.0018 ± .0005	.0147 ± .0006	.0010 ± .0018	.0009 ± .0019
TM1	030319	.0033 ± .0120	.0029 ± .0005	.0154 ± .0007	.0042 ± .0006	.0010 ± .0018
TM1	030325	.0123 ± .0309	.0055 ± .0005	.0068 ± .0010	.0084 ± .0006	.0013 ± .0017
TM1	030605	.0044 ± .0084	.0016 ± .0005	.0118 ± .0006	.0031 ± .0005	.0014 ± .0017
TM1	030611	.0007 ± .0032	.0000 ± .0013	.0029 ± .0005	.0014 ± .0016	.0000 ± .0018
TM1	030617	.0038 ± .0132	.0033 ± .0005	.0069 ± .0006	.0069 ± .0006	.0025 ± .0007
TM1	030623	.0000 ± .0031	.0001 ± .0013	.0023 ± .0004	.0000 ± .0016	.0000 ± .0018
TM1	030629	.0000 ± .0030	.0000 ± .0012	.0008 ± .0011	.0002 ± .0014	.0006 ± .0017
ZS7	021008	.0182 ± .0645	.0112 ± .0006	.0224 ± .0018	.0413 ± .0007	.0064 ± .0005
ZS7	021014	.0069 ± .0161	.0041 ± .0004	.0150 ± .0006	.0083 ± .0005	.0019 ± .0005
ZS7	021020	.0008 ± .0035	.0013 ± .0003	.0022 ± .0003	.0018 ± .0003	.0012 ± .0004
ZS7	021026	.0040 ± .0099	.0047 ± .0004	.0111 ± .0005	.0040 ± .0004	.0019 ± .0004
ZS7	021201	.0200 ± .0302	.0139 ± .0005	.0385 ± .0011	.0077 ± .0006	.0008 ± .0011
ZS7	021207	.0091 ± .0188	.0080 ± .0004	.0108 ± .0007	.0050 ± .0004	.0004 ± .0011
ZS7	021213	.0261 ± .0507	.0116 ± .0005	.0217 ± .0015	.0280 ± .0007	.0027 ± .0005
ZS7	021219	.0225 ± .0387	.0128 ± .0005	.0338 ± .0013	.0132 ± .0006	.0028 ± .0004
ZS7	021225	.0214 ± .0532	.0072 ± .0005	.0586 ± .0017	.0197 ± .0009	.0019 ± .0004
ZS7	030301	.0074 ± .0025	.0020 ± .0003	.0142 ± .0005	.0030 ± .0004	.0021 ± .0004
ZS7	030307	.0146 ± .0340	.0063 ± .0004	.0555 ± .0012	.0079 ± .0008	.0022 ± .0004
ZS7	030313	.0046 ± .0121	.0031 ± .0004	.0246 ± .0007	.0036 ± .0005	.0019 ± .0004
ZS7	030319	.0148 ± .0438	.0064 ± .0005	.0589 ± .0014	.0135 ± .0009	.0019 ± .0004
ZS7	030325	.0089 ± .0265	.0043 ± .0004	.0221 ± .0009	.0101 ± .0006	.0011 ± .0014
ZS7	030605	.0003 ± .0084	.0026 ± .0004	.0081 ± .0005	.0042 ± .0004	.0020 ± .0004
ZS7	030611	.0004 ± .0037	.0010 ± .0003	.0029 ± .0004	.0012 ± .0003	.0010 ± .0012
ZS7	030617	.0083 ± .0199	.0231 ± .0006	.0062 ± .0007	.0068 ± .0004	.0015 ± .0004
ZS7	030623	.0000 ± .0025	.0007 ± .0008	.0020 ± .0003	.0005 ± .0009	.0003 ± .0010
ZS7	030629	.0004 ± .0022	.0000 ± .0009	.0021 ± .0003	.0006 ± .0011	.0000 ± .0012

Site	Date	Yttrium	Zirconium	Molybdenum	Palladium	Silver
CH6	021002	.0000 ± .0020	.0000 ± .0015	.0000 ± .0026	.0000 ± .0026	.0440 ± .0019
CH6	021008	.0000 ± .0019	.0034 ± .0007	.0000 ± .0035	.0022 ± .0033	.0827 ± .0029
CH6	021014	.0000 ± .0029	.0010 ± .0017	.0000 ± .0030	.0011 ± .0029	.0390 ± .0019
CH6	021020	.0000 ± .0020	.0017 ± .0005	.0017 ± .0026	.0004 ± .0026	.0409 ± .0019
CH6	021026	.0000 ± .0019	.0003 ± .0015	.0015 ± .0026	.0010 ± .0028	.0930 ± .0026
CH6	021201	.0003 ± .0016	.0000 ± .0013	.0011 ± .0024	.0000 ± .0025	.0561 ± .0021
CH6	021207	.0000 ± .0021	.0005 ± .0015	.0000 ± .0027	.0012 ± .0028	.1457 ± .0031
CH6	021213	.0000 ± .0018	.0007 ± .0015	.0007 ± .0026	.0019 ± .0026	.0425 ± .0019
CH6	021219	.0000 ± .0026	.0023 ± .0005	.0010 ± .0027	.0000 ± .0026	.0962 ± .0026
CH6	021225	.0004 ± .0016	.0004 ± .0015	.0007 ± .0027	.0000 ± .0027	.0803 ± .0024
CH6	030301	.0000 ± .0028	.0076 ± .0005	.0042 ± .0009	.0000 ± .0026	.1008 ± .0028
CH6	030307	.0003 ± .0019	.0001 ± .0020	.0045 ± .0012	.0000 ± .0035	.1247 ± .0036
CH6	030313	.0000 ± .0047	.0023 ± .0007	.0025 ± .0035	.0024 ± .0034	.0853 ± .0030
CH6	030319	.0000 ± .0018	.0003 ± .0018	.0017 ± .0032	.0020 ± .0034	.0446 ± .0023
CH6	030325	.0000 ± .0025	.0000 ± .0017	.0035 ± .0010	.0000 ± .0028	.1844 ± .0036
CH6	030605	.0000 ± .0026	.0024 ± .0006	.0033 ± .0010	.0000 ± .0031	.1387 ± .0031
CH6	030611	.0000 ± .0018	.0022 ± .0005	.0016 ± .0025	.0011 ± .0025	.0466 ± .0020
CH6	030617	.0001 ± .0017	.0000 ± .0018	.0033 ± .0010	.0016 ± .0027	.1006 ± .0027
CH6	030623	.0015 ± .0016	.0001 ± .0016	.0017 ± .0027	.0000 ± .0025	.0993 ± .0027
CH6	030629	.0003 ± .0016	.0003 ± .0017	.0000 ± .0029	.0000 ± .0028	.0455 ± .0020
CW3	021002	.0010 ± .0020	.0007 ± .0021	.0011 ± .0036	.0000 ± .0036	.0009 ± .0047
CW3	021008	.0001 ± .0021	.0017 ± .0023	.0000 ± .0039	.0004 ± .0034	.0000 ± .0049
CW3	021014	.0002 ± .0017	.0005 ± .0020	.0013 ± .0035	.0000 ± .0033	.0023 ± .0047
CW3	021020	.0000 ± .0019	.0001 ± .0022	.0000 ± .0039	.0018 ± .0037	.0000 ± .0046
CW3	021026	.0000 ± .0023	.0003 ± .0024	.0000 ± .0042	.0000 ± .0041	.0000 ± .0050
CW3	021201	.0000 ± .0019	.0000 ± .0021	.0000 ± .0037	.0000 ± .0035	.0000 ± .0047
CW3	021207	.0000 ± .0019	.0006 ± .0023	.0000 ± .0040	.0000 ± .0043	.0000 ± .0051
CW3	021213	.0003 ± .0020	.0001 ± .0020	.0001 ± .0035	.0001 ± .0035	.0000 ± .0047
CW3	021219	.0000 ± .0019	.0013 ± .0021	.0000 ± .0036	.0000 ± .0036	.0000 ± .0046
CW3	021225	.0006 ± .0019	.0011 ± .0020	.0000 ± .0035	.0015 ± .0035	.0012 ± .0043
CW3	030301	.0005 ± .0021	.0006 ± .0024	.0008 ± .0042	.0001 ± .0044	.0008 ± .0052
CW3	030307	.0000 ± .0024	.0006 ± .0028	.0000 ± .0047	.0000 ± .0041	.0022 ± .0058
CW3	030313	.0003 ± .0022	.0014 ± .0026	.0000 ± .0044	.0000 ± .0046	.0016 ± .0055
CW3	030319	.0000 ± .0023	.0014 ± .0027	.0000 ± .0047	.0000 ± .0046	.0000 ± .0058
CW3	030325	.0000 ± .0025	.0006 ± .0026	.0008 ± .0044	.0016 ± .0044	.0000 ± .0056
CW3	030605	.0010 ± .0022	.0014 ± .0026	.0031 ± .0044	.0037 ± .0046	.0038 ± .0056
CW3	030611	.0002 ± .0018	.0012 ± .0022	.0033 ± .0038	.0000 ± .0039	.0027 ± .0057
CW3	030617	.0002 ± .0021	.0019 ± .0023	.0018 ± .0040	.0000 ± .0039	.0000 ± .0050
CW3	030623	.0000 ± .0022	.0000 ± .0026	.0029 ± .0045	.0000 ± .0045	.0000 ± .0055
CW3	030629	.0007 ± .0022	.0000 ± .0027	.0000 ± .0046	.0009 ± .0044	.0054 ± .0056
GZ5	021002	.0000 ± .0028	.0012 ± .0024	.0000 ± .0042	.0018 ± .0036	.0001 ± .0049
GZ5	021008	.0000 ± .0023	.0013 ± .0023	.0000 ± .0040	.0007 ± .0038	.0008 ± .0047
GZ5	021014	.0000 ± .0044	.0045 ± .0008	.0000 ± .0039	.0000 ± .0035	.0030 ± .0047
GZ5	021020	.0000 ± .0028	.0011 ± .0020	.0011 ± .0035	.0008 ± .0033	.0007 ± .0045
GZ5	021026	.0002 ± .0025	.0000 ± .0022	.0000 ± .0039	.0004 ± .0040	.0000 ± .0049
GZ5	021201	.0000 ± .0046	.0019 ± .0021	.0023 ± .0036	.0000 ± .0035	.0020 ± .0048

Site	Date	Yttrium	Zirconium	Molybdenum	Palladium	Silver
GZ5	021207	.0002 ± .0037	.0031 ± .0007	.0004 ± .0037	.0006 ± .0037	.0008 ± .0049
GZ5	021213	.0000 ± .0024	.0004 ± .0020	.0000 ± .0035	.0000 ± .0034	.0000 ± .0047
GZ5	021219	.0000 ± .0036	.0027 ± .0008	.0000 ± .0039	.0015 ± .0036	.0020 ± .0045
GZ5	021225	.0002 ± .0023	.0011 ± .0021	.0000 ± .0036	.0001 ± .0034	.0000 ± .0047
GZ5	030301	.0000 ± .0032	.0043 ± .0009	.0004 ± .0046	.0000 ± .0048	.0002 ± .0059
GZ5	030307	.0000 ± .0029	.0006 ± .0028	.0000 ± .0047	.0000 ± .0045	.0020 ± .0060
GZ5	030313	.0011 ± .0045	.0011 ± .0030	.0000 ± .0052	.0000 ± .0046	.0009 ± .0062
GZ5	030319	.0001 ± .0025	.0000 ± .0026	.0000 ± .0045	.0000 ± .0043	.0020 ± .0055
GZ5	030325	.0000 ± .0040	.0029 ± .0009	.0000 ± .0046	.0000 ± .0045	.0088 ± .0021
GZ5	030605	.0000 ± .0025	.0022 ± .0025	.0020 ± .0043	.0000 ± .0046	.0000 ± .0056
GZ5	030611	.0012 ± .0034	.0070 ± .0008	.0051 ± .0014	.0025 ± .0042	.0023 ± .0049
GZ5	030617	.0000 ± .0048	.0068 ± .0011	.0000 ± .0053	.0000 ± .0046	.0035 ± .0061
GZ5	030623	.0012 ± .0038	.0069 ± .0010	.0000 ± .0048	.0000 ± .0045	.0014 ± .0062
GZ5	030629	.0008 ± .0026	.0028 ± .0008	.0037 ± .0041	.0000 ± .0040	.0012 ± .0052
SZ4	021002	.0000 ± .0023	.0008 ± .0022	.0000 ± .0038	.0012 ± .0036	.0000 ± .0044
SZ4	021008	.0000 ± .0025	.0015 ± .0021	.0000 ± .0037	.0000 ± .0036	.0028 ± .0047
SZ4	021014	.0000 ± .0019	.0000 ± .0022	.0000 ± .0038	.0009 ± .0034	.0005 ± .0046
SZ4	021020	.0002 ± .0017	.0008 ± .0020	.0000 ± .0036	.0002 ± .0036	.0024 ± .0047
SZ4	021026	.0000 ± .0025	.0005 ± .0025	.0000 ± .0043	.0014 ± .0038	.0000 ± .0047
SZ4	021201	.0000 ± .0017	.0000 ± .0019	.0000 ± .0033	.0031 ± .0033	.0000 ± .0042
SZ4	021207	.0000 ± .0018	.0012 ± .0021	.0000 ± .0036	.0006 ± .0036	.0022 ± .0048
SZ4	021213	.0020 ± .0063	.0028 ± .0070	.0076 ± .0122	.0000 ± .0117	.0135 ± .0158
SZ4	021221	.0000 ± .0069	.0070 ± .0074	.0059 ± .0127	.0000 ± .0125	.0124 ± .0158
SZ4	021225	.0000 ± .0022	.0003 ± .0022	.0000 ± .0038	.0000 ± .0037	.0002 ± .0045
SZ4	030102	.0014 ± .0026	.0000 ± .0021	.0000 ± .0037	.0008 ± .0037	.0013 ± .0049
SZ4	030301	.0011 ± .0022	.0006 ± .0025	.0028 ± .0043	.0000 ± .0045	.0000 ± .0057
SZ4	030307	.0013 ± .0026	.0005 ± .0024	.0024 ± .0042	.0000 ± .0040	.0023 ± .0058
SZ4	030313	.0000 ± .0023	.0000 ± .0026	.0009 ± .0045	.0010 ± .0045	.0038 ± .0056
SZ4	030319	.0002 ± .0024	.0018 ± .0025	.0028 ± .0044	.0000 ± .0048	.0000 ± .0061
SZ4	030325	.0000 ± .0028	.0023 ± .0028	.0005 ± .0048	.0000 ± .0045	.0005 ± .0064
SZ4	030605	.0006 ± .0023	.0006 ± .0026	.0026 ± .0045	.0000 ± .0042	.0029 ± .0054
SZ4	030611	.0012 ± .0021	.0011 ± .0025	.0023 ± .0043	.0026 ± .0041	.0039 ± .0051
SZ4	030617	.0000 ± .0024	.0000 ± .0027	.0000 ± .0046	.0000 ± .0043	.0099 ± .0019
SZ4	030623	.0004 ± .0021	.0010 ± .0025	.0007 ± .0044	.0037 ± .0043	.0033 ± .0053
SZ4	030629	.0000 ± .0021	.0009 ± .0025	.0031 ± .0043	.0000 ± .0044	.0013 ± .0056
TC2	021002	.0000 ± .0020	.0013 ± .0020	.0002 ± .0036	.0000 ± .0035	.0031 ± .0046
TC2	021008	.0000 ± .0020	.0012 ± .0021	.0000 ± .0037	.0000 ± .0035	.0000 ± .0045
TC2	021014	.0000 ± .0019	.0000 ± .0022	.0000 ± .0038	.0000 ± .0036	.0007 ± .0047
TC2	021020	.0003 ± .0017	.0008 ± .0020	.0000 ± .0034	.0001 ± .0031	.0024 ± .0044
TC2	021026	.0000 ± .0020	.0000 ± .0020	.0000 ± .0036	.0000 ± .0034	.0015 ± .0046
TC2	021201	.0000 ± .0017	.0000 ± .0018	.0002 ± .0032	.0000 ± .0034	.0000 ± .0044
TC2	021207	.0000 ± .0017	.0000 ± .0020	.0000 ± .0036	.0000 ± .0032	.0001 ± .0042
TC2	021213	.0000 ± .0022	.0012 ± .0022	.0000 ± .0038	.0018 ± .0038	.0000 ± .0048
TC2	021219	.0000 ± .0020	.0000 ± .0023	.0000 ± .0040	.0000 ± .0039	.0000 ± .0049
TC2	021225	.0004 ± .0021	.0008 ± .0020	.0014 ± .0035	.0000 ± .0033	.0053 ± .0014
TC2	030301	.0001 ± .0023	.0012 ± .0027	.0000 ± .0046	.0004 ± .0042	.0045 ± .0055
TC2	030307	.0002 ± .0026	.0023 ± .0027	.0018 ± .0046	.0011 ± .0043	.0010 ± .0060
TC2	030313	.0000 ± .0024	.0000 ± .0029	.0000 ± .0050	.0000 ± .0045	.0022 ± .0057
TC2	030319	.0016 ± .0023	.0020 ± .0026	.0027 ± .0045	.0034 ± .0048	.0012 ± .0056

Site	Date	Yttrium	Zirconium	Molybdenum	Palladium	Silver
TC2	030325	.0000 ± .0025	.0011 ± .0027	.0000 ± .0047	.0000 ± .0045	.0000 ± .0057
TC2	030605	.0001 ± .0024	.0010 ± .0028	.0000 ± .0048	.0014 ± .0046	.0021 ± .0055
TC2	030611	.0009 ± .0023	.0014 ± .0028	.0000 ± .0048	.0023 ± .0043	.0037 ± .0052
TC2	030617	.0000 ± .0022	.0006 ± .0024	.0025 ± .0042	.0013 ± .0038	.0000 ± .0054
TC2	030623	.0006 ± .0020	.0009 ± .0024	.0001 ± .0042	.0018 ± .0041	.0050 ± .0053
TC2	030629	.0010 ± .0020	.0007 ± .0024	.0000 ± .0042	.0000 ± .0043	.0000 ± .0056
TM1	021002	.0000 ± .0022	.0005 ± .0022	.0005 ± .0040	.0000 ± .0037	.0000 ± .0046
TM1	021008	.0000 ± .0021	.0012 ± .0021	.0000 ± .0037	.0000 ± .0034	.0027 ± .0046
TM1	021014	.0000 ± .0019	.0000 ± .0022	.0000 ± .0039	.0000 ± .0036	.0008 ± .0046
TM1	021020	.0006 ± .0019	.0022 ± .0022	.0000 ± .0038	.0000 ± .0035	.0000 ± .0049
TM1	021026	.0000 ± .0024	.0000 ± .0025	.0000 ± .0043	.0000 ± .0041	.0000 ± .0051
TM1	021201	.0001 ± .0018	.0000 ± .0019	.0000 ± .0034	.0000 ± .0031	.0000 ± .0042
TM1	021207	.0002 ± .0016	.0012 ± .0019	.0000 ± .0032	.0000 ± .0036	.0000 ± .0043
TM1	021213	.0000 ± .0021	.0011 ± .0021	.0000 ± .0036	.0000 ± .0036	.0006 ± .0046
TM1	021219	.0000 ± .0019	.0006 ± .0020	.0000 ± .0035	.0000 ± .0033	.0014 ± .0044
TM1	021225	.0000 ± .0019	.0000 ± .0018	.0000 ± .0032	.0019 ± .0033	.0010 ± .0041
TM1	030301	.0011 ± .0021	.0003 ± .0025	.0000 ± .0042	.0000 ± .0043	.0049 ± .0057
TM1	030307	.0000 ± .0024	.0013 ± .0027	.0025 ± .0047	.0000 ± .0047	.0014 ± .0060
TM1	030313	.0015 ± .0023	.0000 ± .0026	.0005 ± .0046	.0004 ± .0048	.0026 ± .0060
TM1	030319	.0000 ± .0022	.0010 ± .0025	.0026 ± .0044	.0000 ± .0048	.0023 ± .0058
TM1	030325	.0000 ± .0025	.0007 ± .0023	.0021 ± .0040	.0000 ± .0041	.0023 ± .0055
TM1	030605	.0017 ± .0020	.0000 ± .0023	.0016 ± .0040	.0000 ± .0038	.0022 ± .0050
TM1	030611	.0007 ± .0022	.0011 ± .0026	.0000 ± .0045	.0004 ± .0043	.0032 ± .0057
TM1	030617	.0002 ± .0024	.0008 ± .0027	.0000 ± .0047	.0000 ± .0045	.0000 ± .0053
TM1	030623	.0000 ± .0021	.0007 ± .0026	.0000 ± .0045	.0000 ± .0043	.0059 ± .0019
TM1	030629	.0000 ± .0020	.0000 ± .0024	.0024 ± .0041	.0000 ± .0045	.0000 ± .0054
ZS7	021008	.0000 ± .0041	.0033 ± .0006	.0022 ± .0032	.0008 ± .0032	.0808 ± .0026
ZS7	021014	.0000 ± .0018	.0002 ± .0018	.0000 ± .0032	.0000 ± .0028	.0574 ± .0022
ZS7	021020	.0001 ± .0013	.0002 ± .0016	.0000 ± .0027	.0000 ± .0025	.0109 ± .0014
ZS7	021026	.0000 ± .0015	.0011 ± .0016	.0004 ± .0028	.0000 ± .0027	.0000 ± .0038
ZS7	021201	.0003 ± .0021	.0021 ± .0005	.0013 ± .0027	.0030 ± .0009	.0133 ± .0014
ZS7	021207	.0000 ± .0016	.0023 ± .0005	.0000 ± .0026	.0001 ± .0025	.0037 ± .0012
ZS7	021213	.0000 ± .0033	.0035 ± .0006	.0000 ± .0031	.0000 ± .0028	.0067 ± .0014
ZS7	021219	.0000 ± .0026	.0047 ± .0006	.0000 ± .0031	.0000 ± .0030	.0054 ± .0014
ZS7	021225	.0000 ± .0033	.0016 ± .0018	.0000 ± .0031	.0000 ± .0029	.0254 ± .0018
ZS7	030301	.0004 ± .0015	.0010 ± .0017	.0128 ± .0010	.0000 ± .0034	.4433 ± .0055
ZS7	030307	.0016 ± .0022	.0020 ± .0005	.0016 ± .0027	.0000 ± .0026	.0218 ± .0016
ZS7	030313	.0001 ± .0016	.0015 ± .0018	.0016 ± .0031	.0000 ± .0027	.0491 ± .0021
ZS7	030319	.0000 ± .0027	.0019 ± .0006	.0060 ± .0010	.0000 ± .0030	.1219 ± .0030
ZS7	030325	.0006 ± .0022	.0007 ± .0019	.0000 ± .0033	.0000 ± .0029	.0229 ± .0017
ZS7	030605	.0005 ± .0017	.0000 ± .0019	.0000 ± .0032	.0018 ± .0030	.0427 ± .0020
ZS7	030611	.0005 ± .0014	.0014 ± .0017	.0022 ± .0029	.0001 ± .0028	.0007 ± .0034
ZS7	030617	.0000 ± .0017	.0025 ± .0005	.0017 ± .0027	.0000 ± .0028	.0236 ± .0017
ZS7	030623	.0005 ± .0012	.0006 ± .0014	.0002 ± .0025	.0014 ± .0026	.0021 ± .0033
ZS7	030629	.0000 ± .0015	.0006 ± .0017	.0000 ± .0030	.0000 ± .0028	.0279 ± .0018

Site	Date	Cadmium	Indium	Tin	Antimony	Barium
CH6	021002	.0043 ± .0012	.0000 ± .0040	.0138 ± .0024	.0067 ± .0074	.0393 ± .0109
CH6	021008	.0000 ± .0045	.0000 ± .0059	.0073 ± .0096	.0051 ± .0095	.0000 ± .0432
CH6	021014	.0115 ± .0015	.0015 ± .0047	.0255 ± .0027	.0144 ± .0028	.0000 ± .0344
CH6	021020	.0027 ± .0035	.0000 ± .0040	.0100 ± .0023	.0045 ± .0073	.0000 ± .0328
CH6	021026	.0033 ± .0037	.0000 ± .0040	.0297 ± .0028	.0157 ± .0025	.0177 ± .0325
CH6	021201	.0011 ± .0034	.0000 ± .0041	.0228 ± .0024	.0110 ± .0022	.0000 ± .0306
CH6	021207	.0031 ± .0036	.0000 ± .0043	.0171 ± .0031	.0095 ± .0024	.0000 ± .0322
CH6	021213	.0000 ± .0034	.0010 ± .0040	.0183 ± .0024	.0130 ± .0025	.0155 ± .0327
CH6	021219	.0031 ± .0034	.0021 ± .0044	.0492 ± .0031	.0095 ± .0025	.0000 ± .0320
CH6	021225	.0016 ± .0034	.0000 ± .0042	.0226 ± .0028	.0051 ± .0075	.0000 ± .0325
CH6	030301	.0022 ± .0038	.0000 ± .0044	.0550 ± .0034	.0074 ± .0077	.0179 ± .0343
CH6	030307	.0031 ± .0050	.0000 ± .0057	.0181 ± .0039	.0027 ± .0102	.0000 ± .0473
CH6	030313	.0049 ± .0050	.0033 ± .0060	.0786 ± .0042	.0246 ± .0036	.0309 ± .0448
CH6	030319	.0000 ± .0043	.0000 ± .0050	.0196 ± .0031	.0050 ± .0094	.0272 ± .0420
CH6	030325	.0015 ± .0040	.0000 ± .0046	.0269 ± .0038	.0130 ± .0028	.0000 ± .0370
CH6	030605	.0037 ± .0041	.0000 ± .0047	.0145 ± .0034	.0045 ± .0085	.0372 ± .0122
CH6	030611	.0002 ± .0035	.0000 ± .0041	.0109 ± .0026	.0021 ± .0076	.0123 ± .0338
CH6	030617	.0035 ± .0040	.0000 ± .0046	.0110 ± .0029	.0001 ± .0081	.0092 ± .0372
CH6	030623	.0000 ± .0036	.0002 ± .0044	.0055 ± .0083	.0000 ± .0075	.0077 ± .0343
CH6	030629	.0000 ± .0034	.0000 ± .0045	.0041 ± .0076	.0000 ± .0078	.0000 ± .0368
CW3	021002	.0019 ± .0048	.0000 ± .0058	.0154 ± .0029	.0105 ± .0032	.0240 ± .0454
CW3	021008	.0002 ± .0049	.0036 ± .0062	.0095 ± .0030	.0050 ± .0100	.0042 ± .0465
CW3	021014	.0008 ± .0046	.0025 ± .0057	.0260 ± .0031	.0001 ± .0094	.0000 ± .0445
CW3	021020	.0000 ± .0047	.0000 ± .0062	.0116 ± .0031	.0037 ± .0099	.0216 ± .0472
CW3	021026	.0003 ± .0049	.0016 ± .0065	.0223 ± .0034	.0012 ± .0108	.0200 ± .0489
CW3	021201	.0005 ± .0049	.0000 ± .0060	.0271 ± .0034	.0047 ± .0099	.0215 ± .0452
CW3	021207	.0000 ± .0050	.0000 ± .0060	.0129 ± .0031	.0000 ± .0103	.0000 ± .0473
CW3	021213	.0061 ± .0016	.0048 ± .0059	.0283 ± .0032	.0134 ± .0032	.0427 ± .0449
CW3	021219	.0015 ± .0044	.0023 ± .0056	.0184 ± .0030	.0010 ± .0095	.0207 ± .0444
CW3	021225	.0046 ± .0049	.0000 ± .0056	.0155 ± .0030	.0035 ± .0094	.0000 ± .0431
CW3	030301	.0071 ± .0020	.0026 ± .0071	.0111 ± .0115	.0000 ± .0120	.0217 ± .0564
CW3	030307	.0030 ± .0060	.0037 ± .0073	.0105 ± .0117	.0009 ± .0133	.0326 ± .0600
CW3	030313	.0000 ± .0055	.0000 ± .0071	.0045 ± .0112	.0084 ± .0125	.0118 ± .0581
CW3	030319	.0000 ± .0063	.0000 ± .0073	.0459 ± .0044	.0000 ± .0128	.0261 ± .0593
CW3	030325	.0038 ± .0058	.0012 ± .0071	.0320 ± .0043	.0000 ± .0128	.0000 ± .0579
CW3	030605	.0000 ± .0058	.0000 ± .0075	.0032 ± .0117	.0000 ± .0124	.0287 ± .0569
CW3	030611	.0000 ± .0052	.0047 ± .0067	.0000 ± .0100	.0000 ± .0114	.0000 ± .0530
CW3	030617	.0063 ± .0019	.0003 ± .0067	.0244 ± .0039	.0000 ± .0120	.0047 ± .0548
CW3	030623	.0001 ± .0058	.0000 ± .0070	.0000 ± .0109	.0008 ± .0123	.0142 ± .0568
CW3	030629	.0002 ± .0055	.0000 ± .0069	.0000 ± .0106	.0002 ± .0125	.0000 ± .0594
GZ5	021002	.0036 ± .0054	.0041 ± .0061	.0292 ± .0033	.0153 ± .0037	.0031 ± .0495
GZ5	021008	.0068 ± .0017	.0035 ± .0060	.0115 ± .0031	.0139 ± .0037	.0000 ± .0481
GZ5	021014	.0120 ± .0017	.0016 ± .0061	.0531 ± .0037	.0203 ± .0035	.0509 ± .0158
GZ5	021020	.0011 ± .0046	.0000 ± .0054	.0225 ± .0030	.0128 ± .0033	.0000 ± .0446
GZ5	021026	.0041 ± .0050	.0000 ± .0058	.0279 ± .0034	.0130 ± .0036	.0066 ± .0478
GZ5	021201	.0000 ± .0049	.0000 ± .0056	.0799 ± .0039	.0275 ± .0036	.0000 ± .0439

Site	Date	Cadmium	Indium	Tin	Antimony	Barium
GZ5	021207	.0037 ± .0051	.0033 ± .0057	.0287 ± .0030	.0321 ± .0036	.0000 ± .0448
GZ5	021213	.0000 ± .0050	.0000 ± .0058	.0183 ± .0030	.0143 ± .0032	.0000 ± .0441
GZ5	021219	.0000 ± .0050	.0039 ± .0055	.0302 ± .0032	.0269 ± .0036	.0057 ± .0457
GZ5	021225	.0016 ± .0048	.0014 ± .0058	.0487 ± .0034	.0100 ± .0032	.0200 ± .0442
GZ5	030301	.0034 ± .0063	.0007 ± .0073	.0229 ± .0040	.0160 ± .0045	.0409 ± .0594
GZ5	030307	.0068 ± .0022	.0000 ± .0078	.0070 ± .0122	.0131 ± .0139	.0198 ± .0602
GZ5	030313	.0000 ± .0070	.0018 ± .0077	.0470 ± .0048	.0200 ± .0051	.0205 ± .0636
GZ5	030319	.0003 ± .0058	.0000 ± .0068	.0231 ± .0040	.0070 ± .0127	.0000 ± .0584
GZ5	030325	.0128 ± .0021	.0000 ± .0070	.0406 ± .0044	.0068 ± .0132	.0000 ± .0592
GZ5	030605	.0018 ± .0054	.0000 ± .0068	.0140 ± .0039	.0000 ± .0123	.0100 ± .0563
GZ5	030611	.0000 ± .0058	.0018 ± .0065	.0121 ± .0038	.0203 ± .0044	.0330 ± .0542
GZ5	030617	.0122 ± .0022	.0008 ± .0078	.0362 ± .0044	.0156 ± .0047	.0671 ± .0210
GZ5	030623	.0018 ± .0061	.0041 ± .0074	.0116 ± .0120	.0000 ± .0133	.0000 ± .0596
GZ5	030629	.0000 ± .0055	.0000 ± .0068	.0000 ± .0109	.0000 ± .0126	.0000 ± .0547
SZ4	021002	.0091 ± .0017	.0000 ± .0058	.0216 ± .0032	.0126 ± .0035	.0134 ± .0459
SZ4	021008	.0043 ± .0050	.0000 ± .0054	.0210 ± .0030	.0120 ± .0034	.0210 ± .0452
SZ4	021014	.0000 ± .0048	.0000 ± .0061	.0100 ± .0030	.0068 ± .0100	.0000 ± .0468
SZ4	021020	.0000 ± .0043	.0016 ± .0057	.0131 ± .0029	.0060 ± .0095	.0000 ± .0448
SZ4	021026	.0028 ± .0053	.0000 ± .0064	.0274 ± .0033	.0100 ± .0109	.0095 ± .0494
SZ4	021201	.0017 ± .0044	.0000 ± .0054	.0140 ± .0030	.0019 ± .0094	.0000 ± .0428
SZ4	021207	.0049 ± .0016	.0034 ± .0054	.0181 ± .0029	.0043 ± .0096	.0056 ± .0446
SZ4	021213	.0000 ± .0160	.0121 ± .0200	.0017 ± .0305	.0000 ± .0355	.0000 ± .1617
SZ4	021221	.0064 ± .0159	.0000 ± .0214	.0287 ± .0350	.0324 ± .0369	.0000 ± .1670
SZ4	021225	.0050 ± .0016	.0009 ± .0057	.0150 ± .0030	.0000 ± .0099	.0141 ± .0452
SZ4	030102	.0018 ± .0049	.0022 ± .0059	.0340 ± .0033	.0114 ± .0033	.0000 ± .0448
SZ4	030301	.0024 ± .0057	.0000 ± .0070	.0112 ± .0037	.0000 ± .0123	.0261 ± .0578
SZ4	030307	.0095 ± .0022	.0031 ± .0065	.0051 ± .0107	.0055 ± .0124	.0000 ± .0555
SZ4	030313	.0015 ± .0059	.0014 ± .0074	.0119 ± .0122	.0002 ± .0128	.0000 ± .0586
SZ4	030319	.0027 ± .0061	.0000 ± .0073	.0107 ± .0124	.0000 ± .0135	.0181 ± .0595
SZ4	030325	.0073 ± .0022	.0022 ± .0074	.0414 ± .0044	.0081 ± .0134	.0543 ± .0609
SZ4	030605	.0004 ± .0058	.0006 ± .0074	.0093 ± .0117	.0000 ± .0126	.0094 ± .0581
SZ4	030611	.0047 ± .0055	.0020 ± .0067	.0047 ± .0111	.0000 ± .0118	.0020 ± .0558
SZ4	030617	.0006 ± .0054	.0000 ± .0078	.0123 ± .0125	.0000 ± .0131	.0570 ± .0577
SZ4	030623	.0005 ± .0054	.0000 ± .0070	.0000 ± .0109	.0000 ± .0118	.0454 ± .0564
SZ4	030629	.0000 ± .0057	.0000 ± .0069	.0000 ± .0111	.0007 ± .0126	.0186 ± .0559
TC2	021002	.0000 ± .0046	.0000 ± .0057	.0129 ± .0029	.0081 ± .0095	.0000 ± .0430
TC2	021008	.0027 ± .0049	.0000 ± .0057	.0028 ± .0084	.0000 ± .0097	.0000 ± .0448
TC2	021014	.0000 ± .0046	.0000 ± .0057	.0089 ± .0029	.0055 ± .0097	.0156 ± .0460
TC2	021020	.0024 ± .0045	.0021 ± .0052	.0075 ± .0079	.0034 ± .0090	.0000 ± .0428
TC2	021026	.0062 ± .0016	.0000 ± .0053	.0172 ± .0029	.0013 ± .0094	.0000 ± .0441
TC2	021201	.0000 ± .0043	.0000 ± .0049	.0152 ± .0027	.0071 ± .0088	.0000 ± .0408
TC2	021207	.0038 ± .0044	.0035 ± .0054	.0000 ± .0080	.0016 ± .0095	.0011 ± .0430
TC2	021213	.0000 ± .0048	.0000 ± .0061	.0118 ± .0031	.0039 ± .0100	.0000 ± .0455
TC2	021219	.0000 ± .0050	.0007 ± .0064	.0165 ± .0030	.0043 ± .0101	.0000 ± .0476
TC2	021225	.0000 ± .0046	.0039 ± .0060	.0215 ± .0030	.0040 ± .0094	.0000 ± .0428
TC2	030301	.0000 ± .0057	.0010 ± .0072	.0025 ± .0114	.0060 ± .0129	.0809 ± .0199
TC2	030307	.0084 ± .0022	.0000 ± .0075	.0011 ± .0116	.0124 ± .0133	.0527 ± .0598
TC2	030313	.0067 ± .0020	.0042 ± .0068	.0112 ± .0113	.0000 ± .0130	.0000 ± .0626
TC2	030319	.0042 ± .0060	.0000 ± .0073	.0094 ± .0124	.0000 ± .0128	.0827 ± .0196

Site	Date	Cadmium	Indium	Tin	Antimony	Barium
TC2	030325	.0017 ± .0059	.0041 ± .0077	.0231 ± .0042	.0000 ± .0134	.0000 ± .0600
TC2	030605	.0040 ± .0062	.0000 ± .0077	.0047 ± .0117	.0000 ± .0128	.0267 ± .0594
TC2	030611	.0018 ± .0060	.0000 ± .0073	.0000 ± .0116	.0000 ± .0130	.0143 ± .0595
TC2	030617	.0019 ± .0061	.0011 ± .0073	.0247 ± .0039	.0041 ± .0125	.0417 ± .0561
TC2	030623	.0012 ± .0054	.0000 ± .0064	.0000 ± .0102	.0047 ± .0115	.0042 ± .0556
TC2	030629	.0000 ± .0056	.0000 ± .0069	.0000 ± .0103	.0026 ± .0119	.0145 ± .0554
TM1	021002	.0025 ± .0048	.0000 ± .0061	.0146 ± .0032	.0000 ± .0101	.0000 ± .0468
TM1	021008	.0000 ± .0049	.0000 ± .0054	.0026 ± .0083	.0054 ± .0094	.0065 ± .0451
TM1	021014	.0000 ± .0048	.0000 ± .0065	.0012 ± .0090	.0038 ± .0102	.0000 ± .0469
TM1	021020	.0000 ± .0049	.0000 ± .0059	.0049 ± .0089	.0000 ± .0099	.0296 ± .0460
TM1	021026	.0014 ± .0053	.0000 ± .0066	.0236 ± .0034	.0024 ± .0105	.0125 ± .0496
TM1	021201	.0000 ± .0046	.0028 ± .0058	.0143 ± .0029	.0069 ± .0090	.0099 ± .0430
TM1	021207	.0027 ± .0043	.0000 ± .0052	.0108 ± .0028	.0000 ± .0091	.0000 ± .0424
TM1	021213	.0038 ± .0045	.0016 ± .0059	.0193 ± .0030	.0075 ± .0096	.0222 ± .0449
TM1	021219	.0005 ± .0044	.0044 ± .0055	.0257 ± .0030	.0000 ± .0097	.0034 ± .0435
TM1	021225	.0070 ± .0015	.0011 ± .0054	.0171 ± .0029	.0026 ± .0091	.0042 ± .0422
TM1	030301	.0023 ± .0055	.0013 ± .0070	.0093 ± .0114	.0000 ± .0122	.0240 ± .0575
TM1	030307	.0000 ± .0062	.0000 ± .0077	.0043 ± .0121	.0007 ± .0132	.0037 ± .0602
TM1	030313	.0021 ± .0062	.0000 ± .0075	.0010 ± .0115	.0000 ± .0129	.0000 ± .0603
TM1	030319	.0058 ± .0059	.0059 ± .0072	.0150 ± .0040	.0026 ± .0127	.0000 ± .0580
TM1	030325	.0081 ± .0017	.0033 ± .0063	.0670 ± .0045	.0012 ± .0118	.0157 ± .0557
TM1	030605	.0000 ± .0053	.0005 ± .0066	.0000 ± .0100	.0000 ± .0113	.0263 ± .0549
TM1	030611	.0043 ± .0058	.0025 ± .0067	.0014 ± .0107	.0000 ± .0122	.0130 ± .0573
TM1	030617	.0000 ± .0059	.0000 ± .0074	.0149 ± .0042	.0000 ± .0130	.0155 ± .0594
TM1	030623	.0033 ± .0055	.0000 ± .0071	.0000 ± .0109	.0000 ± .0121	.0000 ± .0576
TM1	030629	.0000 ± .0053	.0000 ± .0065	.0000 ± .0104	.0000 ± .0117	.0000 ± .0548
ZS7	021008	.0061 ± .0014	.0000 ± .0047	.0255 ± .0030	.0115 ± .0028	.0000 ± .0372
ZS7	021014	.0024 ± .0040	.0000 ± .0047	.0280 ± .0029	.0029 ± .0082	.0055 ± .0377
ZS7	021020	.0016 ± .0034	.0000 ± .0044	.0000 ± .0066	.0020 ± .0074	.0096 ± .0346
ZS7	021026	.0104 ± .0015	.0001 ± .0043	.0062 ± .0068	.0017 ± .0077	.0075 ± .0348
ZS7	021201	.0059 ± .0013	.0028 ± .0041	.0262 ± .0026	.0080 ± .0081	.0359 ± .0112
ZS7	021207	.0000 ± .0036	.0000 ± .0042	.0098 ± .0022	.0049 ± .0071	.0014 ± .0329
ZS7	021213	.0000 ± .0041	.0019 ± .0048	.0296 ± .0028	.0170 ± .0029	.0000 ± .0371
ZS7	021219	.0041 ± .0042	.0000 ± .0045	.0383 ± .0027	.0282 ± .0029	.0312 ± .0360
ZS7	021225	.0033 ± .0042	.0009 ± .0048	.0244 ± .0026	.0075 ± .0081	.0238 ± .0357
ZS7	030301	.0000 ± .0041	.0000 ± .0051	.0000 ± .0187	.0016 ± .0086	.0653 ± .0126
ZS7	030307	.0073 ± .0013	.0000 ± .0043	.0185 ± .0027	.0057 ± .0078	.0000 ± .0359
ZS7	030313	.0023 ± .0039	.0000 ± .0049	.0168 ± .0028	.0072 ± .0084	.0090 ± .0384
ZS7	030319	.0000 ± .0037	.0000 ± .0045	.0264 ± .0033	.0076 ± .0082	.0083 ± .0366
ZS7	030325	.0047 ± .0014	.0000 ± .0048	.0406 ± .0031	.0064 ± .0087	.0412 ± .0132
ZS7	030605	.0015 ± .0039	.0000 ± .0046	.0118 ± .0027	.0000 ± .0085	.0046 ± .0388
ZS7	030611	.0000 ± .0038	.0003 ± .0047	.0000 ± .0070	.0000 ± .0081	.0140 ± .0374
ZS7	030617	.0167 ± .0016	.0040 ± .0044	.0221 ± .0026	.0094 ± .0027	.0376 ± .0120
ZS7	030623	.0008 ± .0033	.0012 ± .0043	.0002 ± .0063	.0000 ± .0073	.0048 ± .0343
ZS7	030629	.0014 ± .0034	.0015 ± .0046	.0034 ± .0076	.0000 ± .0081	.0000 ± .0374

Site	Date	Gold	Mercury	Thallium	Lead	Uranium
CH6	021002	.0000 ± .0079	.0000 ± .0015	.0030 ± .0042	.1639 ± .0021	.0000 ± .0029
CH6	021008	.0000 ± .0054	.0000 ± .0019	.0018 ± .0028	.0858 ± .0020	.0000 ± .0031
CH6	021014	.0000 ± .0199	.0000 ± .0018	.0026 ± .0066	.2686 ± .0027	.0000 ± .0041
CH6	021020	.0000 ± .0116	.0004 ± .0015	.0015 ± .0042	.1632 ± .0021	.0000 ± .0032
CH6	021026	.0000 ± .0106	.0000 ± .0014	.0017 ± .0038	.1430 ± .0020	.0000 ± .0031
CH6	021201	.0001 ± .0083	.0011 ± .0014	.0026 ± .0027	.0923 ± .0016	.0000 ± .0031
CH6	021207	.0000 ± .0062	.0008 ± .0016	.0025 ± .0044	.1730 ± .0021	.0000 ± .0035
CH6	021213	.0000 ± .0095	.0009 ± .0015	.0014 ± .0034	.1274 ± .0019	.0000 ± .0029
CH6	021219	.0000 ± .0116	.0011 ± .0017	.0021 ± .0059	.2393 ± .0025	.0000 ± .0038
CH6	021225	.0000 ± .0070	.0000 ± .0015	.0010 ± .0027	.0951 ± .0017	.0012 ± .0028
CH6	030301	.0003 ± .0123	.0011 ± .0017	.0089 ± .0024	.2802 ± .0028	.0000 ± .0038
CH6	030307	.0011 ± .0053	.0008 ± .0020	.0000 ± .0032	.0939 ± .0021	.0000 ± .0032
CH6	030313	.0000 ± .0309	.0012 ± .0024	.0040 ± .0114	.4614 ± .0040	.0000 ± .0080
CH6	030319	.0012 ± .0067	.0013 ± .0018	.0000 ± .0030	.0933 ± .0020	.0000 ± .0031
CH6	030325	.0000 ± .0173	.0000 ± .0018	.0026 ± .0058	.2249 ± .0025	.0000 ± .0037
CH6	030605	.0000 ± .0100	.0012 ± .0018	.0065 ± .0017	.1885 ± .0024	.0000 ± .0055
CH6	030611	.0000 ± .0078	.0000 ± .0014	.0012 ± .0033	.1163 ± .0019	.0000 ± .0034
CH6	030617	.0000 ± .0091	.0005 ± .0017	.0021 ± .0028	.0890 ± .0018	.0008 ± .0029
CH6	030623	.0000 ± .0042	.0000 ± .0015	.0024 ± .0008	.0713 ± .0016	.0015 ± .0028
CH6	030629	.0000 ± .0039	.0002 ± .0016	.0021 ± .0007	.0540 ± .0015	.0000 ± .0029
CW3	021002	.0000 ± .0110	.0000 ± .0019	.0032 ± .0032	.0975 ± .0021	.0000 ± .0032
CW3	021008	.0000 ± .0094	.0001 ± .0021	.0003 ± .0029	.0862 ± .0021	.0000 ± .0034
CW3	021014	.0020 ± .0037	.0000 ± .0019	.0003 ± .0017	.0119 ± .0013	.0024 ± .0029
CW3	021020	.0000 ± .0037	.0003 ± .0021	.0000 ± .0018	.0064 ± .0014	.0017 ± .0032
CW3	021026	.0000 ± .0121	.0000 ± .0023	.0012 ± .0032	.0940 ± .0022	.0000 ± .0037
CW3	021201	.0000 ± .0090	.0000 ± .0020	.0017 ± .0027	.0719 ± .0019	.0028 ± .0032
CW3	021207	.0000 ± .0046	.0000 ± .0021	.0000 ± .0019	.0103 ± .0015	.0000 ± .0033
CW3	021213	.0000 ± .0102	.0005 ± .0019	.0002 ± .0033	.1102 ± .0022	.0001 ± .0033
CW3	021219	.0000 ± .0069	.0000 ± .0019	.0016 ± .0024	.0620 ± .0018	.0000 ± .0030
CW3	021225	.0000 ± .0111	.0000 ± .0019	.0015 ± .0029	.0840 ± .0020	.0000 ± .0031
CW3	030301	.0054 ± .0055	.0002 ± .0024	.0010 ± .0024	.0267 ± .0017	.0000 ± .0034
CW3	030307	.0000 ± .0120	.0000 ± .0026	.0023 ± .0032	.0764 ± .0024	.0000 ± .0041
CW3	030313	.0008 ± .0064	.0000 ± .0023	.0000 ± .0024	.0296 ± .0018	.0000 ± .0036
CW3	030319	.0000 ± .0067	.0000 ± .0025	.0003 ± .0026	.0362 ± .0020	.0000 ± .0038
CW3	030325	.0000 ± .0114	.0000 ± .0025	.0028 ± .0043	.1331 ± .0028	.0000 ± .0038
CW3	030605	.0000 ± .0069	.0000 ± .0023	.0011 ± .0028	.0503 ± .0020	.0000 ± .0037
CW3	030611	.0000 ± .0047	.0000 ± .0021	.0000 ± .0020	.0064 ± .0014	.0002 ± .0031
CW3	030617	.0031 ± .0107	.0005 ± .0022	.0000 ± .0030	.0707 ± .0021	.0008 ± .0035
CW3	030623	.0000 ± .0042	.0004 ± .0024	.0007 ± .0021	.0000 ± .0045	.0004 ± .0037
CW3	030629	.0000 ± .0042	.0005 ± .0025	.0001 ± .0021	.0024 ± .0047	.0000 ± .0038
GZ5	021002	.0000 ± .0145	.0000 ± .0024	.0045 ± .0056	.2001 ± .0029	.0007 ± .0043
GZ5	021008	.0000 ± .0075	.0000 ± .0022	.0027 ± .0039	.1252 ± .0024	.0000 ± .0038
GZ5	021014	.0000 ± .0242	.0009 ± .0025	.0080 ± .0104	.4237 ± .0039	.0000 ± .0068
GZ5	021020	.0000 ± .0365	.0004 ± .0021	.0021 ± .0065	.2517 ± .0030	.0000 ± .0035
GZ5	021026	.0000 ± .0101	.0000 ± .0022	.0017 ± .0046	.1606 ± .0026	.0000 ± .0037
GZ5	021201	.0000 ± .0235	.0017 ± .0025	.0040 ± .0117	.4795 ± .0040	.0000 ± .0048

Site	Date	Gold	Mercury	Thallium	Lead	Uranium
GZ5	021207	.0000 ± .0174	.0019 ± .0024	.0049 ± .0088	.3563 ± .0035	.0000 ± .0052
GZ5	021213	.0020 ± .0094	.0006 ± .0020	.0038 ± .0048	.1750 ± .0026	.0000 ± .0039
GZ5	021219	.0000 ± .0204	.0007 ± .0024	.0046 ± .0085	.3410 ± .0035	.0000 ± .0043
GZ5	021225	.0000 ± .0086	.0000 ± .0020	.0035 ± .0046	.1659 ± .0025	.0013 ± .0035
GZ5	030301	.0000 ± .0263	.0015 ± .0028	.0036 ± .0069	.2499 ± .0036	.0022 ± .0043
GZ5	030307	.0000 ± .0116	.0000 ± .0027	.0033 ± .0055	.1866 ± .0032	.0000 ± .0044
GZ5	030313	.0000 ± .0261	.0000 ± .0030	.0080 ± .0102	.3912 ± .0044	.0000 ± .0065
GZ5	030319	.0000 ± .0097	.0000 ± .0025	.0020 ± .0039	.1090 ± .0026	.0000 ± .0045
GZ5	030325	.0000 ± .0196	.0000 ± .0028	.0059 ± .0096	.3695 ± .0042	.0000 ± .0053
GZ5	030605	.0026 ± .0165	.0012 ± .0025	.0000 ± .0044	.1409 ± .0028	.0000 ± .0039
GZ5	030611	.0000 ± .0382	.0020 ± .0026	.0034 ± .0081	.2959 ± .0038	.0000 ± .0043
GZ5	030617	.0000 ± .0351	.0000 ± .0032	.0093 ± .0113	.4363 ± .0048	.0000 ± .0069
GZ5	030623	.0000 ± .0276	.0000 ± .0028	.0072 ± .0086	.3254 ± .0039	.0000 ± .0049
GZ5	030629	.0000 ± .0118	.0000 ± .0023	.0042 ± .0056	.1940 ± .0031	.0000 ± .0034
SZ4	021002	.0000 ± .0144	.0000 ± .0021	.0025 ± .0042	.1513 ± .0025	.0032 ± .0038
SZ4	021008	.0000 ± .0164	.0000 ± .0020	.0014 ± .0047	.1735 ± .0026	.0000 ± .0038
SZ4	021014	.0000 ± .0051	.0000 ± .0020	.0000 ± .0020	.0275 ± .0016	.0005 ± .0031
SZ4	021020	.0000 ± .0044	.0000 ± .0019	.0003 ± .0018	.0148 ± .0014	.0000 ± .0029
SZ4	021026	.0000 ± .0154	.0000 ± .0023	.0000 ± .0039	.1340 ± .0025	.0012 ± .0040
SZ4	021201	.0016 ± .0074	.0005 ± .0018	.0001 ± .0025	.0643 ± .0018	.0005 ± .0028
SZ4	021207	.0000 ± .0064	.0000 ± .0019	.0030 ± .0007	.0421 ± .0017	.0006 ± .0031
SZ4	021213	.0029 ± .0255	.0000 ± .0066	.0012 ± .0085	.2042 ± .0063	.0000 ± .0103
SZ4	021221	.0053 ± .0280	.0000 ± .0069	.0047 ± .0107	.3050 ± .0073	.0000 ± .0109
SZ4	021225	.0000 ± .0125	.0008 ± .0021	.0011 ± .0037	.1256 ± .0023	.0017 ± .0036
SZ4	030102	.0000 ± .0122	.0000 ± .0020	.0031 ± .0050	.1856 ± .0027	.0000 ± .0040
SZ4	030301	.0031 ± .0077	.0000 ± .0024	.0002 ± .0028	.0515 ± .0020	.0000 ± .0036
SZ4	030307	.0000 ± .0134	.0009 ± .0024	.0000 ± .0046	.1532 ± .0029	.0000 ± .0039
SZ4	030313	.0000 ± .0116	.0014 ± .0026	.0011 ± .0030	.0642 ± .0022	.0000 ± .0038
SZ4	030319	.0009 ± .0119	.0000 ± .0024	.0023 ± .0039	.1120 ± .0026	.0000 ± .0039
SZ4	030325	.0000 ± .0184	.0000 ± .0026	.0015 ± .0049	.1593 ± .0030	.0000 ± .0042
SZ4	030605	.0000 ± .0073	.0018 ± .0025	.0019 ± .0028	.0476 ± .0020	.0000 ± .0039
SZ4	030611	.0000 ± .0055	.0004 ± .0023	.0000 ± .0023	.0290 ± .0018	.0010 ± .0036
SZ4	030617	.0000 ± .0103	.0000 ± .0025	.0000 ± .0032	.0801 ± .0024	.0006 ± .0041
SZ4	030623	.0000 ± .0041	.0000 ± .0023	.0005 ± .0022	.0053 ± .0015	.0006 ± .0036
SZ4	030629	.0041 ± .0041	.0000 ± .0024	.0004 ± .0020	.0051 ± .0015	.0000 ± .0035
TC2	021002	.0000 ± .0107	.0000 ± .0019	.0008 ± .0031	.1040 ± .0021	.0012 ± .0032
TC2	021008	.0000 ± .0101	.0000 ± .0020	.0010 ± .0029	.0884 ± .0020	.0015 ± .0035
TC2	021014	.0000 ± .0036	.0000 ± .0020	.0014 ± .0020	.0211 ± .0015	.0010 ± .0032
TC2	021020	.0000 ± .0032	.0000 ± .0018	.0010 ± .0017	.0073 ± .0012	.0000 ± .0027
TC2	021026	.0000 ± .0140	.0002 ± .0020	.0021 ± .0032	.1021 ± .0021	.0000 ± .0033
TC2	021201	.0021 ± .0075	.0003 ± .0018	.0015 ± .0024	.0634 ± .0017	.0005 ± .0027
TC2	021207	.0000 ± .0034	.0002 ± .0019	.0011 ± .0017	.0027 ± .0037	.0025 ± .0029
TC2	021213	.0000 ± .0099	.0000 ± .0020	.0010 ± .0034	.1098 ± .0022	.0000 ± .0035
TC2	021219	.0000 ± .0050	.0001 ± .0022	.0014 ± .0022	.0389 ± .0017	.0000 ± .0033
TC2	021225	.0000 ± .0132	.0000 ± .0019	.0023 ± .0036	.1212 ± .0022	.0002 ± .0033
TC2	030301	.0009 ± .0048	.0000 ± .0025	.0013 ± .0023	.0190 ± .0018	.0000 ± .0038
TC2	030307	.0000 ± .0145	.0010 ± .0026	.0029 ± .0045	.1466 ± .0029	.0000 ± .0040
TC2	030313	.0000 ± .0056	.0004 ± .0027	.0023 ± .0026	.0215 ± .0019	.0000 ± .0041
TC2	030319	.0010 ± .0080	.0000 ± .0024	.0000 ± .0029	.0555 ± .0021	.0026 ± .0038

Site	Date	Gold	Mercury	Thallium	Lead	Uranium
TC2	030325	.0000 ± .0087	.0000 ± .0025	.0000 ± .0036	.1010 ± .0026	.0000 ± .0039
TC2	030605	.0000 ± .0072	.0000 ± .0025	.0019 ± .0028	.0542 ± .0022	.0000 ± .0041
TC2	030611	.0007 ± .0044	.0000 ± .0025	.0004 ± .0024	.0012 ± .0048	.0009 ± .0040
TC2	030617	.0013 ± .0092	.0013 ± .0024	.0011 ± .0031	.0719 ± .0022	.0000 ± .0036
TC2	030623	.0000 ± .0038	.0001 ± .0023	.0007 ± .0020	.0024 ± .0043	.0008 ± .0035
TC2	030629	.0007 ± .0039	.0002 ± .0023	.0000 ± .0019	.0002 ± .0042	.0015 ± .0035
TM1	021002	.0000 ± .0097	.0000 ± .0022	.0033 ± .0035	.1108 ± .0023	.0013 ± .0036
TM1	021008	.0000 ± .0099	.0000 ± .0020	.0016 ± .0031	.1004 ± .0021	.0011 ± .0034
TM1	021014	.0000 ± .0036	.0000 ± .0020	.0004 ± .0019	.0066 ± .0014	.0027 ± .0032
TM1	021020	.0000 ± .0035	.0002 ± .0021	.0002 ± .0018	.0054 ± .0013	.0000 ± .0030
TM1	021026	.0000 ± .0151	.0000 ± .0024	.0004 ± .0035	.1115 ± .0024	.0008 ± .0039
TM1	021201	.0000 ± .0081	.0008 ± .0019	.0006 ± .0026	.0741 ± .0019	.0000 ± .0029
TM1	021207	.0000 ± .0032	.0000 ± .0017	.0007 ± .0018	.0176 ± .0013	.0004 ± .0026
TM1	021213	.0000 ± .0092	.0000 ± .0020	.0024 ± .0035	.1190 ± .0022	.0017 ± .0035
TM1	021219	.0000 ± .0054	.0000 ± .0019	.0014 ± .0026	.0703 ± .0019	.0000 ± .0030
TM1	021225	.0000 ± .0103	.0000 ± .0017	.0004 ± .0030	.0962 ± .0020	.0000 ± .0031
TM1	030301	.0019 ± .0046	.0000 ± .0023	.0010 ± .0024	.0249 ± .0017	.0023 ± .0036
TM1	030307	.0009 ± .0132	.0013 ± .0026	.0001 ± .0033	.0795 ± .0024	.0000 ± .0040
TM1	030313	.0007 ± .0062	.0000 ± .0025	.0001 ± .0024	.0294 ± .0019	.0004 ± .0038
TM1	030319	.0000 ± .0096	.0000 ± .0023	.0000 ± .0028	.0638 ± .0022	.0000 ± .0037
TM1	030325	.0009 ± .0136	.0009 ± .0023	.0001 ± .0052	.1767 ± .0030	.0000 ± .0037
TM1	030605	.0055 ± .0059	.0000 ± .0022	.0000 ± .0025	.0424 ± .0019	.0000 ± .0034
TM1	030611	.0000 ± .0042	.0009 ± .0025	.0008 ± .0021	.0020 ± .0046	.0003 ± .0037
TM1	030617	.0000 ± .0100	.0000 ± .0025	.0044 ± .0011	.0713 ± .0023	.0000 ± .0041
TM1	030623	.0000 ± .0040	.0000 ± .0023	.0013 ± .0021	.0000 ± .0045	.0027 ± .0037
TM1	030629	.0037 ± .0039	.0000 ± .0022	.0010 ± .0021	.0034 ± .0042	.0002 ± .0034
ZS7	021008	.0000 ± .0175	.0031 ± .0007	.0092 ± .0096	.3968 ± .0033	.0000 ± .0071
ZS7	021014	.0000 ± .0074	.0000 ± .0018	.0020 ± .0029	.0961 ± .0019	.0013 ± .0031
ZS7	021020	.0000 ± .0035	.0000 ± .0015	.0000 ± .0014	.0164 ± .0011	.0005 ± .0023
ZS7	021026	.0000 ± .0055	.0000 ± .0014	.0019 ± .0021	.0571 ± .0015	.0006 ± .0024
ZS7	021201	.0000 ± .0270	.0007 ± .0017	.0036 ± .0048	.1815 ± .0023	.0000 ± .0028
ZS7	021207	.0000 ± .0077	.0015 ± .0016	.0021 ± .0032	.1126 ± .0019	.0000 ± .0023
ZS7	021213	.0000 ± .0168	.0002 ± .0019	.0046 ± .0076	.3105 ± .0029	.0000 ± .0052
ZS7	021219	.0000 ± .0332	.0000 ± .0019	.0050 ± .0060	.2354 ± .0026	.0000 ± .0035
ZS7	021225	.0000 ± .0192	.0006 ± .0020	.0054 ± .0079	.3269 ± .0029	.0000 ± .0043
ZS7	030301	.0000 ± .0056	.0002 ± .0016	.0004 ± .0019	.0384 ± .0014	.0000 ± .0026
ZS7	030307	.0000 ± .0104	.0005 ± .0016	.0022 ± .0052	.1966 ± .0024	.0000 ± .0029
ZS7	030313	.0000 ± .0095	.0004 ± .0017	.0019 ± .0024	.0669 ± .0017	.0000 ± .0027
ZS7	030319	.0000 ± .0150	.0005 ± .0018	.0040 ± .0065	.2545 ± .0027	.0000 ± .0034
ZS7	030325	.0000 ± .0129	.0000 ± .0018	.0036 ± .0042	.1523 ± .0023	.0000 ± .0032
ZS7	030605	.0000 ± .0057	.0010 ± .0018	.0011 ± .0020	.0450 ± .0015	.0000 ± .0028
ZS7	030611	.0017 ± .0031	.0008 ± .0016	.0002 ± .0016	.0157 ± .0012	.0000 ± .0024
ZS7	030617	.0020 ± .0155	.0002 ± .0015	.0009 ± .0033	.1087 ± .0020	.0003 ± .0026
ZS7	030623	.0024 ± .0027	.0005 ± .0014	.0005 ± .0014	.0083 ± .0009	.0000 ± .0020
ZS7	030629	.0000 ± .0027	.0000 ± .0015	.0009 ± .0014	.0023 ± .0031	.0000 ± .0025

APPENDIX C: GREENLAND ICE SHEET AND NIWOT RIDGE – FIELD SAMPLING PREPARATION AND CALCULATIONS

C.1 Sample Bottle Cleaning Analysis

Given the expected low concentrations of organic carbon in the Greenland snow, any contamination due to the sampling materials was tested prior to the 2005 field trip. The selected bottles for snow sampling were Qorpak KaptClean^{TM} (Cole Parmer: EW-34605-70) glass bottles with Teflon-lined plastic caps. While these bottles were certified as pre-cleaned environmental bottles, it was uncertain whether the Qorpak cleaning procedures were sufficient. A week-long comparison test was thus performed, a series of bottles filled with a volume of low total organic carbon (TOC) deionized water and then measured for TOC at 0 hours, 24 hours, 5 days. Twenty bottles were used, ten of which were in their original purchased condition and ten with additional cleaning of both the glass bottle and the lid. For the ten samples with additional cleaning, the glass bottles were heated in a Thermolyne Furnace to a temperature of 550 °C for 12 hours and the Teflon-lined plastic lids were rinsed with certified hexane, certified methanol, and finally with low-TOC deionized water.

As seen in Figure C.1, it was found that the additional cleaning steps did provide a reduction in measured TOC. Also, the cleaned samples were within range of the laboratory DI water, which is usually around 15-25 ppb C. It was concluded that the extra cleaning steps were required for Greenland samples and the bottles were expected to contribute negligible levels of TOC to the samples. Later, further testing determined that methanol and hexane were unnecessary steps in cleaning the sample jar lids – these steps were substituted with a series of two 10-minute sonication baths and a final rinse in low-TOC DI water.

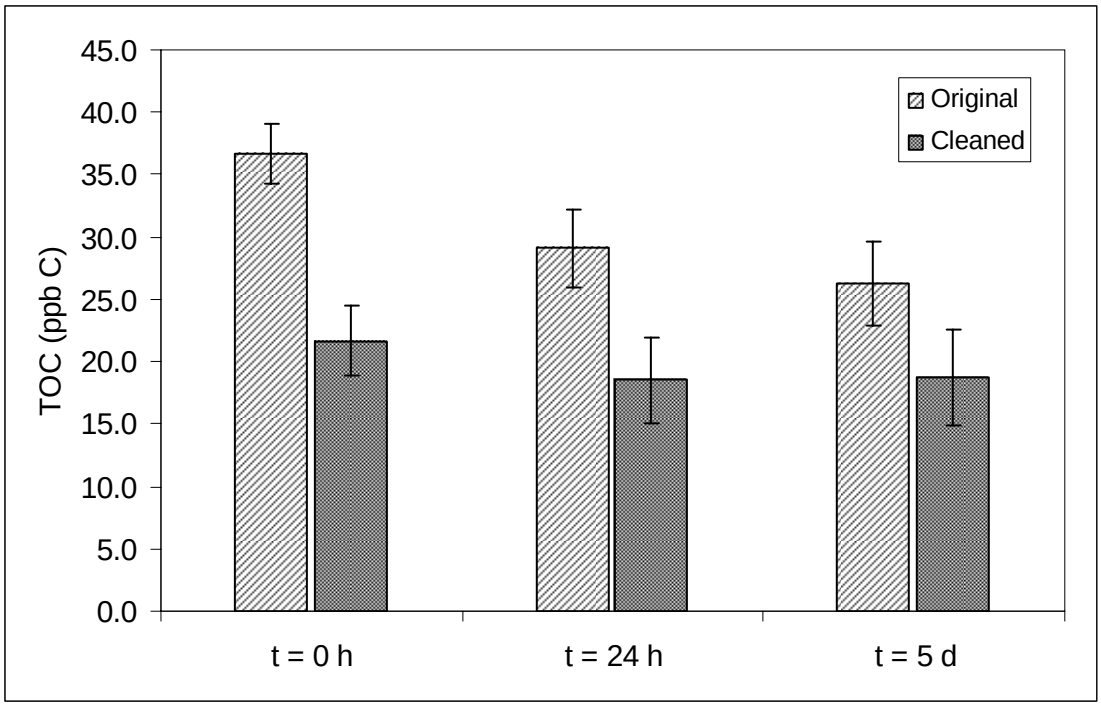

Figure C.1 Comparison of carbon mass in ultraclean water in Kaptclean^{TM} bottles, before and after cleaning.

C.2 Pre-acidification Process for Water-Soluble Organic Carbon Analysis

The Sievers 900 Total Organic Carbon (TOC) Analyzer analyzes water-phase organic carbon (OC) using a UV-based oxidation technique. Briefly, the analyzer splits the incoming sample stream into two portions, one portion passing through a UV-lit region causing the oxidation of OC and the second portion passing through a delay column. Thus, the UV-reacted sample volume now contains fully-oxidized carbon plus inorganic carbon (IC), all in inorganic form (H_2CO_3, HCO_3^-, CO_3^{2-}) and the second sample portion contains only IC. The two sample streams pass through a conductivity detector and organic carbon is calculated as: OC = total carbon – IC. Given low concentrations of OC and/or high IC, significant error can be introduced by this calculation method. The Sievers 900 analyzer recommends that OC be at least 10% of the total carbon for an accurate measurement.

As shown in Figure C.2, the concentration of IC is theoretically dependent upon pH. Given equilibration time with typical ambient CO_2 concentrations ($10^{-3.5}$ atm), the theoretical minimum IC concentration is ~130 ppb C, yielding ~15 ppb C as the lowest reliable measurement of OC by the Sievers instrument. Meanwhile, at a pH of 7, IC is theoretically ~700 ppb C and results in a lower limit of approximately 80 ppb C for trustworthy OC measurement. For typical OC concentrations in surface water and precipitation, a lower limit of 80 ppb C is not a concern. However, for the pristine polar areas, the inorganic contribution to the analyzer's conductivity signal needs to be reduced to resolve organic concentrations as low as 20 ppb C.

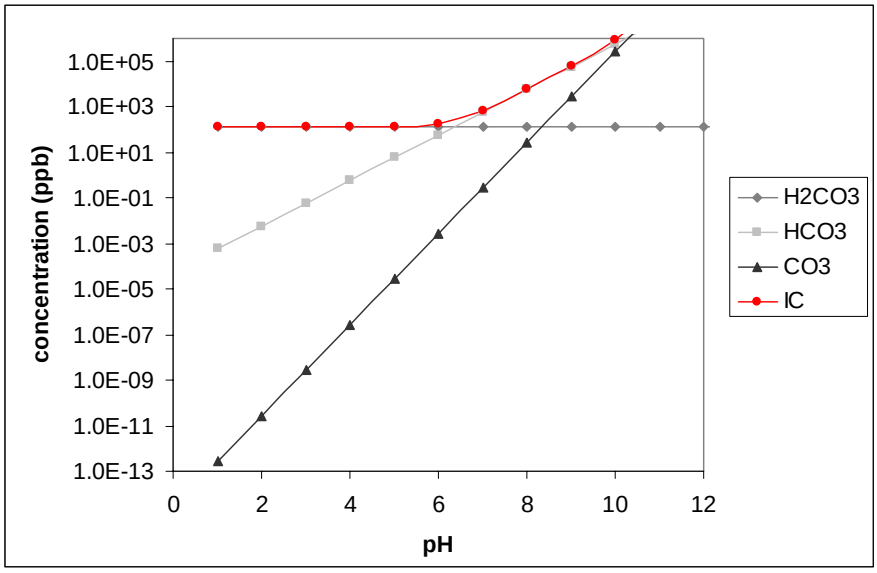

Figure C.2. Calculated inorganic carbon in water given P_{CO2} of $10^{-3.5}$ atm

A series of laboratory tests were performed to determine whether pre-acidifying samples with phosphoric acid would decrease the IC signal without contributing background OC. Figures C.3 and C.4 show the results of 3 samples (each 50 mL of ultrapure water) that were allowed to equilibrate with ambient CO_2 overnight, then measured for initial OC and IC concentrations. Then, a small amount (~20 µL) of 85% phosphoric acid was added to each sample, allowed to equilibrate for 40 minutes, and then re-measured for OC and IC. It can be seen that this acidification step reduced IC from its initial level of 460 ppb to a final 220 ppb. The OC concentration appears to increase from 13 to 34 ppb with acidification, but it is difficult to determine from this experiment whether that is background addition by the phosphoric acid or a consequence of poor OC measurement during the initial high-IC conditions. As a result of the lower IC levels from acidification, the fraction of OC in the total carbon increased from 3% to 13%, as shown in Figure C.4.

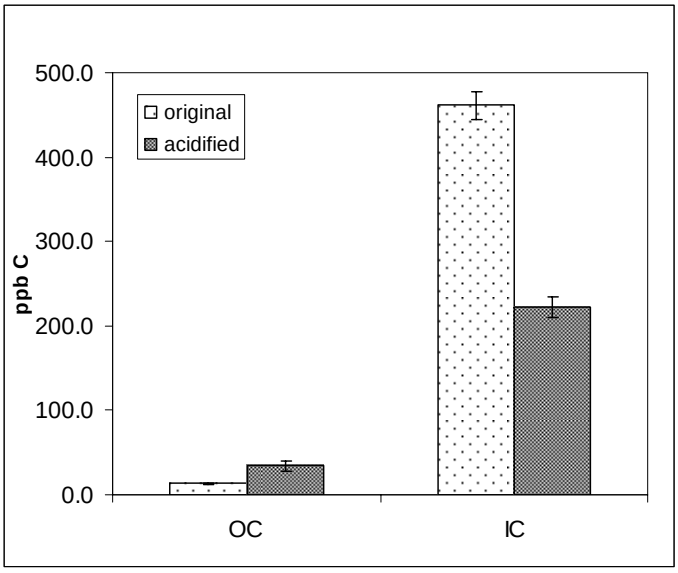

Figure C.3 OC and IC concentrations in aged ultrapure water during acidification tests.

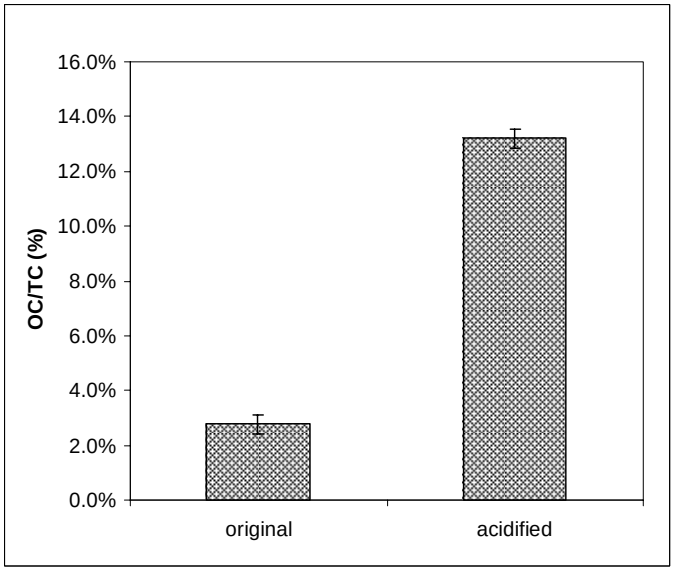

Figure C.4 OC/TC fraction during acidification tests.

To determine whether the phosphoric acid adds background OC, a second series of three 50 mL ultrapure samples were used. This time, however, the ultrapure water was not aged overnight and thus had low initial IC concentrations (<200 ppb) and so low OC concentrations could be reliably measured without pre-acidification. Samples were

initially measured for OC. Then, the samples were acidified with phosphoric acid, allowed to equilibrate for 40 minutes, and measured again for OC. As shown in Figure C.5, it appears that the phosphoric acid adds negligible OC. Thus, this method was deemed suitable for use in the OC-measurement of pristine polar snow samples.

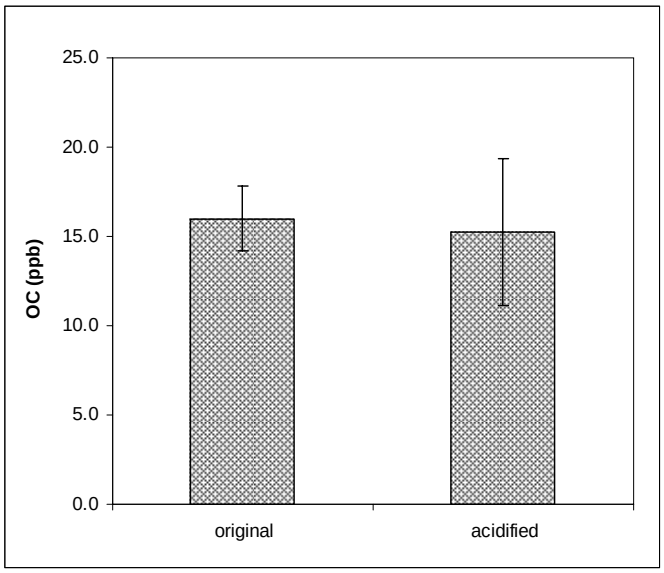

Figure C.5 Tests for background addition by phosphoric acid

C.3 Tests on Overlaying Two Filters in the Sunset Carbon Analyzer

One major challenge faced in the Greenland Ice Sheet study was to minimize the sampling time required to detect atmospheric particulate organic (OC) and elemental carbon (EC). The major constraint on meeting this goal is the EC detection limit of 0.2 μg carbon in our analytical method (Sunset Carbon Analyzer). Given the expected concentrations of EC in the Greenland atmosphere, a minimum run time of 160 hours (~7 days) would be needed to have detectable EC mass. In addition, the actual sampling period would be likely much longer given the sector control system turning off sampling during time periods with potential contamination from camp emissions.

In order to lessen the integrating time period, one proposition was to double the sample material placed into the Sunset Carbon Analyzer, layering two punches of a quartz fiber filter sample instead of the usual one punch. The total carbon mass would be expected to be accurately resolved using two layered punches, as the total carbon is simply related to the amount of carbon evolved from the filter (detected as methane) through progressive heating. However, there may be a concern about the apportioning of carbon mass between the organic and elemental fraction. To split the total carbon into the two fractions, a laser-beam transmittance method is employed. While undergoing a heating regime, a laser beam continuously passes through the sample filter. During the first heating stage, in the presence of helium gas, the initial laser transmittance is usually observed to drop as a portion of organic mass chars. During the second phase of heating, in the presence of oxygen gas, the residual organic mass evolves and the laser

transmittance increases. At the point where the laser transmittance crosses its initial point, a split point is defined and all remaining detected carbon is operationally defined as "elemental carbon". The most significant concern to layering filter punches would be a significant attenuation of the detected laser signal and potentially a misread of the split-point between OC and EC.

To determine whether layering filter punches is a reasonable approach, a set of 3 samples were taken on the rooftop of the Georgia Tech Environmental Science and Technology building in Atlanta, Georgia during September, 2005. Particulate matter samples were collected for in two parallel 25 mm filter holders for 6-18 hours. After collection, one filter sample was measured as a two single punches ("half") and the second filter sample was measured with two layered punches ("layered"). The results are shown below in Figure C.6.

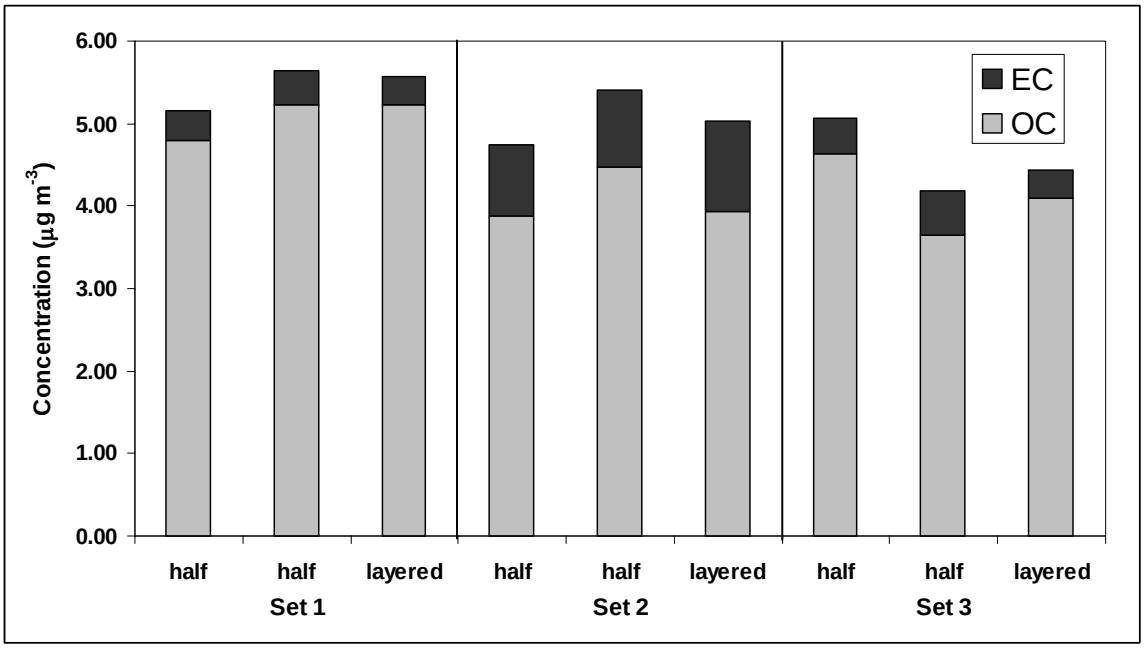

Figure C.6 Layered versus single punches measured on the Sunset Carbon Analyzer.

It can be seen that the layered filter measurements are very similar to the two half-filter punches, both in overall concentration and in apportionment between OC and EC. It is interesting that for all three sets of samples, the two single-punches do not give identical measurements (although are quite close). This is likely due to an imperfect distribution of particulate matter on the filter surface. The layered filters appear to strike nearly in the middle of each pair of half filters and possibly represent an even more accurate of the ambient concentration. Overall, the layered filters agreed reasonably well with the single filter punches for total carbon (average agreement within 8%), OC (7%), and EC (21%) and no consistent bias towards higher or lower EC was observed. For the Greenland ambient samples, it was deemed appropriate to half the required sampling time to 80 hours and layer filter punches in analysis when single punches were below the detection limit.

C.4 Analysis of Camp Impact during July, 2005 at Summit, Greenland

Summit Camp is a small field camp located at the highest point of the Greenland Ice Sheet and used for a variety of scientific measurements ranging from deep ice core drilling to present-day atmospheric measurements. It is a small camp, with researchers and staff numbering about 30 during the summer season (May to August) and 4 staff members in winter (September to April). Currently, the camp has a variety of emission sources that could potentially impact air and snow concentrations of carbonaceous particulates, including a diesel generator, diesel-powered vehicles (snowmobiles and heavy equipment), and aircraft (Twin Otters and LC-130s). Aircraft are the primary method of transporting people and supplies to the ice sheet, with flights arriving and departing approximately every 3 weeks during the summer season. Summit Camp seeks to preserve a "clean air" research area located south of camp by stopping all gasoline or diesel-powered snowmobiles and heavy equipment during days with northerly winds. In addition, the Summit contracting company (VECO Polar Resources) seeks to limit camp energy use as much as possible by introducing electric snowmobiles and having visiting researchers sleeping in unheated tents. However, aircraft transit and the camp generator are not turned off during "north wind days" and can impact the clean air sector. It is also possible, albeit unlikely, that emissions during "south wind days" could track back to impact camp given the right meteorological conditions.

Determining the impact of camp contamination was a major goal of the 2005 field expedition to Summit, Greenland. To detect the impact of camp emissions, measurement

of the particulate absorption coefficient (σ_{ap}) was compared with wind speed and wind direction over a 9-day period of time. In Figures C.7-C.9, intense spikes in the absorption coefficient on July 16th (up to ~40 Mm^{-1}) and July 25th (up to ~100 Mm^{-1}) are observed to be linked with time periods when winds passed through the camp sector. In comparison, significantly lower concentrations are observed during the other time periods.

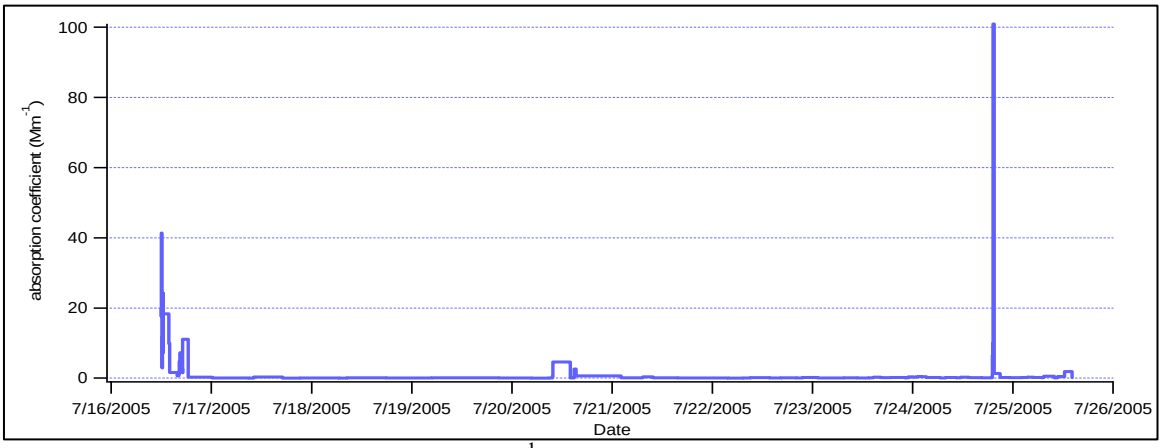

Figure C.7 Absorption coefficient (Mm^{-1}) measured at Summit Camp.

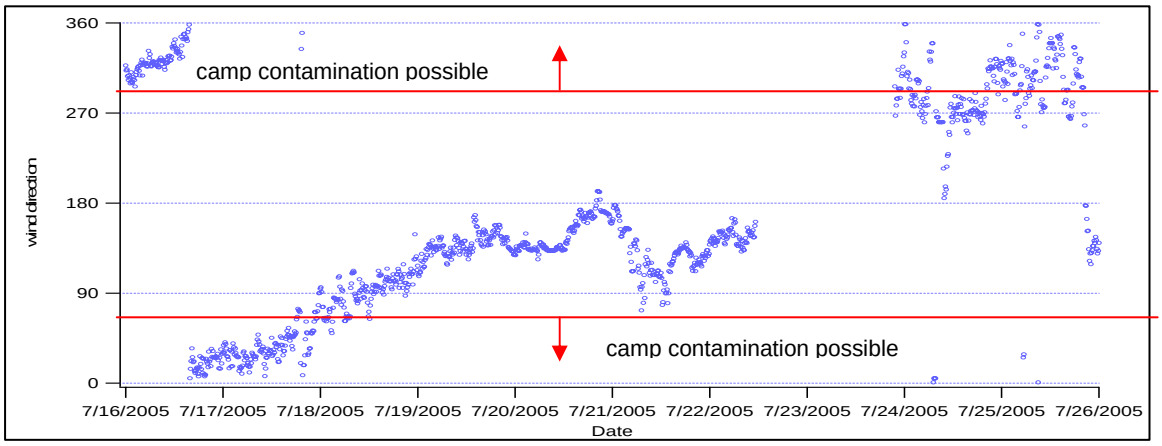

Figure C.8 Wind direction during the July 2005 field campaign, with red lines indicating wind directions that would potentially carry camp emissions toward the sampling instruments.

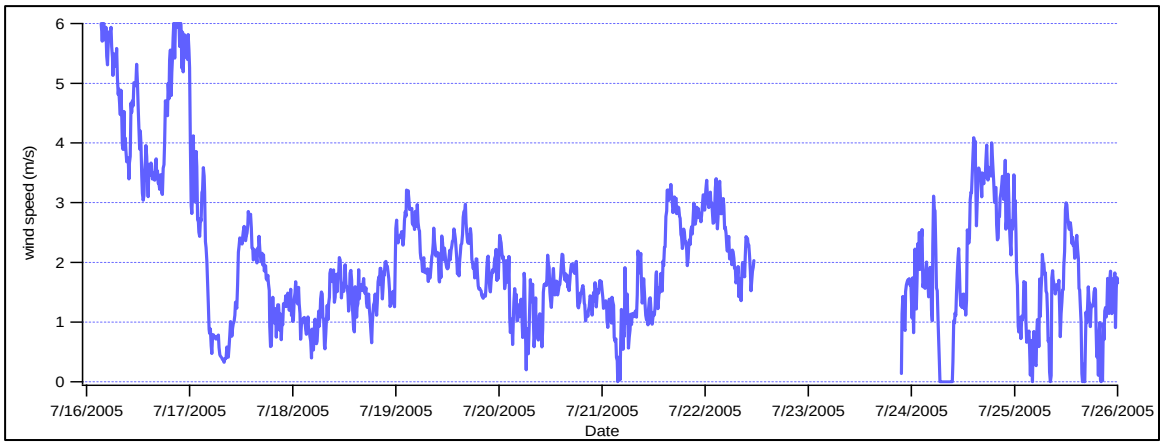

Figure C.9 Wind speeds measured during the July 2005 field campaign.

Based upon these observations, it was decided that the 2006 summer campaign would be relocated to a "satellite camp" located approximately ½ mile from the base camp. In addition, a sector control system was designed to protect the 2006 integrated filter measurements from camp pollution. Computer code for this sector control system is provided in the following section (Appendix C, section C3). Finally, further analysis of camp impact was incorporated into the 2006 campaign through a series of 1 meter snow pits, comparing concentrations near camp and at distances up to 20 kilometers from camp. For more details on the 1 meter snow pit samples, please refer to Chapter 6.

C.5 Sector Control Computer Code (Visual Basic)

```
'CR200 Series
'Declare Variables and Units
Public Batt_Volt
Public WS_ms
Public WindDir
Public Flag(8)
Public PS

Units Batt_Volt=Volts
Units WS_ms=meters/second
Units WindDir=Degrees

'Define Data Tables
DataTable(Table1,True,-1)
	DataInterval(0,1,Min)
	WindVector (WS_ms,WindDir,False,0,1)
	FieldNames("WS_ms_S_WVT,WindDir_D1_WVT")
	Sample (1,PS)
EndTable

'Main Program
BeginProg
	Scan(10,Sec)
		'Default Datalogger Battery Voltage measurement Batt_Volt:
		Battery(Batt_Volt)
		'03001 Wind Sensor measurements WS_ms and WindDir:
		PulseCount(WS_ms,P_LL,1,1,0.75,0.2)
		If WS_ms<0.21 Then WS_ms=0
		ExDelSE(WindDir,1,1,1,mV2500,3000,0.142,0)
		If WindDir>=360 Then WindDir=0
		'Simple Control w/ Deadband:
		If Flag(1)=0 Then
			If WS_ms>0.5 Then
				If WindDir > 45 And WindDir < 288 Then
					PortSet(2,1)
					PortSet(1,1)
					PS=1
				Else
					PortSet(2,0)
					PortSet(1,0)
					PS=0
				EndIf
			Else
				If WS_ms<0.5 Then
					PortSet(2,0)
					PortSet(1,0)
					PS=0
				EndIf
			EndIf
		Else
			PortSet(2,0)
			PortSet(1,0)
			PS=0
		EndIf

		'Call Data Tables and Store Data
		CallTable(Table1)
	NextScan
EndProg
```

C.6 IGOR Code – Calculation of $PM_{0.1\text{-}1.0}$

```
Macro Concentration_calc()
Make/O/N=(numpnts(Sample_Time)) ch0_mass_conc
Make/O/N=(numpnts(Sample_Time)) ch1_mass_conc
Make/O/N=(numpnts(Sample_Time)) ch2_mass_conc
Make/O/N=(numpnts(Sample_Time)) ch3_mass_conc
Make/O/N=(numpnts(Sample_Time)) ch4_mass_conc
Make/O/N=(numpnts(Sample_Time)) ch5_mass_conc
Make/O/N=(numpnts(Sample_Time)) ch6_mass_conc
Make/O/N=(numpnts(Sample_Time)) pm1_mass_conc
Make/O/N=(numpnts(Sample_Time)) ch0_num_conc
Make/O/N=(numpnts(Sample_Time)) ch1_num_conc
Make/O/N=(numpnts(Sample_Time)) ch2_num_conc
Make/O/N=(numpnts(Sample_Time)) ch3_num_conc
Make/O/N=(numpnts(Sample_Time)) ch4_num_conc
Make/O/N=(numpnts(Sample_Time)) ch5_num_conc
Make/O/N=(numpnts(Sample_Time)) ch6_num_conc
Make/O/N=(numpnts(Sample_Time)) ch7_num_conc
Variable i = 0
Variable V_flow=0 //volume of sample
Variable Vp0, Vp1, Vp2, Vp3, Vp4, Vp5, Vp6 //volume of particle
Variable Q=73.3 // flow rate = 0.0733 lpm = 73.3 cm3 p min
Variable pp=1000000 // density of particle = 1 g/cm3 = 10^6 ug/cm3
Variable d0 = 0.15, d1 = 0.25, d2 = 0.35, d3 = 0.45, d4 = 0.6, d5 = 0.85, d6 =
1.5 //midpoint diameters
do
       V_flow = Q*Sample_Interval[i]/60 //volume in cm3
       Vp0 = (d0/2)^3*(4/3)*pi/10^12  //particle volume in cm3
       Vp1 = (d1/2)^3*(4/3)*pi/10^12
       Vp2 = (d2/2)^3*(4/3)*pi/10^12
       Vp3 = (d3/2)^3*(4/3)*pi/10^12
       Vp4 = (d4/2)^3*(4/3)*pi/10^12
       Vp5 = (d5/2)^3*(4/3)*pi/10^12
       Vp6 = (d6/2)^3*(4/3)*pi/10^12

       //conc in ug/m3
       ch0_mass_conc[i]=1000000*Counts_Channel_0[i]*Vp0*pp/V_flow
       ch1_mass_conc[i]=1000000*Counts_Channel_1[i]*Vp1*pp/V_flow
       ch2_mass_conc[i]=1000000*Counts_Channel_2[i]*Vp2*pp/V_flow
       ch3_mass_conc[i]=1000000*Counts_Channel_3[i]*Vp3*pp/V_flow
       ch4_mass_conc[i]=1000000*Counts_Channel_4[i]*Vp4*pp/V_flow
       ch5_mass_conc[i]=1000000*Counts_Channel_5[i]*Vp5*pp/V_flow
       ch6_mass_conc[i]=1000000*Counts_Channel_6[i]*Vp6*pp/V_flow

       pm1_mass_conc[i]=ch0_mass_conc[i]+ch1_mass_conc[i]+
       ch2_mass_conc[i]+ch3_mass_conc[i]+ch4_mass_conc[i]+ ch5_mass_conc[i]

      //conc in N/cm3
       ch0_num_conc[i]=Counts_Channel_0[i]/V_flow
       ch1_num_conc[i]=Counts_Channel_1[i]/V_flow
       ch2_num_conc[i]=Counts_Channel_2[i]/V_flow
       ch3_num_conc[i]=Counts_Channel_3[i]/V_flow
       ch4_num_conc[i]=Counts_Channel_4[i]/V_flow
       ch5_num_conc[i]=Counts_Channel_5[i]/V_flow
       ch6_num_conc[i]=Counts_Channel_6[i]/V_flow
       ch7_num_conc[i]=Counts_Channel_7[i]/V_flow
       i+=1
       print i
while (i<=numpnts(Sample_Time))

End
```

C.7 IGOR Code – Calculation of σ_{ap}

```
Macro bap_calc(tran, timestep)
//import filtered transmittance wave and timestamp wave
String tran
Prompt tran, "select filtered transmittance wave",popup, Wavelist("*",";","")
String timestep
Prompt timestep, "select timestamp data",popup, Wavelist("*",";","")

//make final data waves
Make/O/N=(numpnts($tran)) bap_new
Make/O/N = (numpnts($tran)) bap_new_corr
Make/O/N=(numpnts($tran)) bap_timestamp
Make/O/N=(numpnts($tran)) stop_wave
Make/O/N=(numpnts($tran)) start_wave

appendtotable bap_new, bap_timestamp, start_wave, stop_wave

//make set-through variables
Variable i=0
Variable t_min = 0
Variable start = 0
Variable stop = 1
Variable increment = 0
Variable endprog = numpnts($timestep)
Variable tran_avg = 0

//step through data and calculate bap

do
If ($tran[stop] == -99999)
	stop+=1
	start+=1
Endif

If ($tran[stop]>$tran[start])
	stop+=1
	start=stop
Endif

increment = $tran[start]-$tran[stop]

If ($tran[stop]>0)
	If (increment >= 0.003)
		t_min = ($timestep[stop] - $timestep[start])/60
		bap_new[i] = (11407.54958/t_min)*ln($tran[start]/$tran[stop])
		tran_avg = ($tran[start]+$tran[stop])/2
		bap_new_corr[i]=bap_new[i]*1/(2*(0.5398*tran_avg+0.355))
		bap_timestamp[i]=$timestep[start]
		start_wave[i]=start
		stop_wave[i]=stop
		start=stop+1
		stop+=1
		i+=1
	Else
		stop+=1
	Endif

Endif

while ((stop<=endprog))
End
```

C.8 IGOR Code – Filtering Flagged Time Periods (LASAIR and PSAP data)

PSAP program:

```
Macro bap_met_calc(bap_in, bap_time, ps_time, ps_in)
//goal of this macro is to look at met values and set bap to zero during camp
winds

String bap_in
Prompt bap_in, "select calculated bap wave",popup, Wavelist("*",";","")
String bap_time
Prompt bap_time, "select bap timestamp data",popup, Wavelist("*",";","")
String ps_time
Prompt ps_time, "select power strip timestamp data",popup, Wavelist("*",";","")
String ps_in
Prompt ps_in, "select power strip on/off data",popup, Wavelist("*",";","")

//make new bap wave for final adjustment
Duplicate/O $bap_in, bap_met_adjust
Make/O/N=(numpnts($bap_in)) ps_start
Make/O/N=(numpnts($bap_in)) ps_end
appendtotable bap_met_adjust, ps_start, ps_end

Variable m_start = 0
Variable m_end = 1
Variable b_start = 0
Variable b_end = 1
Variable i = 0
Variable test = 0
Variable endprog = numpnts($bap_in)
Variable new_start = 0
Variable count = 0

//step through data and calculate adjusted bap
do

//align time periods of bap and sector control waves
do
       m_start +=1
       m_end +=1
while(($bap_time[b_start]>$ps_time[m_start]))

do
       m_end +=1
while (($bap_time[b_end]>$ps_time[m_end]))

//indicate start and end powerstrip times
ps_start[i] = m_start
ps_end[i] = m_end
new_start = m_start

//to be conservative, create test variable that will increase for each 10-
// minute period experiencing camp contamination for 40 minutes prior to PSAP

If ($ps_in[m_start-1]==0)
       test+=1
Endif

If ($ps_in[m_start-2]==0)
       test+=1
Endif
```

```
If ($ps_in[m_start-3]==0)
       test+=1
Endif

If ($ps_in[m_start-4]==0)
       test+=1
Endif

If ($ps_in[m_start-5]==0)
       test+=1
Endif

do
If ($ps_in[m_start]==0)
       test+=1
Endif
       m_start+=1
while((m_start<=m_end))

//given that camp contamination flagged 3 times within an hour of the
//measurement, set bap to O during time period

If (test>2)
bap_met_adjust[i]=0
count +=1
Endif

test = 0
m_start = new_start
m_end = new_start + 1
i +=1
b_start = b_end
b_end +=1

while((i<=endprog))

print count

End
```

LAISAIR program:

```
Macro laisair_met_calc(pm1_in, pm1_time, ps_time, ps_in)
//goal of this macro is to look at met values and set to zero during camp winds
String pm1_in
Prompt pm1_in, "select calculated pm1 wave",popup, Wavelist("*",";","")
String pm1_time
Prompt pm1_time, "select pm1 timestamp data",popup, Wavelist("*",";","")
String ps_time
Prompt ps_time, "select power strip timestamp data",popup, Wavelist("*",";","")
String ps_in
Prompt ps_in, "select power strip on/off data",popup, Wavelist("*",";","")

//make new bap wave for final adjustment
Duplicate/O $pm1_in, pm1_met_adjust
Duplicate/O ch0_num_conc, ch0_num_met
Duplicate/O ch1_num_conc, ch1_num_met
Duplicate/O ch2_num_conc, ch2_num_met
Duplicate/O ch3_num_conc, ch3_num_met
Duplicate/O ch4_num_conc, ch4_num_met
Duplicate/O ch5_num_conc, ch5_num_met
Make/O/N=(numpnts($pm1_in)) ps_start
```

```
Make/O/N=(numpnts($pm1_in)) ps_end
appendtotable pm1_met_adjust, ps_start, ps_end

Variable m_start = 0
Variable m_end = 1
Variable i = 0
Variable test = 0
Variable endprog = numpnts($pm1_in)
Variable new_start = 0
Variable count = 0
Variable inc = 600
Variable test_inc = 0

//step through data and calculate adjusted waves

do

	do
		If ($pm1_time[i]<$ps_time[m_start])
			i+=1
			print i
		Else
			break
		Endif
	while(($pm1_time[i]<$ps_time[m_start]))

	test_inc = $pm1_time[i]-$ps_time[m_start]

	If (test_inc>inc)
		m_start+=1
		m_end+=1
	Endif

	test_inc = 0

	//indicate start and end powerstrip times
	ps_start[i] = m_start
	ps_end[i] = m_end

	If ($ps_in[m_start-1]==0)
		test+=1
	Endif

	If ($ps_in[m_start-2]==0)
		test+=1
	Endif

	If ($ps_in[m_start-3]==0)
		test+=1
	Endif

	If ($ps_in[m_start-4]==0)
		test+=1
	Endif

	If ($ps_in[m_start-5]==0)
		test+=1
	Endif

	If ($ps_in[m_start]==0)
		test+=1
	Endif
```

```
        If (test>2)
        pm1_met_adjust[i]=0
        ch0_num_met[i]=0
        ch1_num_met[i]=0
        ch2_num_met[i]=0
        ch3_num_met[i]=0
        ch4_num_met[i]=0
        ch5_num_met[i]=0
        count +=1
        Endif

        test = 0
        i+=1

        print i
while((i<=endprog))

print count

End
```

APPENDIX D: GREENLAND ICE SHEET – ADDITIONAL DATA

D.1 10-Day Back-Trajectories During Summer 2006 at Summit, Greenland

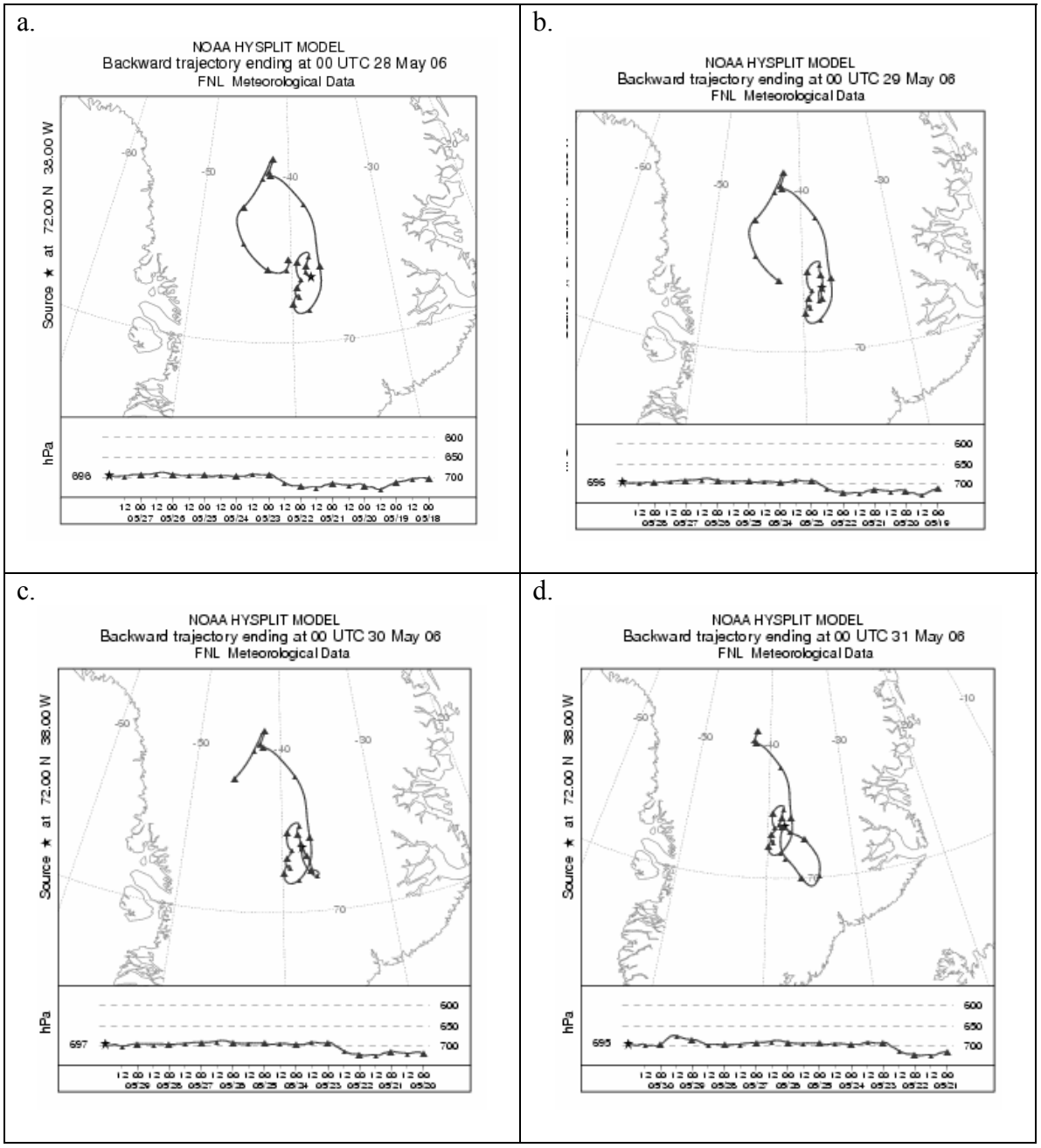

Figure D.1 Calculated 10-day isobaric trajectories arriving at Summit, Greenland on 28 May 2006 (a), 29 May 2006 (b), 30 May 2006 (c), and 31 May 2006 (d).

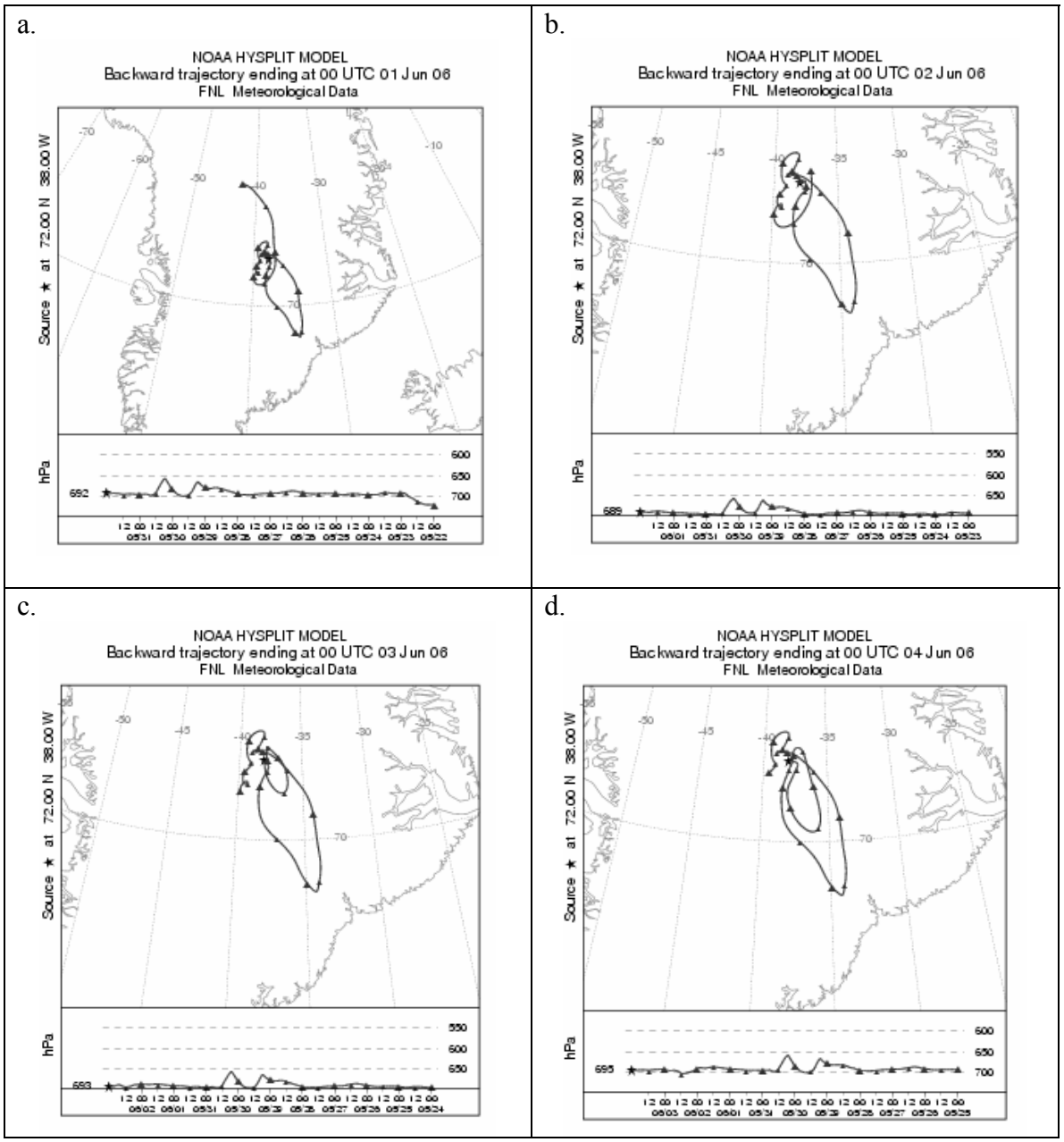

Figure D.2 Calculated 10-day isobaric trajectories arriving at Summit, Greenland on 1 June 2006 (a), 2 June 2006 (b), 3 June 2006 (c), and 4 June 2006 (d).

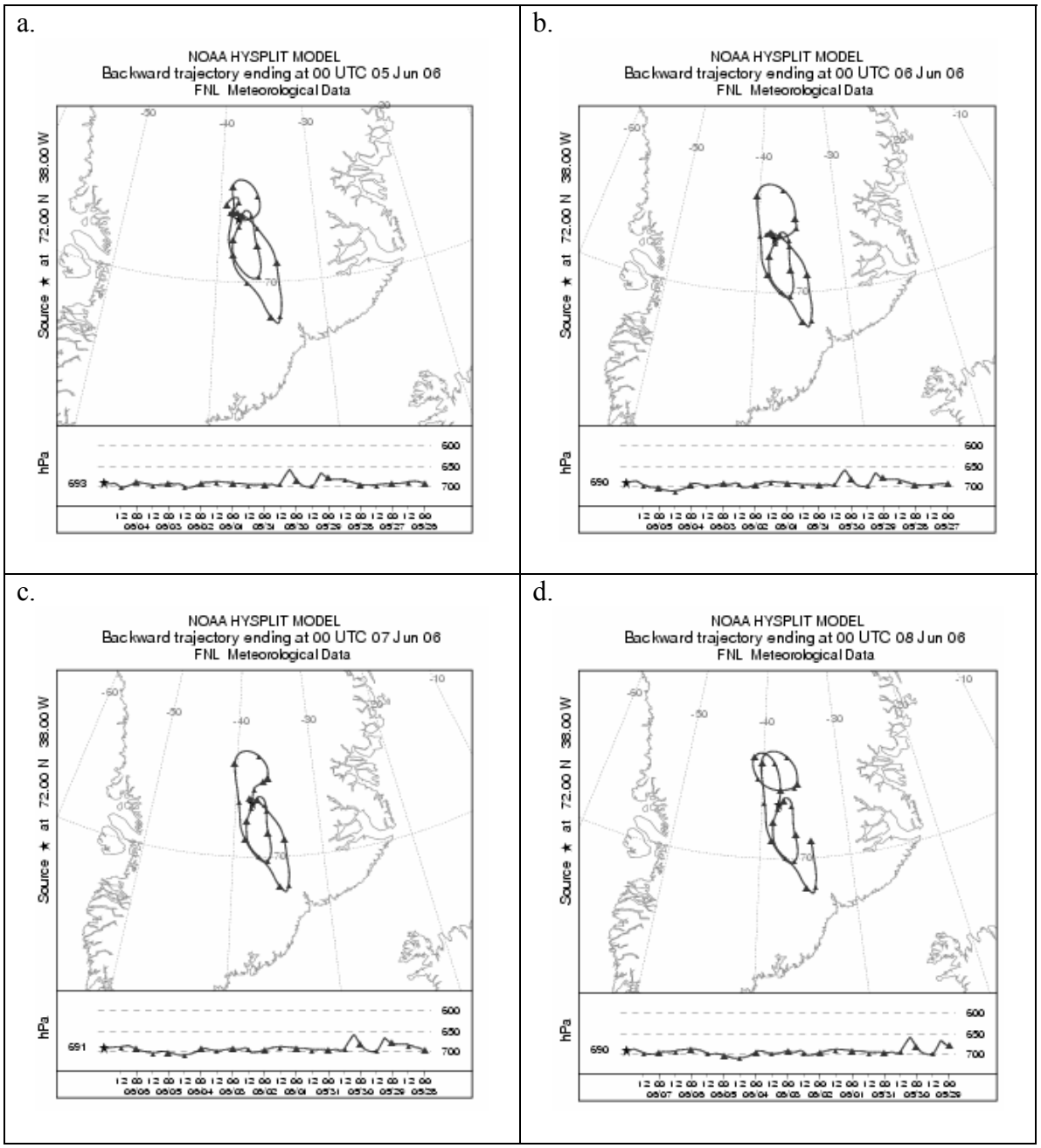

Figure D.3 Calculated 10-day isobaric trajectories arriving at Summit, Greenland on 5 June 2006 (a), 6 June 2006 (b), 7 June 2006 (c), and 8 June 2006 (d).

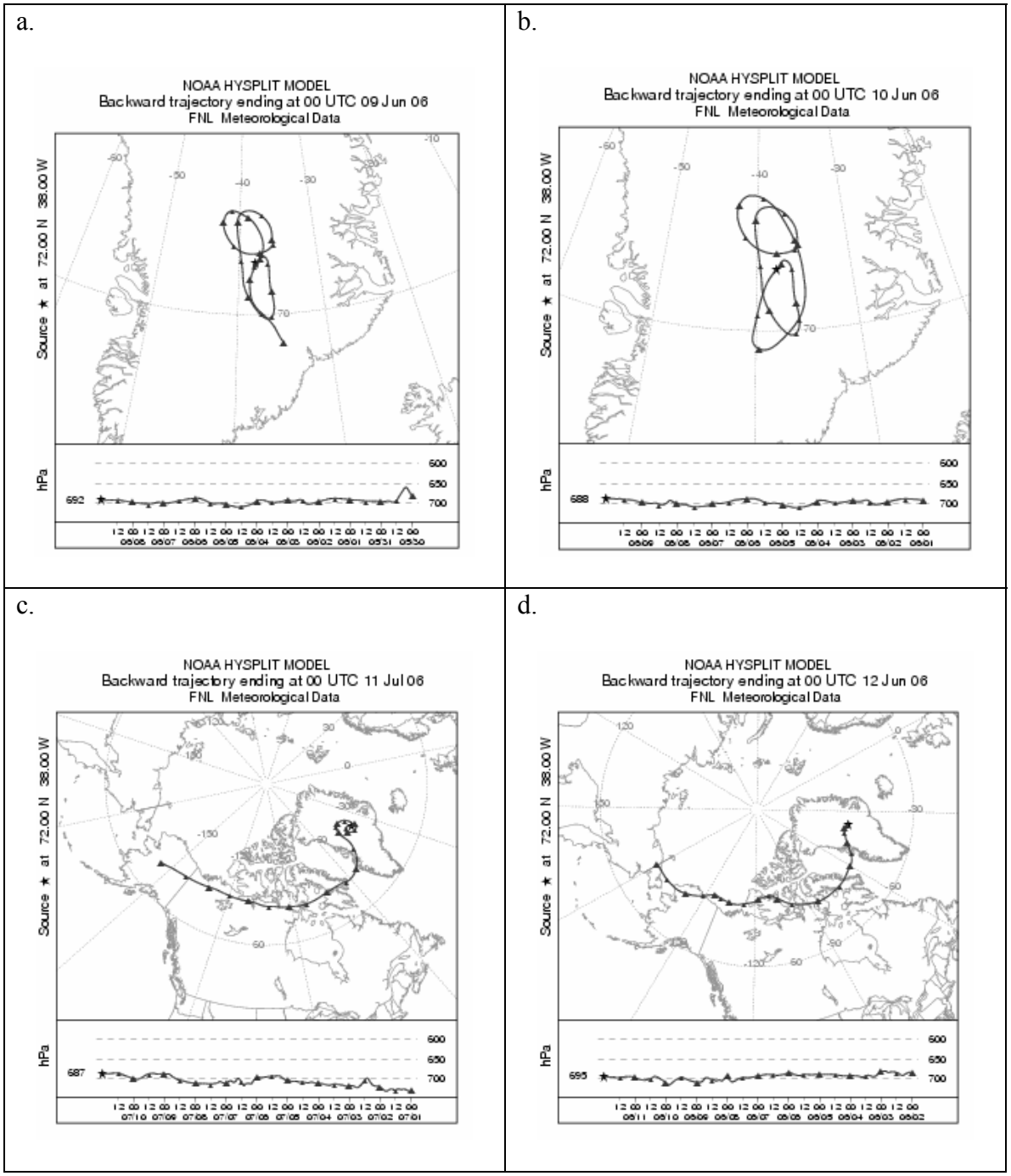

Figure D.4 Calculated 10-day isobaric trajectories arriving at Summit, Greenland on 9 June 2006 (a), 10 June 2006 (b), 11 June 2006 (c), and 12 June 2006 (d).

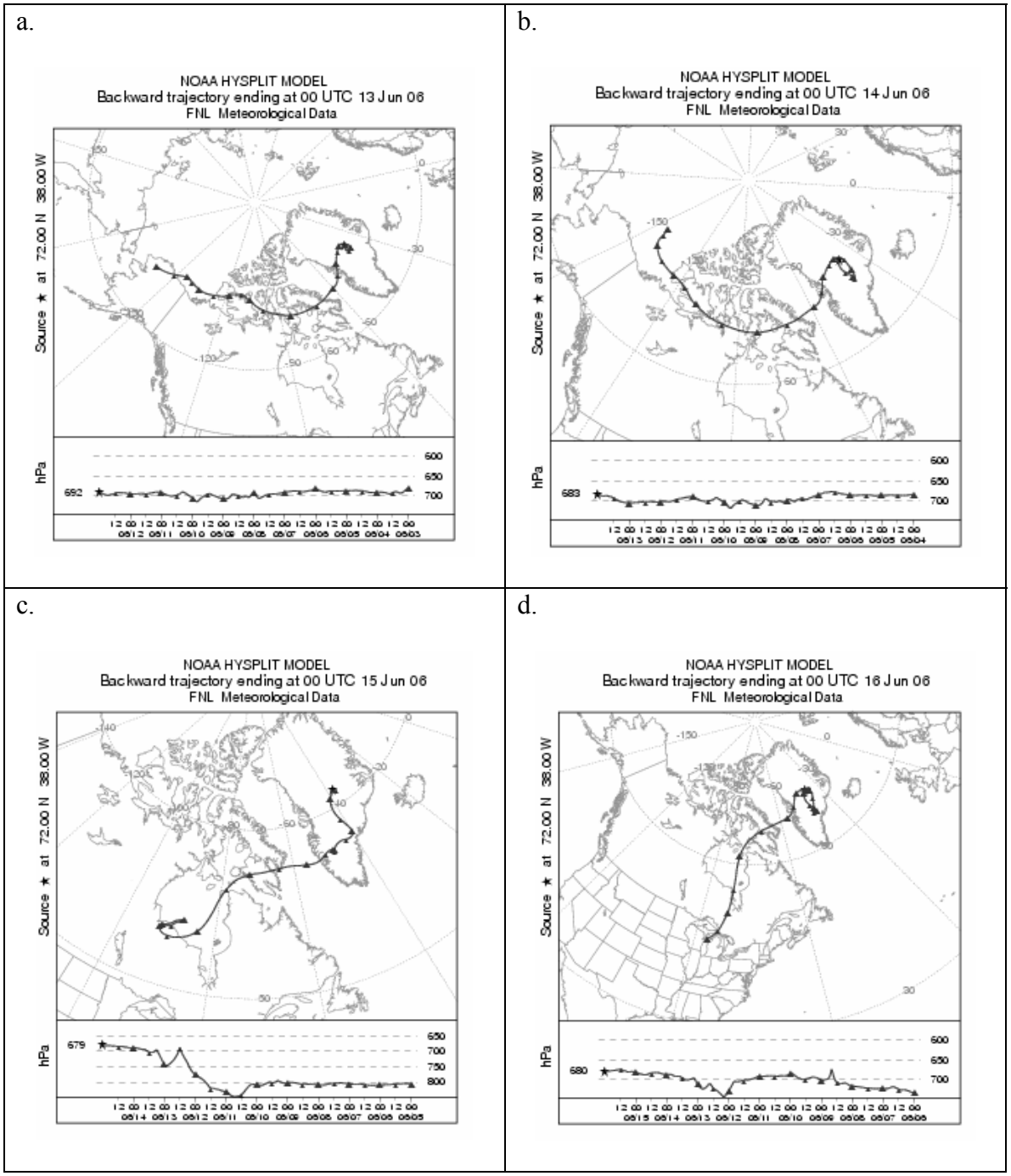

Figure D.5 Calculated 10-day isobaric trajectories arriving at Summit, Greenland on 13 June 2006 (a), 14 June 2006 (b), 15 June 2006 (c), and 16 June 2006 (d).

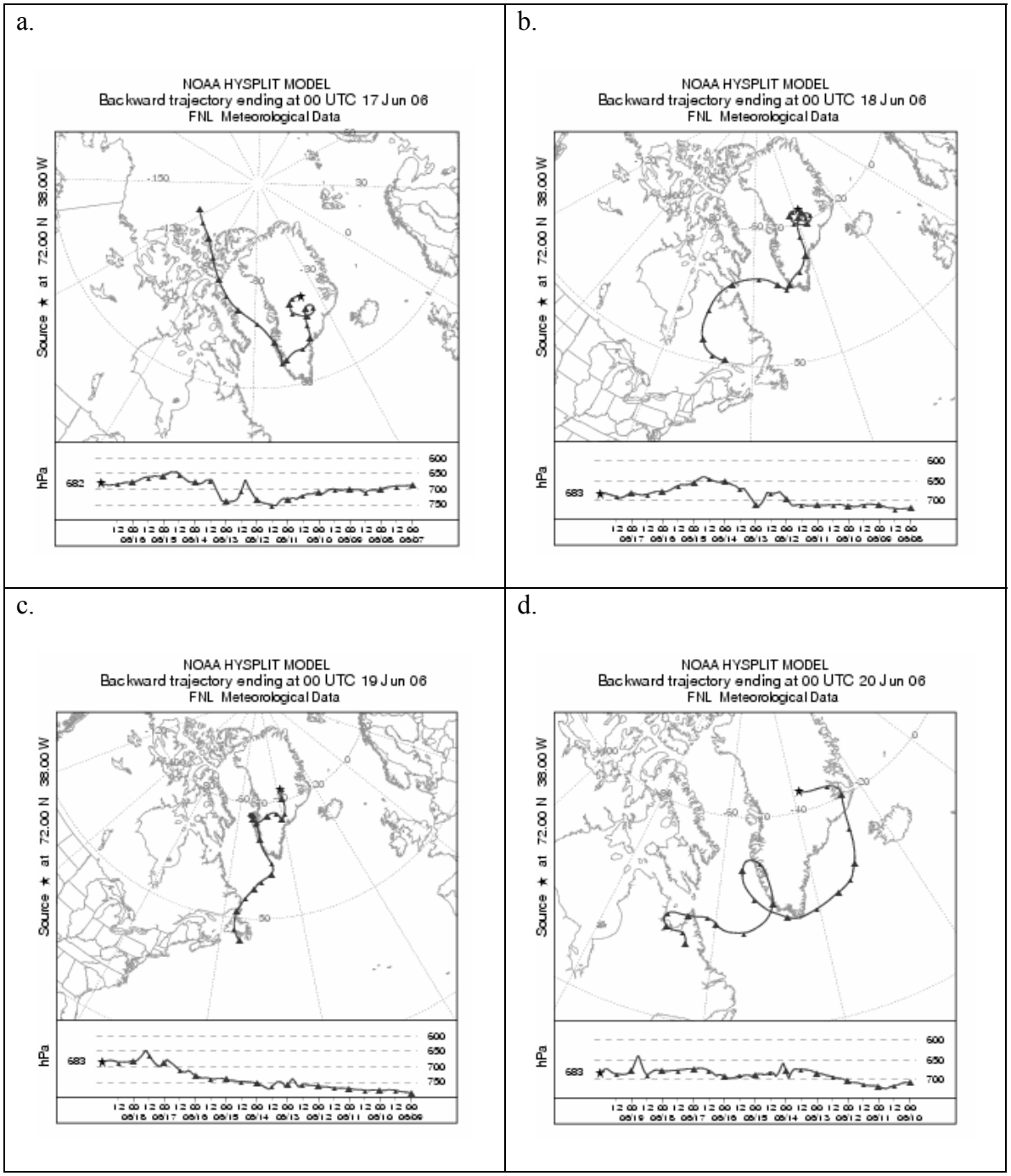

Figure D.6 Calculated 10-day isobaric trajectories arriving at Summit, Greenland on 17 June 2006 (a), 18 June 2006 (b), 19 June 2006 (c), and 20 June 2006 (d).

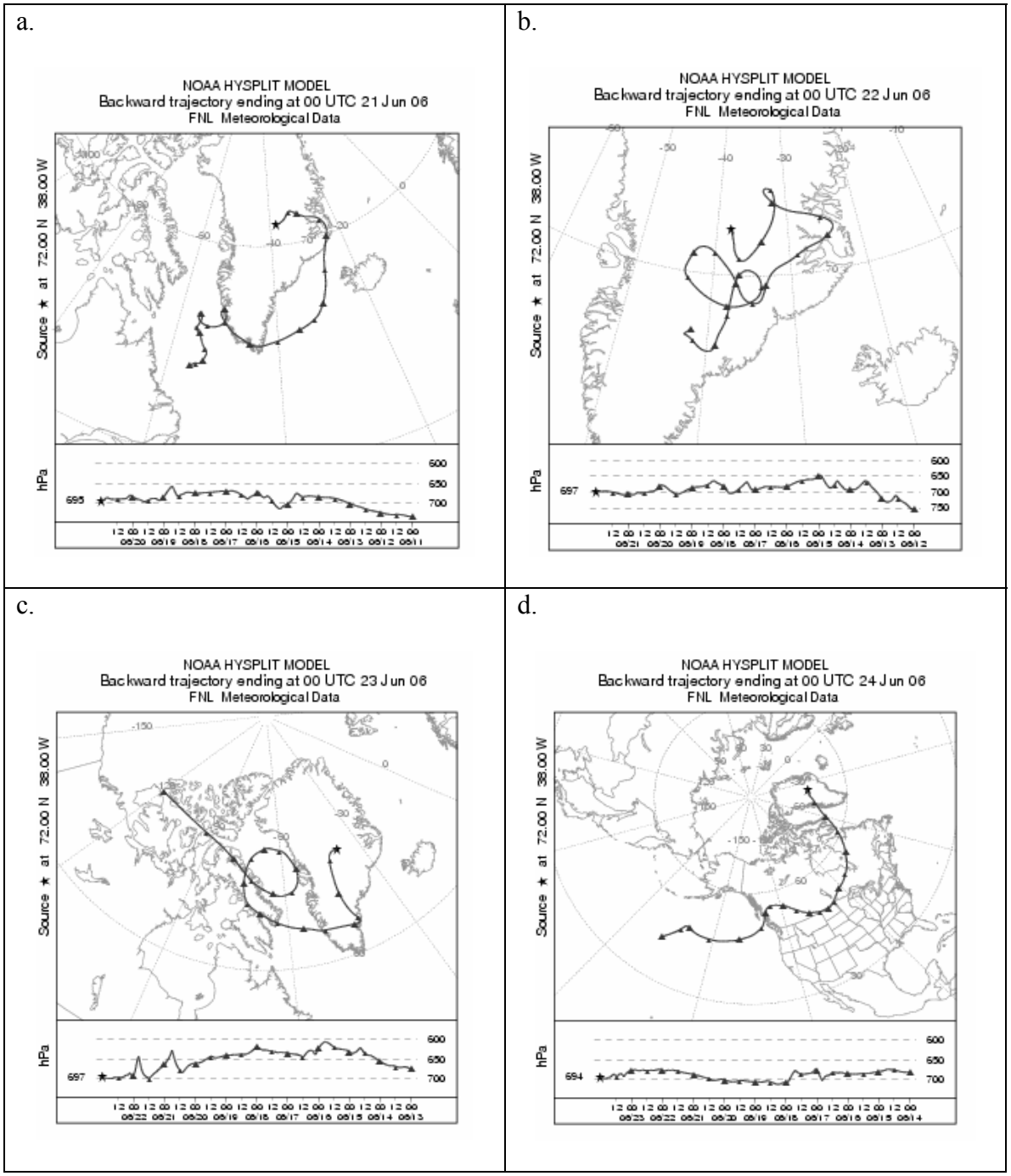

Figure D.7 Calculated 10-day isobaric trajectories arriving at Summit, Greenland on 21 June 2006 (a), 22 June 2006 (b), 23 June 2006 (c), and 24 June 2006 (d).

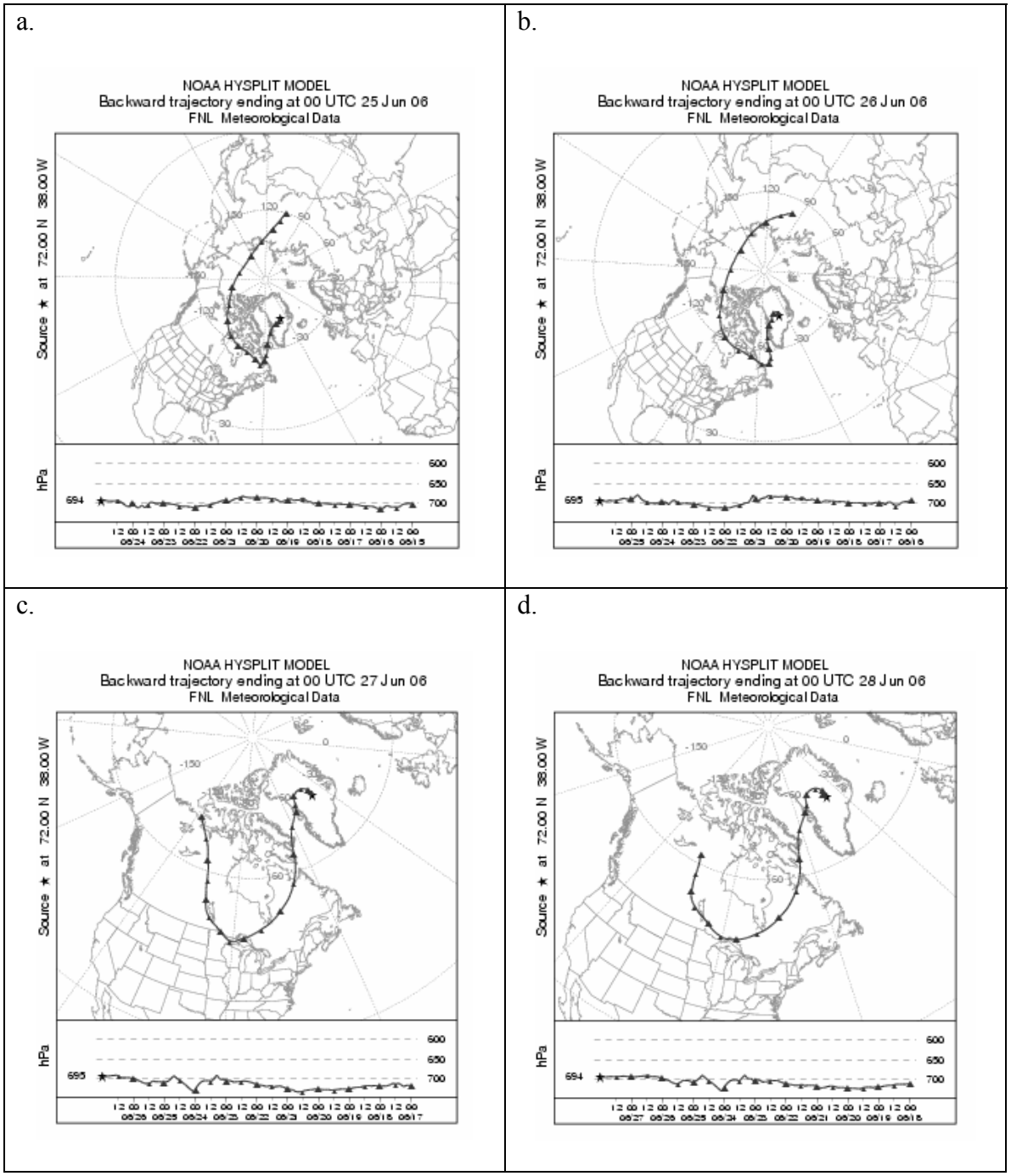

Figure D.8 Calculated 10-day isobaric trajectories arriving at Summit, Greenland on 25 June 2006 (a), 26 June 2006 (b), 27 June 2006 (c), and 28 June 2006 (d).

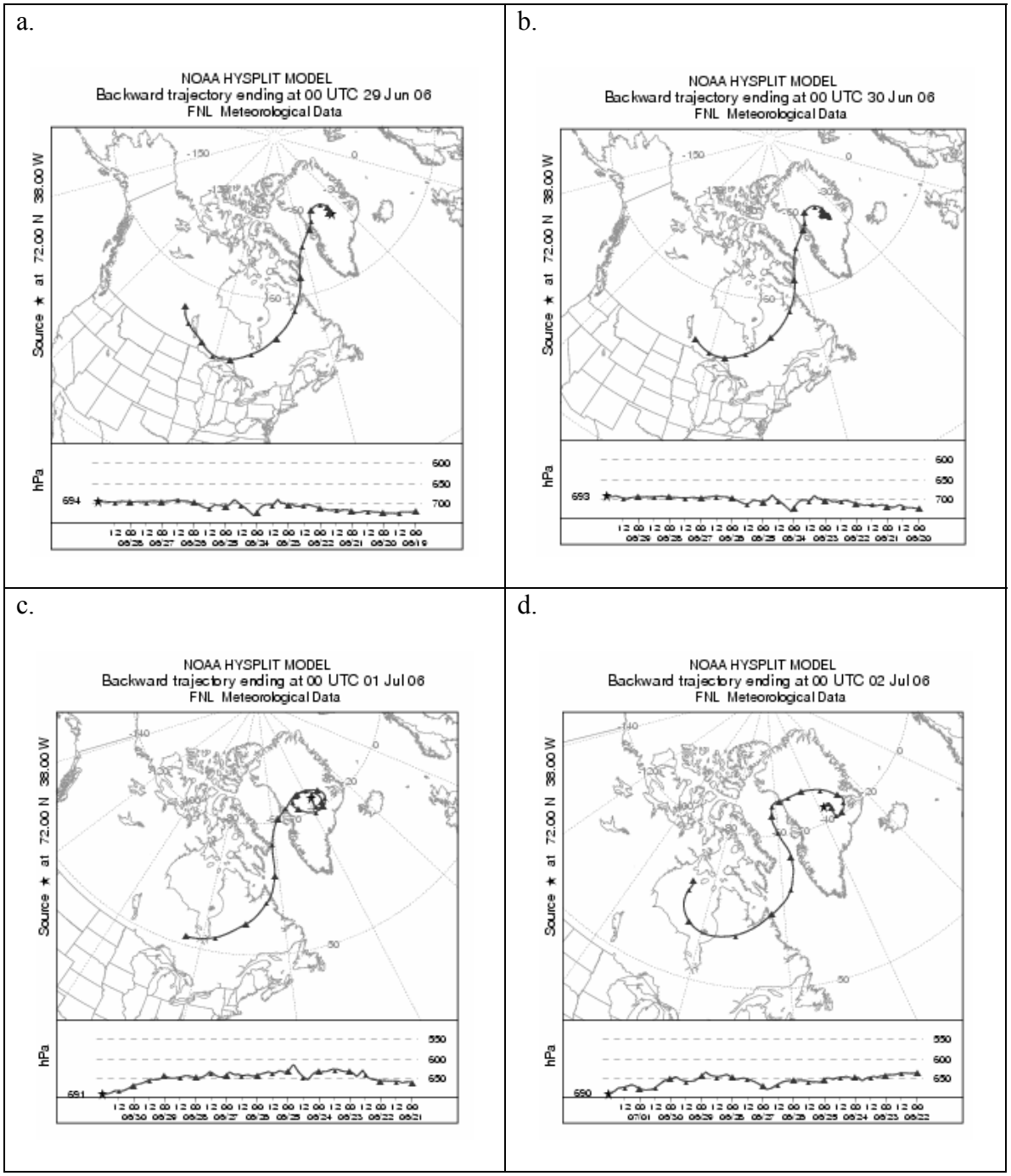

Figure D.9 Calculated 10-day isobaric trajectories arriving at Summit, Greenland on 29 June 2006 (a), 30 June 2006 (b), 1 July 2006 (c), and 2 July 2006 (d).

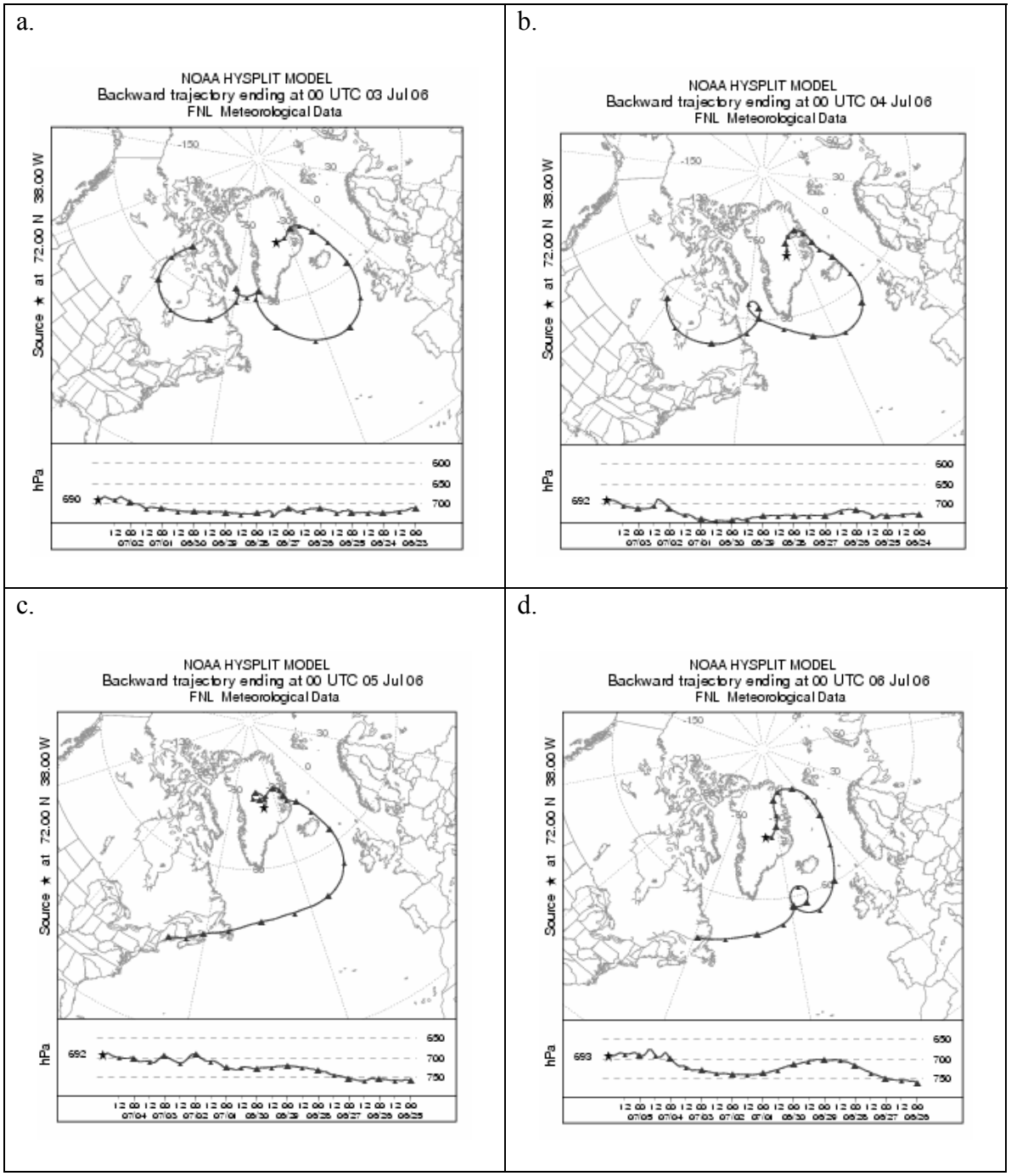

Figure D.10 Calculated 10-day isobaric trajectories arriving at Summit, Greenland on 3 July 2006 (a), 4 June 2006 (b), 5 July 2006 (c), and 6 July 2006 (d).

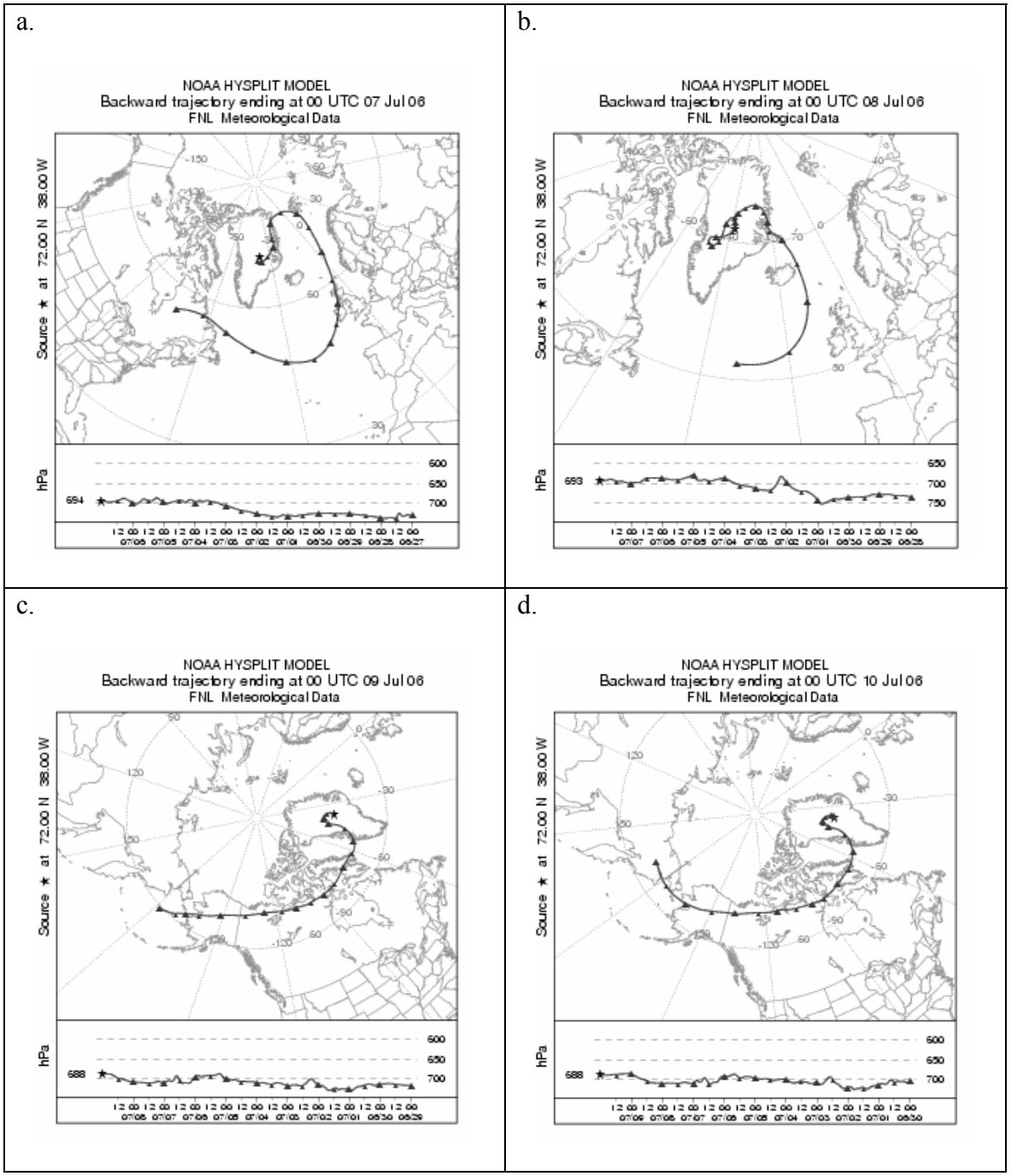

Figure D.11 Calculated 10-day isobaric trajectories arriving at Summit, Greenland on 7 July 2006 (a), 8 June 2006 (b), 9 July 2006 (c), and 10 July 2006 (d).

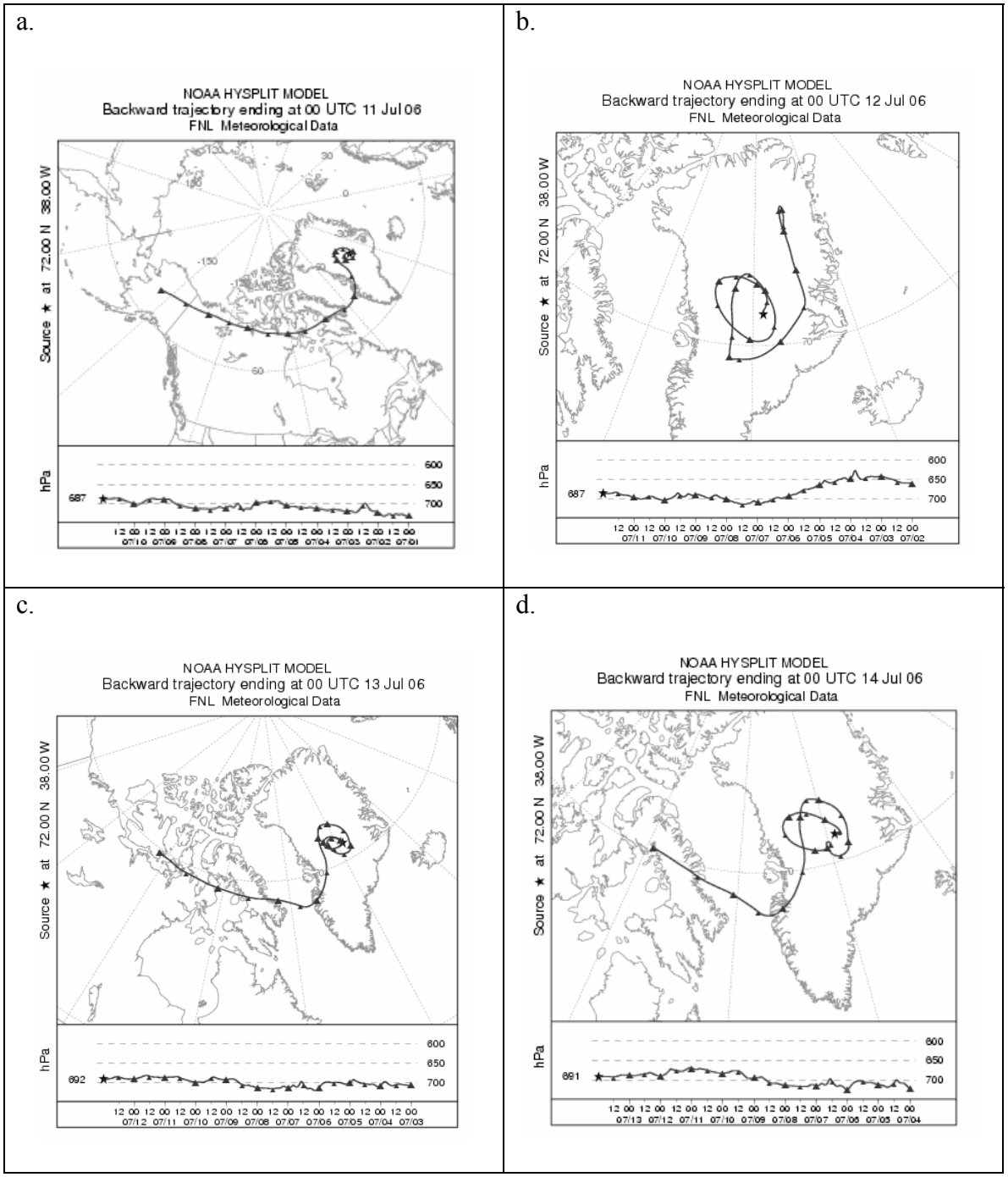

Figure D.12 Calculated 10-day isobaric trajectories arriving at Summit, Greenland on 11 July 2006 (a), 12 July 2006 (b), 13 July 2006 (c), and 14 July 2006 (d).

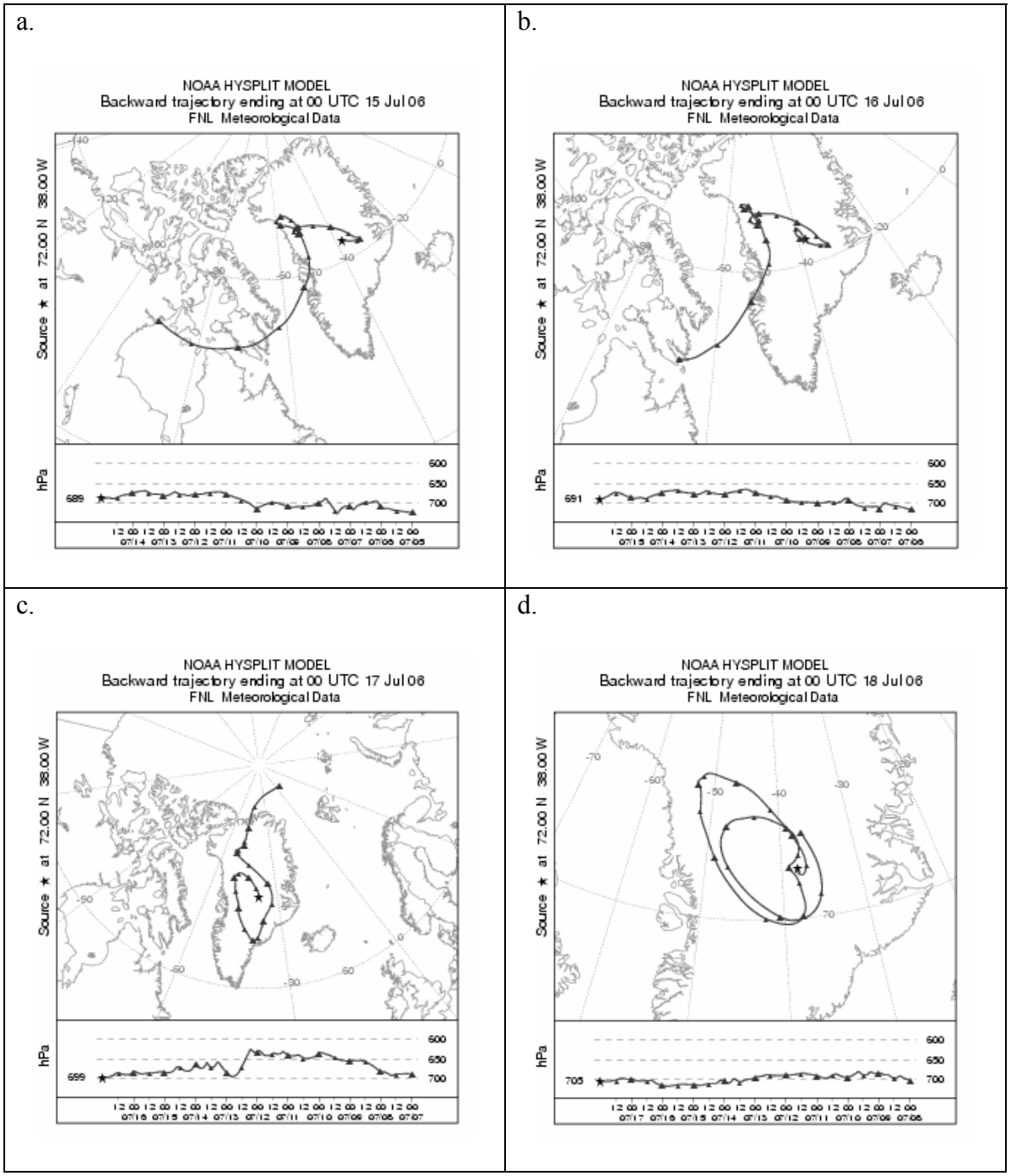

Figure D.13 Calculated 10-day isobaric trajectories arriving at Summit, Greenland on 15 July 2006 (a), 16 July 2006 (b), 17 July 2006 (c), and 18 July 2006 (d).

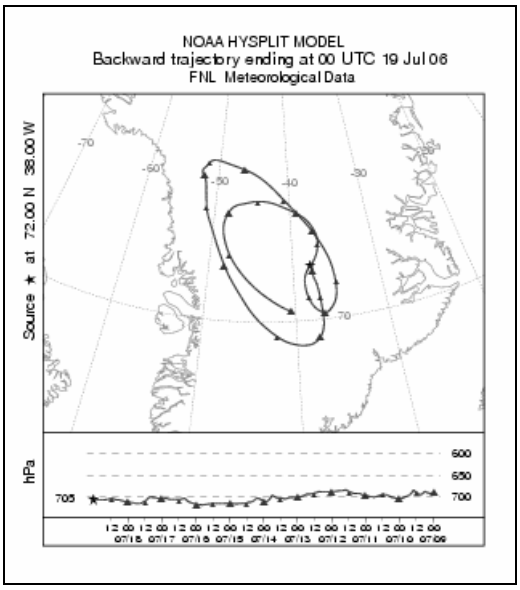

Figure D.14 Calculated 10-day isobaric trajectories arriving at Summit, Greenland on 19 July 2006.

D.2 Additional 3-meter Snow Pit Profiles – Greenland Ice Sheet, Summer 2006

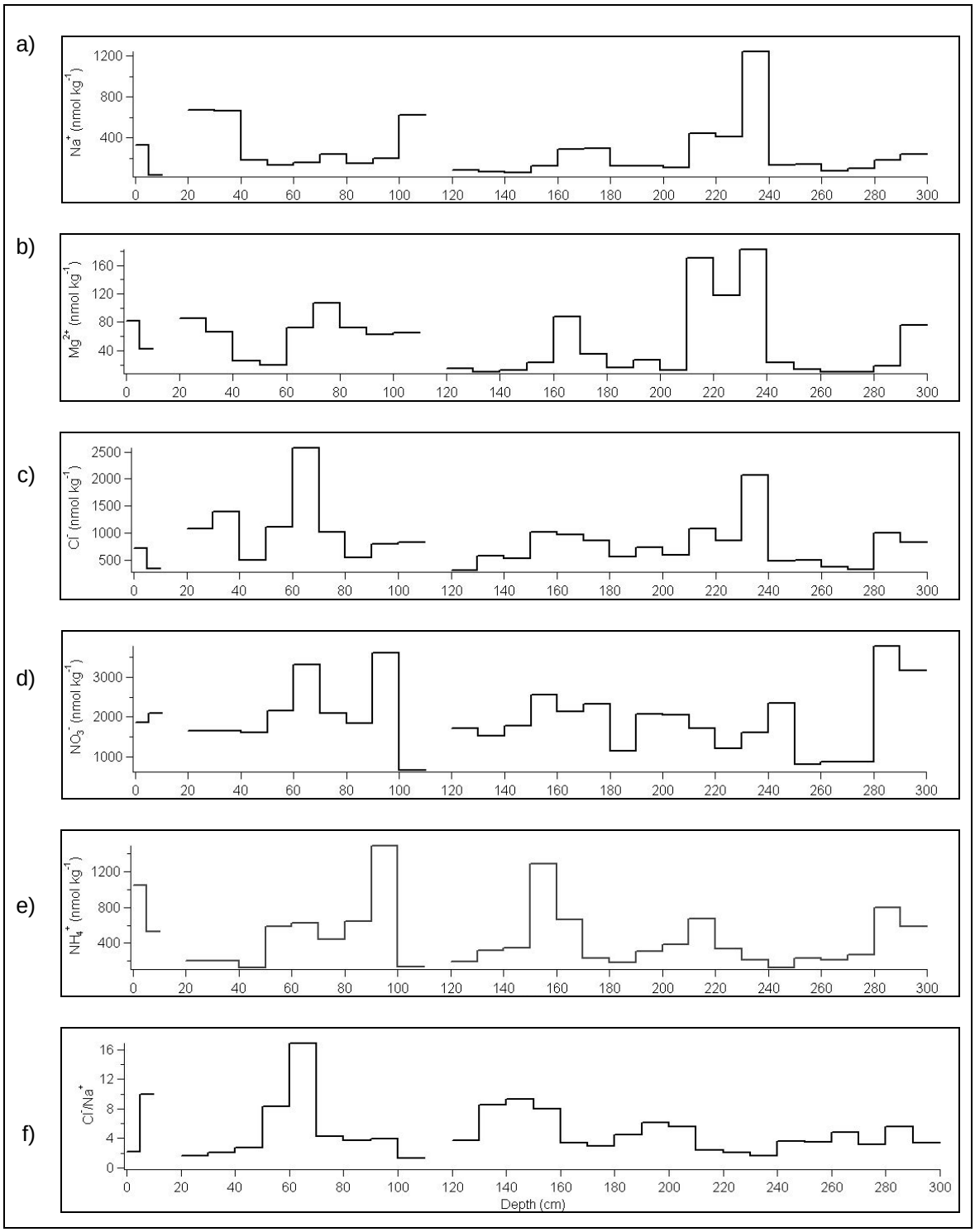

Figure D.15 Profiles of ions measured in a 3-meter snow pit at Summit, Greenland, Summer 2006.

D.3 1-meter Snow Pit Profiles – Greenland Ice Sheet, Summer 2006

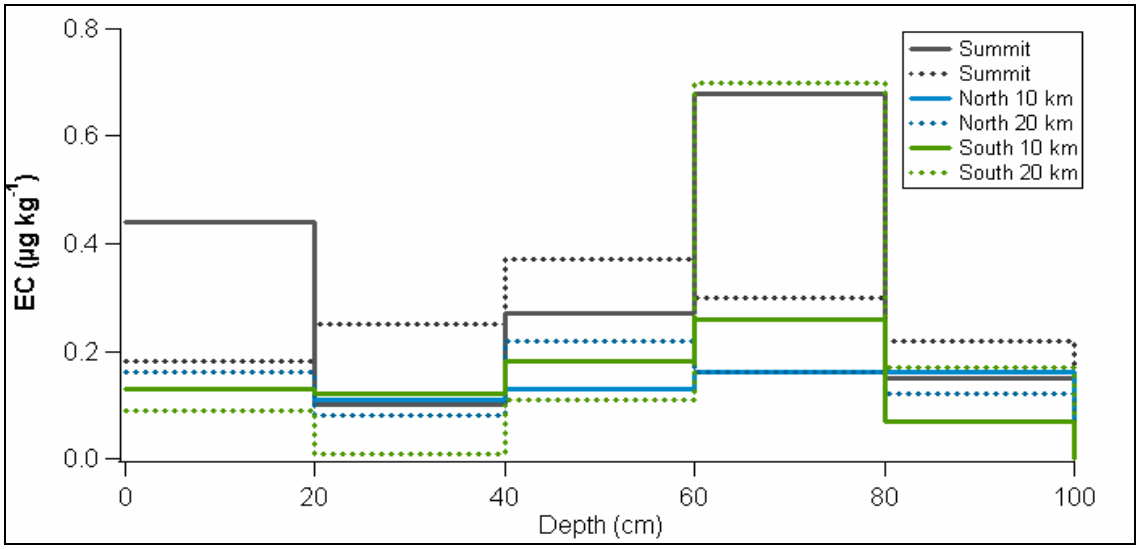

Figure D.16 1-meter profile of elemental carbon (EC) at Summit, Greenland and up to 20 km North or South of Summit, Summer 2006

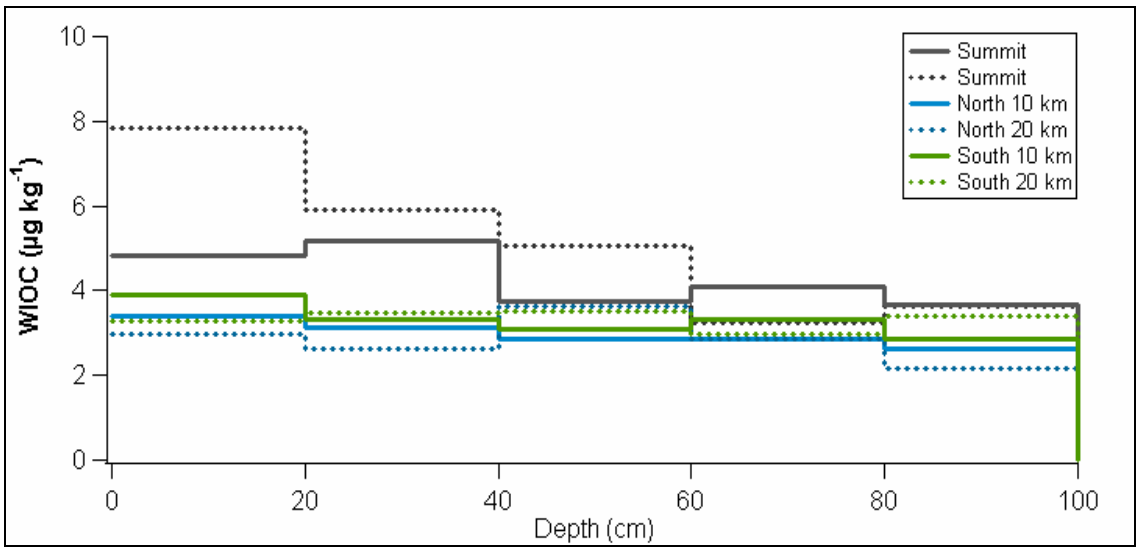

Figure D.17 1-meter profile of water-insoluble organic carbon (OC) at Summit, Greenland and up to 20 km North or South of Summit, Summer 2006

D.4 Results from the 2005 Field Campaign to the Greenland Ice Sheet

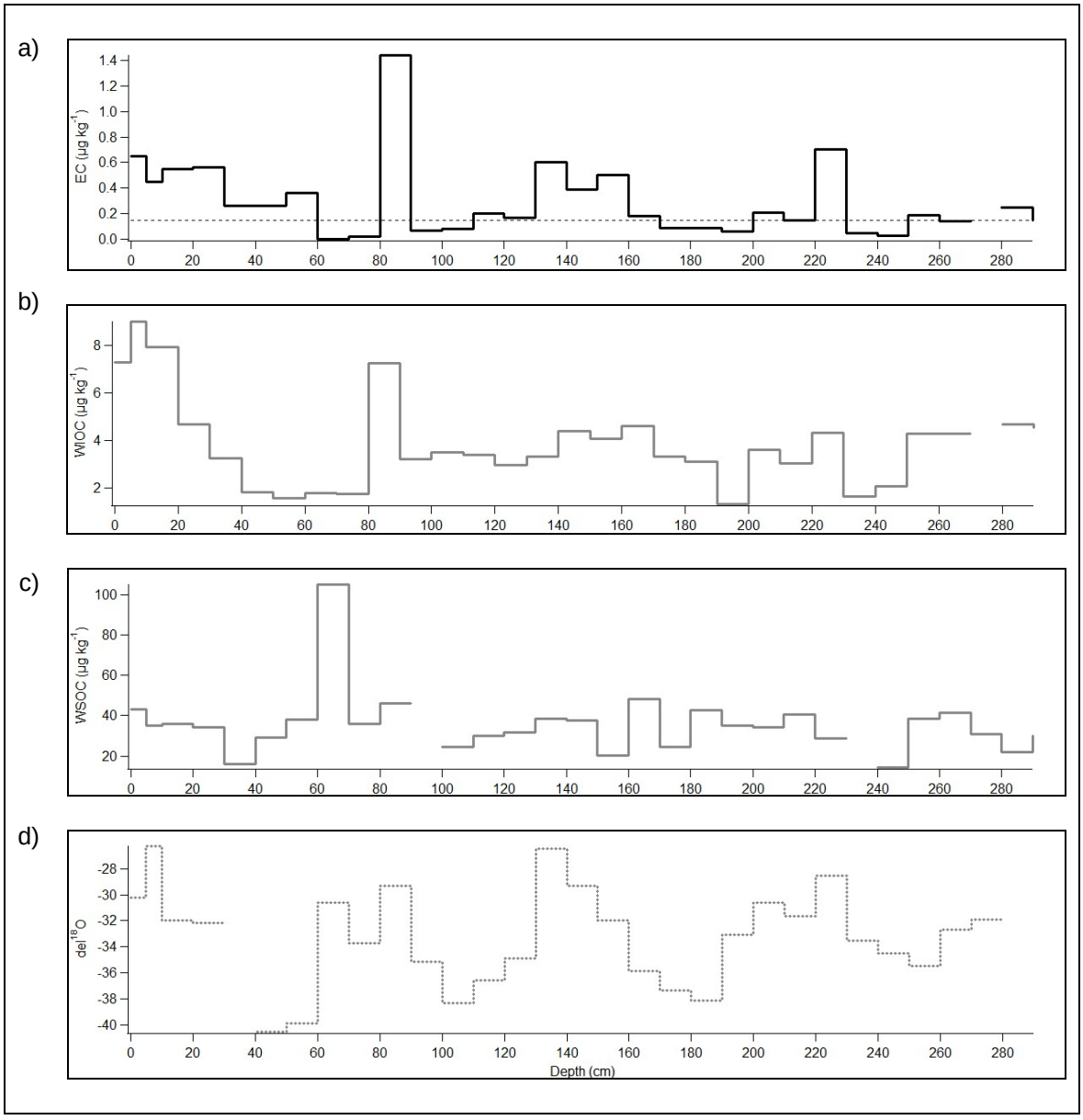

Figure D.18 3-meter snow pit carbonaceous species and oxygen-isotope ratio, Greenland Ice Sheet, July 2005. A number of EC values were below the detection limit (dashed line in (a)).

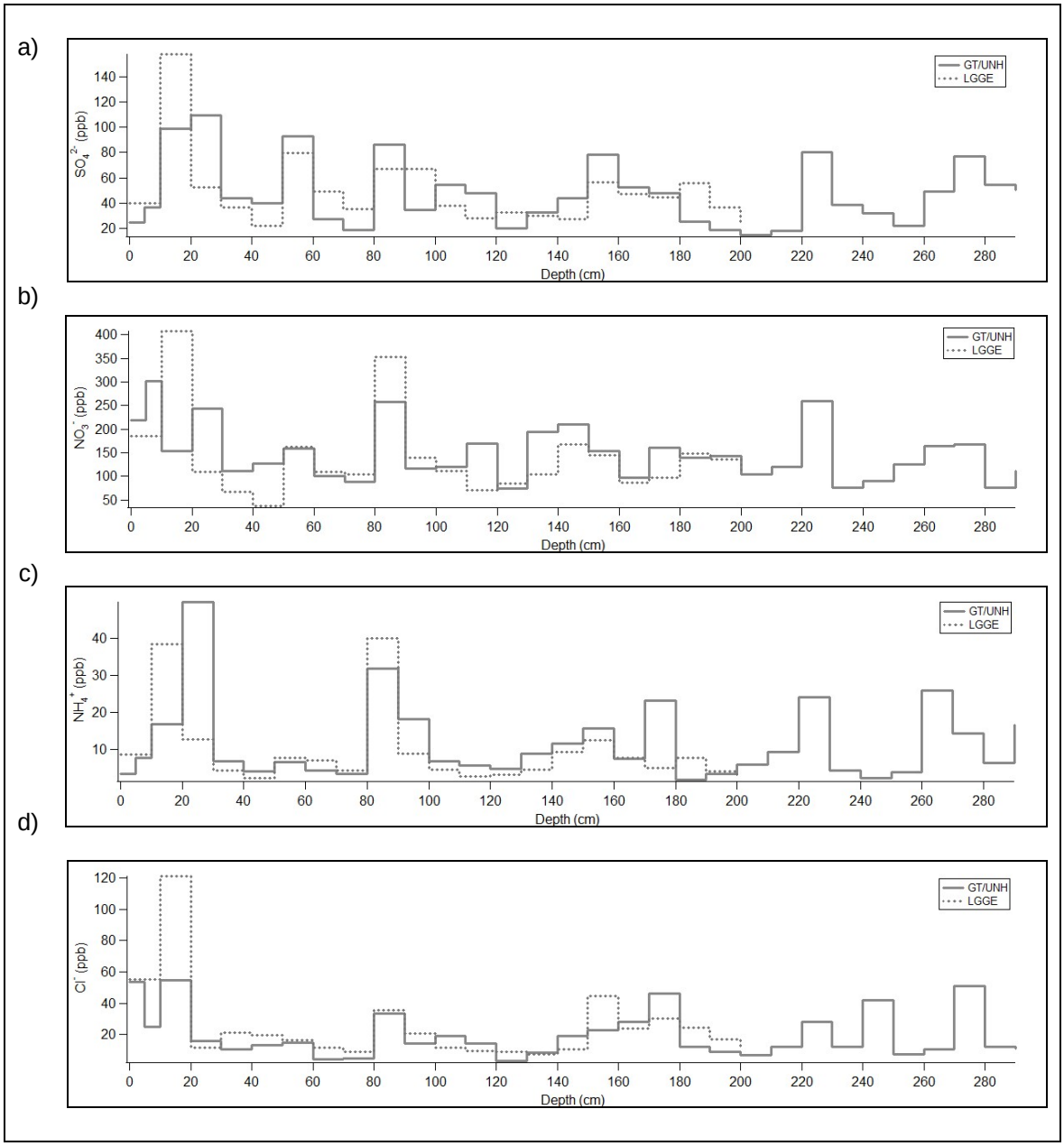

Figure D.19 3-meter snow pit ions and comparison of GT/UNH sampling with samples from a parallel 2-meter snow pit taken by the Xavier Fain of the Laboratoire de Glaciologie et Géophysique de l'Environnement (LGGE), Greenland Ice Sheet, July 2005. Several ions are not shown due to known sample-bottle contamination issues (Na^+, Mg^{2+}, Ca^{2+}).

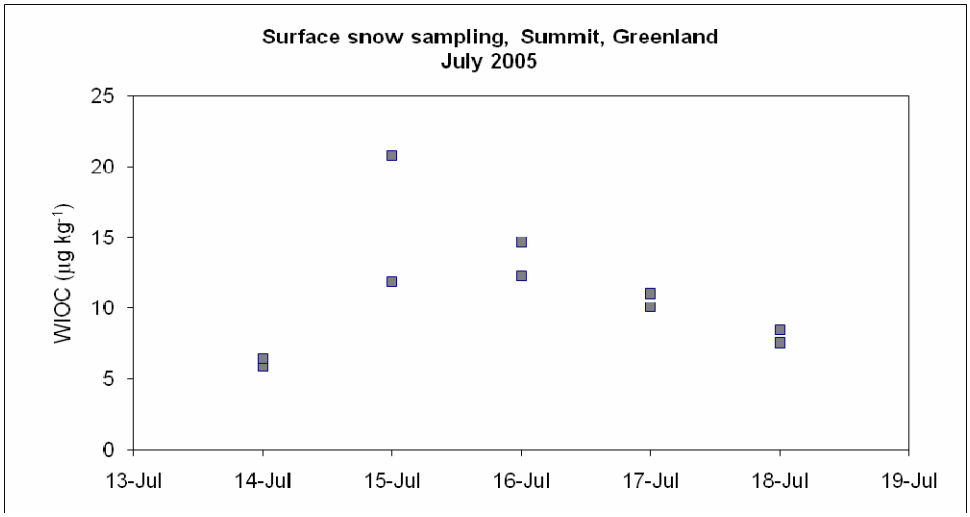

Figure D.20 Water-insoluble organic carbon (WIOC) measured in the surface snow during the July 2005 field campaign in Summit, Greenland.

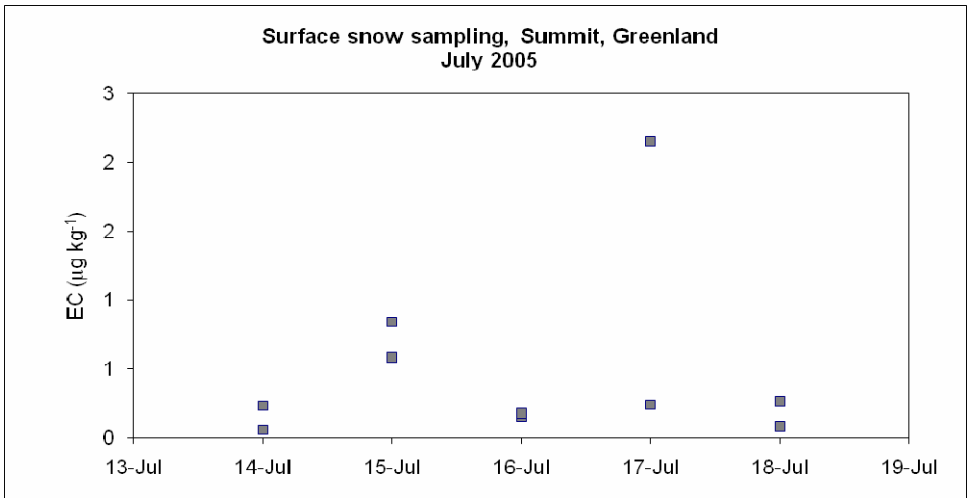

Figure D.21 Elemental carbon (EC) measured in the surface snow during the July 2005 field campaign in Summit, Greenland.

REFERENCES

Akimoto, H., Ohara, T., Kurokawa, J. and Horii, N., 2006. Verification of energy consumption in China during 1996-2003 by using satellite observational data. Atmospheric Environment, 40: 7663-7667.

Albert, M.R. and Shultz, E.F., 2002. Snow and firn properties and air-snow transport processes at Summit, Greenland. Atmospheric Environment, 36(15-16): 2789-2797.

Anderson, C. et al., 2001. Water-soluble organic carbon measurements at Summit, Greenland. Journal of Geophysical Research-Atmospheres, in preparation.

Asiaweek, 2000. Best Cities in Asia, Asiaweek.com. (Date accessed: March, 2007)

Aunan, K. and Pan, X.C., 2004. Exposure-response functions for health effects of ambient air pollution applicable for China - a meta-analysis. Science Of The Total Environment, 329(1-3): 3-16.

Bender, M. et al., 1994. Climate Correlations between Greenland and Antarctica During the Past 100,000 Years. Nature, 372(6507): 663-666.

Bergin, M.H. et al., 1995. The contributions of snow, fog, and dry deposition to the summer flux of anions and cations at Summit, Greenland. Journal of Geophysical Research-Atmospheres, 100(D8): 16275-16288.

Bergin, M.H. et al., 1995. A simple model to estimate atmospheric concentrations of aerosol chemical species based on snow core chemistry at Summit, Greenland. Geophysical Research Letters, 22: 3517-3520.

Birch, M.E. and Cary, R.A., 1996. Elemental carbon-based method for monitoring occupational exposures to particulate diesel exhaust. Aerosol Science And Technology, 25(3): 221-241.

Bolleter, W.T., Bushman, C.J. and Tidwell, P.W., 1961. Spectrophotometric determination of ammonia as indophenol. Analytical Chemistry, 33(4): 592-&.

Bond, T.C., Anderson, T.L. and Campbell, D., 1999. Calibration and intercomparison of filter-based measurements of visible light absorption by aerosols. Aerosol Science And Technology, 30(6): 582-600.

Bond, T.C. and Bergstrom, R.W., 2006. Light absorption by carbonaceous particles: An investigative review. Aerosol Science And Technology, 40(1): 27-67.

Bory, A.J.M., Biscaye, P.E., and Grousset, F.E., 2003. Two distinct seasonal Asian source regions for mineral dust deposited in Greenland (NorthGRIP). Geophysical Research Letters, 30(4).

Bory, A.J.M., Biscaye, P.E., Svensson, A., and Grousset, F.E., 2002. Seasonal variability in the origin of recent atmospheric mineral dust at NorthGRIP, Greenland. Earth and Planetary Science Letters, 196(3-4): 123-134.

Boucher, O. and Lohmann, U., 1995. The sulfate-CCN-cloud albedo effect – a sensitivity study with 2 general-circulation models. Tellus Series B-Chemical and Physical Meteorology, 47(3): 281-300.

Box, J.E., Bromwich, D.H., and Bai, L.S., 2004. Greenland ice sheet surface mass balance 1991-2000: Application of polar MM5 mesoscale model and in situ data. Journal of Geophysical Research-Atmospheres, 109(D16).

Burkhart, J.F., Hutterli, M.A., and Bales, R.C., 2002. Partitioning of formaldehyde between air and ice at -35 degrees C to -5 degrees C. Atmospheric Environment, 36(13): 2157-2163.

Cachier, H. and Pertuisot, M.H., 1994. Particulate carbon in Arctic ice. Analusis, 22(7): M34-M37.

Canadian Forest Service, 2006. Forest fires in Canada: http://fire.cfs.nrcan.gc.ca (Date accessed: March, 2007)

Cao, G., Zhang, X., and Zheng, F., 2006. Inventory of black carbon and organic carbon emissions from China. Atmospheric Environment, 40: 6516-6527.

Cao, J.J. et al., 2003. Characteristics of carbonaceous aerosol in Pearl River Delta Region, China during 2001 winter period. Atmospheric Environment, 37(11): 1451-1460.

Cao, J.J. et al., 2004. Spatial and seasonal variations of atmospheric organic carbon and elemental carbon in Pearl River Delta Region, China. Atmospheric Environment, 38(27): 4447-4456.

Carrico, C.M., Bergin, M.H., Shrestha, A.B., et al., 2003a. The importance of carbon and mineral dust to seasonal aerosol properties in the Nepal Himalaya. Atmospheric Environment, 37(20): 2811-2824.

Carrico, C.M., Bergin, M.H., Xu, J., et al., 2003b. Urban aerosol radiative properties: Measurements during the 1999 Atlanta Supersite Experiment. Journal of Geophysical Research-Atmospheres, 108(D7).

Charlson, R.J. et al., 1992. Climate forcing by anthropogenic aerosols. Science, 255 (5043): 423-430.

CH2M HILL (China) Limited, 2002. Study of air quality in the Pear River Delta Region, Commissioned by the Hong Kong Environmental Protection Department, Hong Kong Special Administrative Region Government.

Chameides, W.L. et al., 1999. Case study of the effects of atmospheric aerosols and regional haze on agriculture: An opportunity to enhance crop yields in China through emission controls? Proceedings from the National Academy of Sciences, 96(24): 13626-13633.

Cheung, H.C., Wang, T., Baumann, K. and Guo, H., 2005. Influence of regional pollution outflow on the concentrations of fine particulate matter and visibility in the coastal area of southern China. Atmospheric Environment, 39(34): 6463-6474.

Cho, H., Shepson, P.B., Barrie, L.A., Cowin, J.P. and Zaveri, R., 2002. NMR investigation of the quasi-brine layer in ice/brine mixtures. Journal of Physical Chemistry B, 106(43): 11226-11232.

Chow, J.C., Watson, J.G., Crow, D., Lowenthal, D.H. and Merrifield, T., 2001. Comparison of IMPROVE and NIOSH carbon measurements. Aerosol Science And Technology, 34(1): 23-34.

Chu, L. and Anastasio, C., 2005. Formation of hydroxyl radical from the photolysis of frozen hydrogen peroxide. Journal of Physical Chemistry A, 109(28): 6264-6271.

Chylek, P., Johnson, B., Damiano, P.A., Taylor, K.C. and Clement, P., 1995. Biomass Burning Record and Black Carbon in the Gisp2 Ice Core. Geophysical Research Letters, 22(2): 89-92.

Chylek, P. and Lohmann, U., 2005. Ratio of the Greenland to global temperature change: Comparison of observations and climate modeling results. Geophysical Research Letters, 32(14).

Clarke, A.D. and Noone, K.J., 1985. Soot in the Arctic snowpack - a cause for perturbations in radiative-transfer. Atmospheric Environment, 19(12): 2045-2053.

Cohen, D.D. et al., 2004. Multielemental analysis and characterization of fine aerosols at several key ACE-Asia sites. Journal of Geophysical Research-Atmospheres, 109(D19).

Cooke, W.F., Liousse, C., Cachier, H. and Feichter, J., 1999. Construction of a 1 degrees x 1 degrees fossil fuel emission data set for carbonaceous aerosol and implementation and radiative impact in the ECHAM4 model. Journal Of Geophysical Research-Atmospheres, 104(D18): 22137-22162.

Cullinane, S., and Cullinane, K., 2003. City profile: Hong Kong. Cities, 20(4): 279-288.

Currie, L. A., Kessler, J.D., Fletcher, R.A., and Dibb, J.E., 2005. Long range transport of biomass aerosol to Greenland: Multi-spectroscopic investigation of particles deposited in the snow, Journal of Radioanalytical and Nuclear Chemistry, 263, 399-411.

Dansgaard, W., Johnsen, S.J., Moller, J. and Langway, C.C., 1969. One thousand centuries of climatic record from Camp Century on Greenland Ice Sheet. Science, 166(3903).

Dassau, T.M. et al., 2002. Investigation of the role of the snowpack on atmospheric formaldehyde chemistry at Summit, Greenland. Journal of Geophysical Research-Atmospheres, 107(D19).

Davidson, C.I. et al., 1987. Radioactive Cesium from the Chernobyl Accident in the Greenland Ice-Sheet. Science, 237(4815): 633-634.

Dibb, J.E. and Arsenault, M., 2002. Shouldn't snowpacks be sources of monocarboxylic acids? Atmospheric Environment, 36(15-16): 2513-2522.

Dibb, J.E. and Fahnestock, M., 2004. Snow accumulation, surface height change, and firn densification at Summit, Greenland: Insights from 2 years of in situ observation. Journal of Geophysical Research-Atmospheres, 109(D24).

Dibb, J.E., Talbot, R.W. and Bergin, M.H., 1994. Soluble Acidic Species in Air and Snow at Summit, Greenland. Geophysical Research Letters, 21(15): 1627-1630.

Dibb, J.E., et al., 1996. Biomass burning signatures in the atmosphere and snow at Summit, Greenland: An event on 5 August 1994. Atmospheric Environment, 30: 553-561.

Dibb, J.E., Whitlow, S.I. and Arsenault, M., 2007. Seasonal variations in the soluble ion content of snow at Summit, Greenland: Constraints from three years of daily surface snow samples. Atmospheric Environment, In press.

Dockery, D.W. et al., 1993. An association between air pollution and mortality in 6 United States cities. New England Journal of Medicine, 329(24): 1753-1759.

Dolinova, J., Ruzicka, R., Kurkova, R., Klanova, J. and Klan, P., 2006. Oxidation of aromatic and aliphatic hydrocarbons by OH radicals photochemically generated from H2O2 in ice. Environmental Science & Technology, 40(24): 7668-7674.

Donarummo, J., Ram, M. and Stoermer, E.F., 2003. Possible deposit of soil dust from the 1930's U.S. dust bowl identified in Greenland ice. Geophysical Research Letters, 30(6).

Drab, E., Gaudichet, A., Jaffrezo, J.L. and Colin, J.L., 2002. Mineral particles content in recent snow at Summit (Greenland). Atmospheric Environment, 36(34): 5365-5376.

Draxler, R.R. and Rolph, G.D., 2003. HYSPLIT (HYbrid Single-Particle Lagrangian Integrated Trajectory) Model access via NOAA ARL READY Website (http://www.arl.noaa.gov/ready/hysplit4.html). NOAA Air Resources Laboratory, Silver Spring, MD. (Date accessed: October, 2006)

Ducret, J. and Cachier, H., 1992. Particulate Carbon Content in Rain at Various Temperate and Tropical Locations. Journal of Atmospheric Chemistry, 15(1): 55-67.

Elmore, D. et al., 1982. Cl-36 Bomb Pulse Measured in a Shallow Ice Core from Dye-3, Greenland. Nature, 300(5894): 735-737.

Englert, N., 2004. Fine particles and human health – a review of epidemiological studies. Toxicology Letters, 149(1-3): 235-242.

Enright, M. and Scott, E., 2002. Boom times on our doorstep. South China Morning Post 25/11/02, 14.

EPA, 1998. Quality Assurance Guidance Document 2.12. US Environmental Protection Agency.

Ford, K.M. et al., 2002. Studies of Peroxyacetyl nitrate (PAN) and its interaction with the snowpack at Summit, Greenland. Journal of Geophysical Research-Atmospheres, 107(D10).

Fung, K., Chow, J.C. and Watson, J.G., 2002. Evaluation of OC/EC speciation by thermal manganese dioxide oxidation and the IMPROVE method. Journal Of The Air & Waste Management Association, 52(11): 1333-1341.

Galbavy, E., Anastasio, C., Lefer, B. and Hall, S., 2006. Light Penetration in the Snowpack at Summit, Greenland: Part 2: Nitrate Photolysis. Atmospheric Environment.

Grannas, A.M., Shepson, P.B. and Filley, T.R., 2004. Photochemistry and nature of organic matter in Arctic and Antarctic snow. Global Biogeochemical Cycles, 18(1).

Hanna, E. et al., 2005. Runoff and mass balance of the Greenland ice sheet: 1958-2003. Journal of Geophysical Research-Atmospheres, 110(D13).

Hansen, J. and Nazarenko, L., 2004. Soot climate forcing via snow and ice albedos. Proceedings of the National

Haywood, J.M. and Shine, K.P., 1995. The effect of anthropogenic sulfate and soot aerosol on the clear-sky planetary radiation budget. Geophysical Research Letters, 22(5): 603-606.

Haywood, J. and Boucher, O., 2000. Estimates of the direct and indirect radiative forcing due to tropospheric aerosols: A review. Reviews of Geophysics, 38(4): 513-543.

Herbert, B.M.J., Halsall, C.J., Villa, S., Jones, K.C. and Kallenborn, R., 2005. Rapid changes in PCB and OC pesticide concentrations in Arctic snow. Environmental Science & Technology, 39(9): 2998-3005.

Ho, K.F. et al., 2003. Characterization of chemical species in $PM_{2.5}$ and PM_{10} aerosols in Hong Kong. Atmospheric Environment, 37(1): 31-39.

Ho, K.F., Lee, S.C., Yu, J.C., Zou, S.C. and Fung, K., 2002. Carbonaceous characteristics of atmospheric particulate matter in Hong Kong. Science Of The Total Environment, 300(1-3): 59-67.

Hong, S.M., Candelone, J.P., Patterson, C.C. and Boutron, C.F., 1994. Greenland Ice Evidence of Hemispheric Lead Pollution 2-Millennia Ago by Greek and Roman Civilizations. Science, 265(5180): 1841-1843.

Hutterli, M.A., Rothlisberger, R. and Bales, R.C., 1999. Atmosphere-to-snow-to-firn transfer studies of HCHO at Summit, Greenland. Geophysical Research Letters, 26(12): 1691-1694.

IPCC (Editor), 2001. Climate Change 2001: The Scientific Basis. Contribution of Working Group I to the Third Assessment Report of the Intergovernmental Panel on Climate Change. Cambridge University Press, Cambridge, United Kingdom and New York, NY, USA, 881 pp.

Jacobi, H.W. et al., 2004. Reactive trace gases measured in the interstitial air of surface snow at Summit, Greenland. Atmospheric Environment, 38(12): 1687-1697.

Jacobi, H.W. et al., 2002. Measurements of hydrogen peroxide and formaldehyde exchange between the atmosphere and surface snow at Summit, Greenland. Atmospheric Environment, 36(15-16): 2619-2628.

Jacobson, M.Z., 2004. Climate response of fossil fuel and biofuel soot, accounting for soot's feedback to snow and sea ice albedo and emissivity. Journal of Geophysical Research-Atmospheres, 109(D21).

Jaffrezo, J.L., Clain, M.P. and Masclet, P., 1994. Polycyclic Aromatic-Hydrocarbons in the Polar Ice of Greenland - Geochemical Use of These Atmospheric Tracers. Atmospheric Environment, 28(6): 1139-1145.

Jaffrezo, J.L. et al., 1998. Biomass burning signatures in the atmosphere of central Greenland. Journal of Geophysical Research-Atmospheres, 103(D23): 31067-31078.

John, W. and Reischl, G., 1980. A Cyclone For Size-Selective Sampling Of Ambient Air. Journal Of The Air Pollution Control Association, 30(8): 872-876.

Jones, A., Roberts, D.L., and Slingo, A., 1994. A climate model study of indirect radiative forcing by anthropogenic sulfate aerosols. Nature, 370(6489): 450-453.

Kahl, J.D.W. et al., 1997. Air mass trajectories to Summit, Greenland: A 44-year climatology and some episodic events. Journal of Geophysical Research-Oceans, 102(C12): 26861-26875.

Kan, H.D. and Chen, B.H., 2004. Particulate air pollution in urban areas of Shanghai, China: health-based economic assessment. Science of the Total Environment, 322(1-3): 71-79.

Klan, P., Klanova, J., Holoubek, I. and Cupr, P., 2003. Photochemical activity of organic compounds in ice induced by sunlight irradiation: The Svalbard project. Geophysical Research Letters, 30(6).

Koch, D. and Hansen, J., 2005. Distant origins of Arctic black carbon: A Goddard Institute for Space Studies ModelE experiment. Journal of Geophysical Research-Atmospheres, 110(D4).

Lavanchy, V.M.H., Gaggeler, H.W., Schotterer, U., Schwikowski, M. and Baltensperger, U., 1999. Historical record of carbonaceous particle concentrations from a European high-alpine glacier (Colle Gnifetti, Switzerland). Journal Of Geophysical Research-Atmospheres, 104(D17): 21227-21236.

Lee, E., Chan, C.K. and Paatero, P., 1999. Application of positive matrix factorization in source apportionment of particulate pollutants in Hong Kong. Atmospheric Environment, 33(19): 3201-3212.

Lee, J.H., Kim, Y.P., Moon, K.C., Kim, H.K. and Lee, C.B., 2001. Fine particle measurements at two background sites in Korea between 1996 and 1997. Atmospheric Environment, 35(4): 635-643.

Lee, Y.L. and Sequeira, R., 2002. Water-soluble aerosol and visibility degradation in Hong Kong during autumn and early winter, 1998. Environmental Pollution, 116(2): 225-233.

Legrand, M., Deangelis, M., Staffelbach, T., Neftel, A. and Stauffer, B., 1992. Large Perturbations of Ammonium and Organic-Acids Content in the Summit-Greenland Ice Core - Fingerprint from Forest-Fires. Geophysical Research Letters, 19(5): 473-475.

Liu, H.P., Chan, J.C.L. and Cheng, A.Y.S., 2001. Internal boundary layer structure under sea-breeze conditions in Hong Kong. Atmospheric Environment, 35: 683-692.

Lough, G. et al., 2005. Emissions of metals associated with motor vehicle roadways. Environmental Science & Technology, 39(3): 826-836.

Louie, P.K.K. et al., 2005. PM2.5 chemical composition in Hong Kong: Urban and regional variations. Science Of The Total Environment, 338(3): 267-281.

Man, C.K. and Shih, M.Y., 2001. Light scattering and absorption properties of aerosol particles in Hong Kong. Journal of Aerosol Science, 32(6): 795-804.

Masclet, P., Hoyau, V., Jaffrezo, J. and Legrand, M., 1995. Evidence for the Presence of Polycyclic Aromatic-Hydrocarbons in the Polar Atmosphere and in the Polar Ice of Greenland. Analusis, 23(6): 250-252.

Masclet, P., Hoyau, V., Jaffrezo, J.L. and Cachier, H., 2000. Polycyclic aromatic hydrocarbon deposition on the ice sheet of Greenland. Part I: Superficial snow. Atmospheric Environment, 34(19): 3195-3207.

Mayewski, P.A. et al., 1986. Sulfate and Nitrate Concentrations from a South Greenland Ice Core. Science, 232(4753): 975-977.

McConnell, J.R., Lamorey, G.W. and Hutterli, M.A., 2002. A 250-year high-resolution record of Pb flux and crustal enrichment in central Greenland. Geophysical Research Letters, 29(23).

Meese, D.A. et al., 1997. The Greenland Ice Sheet Project 2 depth-age scale: Methods and results. Journal of Geophysical Research-Oceans, 102(C12): 26411-26423.

Miyazaki, Y. et al., 2006. Time-resolved measurements of water-soluble organic carbon in Tokyo. Journal Of Geophysical Research-Atmospheres, 111(D23).

National Bureau of Statistics, 2000. China statistical yearbook. Beijing: China Statistics Press.

Nriagu, J.O. and Pacyna, J.M., 1988. Quantitative Assessment of Worldwide Contamination of Air, Water and Soils by Trace-Metals. Nature, 333(6169): 134-139.

Pathak, R.K., Yao, X.H., Lau, A.K.H. and Chan, C.K., 2003. Acidity and concentrations of ionic species of PM2.5 in Hong Kong. Atmospheric Environment, 37(8): 1113-1124.

Patris, N. et al., 2002. First sulfur isotope measurements in central Greenland ice cores along the preindustrial and industrial periods. Journal of Geophysical Research-Atmospheres, 107(D11).

Pope, C.A. et al., 2002. Lung cancer, cardiopulmonary mortality, and long-term exposure to fine particulate air pollution. Journal of the American Medical Association, 287(9): 1132-1141.

Qian, Y., 2003. How Reform Worked in China. In Search of Prosperity. Princeton University Press, Princeton.

Qian, Z.M., Zhang, J.F., Wei, F.H., Wilson, W.E. and Chapman, R.S., 2001. Long-term ambient air pollution levels in four Chinese cities: inter-city and intra-city concentration gradients for epidemiological studies. Journal of Exposure Analysis and Environmental Epidemiology, 11(5): 341-351.

Qin, Y., Chan, C.K. and Chan, L.Y., 1997. Characteristics of chemical compositions of atmospheric aerosols in Hong Kong: spatial and seasonal distributions. Science of the Total Environment, 206(1): 25-37.

Roberts, D.L. and Jones, A., 2004. Climate sensitivity to black carbon aerosol from fossil fuel combustion. Journal of Geophysical Research-Atmospheres, 109(D16).

Roth, C.M., Goss, K.U. and Schwarzenbach, R.P., 2004. Sorption of diverse organic vapors to snow. Environmental Science & Technology, 38(15): 4078-4084.

Russell, L.M., 2003. Aerosol organic-mass-to-organic-carbon ratio measurements. Abstracts Of Papers Of The American Chemical Society, 225: U817-U818.

Schauer, J.J., Rogge, W.F., Hildemann, L.M., Mazurek, M.A. and Cass, G.R., 1996. Source apportionment of airborne particulate matter using organic compounds as tracers. Atmospheric Environment, 30(22): 3837-3855.

Schwartz, J., Dockery, D.W., and Neas, L.M., 1996. Is daily mortality associated specifically with fine particles? Journal of the Air & Waste Management Association, 46(10): 927-939.

Schwartz, S.E., 1996. The Whitehouse effect – Shortwave radiative forcing of climate by anthropogenic aerosols: An overview. Journal of Aerosol Science, 27(3): 359-382.

Simoneit, B.R.T. et al., 1999. Levoglucosan, a tracer for cellulose in biomass burning and atmospheric particles. Atmospheric Environment, 33(2): 173-182.

Sjostedt, S.J., et al., 2007. Observations of hydroxyl and the sum of peroxy radicals at Summit, Greenland during summer 2003. Atmospheric Environment, doi:10.1016/j.atmosenv.2006.06.065.

Slater, J.F., Currie, L.A., Dibb, J.E. and Benner, B.A., 2002. Distinguishing the relative contribution of fossil fuel and biomass combustion aerosols deposited at Summit, Greenland through isotopic and molecular characterization of insoluble carbon. Atmospheric Environment, 36(28): 4463-4477.

Sowers, T., Bender, M., Raynaud, D. and Korotkevich, Y.S., 1992. Delta-N-15 of N2 in Air Trapped in Polar Ice - a Tracer of Gas-Transport in the Firn and a Possible Constraint on Ice Age-Gas Age-Differences. Journal of Geophysical Research-Atmospheres, 97(D14): 15683-15697.

Stohl, A. et al., 2006. Pan-Arctic enhancements of light absorbing aerosol concentrations due to North American boreal forest fires during summer 2004. Journal of Geophysical Research-Atmospheres, 111(D22).

Streets, D.G. et al., 2003. An inventory of gaseous and primary aerosol emissions in Asia in the year 2000. Journal Of Geophysical Research-Atmospheres, 108(D21).

Streets, D.G. et al., 2007. Air quality during the 2008 Beijing Olympic Games. Atmospheric Environment, 41: 480-492.

Streets, D.G. and Waldhoff, S.T., 2000. Present and future emissions of air pollutants in China: SO2, NOx, and CO. Atmospheric Environment, 34(3): 363-374.

Sullivan, A.P. and Weber, R.J., 2006a. Chemical characterization of the ambient organic aerosol soluble in water: 1. Isolation of hydrophobic and hydrophilic fractions with a XAD-8 resin. Journal of Geophysical Research-Atmospheres, 111(D5).

Sullivan, A.P. and Weber, R.J., 2006b. Chemical characterization of the ambient organic aerosol soluble in water: 1. Isolation of acid, neutral, and basic fractions by modified size-exclusion chromatography. Journal of Geophysical Research-Atmospheres, 111(D5).

Sullivan, A.P. et al., 2004. A method for on-line measurement of water-soluble organic carbon in ambient aerosol particles: Results from an urban site. Geophysical Research Letters, 31(13).

Swanson, A.L. et al., 2002. Photochemically induced production of CH3Br, CH3I, C2H5I, ethene, and propene within surface snow at Summit, Greenland. Atmospheric Environment, 36(15-16): 2671-2682.

Tanner, R.L., Parkhurst, W.J., Valente, M.L. and Phillips, W.D., 2004. Regional composition of $PM_{2.5}$ aerosols measured at urban, rural and "background" sites in the Tennessee valley. Atmospheric Environment, 38(20): 3143-3153.

Thomas, R., Frederick, E., Krabill, W., Manizade, S. and Martin, C., 2006. Progressive increase in ice loss from Greenland. Geophysical Research Letters, 33(10).

Tsai, Y.I. and Chen, C.L., 2006. Characterization of Asian dust storm and non-Asian dust storm PM2.5 aerosol in southern Taiwan. Atmospheric Environment, 40(25): 4734-4750.

Twickler, M.S., Spencer, M.J., Lyons, W.B. and Mayewski, P.A., 1986. Measurement of Organic-Carbon in Polar Snow Samples. Nature, 320(6058): 156-158.

Twohy, C.H., Clarke, A.D., Warren, S.G., Radke, L.F. and Charlson, R.J., 1989. Light-Absorbing Material Extracted from Cloud Droplets and Its Effect on Cloud Albedo. Journal of Geophysical Research-Atmospheres, 94(D6): 8623-8631.

Veltkamp, P.R., Hansen, K.J., Barkley, R.M., and Sievers, R.E., 1996. Principal component analysis of summertime organic aerosols at Niwot Ridge, Colorado. Journal of Geophysical Research-Atmospheres, 101(D14).

Wan, Y., Yang, H.W. and Masui, T., 2005. Health and economic impacts of air pollution in China: A comparison of the general equilibrium approach and human capital approach. Biomedical And Environmental Sciences, 18(6): 427-441.

Wang, H. and Mullahy, J., 2006. Willingness to pay for reducing fatal risk by improving air quality: A contingent valuation study in Chongqing, China. Science of the Total Environment, 367(1): 50-57.

Wang, X.P. and Mauzerall, D.L., 2006. Evaluating impacts of air pollution in China on public health: Implications for future air pollution and energy policies. Atmospheric Environment, 40(9): 1706-1721.

Wang, Y.Q., Zhang, X.Y. and Arimoto, R., 2006. The contribution from distant dust sources to the atmospheric particulate matter loadings at XiAn, China during spring. Science Of The Total Environment, 368(2-3): 875-883.

Warren-Rhodes, K. and Koenig, A., 2001. Ecosystem appropriation by Hong Kong and its implications for sustainable development. Ecological Economies, 39: 347-359.

Watson, J.G., Chow, J.C. and Frazier, C.A., 1996. X-Ray fluorescence analysis of ambient air samples. Elemental analysis of airborne particles. Gordon and Breach, Newark, 1-31 pp.

Watson, J.G., Chow, J.C. and Houck, J.E., 2001. PM2.5 chemical source profiles for vehicle exhaust, vegetative burning, geological material, and coal burning in Northwestern Colorado during 1995. Chemosphere, 43(8): 1141-1151.

Weast, R.C. (Editor), 1987. CRC Handbook of Chemistry and Physics, 1st Student Edition. CRC Press, Inc., Boca Raton, FL.

Wei, F. et al., 1999. Ambient concentrations and elemental compositions of PM10 and PM2.5 in four Chinese cities. Environmental Science & Technology, 33(23): 4188-4193.

Weiss, H.V., Koide, M. and Goldberg, E.D., 1971a. Mercury in a Greenland Ice Sheet - Evidence of Recent Input by Man. Science, 174(4010): 692-&.

Weiss, H.V., Koide, M. and Goldberg, E.D., 1971b. Selenium and Sulfur in a Greenland Ice Sheet - Relation to Fossil Fuel Combustion. Science, 172(3980): 261-&.

Whitlow, S., Mayewski, P., Dibb, J., Holdsworth, G. and Twickler, M., 1994. An Ice-Core-Based Record of Biomass Burning in the Arctic and Sub-Arctic, 1750-1980. Tellus Series B-Chemical and Physical Meteorology, 46(3): 234-242.

World Health Organization, 2006. WHO Air quality guidelines for particulate matter, ozone, nitrogen dioxide and sulfur dioxide, Global update 2005. http://whqlibdoc.who.int/hq/2006/WHO_SDE_PHE_OEH_06.02_eng.pdf (Date accessed: April, 2007)

Wong, C.M. et al., 2002. A tale of two cities: Effects of air pollution on hospital admissions in Hong Kong and London compared. Environmental Health Perspectives, 110(1): 67-77.

Wong, C.M., Ma, S., Hedley, A.J. and Lam, T.H., 2001. Effect of air pollution on daily mortality in Hong Kong. Environmental Health Perspectives, 109(4): 335-340.

Wong, C.S.C., Li, X.D., Zhang, G., Qi, S.H. and Peng, X.Z., 2003. Atmospheric deposition of heavy metals in the Pearl River Delta, China. Atmospheric Environment, 37: 767-776.

Wong, S.C., Li, X.D., Zhang, G., Qi, S.H. and Min, Y.S., 2002. Heavy metals in the agricultural soils of the Pearl River Delta, South China. Environmental Pollution, 119: 33-44.

Wong, T.W., Tam, W.S., Yu, T.S. and Wong, A.H.S., 2002. Associations between daily mortalities from respiratory and cardiovascular diseases and air pollution in Hong Kong, China. Occupational And Environmental Medicine, 59(1): 30-35.

Wu, D. et al., 2005. An extremely low visibility event over the Guangzhou region: A case study. Atmospheric Environment, 39(35): 6568-6577.

Zielinski, G.A. et al., 1994. Record of Volcanism since 7000-Bc from the Gisp2 Greenland Ice Core and Implications for the Volcano-Climate System. Science, 264(5161): 948-952.

VITA

Gayle Singleton Willis Hagler is the daughter of Jim and Ann Willis, born in Nashua, New Hampshire as the second of four very blond girls (siblings are Lisa, Allison, and Suzanne). She grew up in the small town of Amherst, New Hampshire and attended local public schools where she was regularly dubbed as "class clown" by her teachers. During high school, she also spent 7 months as a student at the John F. Kennedy Schule in Berlin, Germany, although she spoke essentially no German at the time.

Gayle was initially interested in becoming a professional musician (French horn and piano) but then discovered an untapped passion for physics during her junior year of high school. Her growing interest in science and having an old Suburban in her family's possession quickly elevated Gayle to leadership of her school's astronomy club, as she was the only one capable of transporting the club telescope. After high school, Gayle received a bachelor's degree in Civil Engineering at the Georgia Institution of Technology, followed by specializing in Environmental Engineering at the M.S. and PhD level. Gayle's time spent researching in the field in China led to an honorary second name for easier communication – Li Hong Xia, a traditional Communist-era girl's name meaning "Red Sunset, of the Li family". It should be noted, Gayle is not a member of the Communist Party, although she very much appreciates being given a Chinese name.

In 2004, Gayle married fellow Georgia Tech alum, Ty Hagler. After her graduation, they plan to reside near Research Triangle Park, North Carolina.